

**Exploring the role of mu opioid receptor
(*OPRM1*) and *CYP2B6* gene variations for
methadone pharmacogenomics. Can these
variations be used to advance toxicological
interpretation post-mortem?**

Hannah Bunten

**A thesis submitted in partial fulfilment of the requirements of Bournemouth
University for the degree of Doctor of Philosophy.**

September, 2010



This copy of the thesis has been supplied on condition that anyone who consults it is understood to recognise that its copyright rests with its author and due acknowledgement must always be made of the use of any material conducted in, or derived from, this thesis.

Abstract

“Exploring the role of mu opioid receptor (*OPRM1*) and *CYP2B6* gene variations for methadone pharmacogenomics. Can these variations be used to advance toxicological interpretation post-mortem?”

Hannah Bunten

Methadone is increasingly involved in drug overdose cases and the molecular actions of the drug *in vivo* are largely unknown requiring elucidation. This study set out to examine the relationship between methadone toxicity and *CYP2B6* and mu (μ) opioid receptor (*OPRM1*) single nucleotide polymorphisms (SNPs).

Using SNP genotyping, the association between *OPRM1* A118G and *CYP2B6* T750C, G516T, and A785G variations and post-mortem methadone concentrations were investigated. The allele frequencies of *OPRM1* and *CYP2B6* variants were then studied in a control population of live non-methadone using subjects, to determine the prevalence and distribution of specific variations in post-mortem and living subjects. Further *in vitro* study was conducted to assist in interpreting the association between *OPRM1* and *CYP2B6* variations and individual susceptibility to methadone. Cloning strategies were designed for the studies of promoter activities affected by the T750C promoter SNP on *CYP2B6* expression, and the role of the *OPRM1* A118G variation for receptor internalisation following methadone treatment was investigated.

A significant association was identified between high post-mortem methadone concentrations and G561T and A785G (*CYP2B6**6) variations reflecting poor methadone metabolism. Furthermore, the *OPRM1* A118G SNP significantly correlated with higher post-mortem methadone concentrations and the *in vitro* analysis of A118G indicated that this could be due to a reduction in receptor internalisation in 118 AG subjects.

The findings from the research contribute to pre-determining, in part, individual susceptibility to methadone accumulation and toxicity. Specific screening to identify *CYP2B6**6 and *OPRM1* A118G carriers prior to addiction treatment could therefore be valuable as part of a cost-effective risk management strategy. Furthermore, *CYP2B6**6 and A118G could be used to interpret toxicology results identifying subjects with poor metabolism.

List of Contents

Page

Abstract.....	III
Table of Contents.....	IV
Table of Figures.....	X
Table of Tables.....	XII
Acknowledgements.....	XIV
Authors Declaration.....	XV
List of Abbreviations.....	XVI

CHAPTER 1: Introduction.

1.1 Background.....	2
1.1.1 Study Aim and Objectives.....	4
1.2 Methadone pharmacology and mechanisms of action.....	5
1.3 Methadone safety profile (adverse drug reactions).....	9
1.4 Methadone-related deaths.....	10
1.4.1 Cardio-toxicity.....	11
1.4.2 Respiratory depression.....	13
1.4.3 Influence of drug-drug interactions.....	15
1.4.4 Drug Tolerance.....	17
1.5 Toxicological interpretation of methadone cases.....	18
1.5.1 Post-mortem redistribution.....	19
1.5.2 Individual differences in drug metabolism.....	20
1.6 Pharmacogenomics.....	20
1.6.1 Toxicological interpretation and pharmacogenomics.....	22
1.6.2 Pharmacogenomic influences on methadone metabolism.....	24
1.6.3 Pharmacogenomic influences on methadone-receptor binding and response.....	31
1.7 Summary.....	40

CHAPTER 2: Methodology.

2.1 Method Optimisation.....	43
2.1.1 DNA Collection and Extraction.....	44
2.1.1.1 DNA extraction from buccal swabs.....	44
2.1.1.1.1 Buccal DNA quantification.....	44
2.1.1.1.2 Quantifiler® Software Setup.....	45
2.1.1.1.3 Sample Preparation.....	45
2.1.1.2 DNA extraction from whole blood.....	46
2.1.1.2.1 DNA extraction using the Promega Wizard Purification Kit.....	47
2.1.1.2.2 DNA extraction using the Qiagen DNeasy Blood and Tissue kit.....	47
2.1.1.2.3 Quantification of DNA from whole blood.....	48
2.1.2 PCR Amplification of SNP regions of <i>OPRM1</i> gene.....	48
2.1.2.1 Primer design and Rehydration.....	48
2.1.2.2 Primer validation.....	49
2.1.2.3 PCR Development.....	51

2.1.2.3.1 MgCl ₂	51
2.1.2.3.2 Temperature.....	52
2.1.2.4 PCR Validation.....	54
2.1.2.5 A118G identification.....	54
2.1.3 PCR Amplification of SNP regions of <i>CYP2B6</i> gene.....	55
2.1.3.1 Primer design and Rehydration.....	55
2.1.3.2 Primer validation.....	56
2.1.3.3 T750C PCR Validation.....	57
2.1.3.3.1 Temperature.....	57
2.1.3.3.2 MgCl ₂	57
2.1.3.4 T750C Identification.....	58
2.1.3.5 G516T PCR Validation.....	58
2.1.3.5.1 Temperature.....	58
2.1.3.5.2 MgCl ₂	60
2.1.3.6 G516T Identification.....	60
2.1.3.7 A785G PCR Validation.....	61
2.1.3.7.1 Temperature.....	61
2.1.3.8 A785G Identification.....	62
2.2 Post-mortem Sample Examination.....	63
2.2.1 DNA extraction from whole blood.....	64
2.2.2 Quantification of DNA from post-mortem blood.....	64
2.2.3 A118G SNP Genotyping.....	64
2.2.3.1 Software set-up.....	65
2.2.3.2 Sample preparation.....	66
2.2.4 T750C SNP Genotyping.....	67
2.2.4.1. Software set-up.....	67
2.2.4.2 Sample preparation.....	69
2.2.5 G516T SNP Genotyping.....	69
2.2.5.1 Software set-up.....	69
2.2.5.2 Sample preparation.....	71
2.2.6 A785G SNP Genotyping.....	71
2.2.6.1 Software set-up.....	71
2.2.6.2 Sample preparation.....	73
2.2 Control Sample Examination.....	74
2.2.1 DNA Extraction from buccal swabs.....	75
2.2.2 Buccal DNA Quantification.....	75
2.2.3 A118G Genotyping.....	75
2.3.3.1 Software set-up.....	76
2.3.3.2 Sample preparation.....	77
2.2.4 T750C Genotyping.....	77
2.3.4.1 Software set-up.....	78
2.3.4.2 Sample preparation.....	79
2.2.5 G516T Genotyping.....	79
2.3.5.1 Software set-up.....	80
2.3.5.2 Sample preparation.....	81
2.2.6 A785G Genotyping.....	81
2.3.6.1 Software set-up.....	82
2.3.6.2 Sample preparation.....	83
2.3 <i>CYP2B6</i> Cloning.....	84
2.3.1 Primary Cloning strategy.....	85
2.3.2 Plasmid DNA preparation.....	87

2.3.3	<i>Hind</i> III & <i>Xba</i> I digest.....	87
2.3.4	Gel Extraction of EGFP Gene.....	87
2.3.5	Gel Extraction of hSVCT2 Gene.....	88
2.3.6	DNA ligation of EGFP into hSVCT2 vector.....	88
2.3.7	Transformation of EGFP clone into JM109 cells.....	89
2.3.8	PCR amplification of <i>CYP2B6</i> promoter region	89
2.4.8.1	Primer design and Rehydration.....	89
2.4.8.2	Primer validation.....	90
2.4.8.3	PCR temperature development.....	91
2.4.8.4	Amplification of <i>CYP2B6</i> promoter region.....	91
2.4.8.5	Gel Extraction of <i>CYP2B6</i> promoter region.....	92
2.3.9	Alternative Cloning strategy.....	92
2.3.10	<i>CYP2B6</i> promoter insertion into pcDNA3.1/CT-GFP-TOPO® vector.....	94
2.4.10.1	DNA ligation of <i>CYP2B6</i> into pcDNA3.1/CT-GFP-TOPO® vector.....	94
2.4.10.2	Transformation of p2B6-GFP-HB clones into OneShot® TOP10 <i>E. coli</i>	94
2.4.10.3	p2B6-GFP-HB Clone Sequencing.....	95
2.4	A118G Methadone Binding Study.....	96
2.4.1	B-Cell line DNA extraction.....	97
2.4.2	Quantification of DNA from post-mortem blood.....	97
2.4.3	A118G SNP Genotyping.....	97
2.5.3.1	Software set-up.....	97
2.5.3.2	Sample preparation.....	99
2.4.4	Receptor Internalisation.....	99
2.5.4.1	Primary anti- μ and secondary anti-rabbit IgGFITC Optimisation.....	99
2.5.4.2	Blockage of Fc receptors to improve Antibody-Receptor Binding.....	101
2.5.4.3	Primary anti- μ and secondary anti-rabbit IgGPE Optimisation.....	101
2.5.4.4	Primary anti- μ and secondary anti-rabbit IgGFITC Optimisation.....	103
2.4.5	Racemic Methadone Binding Study.....	104
2.5.5.1	The effects of cell culture incubation interval on cell apoptosis.....	104
2.5.5.2	Cell apoptosis Trial.....	104
2.5.5.3	Cell Culture of B-lymphocytes in methadone.....	105
2.5.5.4	Cell apoptosis Trial.....	106
2.5.5.5	μ receptor Internalisation.....	106
2.5	Statistical Analysis.....	108
2.5.1	Data Normalisation.....	109
2.5.2	Post-mortem drug-drug correlations.....	109
2.6.2.1	Post-mortem drug concentrations.....	109
2.5.3	Independent T-test.....	110
2.5.4	Hardy Weinberg equilibrium.....	110
2.5.5	<i>CYP2B6</i> & <i>OPRM1</i> SNP-SNP Correlations.....	111
2.5.6	Comparing the prevalence of <i>CYP2B6</i> and <i>OPRM1</i> variations in a post- mortem and a control population.....	111
2.5.7	The influence of Age, Gender and Involvement in Methadone Maintenance.....	111

CHAPTER 3: Results.

3.1 Method Optimisation.....	113
3.1.1 DNA Extraction.....	114
3.1.1.1 DNA extraction from buccal swabs.....	114
3.1.1.2 DNA extraction from whole blood.....	116
3.1.2 PCR Amplification of SNP regions of the human <i>OPRM1</i> gene	118
3.1.2.1 MgCl ₂	118
3.1.2.2 Temperature.....	119
3.1.2.2.1 Gradient PCR reaction.....	119
3.1.2.2.2 Temperatures selected from the Gradient Reaction.....	120
3.1.2.2.3 Temperature optimisation to increase specificity.....	121
3.1.2.2.4 SNPs revealed by DNA sequencing results.....	123
3.1.2.3 A118G identification.....	131
3.1.2.3.1 A118G sequencing results.....	132
3.1.3 PCR Amplification of SNP regions of the human <i>CYP2B6</i> gene....	134
3.1.3.1 Primer validation.....	134
3.1.3.2 T750C PCR validation.....	135
3.1.3.2.1 Temperature.....	135
3.1.3.2.2 MgCl ₂	136
3.1.3.3 T750C Identification.....	137
3.1.3.3.1 T750C sequencing results.....	137
3.1.3.4 G516T PCR validation.....	139
3.1.3.4.1 Temperature.....	140
3.1.3.4.2 MgCl ₂	140
3.1.3.5 G516T Identification.....	141
3.1.3.5.1 G516T sequencing results.....	142
3.1.3.6 A785G validation.....	144
3.1.3.6.1 Temperature.....	144
3.1.3.7 A785G Identification.....	144
3.1.3.7.1 A785G sequencing results.....	145
3.2 Post-mortem Sample Examination.....	147
3.2.1 Post-mortem sample study.....	148
3.2.1.1 Quantification of DNA from post-mortem blood.....	152
3.2.1.2 A118G SNP Genotyping.....	153
3.2.1.3 T750C SNP Genotyping.....	155
3.2.1.4 G516T SNP Genotyping.....	157
3.2.1.5 A785G SNP Genotyping.....	159
3.3 Control Sample Examination.....	161
3.3.1 Control Sample Study.....	162
3.3.2 Buccal DNA quantification.....	162
3.3.3 A118G SNP genotyping.....	163
3.3.4 T750C SNP genotyping.....	164
3.3.5 G516T SNP genotyping.....	165
3.3.6 A785G SNP genotyping.....	166
3.4 <i>CYP2B6</i> Cloning.....	167
3.4.1 Cloning of promoter region of human <i>CYP2B6</i> gene.....	168
3.4.1.1 Examination of the plasmid by <i>HindIII</i> & <i>XbaI</i> Digest.....	168
3.4.1.2 Gel Extraction of pYEGFP3 Gene.....	169
3.4.1.3 Gel Extraction of hSVCT2 Vector.....	170
3.4.1.4. Ligation of pyEGFP into hSVCT2 vector.....	171

3.4.1.5. <i>NdeI</i> confirmation of hSVCT2-EGFP vector transformation.....	171
3.4.1.6. <i>CYP2B6</i> Promoter Region Primer Validation.....	173
3.4.1.7 PCR Temperature Development.....	174
3.4.1.8 Amplification of <i>CYP2B6</i> promoter region.....	175
3.4.1.9 Transformation of <i>CYP2B6</i> 750TT, 750TC, & 750CC into TOPO® vector.....	175
3.5 A118G Methadone Binding Study.....	178
3.5.1 B-cell line DNA Quantification.....	179
3.5.2 A118G SNP Genotyping.....	180
3.5.3 Receptor Internalisation.....	180
3.5.3.1 Primary anti- μ and secondary anti-rabbit IgGFITC Optimisation.....	180
3.5.3.2 Blockage of Fc Receptors to improve Antibody-Receptor Binding.....	181
3.5.3.3 Primary anti- μ and secondary anti-rabbit IgGPE Optimisation.....	182
3.5.3.4 Primary anti- μ and secondary anti-rabbit IgGFITC Optimisation..	183
3.5.4 Racemic Methadone Binding Study.....	184
3.5.4.1 The effects of cell culture incubation interval on cell apoptosis.....	184
3.5.4.2 Cell culture of B-lymphocytes in methadone.....	184
3.5.4.2.1 Cell Apoptosis Trial.....	184
3.5.4.2.2 μ Receptor Internalisation.....	188
3.6 Statistical Analysis.....	190
3.6.1 Data Normalisation.....	191
3.6.2 Post-mortem Drug Correlations.....	191
3.6.2.1 Post-mortem Drug Concentrations.....	191
3.6.3 Independent T test.....	195
3.6.4 Hardy Weinberg equilibrium.....	195
3.6.4.1 <i>CYP2B6</i>	195
3.6.4.1.1 T750C SNP.....	195
3.6.4.1.2 G516T SNP.....	196
3.6.4.1.3 A785G SNP.....	197
3.6.4.2 <i>OPRM1</i>	198
3.6.4.2.1 A118G SNP.....	198
3.6.5 <i>CYP2B6</i> and <i>OPRM1</i> SNP-SNP Correlations.....	199
3.6.6 The Influence of Age, Gender and Involvement in Methadone Maintenance.....	200

CHAPTER 4: Identification of a rapid screening method to differentiate methadone susceptible individuals using *OPRM1* and *CYP2B6* gene variants.

4.1 Abstract.....	202
4.2 Introduction.....	202
4.3 Materials and Methods.....	205
4.4 Results.....	208
4.5 Discussion.....	216

CHAPTER 5: Validation of a screening method to differentiate methadone susceptible individuals using *OPRM1* and *CYP2B6* gene variants.

5.1 Abstract.....	223
5.2 Introduction.....	224
5.3 Materials and Methods.....	226
5.4 Results.....	228
5.5 Discussion.....	233

CHAPTER 6: Inter-individual variability in the prevalence of <i>OPRM1</i> and <i>CYP2B6</i> gene variations identify drug susceptible populations.	
6.1 Abstract.....	240
6.2 Introduction.....	241
6.3 Materials and Methods.....	242
6.4 Results.....	244
6.5 Discussion.....	249
CHAPTER 7: The T750C single nucleotide polymorphism may be associated with <i>CYP2B6</i> gene expression.	
7.1 Abstract.....	255
7.2 Introduction.....	256
7.3 Materials and Methods.....	257
7.4 Results.....	259
7.5 Discussion.....	261
CHAPTER 8: The effects of the <i>OPRM1</i> A118G variation on cellular apoptosis and μ-receptor internalisation following methadone treatment.	
8.1 Abstract.....	267
8.2 Introduction.....	268
8.3 Materials and Methods.....	269
8.4 Results.....	272
8.5 Discussion.....	276
CHAPTER 9: Thesis Conclusions, Limitations & Future Work.	
9.1 Thesis Summary.....	283
9.2 Results Summary.....	284
9.2.1 Conclusions.....	285
9.2.2 Limitations of this Study.....	292
9.3 Further Work.....	295
References.....	303
Appendix.....	330
Glossary.....	350

List of Figures

- Figure 1 Main metabolic pathway of methadone.
- Figure 2 The chemical structure of r(-)-methadone and s(+)-methadone.
- Figure 3 Loss of Tolerance Following Methadone Abstinence.
- Figure 4 Molecular cloning strategy for *CYP2B6* promoter region.
- Figure 5 Molecular Cloning Strategy for p2B6-GFP-HB.
- Figure 6 Standard curve for buccal extraction run 1.
- Figure 7 Standard curve for buccal extraction run 2.
- Figure 8 Standard curve for Quantification of Promega Samples
- Figure 9 Standard curve for Quantification of Qiagen Samples.
- Figure 10 The effect of MgCl₂ on PCR success.
- Figure 11 Gradient PCR reaction for PRO554 and PRO995 primers
- Figure 12 Temperature reaction for PRO554 and PRO995 primers.
- Figure 13 Improved banding efficiency following annealing temperature optimisation.
- Figure 14 Improved PRO554 annealing following a decrease in temperature.
- Figure 15 Improved PR0995 annealing following an increase in temperature.
- Figure 16 DNA sequencing results for EX1_HB primer amplification of *OPRM1* A118G SNP.
- Figure 17 DNA sequencing results for EX1_HB primer amplification of the *OPRM1* C17T SNP.
- Figure 18 DNA sequencing results for EX2_HB primer amplification of *OPRM1* C440G SNP.
- Figure 19 DNA sequencing results for EX2_HB primer amplification of *OPRM1* A454G SNP.
- Figure 20 DNA sequencing results for EX3_HB primer amplification of *OPRM1* G779A SNP.
- Figure 21 DNA sequencing results for EX3_HB primer amplification of *OPRM1* C793T SNP.
- Figure 22 DNA sequencing results for EX3_HB primer amplification of *OPRM1* G820A SNP.
- Figure 23 DNA sequencing results for EX3_HB primer amplification of *OPRM1* G877A SNP.
- Figure 24 DNA sequencing results for EX3_HB primer amplification of *OPRM1* G942A SNP.
- Figure 25 DNA sequencing for PRO554_HB primer amplification.
- Figure 26 DNA sequencing for PRO995_HB primer amplification.
- Figure 27 Amplification of *OPRM1* exon 1 region using EX1_HB primers PCR 1.
- Figure 28 Amplification of *OPRM1* exon 1 region using EX1_HB primers PCR 2.
- Figure 29 A comparison of two SNP Genotypes for the A118G genotype (118 AA and 118 AG).
- Figure 30 PCR validation for C2B6E4 & C2B6E5 primers.
- Figure 31 PCR validation for C2B6Pr primers.
- Figure 32 PCR temperature optimisation for C2B6Pr.
- Figure 33 PCR MgCl₂ optimisation for C2B6Pr.
- Figure 34 Amplification of *CYP2B6* promoter region using C2B6PR primers.
- Figure 35 A comparison of two SNP Genotypes for the T750C genotype (750 TC and 750 CC).
- Figure 36 Gradient PCR amplification for C2B6E4.
- Figure 37 C2B6E4 banding following a decrease in annealing temperature.
- Figure 38 The effect of MgCl₂ concentration on C2B6E4 amplification.
- Figure 39 Amplification of *CYP2B6* exon 4 region using C2B6E4 primers run 1.
- Figure 40 Amplification of *CYP2B6* exon 4 region using C2B6E4 primers run 2.
- Figure 41 A comparison of two SNP Genotypes for the G516T genotype (516 GG and 516 GT).
- Figure 42 C2B6E5 banding following an increase in annealing temperature.
- Figure 43 Amplification of *CYP2B6* exon 5 region using C2B6E5 primers run 1.
- Figure 44 Amplification of *CYP2B6* exon 5 region using C2B6E5 primers run 2.
- Figure 45 A comparison of two SNP Genotypes for the A785G genotype (785 AA and 785 AG).
- Figure 46 A typical allelic discrimination plot for the A118G SNP.
- Figure 47 A typical allelic discrimination plot for the T750C SNP.
- Figure 48 A typical allelic discrimination plot for the G516T SNP.
- Figure 49 A typical allelic discrimination plot for the A785G SNP.
- Figure 50 Double restriction digest using *HindIII* and *XbaI* for Cloning method development.
- Figure 51 Double restriction digest of pyEGFP using *HindIII* and *XbaI* for Gel Extraction.
- Figure 52 Gel Extracted pyEGFP inserts for cloning strategy.
- Figure 53 Triple restriction digest of hSVCT2 using *HindIII*, *BamHI* and *XbaI* for Gel Extraction.
- Figure 54 Gel Extracted hSVCT2 vector for cloning strategy.
- Figure 55 Ligated Lamda-*HindIII* positive controls.
- Figure 56 Single restriction digest of hSVCT2-EGFP clone using *NdeI*.
- Figure 57 Single restriction digest of hSVCT2-EGFP clone using *NdeI*.
- Figure 58 Single restriction digest of hSVCT2-EGFP clone using *NdeI*.

- Figure 59 Single restriction digest of hSVCT2-EGFP clone using *NdeI*.
- Figure 60 Amplification of *CYP2B6* promoter region for primer optimisation.
- Figure 61 Gradient reaction to improve amplification selectivity for *CYP2B6* promoter.
- Figure 62 Amplification of *CYP2B6* promoter regions for 750TT, 750TC, & 750CC genotypes.
- Figure 63 Validation of the *CYP2B6* promoter region transformation and orientation for the 750 TT genotype.
- Figure 64 Validation of the *CYP2B6* promoter region transformation and orientation for the 750 TC genotype.
- Figure 65 Validation of the *CYP2B6* promoter region transformation and orientation for the 750 CC genotype.
- Figure 66 The influence of cell culture incubation time on cell apoptosis following freezing and thawing.
- Figure 67 The influence of methadone concentration on early stage cell apoptosis for 118 AA subjects, determined by the % of Annexin V-FITC positive cells.
- Figure 68 The influence of methadone concentration on early stage cell apoptosis for 118 AG subjects, determined by the % of Annexin V-FITC positive cells.
- Figure 69 The influence of methadone concentration on late stage cell apoptosis for 118 AA subjects, determined by the % of propidium iodide permeabilised cells.
- Figure 70 The influence of methadone concentration on late stage cell apoptosis for 118 AG subjects, determined by the % of propidium iodide permeabilised cells.
- Figure 71 The influence of methadone concentration on late stage cell apoptosis for 118 AA subjects, determined by the % of propidium iodide fragmented cells.
- Figure 72 The influence of methadone concentration on late stage cell apoptosis for 118 AG subjects, determined by the % of propidium iodide fragmented cells.
- Figure 73 The influence of methadone concentration on μ opioid receptor internalisation for 118 AA subjects.
- Figure 74 The influence of methadone concentration on μ opioid receptor internalisation for 118 AG subjects.
- Figure 75 The correlation between post-mortem methadone concentrations and post-morphine concentrations.
- Figure 76 The correlation between post-mortem methadone concentrations and post-mortem benzodiazepine concentrations.
- Figure 77 The correlation between post-mortem methadone concentrations and post-mortem SSRI concentrations.
- Figure 78 The correlation between post-mortem methadone concentrations and post-mortem SNRI concentrations.
- Figure 79 The correlation between post-mortem methadone concentrations and post-mortem ethanol concentrations.
- Figure 80 The correlation between post-mortem methadone concentrations and post-mortem tricyclic antidepressant concentrations.
- Figure 81 Distribution (median and interquartile range) of post-mortem methadone concentrations for the 516GG, 516GT, and 516TT genotypes.
- Figure 82 Distribution (median and interquartile range) of post-mortem methadone concentrations for the 785AA, 785AG and 785 GG genotypes.
- Figure 83 Distribution (median and interquartile range) of post-mortem methadone concentrations for the 118AA, 118AG and 118GG genotypes.
- Figure 84 Distribution (median and interquartile range) of post-mortem benzodiazepine concentrations for the 118AA, 118AG and 118GG genotypes.
- Figure 85 The association between post-mortem methadone concentration (mg/L) and methadone maintenance daily dosage (mg/L).
- Figure 86 Heterozygous frequencies for *OPRM1* A118G & *CYP2B6* G516T, A785G & T750C genotypes.
- Figure 87 Homozygous variant frequencies for *OPRM1* A118G & *CYP2B6* G516T, A785G & T750C genotypes.
- Figure 88 Total number of *CYP2B6* transformants obtained for T750C variants.
- Figure 89 Mean receptor fluorescence for 118 AA and 118 AG/GG subjects following methadone treatment.
- Figure 90 The network of genes involved in methadone action and response *in vivo*.

List of Tables

Table 1	Inhibitors and inducers of CYP3A4 and CYP2B6, methadone's primary metabolising enzymes.
Table 2	DNA sample identification for the buccal extractions.
Table 3	Standard dilution series of the 200 ng purified DNA standard for quantification.
Table 4	Quantifiler® Reaction Mix Components.
Table 5	Promega Wizard Purification Extraction components and volumes.
Table 6	Qiagen DNeasy Extraction Components and Volumes.
Table 7	<i>OPRM1</i> Primer rehydration volumes.
Table 8	<i>OPRM1</i> primer sequence information.
Table 9	Reaction components for MgCl ₂ optimisation
Table 10	<i>CYP2B6</i> Primer rehydration volumes
Table 11	<i>CYP2B6</i> primer sequence information
Table 12	Reaction components for MgCl ₂ optimisation protocol.
Table 13	Taqman™ SNP Genotyping Reaction Mix Components.
Table 14	Reaction components for the DNA ligation of EGFP into the hSVCT2 vector.
Table 15	<i>CYP2B6</i> promoter primer sequences.
Table 16	<i>CYP2B6</i> promoter primer rehydration volumes.
Table 17	Reaction components for the DNA ligation of <i>CYP2B6</i> into the pcDNA3.1/CT-GFP-TOPO® vector.
Table 18	Qiagen DNeasy Extraction Components and Volumes.
Table 19	Reaction strategy 1 to determine optimal antibody concentration.
Table 20	Reaction strategy 2 to determine optimal antibody concentration
Table 21	Reaction strategy 3 to determine optimal antibody concentration.
Table 22	Reaction strategy for sample cell culture in methadone.
Table 23	Mean DNA yield for the three buccal swabs.
Table 24	Mean DNA yield for the Promega and Qiagen extraction kits examined.
Table 25	The effects of different whole blood preservatives on DNA yield.
Table 26	Toxicology for samples DC1-DC84 where the deaths had been attributed to methadone.
Table 27	DNA yield for methadone and morphine associated post-mortem whole blood extractions.
Table 28	A118G genotypes for the 84 post-mortem samples.
Table 29	T750C genotypes for the 84 post-mortem samples.
Table 30	G516T genotypes for the 84 post-mortem samples.
Table 31	A785G genotypes for the 84 post-mortem samples.
Table 32	DNA yield for control group buccal extractions.
Table 33	A118G genotypes for the 100 control samples.
Table 34	T750C genotypes for the 100 control samples.
Table 35	G156T genotypes for the 100 control samples.
Table 36	A785G genotypes for the 100 control samples.
Table 37	DNA yield for human CLL cell lines.
Table 38	A118G SNP Genotypes for CLL Subjects.
Table 39	The mean fluorescence intensity for antibody bound μ opioid receptors.
Table 40	The mean fluorescence intensity for antibody bound μ opioid receptors following HAB blocking of Fc receptors.
Table 41	The mean fluorescence intensity for PE antibody bound μ opioid receptors.
Table 42	The mean fluorescence intensity for FITC and PE antibody bound μ opioid receptors.
Table 43	Post-mortem expected and observed frequencies for the T750C SNP.
Table 44	Hardy Weinberg results for the T750C SNP in the post-mortem population.
Table 45	Control expected and observed frequencies for the T750C SNP.
Table 46	Hardy Weinberg results for the T750C SNP in the control population.
Table 47	Post-mortem expected and observed frequencies for the G516T SNP.
Table 48	Hardy Weinberg results for the G516T SNP in the post-mortem population.
Table 49	Control expected and observed frequencies for the G516T SNP.
Table 50	Hardy Weinberg results for the G516T SNP in the control population.
Table 51	Post-mortem expected and observed frequencies for the A785G SNP.
Table 52	Hardy Weinberg results for the A785G SNP in the post-mortem population.
Table 53	Control expected and observed frequencies for the A785G SNP.

Table 54	Hardy Weinberg results for the A785G SNP in the control population.
Table 55	Post-mortem expected and observed frequencies for the A118G SNP.
Table 56	Hardy Weinberg results for the A118G SNP in the post-mortem population.
Table 57	Control expected and observed frequencies for the A118G SNP.
Table 58	Hardy Weinberg results for the A118G SNP in the control population.
Table 59	Variables entered into the Binary Logistic Regression Equation to determine the effects of Age and Gender on <i>CYP2B6</i> and <i>OPRM1</i> SNP prevalence.
Table 60	Drugs detected at post-mortem in 40 fatalities attributed to methadone as a cause of death.
Table 61	<i>CYP2B6</i> *4, *9, and *6 alleles and post-mortem methadone blood concentrations.
Table 62	<i>OPRM1</i> and <i>CYP2B6</i> Genotyping Data for the Post-mortem Methadone-attributed fatalities.
Table 63	A118G genotypes and post-mortem methadone and benzodiazepine concentrations for a population of methadone-attributed fatalities (population 1) and A118G genotypes and post-mortem morphine and benzodiazepine concentrations for a population of morphine-attributed fatalities (population 2).
Table 64	<i>CYP2B6</i> *4, *9, and *6 alleles and <i>OPRM1</i> A118G post-mortem methadone blood concentrations.
Table 65	The effect of <i>CYP2B6</i> T750C, G516T, A785G, <i>OPRM1</i> A118G, Gender and Age on subject participation in maintenance and daily methadone dosage.
Table 66	Genotype prevalence between the healthy control population and the post-mortem population whose deaths have been associated with methadone.
Table 67	The effect of the A118G variation on the total % of Annexin V negative cells.
Table 68	The association between the Total % of Annexin V positive cells and the Total % of Propidium Iodide Live, Fragmented and Permeabilised Cells.

Acknowledgements

Over the last three years I have been on an exciting journey of discovery, in both the academic and personal sense. Along the way, I have encountered many people who have encouraged and supported this research, a few of whom I would like to take the opportunity to thank.

Firstly I would like to thank Bournemouth University for giving me this opportunity and my supervisors Professor David Osselton and Dr Wei-Jun Liang who always believed in me. Their support has been constant and has helped to ensure that this study was successfully completed with minimal moments of stress.

Thanks also go to Professor Derrick Pounder and all the laboratory staff at the Centre for Legal and Forensic Medicine, Dundee University. Working together with the centre was an amazing research opportunity.

I would like to thank Dr Anton Parker and all the staff from the Molecular Pathology Department at the Royal Bournemouth Hospital for welcome advice, assistance with the flow cytometer and always making me smile.

I would like to thank Dr John Beavis for much patience and assistance with statistics.

Finally I would like to thank my family and friends. My parents have been a constant rock of support throughout this PhD and I couldn't have done it without them. I would also like to thank my partner Alan, who helped me get through those despairing moments and kept me determined to produce a piece of work I was truly proud of.

Authors Declaration

In the course of collecting data and refining idea and arguments that underpin this thesis, two journal articles have been accepted for publication. These are acknowledged below.

Bunten, H., Liang, W., Pounder, D.J., Seneviratne, C., Osselton, D. (2010). *OPRM1* and *CYP2B6* gene variants as risk factors in methadone-related deaths. *Clinical Pharmacology and Therapeutics*, 88, (3), 383-389.

Bunten, H., Liang, W., Pounder, D.J., Seneviratne, C., Osselton, D. (2011). *CYP2B6* and *OPRM1* gene variations predict methadone-related deaths. *Addiction Biology*, 16, 142-144.

List of Abbreviations

cAMP.....	Cyclic adenosine monophosphate.
CAR.....	Constitutive androstane receptor.
CHO cells.....	Chinese hamster ovary cells.
CLL.....	Chronic lymphocytic leukaemia.
COMT.....	Catechol- <i>O</i> -methyl transferase.
CNS.....	Central nervous system.
CSAT.....	Centre for Substance Abuse Treatment.
DIS-III-R.....	Diagnostic Interview Schedule, revision 3.
DNA.....	Deoxyribonucleic acid.
DRD.....	Dopamine receptor.
DUID.....	Driving under the influence.
EDDP.....	2-ethylidene-1, 5-dimethyl-3, 3-diphenylpyrrolidine.
EGFP.....	Enhanced green fluorescent protein.
EMDP.....	2-ethyl-5-methyl-3, 3-diphenyl-1-pyrrolidine.
FACs.....	Fluorescent activated cell-sorting.
FDA.....	Food and Drug Administration.
hERG.....	Human <i>Ether-à-go-go</i> gene
HIV.....	Human immunodeficiency virus.
IDU.....	Injecting drug user.
LB.....	Luria-Bertani Broth
M6G.....	Morphine-6-glucuronide.
MFI.....	Mean fluorescence intensity.
mRNA.....	Messenger ribonucleic acid.
P-gp.....	P-glycoprotein.
PTX.....	Pertussis toxin.
SAMHSA.....	Substance Abuse and Mental Health Service Administration.
SNP.....	Single nucleotide polymorphism.
SNRI.....	Serotonin-norepinephrine re-uptake inhibitor.
SOC.....	Super Optimal Broth with catabolite repression.
SSRI.....	Selective serotonin re-uptake inhibitor.
SV.....	Splice variant.
TdP.....	Torsades de Pointes.

Chapter 1

Introduction

1.1 Background

Methadone is a medication valued for its effectiveness in reducing the mortality associated with heroin addiction as well as reducing anxieties commonly associated with drug addiction. It is a potent drug associated with many fatal poisonings each year (Corkery *et al.* 2004; Shields *et al.* 2007; Modesto-Lowe *et al.* 2010). Amongst patients in addiction treatment, the largest proportion of methadone associated deaths occur during the drugs induction phase, when either drug tolerance is overestimated or other drugs are also used (Heinemann *et al.* 2000; Buster *et al.* 2002; Maxwell *et al.* 2005; Modesto-Lowe *et al.* 2010).

It is postulated that significant inter-individual variability in blood methadone concentrations and individual susceptibility to methadone toxicity may be explained through genetic variations of the genes encoding metabolism enzymes. Methadone is metabolised by CYP2B6, CYP3A4, and to a lesser extent CYP2D6. CYP2B6 is highly polymorphic with a number of different genotypes identified (Lang *et al.* 2001). Furthermore live patient studies demonstrated that the CYP2B6*6 allele (resulting from a combination of the exon 4 G516T and exon 5 A785G polymorphisms) is linked with poor drug metabolism (Eap *et al.* 2007). The influence of CYP2B6 variations on methadone toxicity post-mortem however has not yet been examined.

The mu (μ) opioid receptor *OPRM1* is the preferential binding target for many opioids including methadone and morphine, *OPRM1* gene variants are therefore likely to influence methadone action *in vivo*. There has been an exponential increase in the number of studies examining morphine pharmacogenomics due its clinical importance, and significant variability in inter-individual drug response (Ross *et al.* 2005; Paice,

2007; Ishani *et al.* 2010). In comparison few studies have examined the association between the μ opioid receptor and methadone response despite reports of significant variability in individual methadone blood concentrations. Methadone is often concomitantly prescribed or abused together with benzodiazepines, and many deaths attributed to methadone also involve benzodiazepines (Caplehorn & Drummer, 2002; Corkery *et al.* 2004; Shields *et al.* 2007). It has been well documented that these two drugs in combination induce lethal respiratory depression (McCormick *et al.* 1984; Borron *et al.* 2002; Lintzeris *et al.* 2007; Poisnel *et al.* 2009; Lintzeris & Nielsen, 2010) however the molecular mechanisms responsible for this remain obscure.

Methadone is a chiral drug, with two enantiomers (*R*)-methadone and (*S*)-methadone that demonstrate stereoselectivity. Until recently the pharmacogenomic importance of this has received little attention, which may in part be a reflection of the pharmacological inactivity of the (*S*)-methadone enantiomer. Although it was suggested that a link between (*S*)-methadone and cardiotoxicity may influence individual susceptibility to methadone (Eap *et al.* 2007). Methadone is known to induce a condition termed “torsades de pointes”, which involves a prolongation of the QT interval resulting in arrhythmia and sudden cardiac death (Krantz *et al.*, 2002). It is postulated that differences in enantiomer distribution is demonstrative of a key stereoselective relationship that could explain occurrences of sudden cardiac death following methadone exposure. Additionally it was also hypothesised that *OPRM1* and *CYP2B6* variations could be associated with this, particularly variations located in areas linked with gene expression (promoter regions). Of particular significance are the T750C polymorphism in the promoter region of the *CYP2B6* gene and the *OPRM1* A118G variation located in exon 1. A118G is located in the receptor binding pocket and has been linked with reductions in β -endorphin binding but not morphine

or racemic methadone (Bond *et al.* 1998). The influence on (*R*)-methadone and (*S*)-methadone separately has not yet been examined.

1.1.1 Study Aim & Objectives

The purpose of this project was to examine whether pharmacogenomics can be used to predict whether methadone programme participants are at higher risk of methadone related-death, whilst advancing current toxicological interpretation of post-mortem methadone concentrations. This aim will be addressed by examining two genes intimately linked with methadone metabolism and response, the gene encoding the cytochrome P450 enzyme *CYP2B6* and the μ opioid receptor gene (*OPRM1*). Methodologies to amplify and genotype *CYP2B6* T750C, G516T and A785G, and *OPRM1* A118G polymorphisms will be developed and optimised (Chapter 2). The results from this will then be analysed and discussed in Chapter 3. The association between *CYP2B6* (G516 T, A785G, T750C) and *OPRM1* (A118G) gene variations and blood methadone concentrations in fatalities attributed to methadone will be examined to determine whether high blood methadone concentrations are linked with *OPRM1* and *CYP2B6* gene variations (Chapters 4 and 5). After this, the post-mortem allele frequencies will be compared against a healthy control population to identify drug susceptibility gene markers (Discussed in Chapter 6).

This study will also conduct *in vitro* studies to explore the effects of *CYP2B6* and *OPRM1* polymorphisms in a controlled environment, to provide a theoretical concept to clarify *OPRM1* and *CYP2B6* gene effects *in vivo*. This concept could then be used to elucidate the molecular actions of methadone. This will involve the molecular cloning of the *CYP2B6* promoter region to create 750 TT, and 750 TC, reporter

constructs (Chapter 7). Finally this study will explore the effects of methadone on μ -receptor internalisation using CLL cells, to develop a method to examine *OPRM1* A118G effects on receptor internalisation (Chapter 8). The overall conclusions and suggestions for further research will be discussed in Chapter 9.

1.2 Methadone pharmacology and mechanisms of action

Methadone is a synthetic opioid originally created as a substitute for morphine during World War II (Crettol *et al.* 2008). Approved as an analgesic by the Food and Drug Administration (FDA) in 1947, methadone is now routinely used for the treatment of opioid addiction and dependence worldwide, leading to significant reductions in heroin use and mortalities associated with heroin addiction (Centre for Substance Abuse Treatment, (CSAT), 2004). A substance abuse and mental health services administration (SAMHSA) report in 2000 documented that over 3 million persons in the US had used heroin at some point, with an estimated number of 0.8 to 1.2 million individuals addicted to the drug (SAMHSA, 2000). In the UK methadone prescription increased sevenfold between 1993 and 2000 and current UK statistics report that 147,000 individuals are enrolled in drug maintenance programmes, with methadone prescription accounting for a significant percentage of this. The 2008 SAMHSA report examined drug use between 2006 and 2007, noting a reduction in the number of current heroin users from 338,000 (0.14%) in 2006 and 153,000 (0.06%) in 2007 (SAMHSA, 2008).

Prescribed orally, methadone is a liposoluble basic drug with a pK_a of 9.2, available as a solid tablet, a rapidly dissolving wafer or as a premixed liquid (Garrido & Trocóniz, 1999; Baselt, 2004). Administered in a racemic mixture, oral methadone has a long plasma elimination half-life and high oral bioavailability (70-

90%), appearing in the blood 30 minutes following administration, the unique pharmacological properties that make it an appropriate choice for the treatment of opioid addiction and pain relief (Wolff *et al.* 1997; Foster *et al.* 1999; Corkery *et al.* 2004; Nettleton *et al.* 2007). Extensively metabolised in the liver (Figure 1), methadone is converted into its primary metabolites 2-ethylidene-1, 5-dimethyl-3, 3-diphenylpyrrolidine (EDDP) and 2-ethyl-5-methyl-3, 3-diphenyl-1-pyrrolidine (EMDP) by the cytochrome P450 enzymes CYP3A4, CYP2B6 and to a lesser extent CYP2D6 (Sullivan & Due, 1973; Eap *et al.* 2007; Pimentel & Mayo, 2008). The two metabolites are widely considered pharmacologically inactive and are eliminated from the body in the faeces and urine together with any unchanged methadone (Corkery *et al.* 2004).

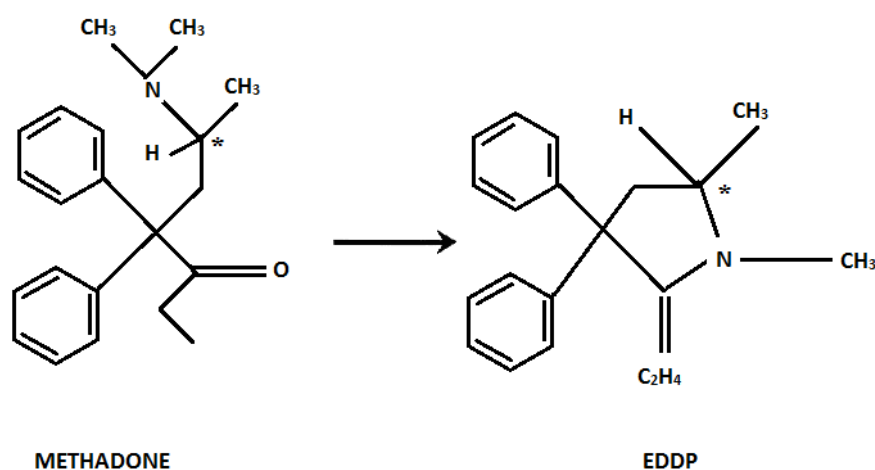


Figure 1: Main metabolic pathway of methadone (asterisk (*) denotes chiral centre).

The percentage of free (unbound) pharmacologically active drug is very low at 6-14% (Wolff, 2003). Drug metabolism can be affected by other drugs through enzymatic inhibition or induction (Table 1), affecting the elimination half life and plasma concentrations (Shields *et al.* 2007). Typically the elimination half life for methadone averages 24-36 hours at steady state, but this can vary from anywhere

between 4 and 91 hours (Ayonrinde & Bridge, 2000). This variability complicates patient steady-state blood levels by affecting the equilibrium between drug elimination and the amount of active drug remaining in the body. During treatment induction this balance usually takes between 4 and 5 days to achieve, however for some individuals this can take a significantly longer time (CSAT, 2004). Extensive (17-fold) inter-individual variability has been documented for blood methadone concentrations, and the prevalence of methadone toxicity following inappropriately short dosing intervals has increased in frequency (Foster *et al.* 2005).

Methadone is a chiral drug (Figures 1 & 2 demonstrate the chiral center) with two enantiomeric forms (*R*)-methadone (which is thought to account for most of the drug's pharmacological activity) and (*S*)-methadone (often described as being pharmacologically inactive) that may be an important determinant in the adverse responses reported for methadone (Eap *et al.*, 2002; Megarbane *et al.*, 2007). A 25-50 fold difference between the analgesic potency of (*R*)-methadone and (*S*)-methadone has been described (Pham-Huy *et al.*, 1997).

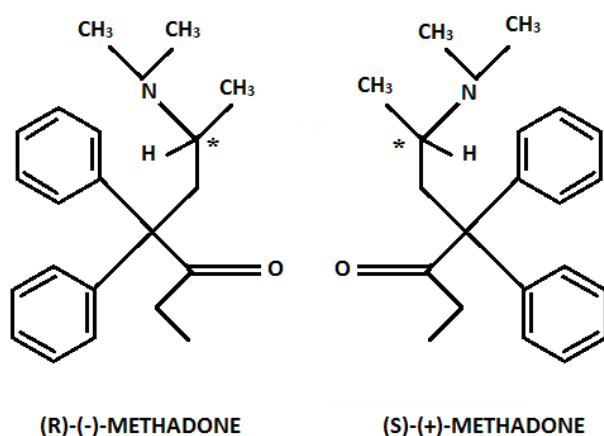


Figure 2: The chemical structure of r-(-)-methadone and s-(+)-methadone (asterisk (*) denotes chiral centre).

Pharmacological activity is induced through selective binding of methadone at the opioid receptors, which include the μ -opioid receptor, the delta (δ)-opioid receptor and the kappa (κ)-opioid receptor. The μ -opioid receptor is the preferential binding target for methadone with a recorded K_i value of 3.7 ± 0.03 (nM) (Mestek *et al.* 1995). This receptor is a member of the G-protein coupled receptor (GPCR) family and ligand-receptor binding induces signal transduction cascades affecting analgesia, respiratory activity, protein phosphorylation, neurotransmitter release, and *OPRM1* gene expression (Mestek *et al.* 1995; Chartuvedi *et al.* 2000). Methadone also binds with low affinity to *N*-methyl-D-aspartic acid (NMDA) receptors, which may result in alterations to the development of drug tolerance (Lewanowitsch *et al.* 2004).

Table 1: Inhibitors and inducers of CYP3A4 and CYP2B6, methadone’s primary metabolising enzymes.

Inducers	Inhibitors
CYP3A4	
Phenobarbital (Runge <i>et al.</i> 2000)	Itraconazole (Raaska & Neuvonen, 1998)
Carbamazepine (Magnusson <i>et al.</i> 2008)	Ritonavir (Eagling <i>et al.</i> 1997)
Phenytoin (Tomlinson <i>et al.</i> 1996)	Nelfinavir (Lillibridge <i>et al.</i> 1998)
Dexamethasone (LeCluyse <i>et al.</i> 2000)	Verapamil (Kantola <i>et al.</i> 1998)
Nevirapine (Lamson <i>et al.</i> 1999)	Erythromycin (Funderburg <i>et al.</i> 1994)
Topiramate (Nallani <i>et al.</i> 2003)	Ketoconazole (Baldwin <i>et al.</i> 1995)
Rifampicin (Lehmann <i>et al.</i> 1998)	Fluconazole (Ahonen <i>et al.</i> 1997)
Efavirenz (Clarke <i>et al.</i> 2001)	Clarithromycin (Quinney <i>et al.</i> 2008)
CYP2B6	
Phenytoin (Wang <i>et al.</i> 2004)	Nelfinavir (Hesse <i>et al.</i> 2001)
Carbamazepine (Ketter <i>et al.</i> 1995)	Ticlopidine (Turpeinen <i>et al.</i> 2004)
Rifampin (Ribera <i>et al.</i> 2001)	Clopidogrel (Richter <i>et al.</i> 2004)
Efavirenz (Robertson <i>et al.</i> 2008)	Paroxetine (Walsky <i>et al.</i> 2006)
Phenobarbital (Rencurel <i>et al.</i> 2005)	Sertraline (Walsky <i>et al.</i> 2006)

1.3 Methadone safety profile (adverse drug reactions)

Opiate addicts are at increased risk of accidental death, principally through drug overdose. Substitution with methadone has been used in the treatment of opioid addiction for a number of years and it has been well documented that methadone prescription reduces heroin use and the related crime and health problems improving overall survival rates (Bertschy, 1995; Neeleman & Farrell, 1997; Esteban *et al.* 2003). The prevalence of communicable diseases such as human immunodeficiency virus (HIV) and hepatitis C are high in injecting drug users (IDU'S) and participation in methadone maintenance programmes has significantly reduced disease prevalence (Harding-Pink, 1993; Caplehorn & Ross, 1995; Broers *et al.* 1998; Wong *et al.* 2003; Gowing *et al.* 2006; Tross *et al.* 2008; Wilson *et al.* 2010).

Initially, UK treatment practises implemented general controls for drug prescription in place of regimented protocols which impacted individual prescription periods (two weeks through to unlimited duration) and encouraged illicit drug abuse (Gossop *et al.* 2001). Increased supervision of maintenance programmes and reduced prescription of methadone tablets significantly improved methadone's safety profile (Zador *et al.* 2006). A relevant proportion of heroin users who start methadone maintenance will however continue concomitant heroin use at least intermittently for some time (Heinemann *et al.* 2000).

Clinical research demonstrated that methadone maintenance reduces the mortality associated with heroin use. However methadone is also dangerous in overdose and increased numbers of methadone-associated deaths suggest stricter reviewing of maintenance practises (Neeleman & Farrell, 1997; CSAT, 2004).

Overdose risk during the drug induction period is central to this and prescriptions that exceed the recommended daily doses of 20-40 mg should be monitored (Heinemann

et al. 2000). The UK Department of Health recommended an initial daily dose of 10-40 mg and for drug tolerant patients 25-40 mg (Department of Health, 1999). More recently, a study reported the mean methadone daily dosage across 157 methadone treatment practises to be 47 mg (Joseph & Moselhy, 2005).

Caplehorn, (2000) documented that only 14 % of clinic staff in the US (a study group of 149 individuals) were aware that the risk of methadone-associated death is significantly increased during the first two weeks of treatment. Furthermore, only 15% of staff understood that prescription of daily dose's of 30-40 mg were unsafe for methadone naïve patients. A 2009 CSAT report noted that adverse events during methadones induction phase are due to an overestimation of drug tolerance by clinic staff. Reports of this nature suggest education is critical to improve methadone's safety profile with particular emphasis on the dangers of the drug induction phase.

1.4 Methadone-related deaths

Large doses of methadone, concomitant use with other substances and accidental ingestion by intolerant persons can all result in toxic reactions and overdose fatalities (Laberke & Bartsch, 2010; Modesto-Lowe *et al.* 2010; Romelsjö *et al.* 2010).

Amongst the more common adverse effects of methadone are nausea, vomiting, dizziness, clouding of consciousness, anorexia, dry mouth and excessive sweating.

Indicators of drug overdose include respiratory depression, pinpoint pupils, hypotension, pulmonary oedema and coma (Davis & Walsh, 2001; Corkery *et al.* 2004). Deaths typically occur during the induction phase of treatment when drug tolerance is overestimated or during maintenance when several days' doses are combined (Harding-Pink, 1993; Heinemann *et al.* 2000). Maxwell *et al.* (2005)

reported a total of 766 patients in methadone maintenance to have died in Texas between 1994 and 2002, the causes of death ranged from cardiovascular and respiratory disease through to drug overdose. At least three-fifths of deaths associated with methadone in England and Wales are due to illicit methadone use (Ghodse *et al.* 2003). In the UK between 1993 and 2002 there were 3604 deaths where methadone was noted on the death certificate (Corkery *et al.* 2004), it is therefore important to identify why these deaths are occurring. Typically there are three possible scenarios for methadone related fatalities all of which can lead to cardio-toxicity and respiratory depression. Illicitly obtained methadone used in excessive doses to experience drug induced euphoria; concomitant use of methadone with other prescription medications such as benzodiazepines; and toxic drug accumulation during the induction period of methadone maintenance (CSAT, 2004).

1.4.1 Cardio-toxicity

There is a clear association between methadone use and cardiotoxicity and it is postulated that this is a result of (*S*)-methadone. Several studies have documented an association between methadone treatment and QT interval prolongation, leading to cardio-toxicity and fatal ventricular arrhythmias (Kornick *et al.* 2003; Routhier *et al.* 2006, Eap *et al.* 2007; Chugh *et al.* 2008). The QT interval is a measurement of cardiac repolarisation. The normal upper limits of the QT interval are < 430 milliseconds (ms) in males and < 450 ms in females, QT intervals greater than 440 ms and 460 ms are classed as being prolonged (Hancox *et al.* 2008). QT prolongation has been associated with congenital long-QT syndrome as a result of gene mutations, ionic disorders, and drug administration (Fonseca *et al.* 2009). High doses of methadone prolong the QT interval by blocking the cardiac potassium channel expressed by the human *ether-a-go-go* gene (hERG or *KCNH2*), as demonstrated in

in vitro in human cell lines (Katchman *et al.* 2002). This induces polymorphic ventricular tachycardia (an electrophysiological disorder of the heart occurring in genetically predisposed individuals), a condition termed Torsades de Pointes (TdP), which if uncorrected can result in sudden cardiac death (Kornick *et al.* 2003; Eap *et al.* 2007).

A number of studies have reported methadone induced TdP (Krantz *et al.* 2002; Gil *et al.* 2003; Kornick *et al.* 2003; Walker *et al.* 2003; Martell *et al.* 2005; Sánchez Hernández *et al.* 2005; Skverjold *et al.* 2006; Fanoë *et al.* 2007; Routhier *et al.* 2006; Pimentel & Mayo, 2008) with several reporting sudden cardiac death as a consequence of methadone treatment (Kornick *et al.* 2003; Pearson & Woosley, 2005; Ehret *et al.* 2006; Gupta *et al.* 2007; Chugh *et al.* 2008; Darke *et al.* 2010). Krantz *et al.* (2002) reported 17 cases of TdP in patients in methadone treatment, the individual doses for these cases were significantly higher than average ranging from 65 to 1000 mg/day. Martel *et al.* (2005) examined 132 patients during the induction phase of methadone treatment reporting a significant prolongation in individual QT intervals. Skverjold *et al.* (2006) found that high concentrations of (*R*)-methadone correlated with QTc values in the upper range, this result was not repeated for (*S*)-methadone and racemic methadone. Chugh *et al.* (2008) examined sudden cardiac death cases in the presence and absence of methadone, reporting a significantly lower prevalence of cardiac abnormalities in the cases where methadone was present, implying methadone as the factor responsible for sudden death. Darke *et al.* (2010) reported higher levels of heart disease in methadone associated fatalities when examined against heroin associated fatalities. Increased frequencies of myocardial fibrosis, cardiomyopathy and myocarditis were documented for the methadone deaths. Darke *et al.* (2010) emphasised that these findings should not be taken to imply that enrolment in

methadone treatment will result in organ damage however the predisposition to methadone induced cardio-toxicity may be explained by these findings.

Therefore, chronic opioid use could have a detrimental effect on the physiology and functionality of the cardiac network. Kienbaum *et al.* (2002) noted that humans addicted to opioids for a number of years (10 years) displayed reductions in central nervous system (CNS) responses to arterial hypotension (where the heart pumps insufficient quantity of blood) as a result of chronic μ -opioid receptor stimulation. Experimental studies have demonstrated that stimulation of the opioid receptors is a predisposing factor in TdP due to a decreased heart rate (Sánchez Hernández *et al.* 2005). The precise role of opioid receptors for cardio-toxicity is still however unclear.

Although methadone has been used for over 40 years TdP has only recently been recognised as a factor in methadone associated deaths (Justo *et al.* 2006; Zünkler & Wos-Maganga, 2010). Therefore it is possible that many cases of TdP during methadone treatment have been misdiagnosed as respiratory in nature.

1.4.2 Respiratory depression

Respiratory depression is the leading cause of death in cases of methadone overdose following the activation of the opioid system. Harding-Pink, (1993) stated that the foremost toxic effect of methadone is respiratory depression with pulmonary oedema and aspiration pneumonia. Respiration is largely an involuntary activity induced by nervous stimulation of the diaphragm and intercostal muscles (Francisco, 2007).

Respiratory depression is generally manifested as a dose-dependent reduction in tidal volume and the slowing of the respiratory rate. This is primarily mediated through the central nervous system. However peripheral chemosensors are also thought to be involved (McDonald, 1981; Francisco, 2007; Chevillard *et al.* 2009). Chevillard *et al.*

(2009) discussed two central sites for opioid induced respiratory depression, the brainstem which integrates sensory signals and controls the switch between inspiration and expiration and the pre-Bötzinger complex which is located in the medulla and represents the active component of inspiration. The medulla determines the need to breathe through partial pressure levels of carbon dioxide (pCO₂) detected by chemosensors in the carotid arteries. An accumulation of pCO₂ will induce the medulla to stimulate the diaphragm and intercostals to breathe deeper, quicker and more rhythmically increasing oxygen intake (Francisco, 2007). Opioid exposure desensitises the medulla resulting in hypoventilation and hypoxemia, occurring 12-14 hours after methadone ingestion (Kreek, 1978; White & Irvine, 1999; Eilers & Schumacher, 2004; Lötsch *et al.* 2005).

The depressive properties of methadone are generally attributed to the (*R*)-enantiomer, however *S*-methadone may also be involved. Silverman *et al.* (2009) documented that in the neonatal guinea pig (*R*)-methadone caused significantly reduced respiratory depression compared with that of racemic methadone. This result suggests a synergistic role for (*S*)-methadone in opioid induced respiratory depression. It should however be cautioned that this result could reflect developmental changes in the neonate, with no influential role on respiratory function after maturation.

Animal models indicate that on a molecular level the mechanism responsible for opioid-induced respiratory depression involves μ -opioid receptor blockade of specialised respiratory neurons in the brainstem (Takeda *et al.* 2001; Lalley, 2003; Eilers & Schumacher, 2004; Mutolo *et al.* 2007). A study on the effects of fentanyl on the cat respiratory network documented that blockade of the dopamine D1 receptor increased the effects of μ -opioid receptor activation and as a consequence increased fentanyl induced respiratory depression in addition to lengthening the duration of action (Lalley, 2005). Therefore, cross talk between different neural modulatory

systems seemed likely to be an influencing factor in opioid induced respiratory depression.

The prevalence of opioid respiratory complications is high, an analysis of postoperative respiratory depression following opioid treatment revealed that out of 20, 000 patients, 17% (3,400) experienced depressive effects (Lötsch *et al.* 2005). Furthermore, earlier studies showed that chronic drug exposure like methadone maintenance treatment can cause respiration to remain depressed even after the development of drug tolerance (Santiago *et al.* 1977; Dyer *et al.* 1999). Because of methadone's long elimination half-life the effects of respiratory depression were observed for more than 24 hours after a dose has been administered (Maxwell *et al.* 2005). This potential for delayed toxicity sets methadone apart from other opioids, it stays in the body for increased periods of time causing plasma levels to rise quicker than realised in many cases (Wolff, 2002; Corkery *et al.* 2004). Interestingly, opioid-induced respiratory depression does not occur in subjects experiencing pain as the pain acts as a physiological antidote to the depressive effects of the administered drug. The mechanisms responsible for this remain obscure however this could simply reflect the lower drug levels required for sufficient analgesia compared with that required to induce respiratory depression (Francisco *et al.* 2007). Alternatively, this could reflect differences in cellular signalling. Kieffer *et al.* (2009) documented that for opioids it is likely that separate signalling pathways exist and the pathways leading to respiratory depression and drug addiction are different from those that inhibit pain.

1.4.3 Influence of drug-drug interactions

Polydrug use is an important factor in methadone-attributed deaths. Deaths involving methadone are more likely to occur when methadone is used in combination with

other drugs, particularly benzodiazepines and alcohol (Corkery *et al.* 2004; Shields *et al.* 2007; Poisnel *et al.* 2009). It has been well documented that the co-administration of methadone and benzodiazepines can result in lethal respiratory depression with benzodiazepines found in over 50 % of cases of death through overdose (Reynaud *et al.* 1998; Caplehorn & Drummer, 2002). This relationship may not be a result of pharmacokinetic interactions, as plasma drug concentrations following administration of methadone and benzodiazepines do not significantly differ from concentrations following the administration of either drug alone (Preston *et al.* 1986).

Methadone and alcohol in combination will also affect individual drug susceptibility. Donnelly *et al.* (1983) reported an enhanced CNS depressant effect when methadone and alcohol were administered together. Joseph & Appel, (1985) reported that alcohol dependence and alcohol related factors are a leading cause of death in methadone associated fatalities accounting for up to 60% of all mortalities. Co-administration of methadone and CNS depressants like alcohol can result in methadone concentrations below the fatal threshold inducing death. Worm *et al.* (1993) documented that in post-mortem cases where alcohol and methadone were identified together the concentration of methadone required to cause death (0.25 mg/L mean) was significantly lower than methadone alone (0.43 mg/L). As approximately 20-50% of patients in methadone maintenance programmes have alcohol related problems (Dobler-Mikola *et al.* 2005), this interaction requires further investigation.

Other drugs that have been linked with methadone toxicity include fluoxetine, rifampicin, and cocaine. Serotonin-selective re-uptake inhibitors (SSRIs) such as fluoxetine influence the activity of CYP3A4. Co-administration of SSRI agents with methadone will increase methadone serum levels resulting in toxicity and respiratory arrest (Davis & Walsh, 2001). Rifampicin is a CYP3A4 inducer prescribed to treat tuberculosis, a common condition in the AIDS population. The combination of

methadone and rifampin can result in opioid withdrawal as a consequence of CYP3A4 induction. Cocaine administration can lead to an up regulation of opioid receptors altering methadone's efficacy (Unterwald *et al.* 1992).

1.4.4 Drug Tolerance

Drug tolerance is where a subject's response to a drug decreases over time resulting in larger drug dose requirements in order to achieve the same effects and is a significant factor in methadone toxicity and death. Tolerance should not be confused with drug dependence (where a subject requires a drug in order to function normally) or drug addiction (the overpowering desire or need (compulsion) to continue taking a drug). A drug tolerant individual will experience less susceptibility to the effects of a drug as a consequence of its prior administration resulting in increased drug requirements (Shields *et al.*, 2007; Bayerer *et al.*, 2007). Acute tolerance develops in response to a single dose or following repeated doses over a very short period of time. Chronic tolerance is conferred over a longer period of exposure, eventually promoting a reduction in drug effects. Methadone maintenance leads to chronic drug tolerance with some individuals requiring significantly elevated drug doses. For example a fatal dose for an opioid naïve individual may be the same or lower than a daily dose for a methadone maintenance patient (Harding-Pink, 1993). Worm *et al.* (1993) examined 41 methadone fatalities from 1981 and 1989 reporting lower mean and median post-mortem blood methadone concentrations in opioid naïve individuals (median 0.22 mg/L; mean 0.27 mg/L) when compared with subjects who had been enrolled in maintenance programmes (median 0.43 mg/L; 0.47 mg/L).

On a cellular level drug tolerance has been linked with the desensitisation and internalisation of opioid receptors following chronic drug exposure (Koch *et al.* 1998). This reduces agonist response due to a decrease in the number of signalling receptors

(Koch *et al.* 2005). Receptor phosphorylation has been postulated as a key influential factor in acute receptor desensitisation. After desensitisation the recruitment of β -arrestins to the plasma membrane facilitates the uncoupling of the receptor from the G-protein causing internalisation (Ferguson *et al.* 1996). von Zastrow *et al.* (2003) suggested that internalisation acts to sort receptors into either a degradative pathway for destruction or to a recycling pathway returning the receptors back to the cell surface in an activated state. Contrary to this, some argued that receptor internalisation acts to reduce opioid-induced tolerance (Koch *et al.* 1998; Whistler & von Zastrow, 1999; Law *et al.* 2000; Grecksch *et al.* 2006). One theory is that rapid receptor internalisation is an important mechanism to ensure that desensitised receptors are recycled back to the cell surface in an activated state as quickly as possible (Koch *et al.* 1998). This will maintain receptor signalling thus reducing the development of drug tolerance (Zhang *et al.* 1998). A second theory suggests that receptor internalisation terminates signalling processes retarding the development of adaptive changes normally triggered by prolonged opioid exposure (Koch *et al.* 2008). Clearly the specific cellular mechanisms responsible for opioid induced tolerance remain controversial; however it seems probable that this is largely influenced by receptor signalling processes.

1.5 Toxicological interpretation of methadone cases

The toxicological interpretation of methadone-attributed deaths is a complex process complicated further by the acquisition of drug tolerance. Assessing tolerance in drug users is difficult requiring the complete documentation of an individual's drug history (Shields *et al.*, 2007). Tagliaro & De Battisti, (1999) commented on the difficulties faced with drug overdose cases when drug habits, tolerance acquisition and drug

history are unknown. Interpretation of toxicology results in such situations is limited. Another point for consideration is that drug concentrations identified in overdose cases are often significantly lower than those found in living and active users, suggesting a period of abstinence from drug use during the months prior to the fatal incident. Epidemiological data supported this by demonstrating higher incidence of overdose cases in subjects recently released from jail (Binswanger *et al.* 2007; Shields *et al.* 2007; Wakeman *et al.* 2009). The molecular mechanisms responsible for the acquisition and subsequent loss of tolerance are controversial and remain unclear (Figure 3).

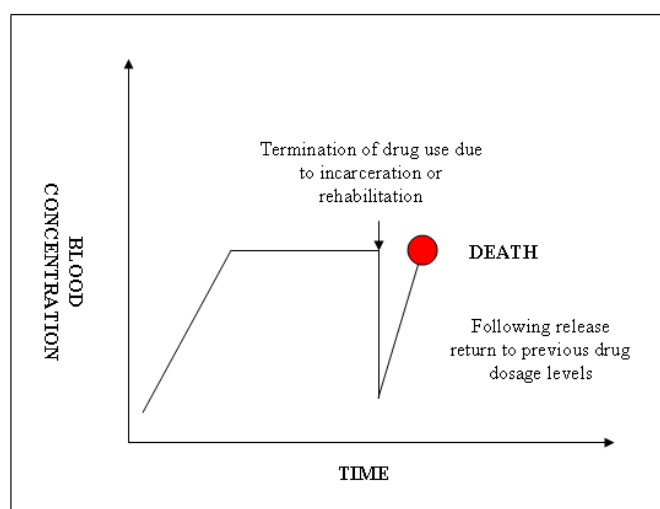


Figure 3: Loss of Tolerance Following Methadone Abstinence.

The loss of tolerance can result in fatalities if previous dosage concentrations are resumed following a period of abstinence.

1.5.1 Post-mortem redistribution

In post-mortem cases particularly where the body has been exhumed toxicological interpretation can be further affected by post-mortem change and redistribution, putrefaction, decomposition and the extent and location of tissues left for sampling

(Prouty & Anderson, 1990). Since methadone is a lipophilic drug with a high volume of distribution the likelihood of post-mortem redistribution is increased, thereby, affecting toxicological interpretation. Detection of a drug and its glucuronide metabolites is of great importance in interpretive forensic and clinical toxicology of a drug. The ability to estimate metabolite/drug ratios may provide information about methadone's route, dose and time of exposure (Kaushik *et al.*, 2006). However it is not possible to definitively identify whether the concentrations identified truly reflect the drug concentrations administered. Drug concentrations in the blood of corpses are often site-dependent following post-mortem redistribution and diffusion (Pounder & Jones, 1990; Cook *et al.* 2000; Kennedy, 2010). Even in femoral venous blood, which is generally believed to be spared post-mortem factors, and in corpses with little putrefaction, drug concentration can change greatly within hours following death (Moriya & Hashimoto, 1999; Ferner, 2008; Butzbach, 2010; Kennedy, 2010).

1.5.2 Individual differences in drug metabolism

In addition to post-mortem redistribution and drug tolerance complicating toxicological interpretation, inter-individual differences in drug metabolism can affect blood methadone concentrations post-mortem. This can be examined through gene analysis of the enzymes responsible for methadone metabolism. The science of attributing genome variations to alterations in drug metabolism and response is termed pharmacogenomics.

1.6 Pharmacogenomics

Pharmacogenetics focuses on individual traits with respect to one compound or drug, and pharmacogenomics focuses on the differences between several compounds and

whole genome responses through the examination of drug modifications on gene expression (White & Wong, 2005). One of the key principles of pharmacogenomics is that the correct drug dose for one individual may not be an appropriate dose or even the most suitable drug for another, due to differences in each individual's genetic makeup. The determination of what is the appropriate dose and, in some cases, what is even the best drug for a given individual constitutes the reasons for the development of the sciences of pharmacogenetics and pharmacogenomics (White & Wong, 2005). In both forensic and clinical practice inter-individual variation in drug response are frequently identified, however the precise mechanisms responsible remain unclear. Clarity may be achieved through the examination of molecular processes in tandem with the continuing advancement of genome research.

Routine application of pharmacogenetics and pharmacogenomics is still in its infancy, however the concept has been in existence for thousands of years, stretching as far back as 510 B.C. when Pythagoras noted that the ingestion of fava beans resulted in a potentially fatal reaction in some, but not all, individuals (Nerbert, 1999). Wider recognition of inter-individual drug sensitivity has since developed. Multiple definitions for pharmacogenetics and pharmacogenomics can be found within the contemporary literatures (Pirmohamed, 2001; Kupiec *et al.* 2006; Catania, 2006). Pirmohamed, (2001) described pharmacogenetics as the study of variability in drug response due to heredity, applicable to genes determining drug metabolism whilst pharmacogenomics encompasses all genes in the genome that may determine drug response. Kupiec *et al.* (2006) stated that pharmacogenetics defines the spectrum of inherited differences in drug metabolism and disposition, whereas pharmacogenomics refers to all the genes that determine drug behaviour and sensitivity. Multiple definitions can be confusing as the distinction between the two is somewhat tenuous,

and the terms are often used interchangeably (Vesell, 2000; Kupiec *et al.* 2006).

Therefore, care must be taken when reviewing this subject area.

For the purpose of this review the following definition for pharmacogenomics will be used, to clarify the molecular actions of methadone with clarity:

pharmacogenomics combines the study of two scientific fields 'pharmacology and genomics' and can be defined as the study of how genetic variation between individuals (genomics) influences drug response and susceptibility to adverse drug reactions (pharmacology) (Catania, 2006).

1.6.1 Toxicological interpretation and pharmacogenomics

Following the publication of the draft sequence of the human genome project in 2001, research examining the association between individual genetic variability and susceptibility to disease, clinical symptoms or treatment responses has increased exponentially heralding a new era in genomics (Skorpen & Laugsand, 2008; Bhatena & Spear, 2008; Harkcom & Abbott, 2010; Savas, 2010). A key topic in innumerable science reports, medical reviews and articles in the lay press, the process of linking basic inheritance to drug discoveries and therapeutics is progressing. The concept that an individual's DNA sequence could be an integral determinant of drug therapy has not yet become a standard notion of clinical medicine, however it is now certainly more than a mere consideration (Giacomini *et al.* 2007).

Clinical discoveries can in turn be utilised to advance scientific progresses within the forensic field particularly with regards to the interpretation of toxicological data. Research conducted by Wong *et al.* (2003) demonstrates that pharmacogenomic studies can be used to identify gene variations for molecular autopsy aiding the interpretation of toxicology results (Wong *et al.* 2003). Current advancements in molecular technologies (such as real-time PCR and DNA chip technology) will situate

pharmacogenomic testing alongside the traditional immunodiagnostics and analytical toxicological tests used currently to correlate *in vivo* drug levels with specific responses.

Toxicological interpretation of biological fluids from either antemortem or postmortem samples is complex. Linking a specific reaction or behaviour to a drug concentration is hindered by many factors including inter-individual differences, development of tolerance, and ambient environment. As discussed previously, this is complicated further in post-mortem samples due to post-mortem redistribution, tissue degradation and the lack of antemortem samples as a means of comparison. Wong *et al.* (2003) proposed that pharmacogenomics may greatly aid in the interpretation of drug toxicity. Pharmaceutical agents are frequently associated with adverse drug responses, and can often be linked with significant morbidity and mortality as discussed in *Section 1.4 Methadone –Related Deaths*. A significant proportion of pharmacogenomic research is clinical and extrapolation from clinical to forensic research may assist in predicting individual susceptibility to methadone in addition to aiding the interpretation of toxicology results in methadone-attributed fatalities.

Clinical research demonstrates that variations in single genes can be linked with unpredictability in the response to drug use. As such single genes are a significant area to concentrate on for the progression of forensic pharmacogenomics, establishing the cause and manner of death can be extremely challenging, especially in unidentified causes of death. Diagnosis of drug toxicity should be made in conjunction with autopsy findings, medical history and gene analysis. Cognizance of variables likely to affect pharmacokinetic and pharmacodynamic parameters would assist with this (Kupiec *et al.* 2006; Weschules *et al.* 2008; Phillips & Mallal, 2010). Genes involved in pharmacokinetic (genes controlling drug metabolism and drug

transport) and pharmacodynamic pathways (genes linked with disease susceptibility or drug targets) should therefore aid toxicological interpretation.

Drug metabolism is a critical component of the final clinical effect of a drug and as such, genes that influence drug pharmacokinetics have become the focus of extensive research. It has been well documented that the genes encoding metabolising enzymes are highly polymorphic (Guttmacher & Collins, 2003; Bhathena & Spear, 2008; Eckhart *et al.* 2009). Alterations to the function of a cytochrome P450 (CYP) enzyme would significantly affect drug efficacy, accounting for inter-individual variations. An individual phenotyped as a poor metaboliser would be expected to exhibit slower drug metabolism resulting in drug accumulation which could lead to drug toxicity (Kupiec *et al.* 2006). Similarly an alteration to the function of a transporter responsible for conveying drugs across the blood brain barrier would have a profound effect on the expected drug response.

Pharmacodynamic pathways are another significant route in which to direct research. It has become increasingly clear over the years that drug receptors are highly polymorphic. It is logical therefore to propose that polymorphisms located in these regions may underlie the target of treatment resistance and super-responders (Kerwin, 1999). The interpretation of post-mortem drug concentrations should therefore be guided by with knowledge of possible pharmacogenomic influences on drug metabolism and drug response. The introduction of alterations at the molecular level can result in significant changes with regards to drug processing and response.

1.6.2 Pharmacogenomic influences on methadone metabolism

Methadone is primarily metabolised in the liver, where it undergoes N-demethylation by CYP3A4 and CYP2B6 (with a minor contribution from CYP2D6) forming the metabolites 2-ethylidene-1, 5-dimethyl-3, 3-diphenylpyrrolidine (EDDP) and 2-ethyl-

5-methyl-3, 3-diphenyl-1-pyrrolidine (EMDP) (Sullivan & Due, 1973; Eap *et al.* 2007). As discussed earlier these enzymes are critical for drug metabolism and the correlation between CYP variations and drug response has been well published for many classes of drugs (de Vos *et al.* 2010; Roberts *et al.* 2005; Lee *et al.* 2010; Suzuki *et al.* 2010). The human genome has 57 different CYP genes (most of which are polymorphic). Only four (*CYP2A6*, *CYP2C9*, *CYP2C19*, and *CYP2D6*) were considered to have “real pharmacogenomic relevance” (Vesell, 2000), however since then a number of pharmacogenomic studies have focused on other CYP genes (Bergmann *et al.* 2010; Li *et al.* 2010; Sagrieya *et al.* 2010; Wang *et al.* 2010)

CYP2D6 has been associated with alterations to drug metabolism. Eap *et al.* (2001) examined the impact of *CYP2D6* on drug metabolism, establishing three metaboliser groupings: poor metaboliser (having a non-functional gene), extensive metaboliser (possessing one or two functional genes) and ultra-rapid metaboliser (having three or more functional genes), supporting the concept of pharmacogenomic relevance. Wong *et al.* (2003) examined whether methadone fatalities could be attributed to *CYP2D6* mutations. The group reviewed case histories for methadone associated deaths from the Milwaukee County Medical Examiner’s Office between 1998 and 2000, using real-time PCR to genotype for *CYP2D6* variations. The genotyping data suggested that *CYP2D6**3(2549 deleted A), *4(C100T, C974A, A984G, & G4180C), and *5 (*CYP2D6* deletion) alleles may assist in molecular autopsy potentially aiding death certification. However the results from this study were not statistically significant and it was noted that further works with larger sample sizes are essential to truly identify a role for *CYP2D6* screening (Wong *et al.* 2003). In addition, the significance of such work is limited, as *CYP2D6* only has a minor role in methadone metabolism.

For pharmacogenomic studies on methadone it would be logical to concentrate on the primary metabolising enzyme *CYP3A4* and *CYP2B6*. However due to a significant lack of literary information on methadone metabolism especially for *CYP3A4*, the toxicity of other substrates in relation to variations of *CYP3A4* may be extrapolated to that of methadone, in order to bridge the knowledge gaps at the molecular level. Today increasing advancements in molecular studies have allowed a number of *CYP3A4* variants to be identified. As *CYP3A4* gene expression levels are often reported to have considerable inter individual variations (40-fold), it is logical to postulate that some of the variability identified in drug metabolism could be explained by these variations (Dai *et al.* 2001; Plant, 2007). Rebbeck *et al.* (1998) reported the discovery of a SNP in the 5' regulatory region of *CYP3A4* when examining the relevance of the gene in prostate cancer. They reported that the A290G (*CYP3A4*1B* allele) polymorphism is located in a transcriptional regulatory element and as a consequence may be responsible for alterations in gene expression. Westlind *et al.* (2001) sequenced the gene promoter and 5' regulatory region of *CYP3A4* in a group of Swedish individuals. The gene promoter region was highly conserved with no other variations identified, it was also concluded that the A290G SNP did not significantly affect the catalytic activity of *CYP3A4*. Dai *et al.* (2001) also examined *CYP3A4* molecular relevance by screening for polymorphisms in 72 individuals from three ethnic groups (Caucasians, African-Americans, and Asians (Taiwanese, Chinese, Melanesian, Indo-Pakistani, Cambodian, and Japanese)) identifying 28 SNPs in total, four of which were novel non synonymous polymorphisms leading to changes of R162Q, F189S, L293P, and P467S. L293P (2% frequency) and P467S (12.5% frequency) were only identified in Asians, where as R162Q only occurred in African-Americans, implicating ethnic relevance in the SNP distributions. Testosterone and the insecticide Chlopyrifos were used to test the effects of the mutations on

metabolism. The F189S allele attributed significantly lower enzyme activity for both substrates whilst L293P increased enzyme activity, this evidenced that the *CYP3A4* variation could be responsible for inter-individual differences in substrate metabolism (Dai *et al.* 2001).

Despite these studies the biological significance of the variants remains questionable and it is clear further work is required. The reported variability in metabolism is likely to be due to the inducibility and inhibition of *CYP3A4* by other drugs (Table 1). Therefore, drug-drug interactions must be taken into account when conducting pharmacogenomic studies to ensure that any relationships identified are truly representative of gene variants and are not otherwise hidden consequences of co-mediations.

CYP2B6 has been studied more frequently and several *CYP2B6* SNPs have been correlated with enzyme efficiency or gene expression levels. Lang *et al.* (2001) screened 35 Caucasian individuals for *CYP2B6* variations. Nine SNPs were identified, five of which were non-synonymous. The C1459T variant was of particular interest, since it causes an amino acid change from arginine to cysteine at position 487. Individuals homozygous for the 'T' allele demonstrated an 8 fold decrease in enzymatic activity compared to wild type individuals. However 'T' allele frequency (14%) within this population could not explain the total extent of metabolism variability identified for this gene. Lamba *et al.* (2003) examined the relationship between *CYP2B6* expression and the transcription factor constitutive androstane receptor (CAR) expression, noting the effects of SNPs located in exonic, intronic and 5' flanking regions on overall gene expression in Caucasian, African and Hispanic American populations. Alternative splicing by resequencing mRNA from liver samples was conducted using TaqMan® fluorescent probes. Sequencing information for both forward and reverse primers was examined noting the presence of base

substitutions. In agreement with Lang *et al.* (2001), the C1459T SNP was associated with a decrease in expression; however this relationship was only identified in females. Another gender trend SNP is located in intron 3 (C15582T). The promoter region (T2320C) also correlated with expression differences in female subjects. Higher mRNA levels of the transcription factor CAR were observed in female subjects, which could perhaps explain the observed gender differences by Lamba *et al.* (2003). The study identified several splicing transcripts, SV1 (the main splice variant, SV) was found in many of the samples examined. This SV lacks sequencing information for exons, 4, 5 and 6. Furthermore, SNPs in exon 4 (G516T) and intron 3 were found to correlate with SV1 presence. Despite positive associations between SNP presence and *CYP2B6* expression Lamba *et al.* (2003) concluded that the identification of functionally important *CYP2B6* genotypes was complicated. Many of the SNPs analysed were found to be in linkage disequilibrium (the non-random association of SNPs at two or more loci but not necessarily on the same chromosome) and therefore associated with different haplotypes. The importance of gender and ethnic difference was noted with the suggestion that future studies should not be limited by focusing on markers of *CYP2B6* phenotype but should instead examine which variants are associated with gender and ethnic differences (Lamba *et al.* 2003). Hoffman *et al.* (2008) examined the relevance of the *CYP2B6**6 allele (G516T and A785G SNP) by constructing *CYP2B6* minigenes and transfecting them into COS-1 and Huh7 cells. *CYP2B6* genotyping was also conducted on a number of liver samples, with the aim of identifying the molecular mechanism responsible for *CYP2B6**6 decreased protein expression and as a consequence protein activity (slow metaboliser phenotype). The study reported the exon 4 SNP (G516T) as being the causal mutation linked to gene function reduction, additionally this mutation was responsible for aberrant splicing resulting in a major splice variant lacking exons 4, 6 and the intronic

regions between. This resulted in the reduction of mRNA transcript length, and total enzyme activity (Hoffman *et al.* 2008). The group also examined the effects of the promoter region SNP (T750C) on expression levels as this SNP is found in tandem with the *CYP2B6**6 allele (Hesse *et al.* 2004). No significant relationship was identified despite a large sample size (235 samples) leading the group to have assumed that the T750C promoter mutation has little effect on transcription. Contrary to Lamba *et al.* (2003) the group were not able to establish a relationship between C15582T (intron 3), hepatic phenotype, and the splice variant SV1. The RT-PCR data did however reveal a significant relationship between the *CYP2B6**1/*1 genotype and the *CYP2B6**6/*6 genotype. For the *1/*1 (T2320C) samples the major transcript detected was the “normal” splice product, for the *6/*6 samples the SV1 transcript was identified. Hoffman *et al.* (2008) concluded that the G516T mutation can be recognised as a causal indicator of expression variability, for predicting inter-individual sensitivity in drug response. The above examples are not specific to methadone, however we postulate that the results from these studies can be used to create a strategy for examining *CYP2B6* effects on methadone metabolism. Further work focusing on methadone metabolism is required to determine the contribution of the *CYP2B6**6 allele for drug metabolism and adverse drug responses.

Methadone stereoselectivity has been associated with many genes including *CYP2D6*, *CYP2B6*, *ABCB1*, *KCNH2* (hERG) (Gerber *et al.* 2004; Wang *et al.* 2004; Crettol *et al.* 2005; Crettol *et al.* 2006; Eap *et al.* 2007). The stereoselective relationship identified between *CYP2B6* and methadone’s enantiomers is of particular interest (Figure 2). Preferential targeting of the (*R*)-enantiomer by *CYP2B6* had been widely demonstrated (Bertschy *et al.* 1994; Eap *et al.* 1997). In addition Gerber *et al.* (2004) identified a stereoselective relationship between *CYP2B6* and (*S*)-methadone, with significantly higher (*S*)-methadone metabolism compared to (*R*)-methadone. The

group also documented that the steady state of (*R*)/(*S*) methadone concentrations in plasma can be controlled by the relative expression of *CYP2B6*. Therefore changes in *CYP2B6* expression could result in greater effects in one enantiomer ((*S*)-methadone) than the other ((*R*)-methadone), complicating the interpretation of toxicology results. Eap *et al.* (2007) examined *CYP2B6* and hERG (human *ether-a-gogo* related gene) stereoselectivity. As discussed previously the human heart is mediated by voltage-gated potassium channels, one of which is the hERG channel. It is known that a number of drugs including methadone can block hERG resulting in malignant ventricular arrhythmias (“torsades de pointes”) and sudden death (Katchman *et al.* 2002; Kornick *et al.* 2003). Using genotyping assays and whole-cell patch-clamp experiments with HEK293 cells Eap *et al.* (2007) identified a stereoselective relationship between (*S*)-methadone and the hERG channel, with (*S*)-methadone reducing I_{hERG} by ~ 65% compared to (*R*)-methadone which reduced I_{hERG} by ~ 40%. Furthermore, the group noted a correlation between the *CYP2B6* *6 genotype (slow metaboliser) and increases in (*S*)-methadone plasma concentrations supporting the relationship identified by Gerber *et al.* (2004). This study suggested a cardiotoxic role for (*S*)-methadone particularly in individuals with the *CYP2B6**6 genotype where (*S*)-methadone concentration levels will be significantly higher than wild type individuals. It should be considered however that this conclusion was based on *in vitro* data, and may not be a true representation of the complexity of the *in vivo* system. Furthermore, Kienbaum *et al.* (2002) noted a relationship between chronic μ receptor stimulation by methadone and the subsequent depression of muscle sympathetic activity in the heart, demonstrating the potential importance of opioid agonists to cardiac response. Nonetheless this is certainly an important aspect that requires further investigation, especially when it is taken into account that *CYP2B6* is expressed in the human heart (Park, 2000).

The importance of studies focused on *CYP2B6* is directly proportional to the increasing incidence of methadone-attributed deaths. Rising occurrences of cardiotoxicity and respiratory depression highlight the significance of methadone pharmacogenomic research, especially when the current data deficiency is considered (Corkery *et al.* 2004; Pimentel & Mayo, 2008). Concentrating pharmacogenomic studies in this area will advance toxicological interpretation and assist in the development of screening methods to identify methadone susceptible individuals.

1.6.3 Pharmacogenomic influences on methadone-receptor binding and response

The μ opioid receptor represents the principle molecular target for methadone binding *in vivo*, with reported K_i values of 3.7 ± 0.3 (nM) (Mestek *et al.* 1995; Wendel & Hoehe, 1998). Despite frequent usage and increasingly reported adverse effects, the studies focusing on methadone actions and *OPRM1* variability has been significantly less than that on morphine. This perhaps reflects the importance of morphine within the clinical environment where most of the studies discussed so far have been conducted. Additionally, the studies that have considered methadone from a pharmacogenomic perspective have done so from a drug metabolism perspective. Only one study examining the relationship between methadone and *OPRM1* variability was found during this study and it was conducted in conjunction with drug metabolism and transport genes. Löttsch *et al.* (2006) examined the effects of levomethadone (r-methadone) on drug response using miosis as an indicator. The group selected not only the genes critical to methadone metabolism and transport namely, *CYP2B6*, *2D6*, *3A*, *1A2*, *2C8*, *2C9*, and *2C19*, p-glycoprotein *ABCB1*, but also the receptor gene *OPRM1*. Of the genes studied the *OPRM1* A118G polymorphism was considered to be the most important factor affecting drug response. Individuals with the 118G allele demonstrated a 1.74 times lower miotic potency

compared to wild type subjects. Despite this association no further work had been conducted since. Contrastingly, studies on *OPRM1* sequence structure, heroin addiction and morphine variability have been extensive. Therefore these studies will be discussed to predict the potential role of *OPRM1* in methadone toxicity.

Wendel & Hoehe, (1996) examined the 5' regulatory and intronic sequence information for *OPRM1* to identify potential transcription sites. The group noted a 40% homology between the human *OPRM1* 5' regulatory region and the rat *OPRM1* gene suggesting that this is a homologous region between species (Mestek *et al.* 1995). The absence of classical TATA and CCAAT regions was interesting since it is usually the "housekeeping" genes that lack these regions for the constitutive expression requirements. Tissue specific expression of *OPRM1* gene might be another explanation. Wendel & Hoehe, (1998) identified 2408 base pairs (bp) of the 5' regulatory region and discovered transcription initiation sites in addition to potential binding sites for transcription regulators. This was a significant contribution to molecular research and extended the known *OPRM1* sequence information to a total of 6968 bp (Wendel & Hoehe, 1998). Such sequence analyses have provided the necessary foundations required for the progression of pharmacogenomic research, assisting in the development of drug – gene orientated studies.

Initially studies on *OPRM1* explored basic drug dependence and addiction, later progressing into genotyping and expression studies. For example Tsuang *et al.* (1998) surveyed drug dependence, examining the probability of drug abuse in 3372 twin males. The Diagnostic Interview Schedule, revision 3 (DIS-III-R) was used to assess abuse and dependence, correlating phenotype (drug use) with the probability of dependence, monitoring gene differences between siblings (Tsuang *et al.* 1998). The group noted that heroin abuse revealed the largest amount of unique genetic variance (38 %) suggesting a key area for pharmacogenomic research. Bond *et al.* (1998) also

examined drug abuse and dependence association however this group applied a molecular examination of *OPRM1* as opposed to the model approach used by Tsuang *et al.* (1998). The study characterised *OPRM1* SNPs in former and current heroin addicts, examining their influence on receptor function. The group studied the *OPRM1* coding regions and identified the following gene variants A118G, C17T, G24A, G779A and G942A, of these only A118G and C17T had previously been identified by Berrettini *et al.* (1997) and Bergen *et al.* (1997). Allele frequencies for African-American, Caucasian and Hispanic ethnic groupings were statistically significant for both A118G (P value of 0.028) and C17T (P value of 0.000002) (Bond *et al.* 1998). Additionally within the Hispanic group it was noted that the 118G allele was present in a higher proportion of non-opioid dependent subjects, although this result was not significant. The group stated that this could be a possible artefact of population admixture, with 118G conferring protection against opioid dependence in a larger sample size (Bond *et al.* 1998). Bond *et al.* (1998) also examined binding affinity in response to A118G by introducing mutant receptors into AV-12 cells and conducting radioligand binding assays. Located in the N-terminal region of the receptor N40D is postulated to induce the loss of a potential glycosylation site (Lötsch & Geisslinger, 2005), resulting in protein modifications (Befort *et al.* 2001). A substantial difference in β -endorphin binding (approximately three fold) was noted between wild type and variant receptors. This was not reciprocated for morphine, methadone, and fentanyl binding, which was not unexpected as a single amino substitution in the N-terminal region is unlikely to affect the tertiary structure of the receptor (Bond *et al.* 1998).

Befort *et al.* (2001) also examined *OPRM1*, screening for genetic variations that could be linked with inter-individual differences in opiate response, and opioid-associated pathophysiology. Similarly to Bond *et al.* (1998), Befort *et al.* (2001)

examined the effects of *OPRM1* mutants (N40D, N152D, R265H, and S268P) on receptor functionality through site directed mutagenesis and transfection of the COS cells. Binding affinity profiles for morphine, [D-Ala², N-MePhe⁴, Gly-ol]-enkephalin (DAMGO), diprenorphine, [D-Phe-Cys-Tyr-Orn-Thr-Pen-Thr-NH₂] CTOP, [Met]enkephalin, β -endorphin, and dynorphin A were analysed for each of the variants. At the amino acid level the A118G DNA polymorphism is N40D, and induces an amino acid change from asparagine to aspartic acid, with an allelic frequency of 10-20%. No significant difference between N40D and wild type receptor densities was observed. N152D and R265H both represent rare mutations with N152D being described for the first time in this study. The relevance of these mutations to opioid pharmacogenomics is therefore limited. S268P was also rare, identified in only 1 subject out of a total of 250 Caucasian subjects. The group however noted that S268P significantly impaired receptor signalling and it was postulated that this represented a functional change in receptor conformation by the proline residue by disrupting the tertiary loop structure, compromising G protein coupling (Koch *et al.* 1997; Befort *et al.* 2001). It was concluded that the degree of receptor signalling impairment warranted further investigation in larger sample groups.

Lötsch *et al.* (2002) studied the effects of the A118G polymorphism on morphine-6-glucuronide toxicity (M6G). The morphine metabolite M6G has a binding affinity similar to that of its parent, a higher analgesic potency and has been reported to accumulate in tissues resulting in drug toxicity (Ashby *et al.* 1997). Therefore gene variations likely to affect this metabolite *in vivo* are of critical importance. Two clinical case studies (patients experiencing unwanted clinical effects) were used to determine the effects of A118G on M6G response. The group noted a decreased M6G potency in carriers of the 118G allele, leading to the hypothesis that A118G confers protection against M6G toxicity (Lötsch *et al.* 2002).

Despite the positive association demonstrated in this study the sample size was too small for this result to be representative of a population trend. Klepstad *et al.* (2004) continued to work in this area noting a correlation between 118G and increased morphine requirements. The study also examined the response to morphine by several other *OPRM1* SNPs (G1727, A118G, IVS2 + G31A, and IVS2 + G691C) located in both exonic and intronic domains. A total of 207 palliative care patients receiving chronic morphine treatment were genotyped and it was noted that subjects homozygous for 118G required significantly more morphine than heterozygous and wild type individuals (Klepstad *et al.* 2004). Combining the works of Löttsch *et al.* (2002) the 118G reflected inter-individual differences in M6G efficacy. However the relevance of such results was limited by a small sample size with only four subjects found to be 118G homozygous. Romberg *et al.* (2005) searched for a link between A118G and respiratory depression, with the hypothesis of Löttsch *et al.* (2002) that this mutation conferred some protection against M6G induced respiratory depression. However, Romberg *et al.* (2005) did not find a significant relationship between A118G and respiratory depression. An association was however noticed between A118G and a reduction in analgesic efficiency. The relevance of such results is somewhat contentious as the study sampled only 16 individuals with no 118G homozygous individuals identified. In comparison Löttsch *et al.* (2002) examined 207 subjects finding 4 individuals homozygous for 118G, and yet this was considered to be a limiting sample size. Therefore the study conducted by Romberg *et al.* (2005) was severely hindered by sample size.

Bart *et al.* (2004) re-examined the A118G variant from a different perspective searching for a link between this SNP and drug addiction in a cohort of Swedish heroin addicts. A118G distribution was found to be in Hardy-Weinberg equilibrium for all of the subgroups with an allelic frequency of 11%. The group discovered a

significant odds ratio between the 118G allele and increased heroin addiction, with the results indicating a 21% risk of heroin addiction mediated by the 118G allele, contrasting with the works of Bond *et al.* (1998). The group also examined A118G relevance in drug addiction and alcohol dependence (Bart *et al.*, 2005).

Zhang *et al.* (2005) conducted a study to elucidate the contribution of A118G to allelic-specific expression. Genomic DNA and total RNA were extracted from post-mortem brain tissue samples to measure allelic imbalance in mRNA expression. The study documented a significant difference in mRNA expression in brain tissues and transfected cells as a result of the A118G polymorphism. Allele-specific expression analysis demonstrated a 2-fold increase in the expression of 118 AA (wild-type) compared with 118 AG heterozygous individuals, potentially explained by the existence of a *cis*-acting factor (Zhang *et al.* 2005). 118 AA yielded 10-fold more binding sites than 118 AG. It was postulated that 118G substitutions may affect translation, post translational processing, or *OPRM1* protein turnover and further work was required to definitively identify the contribution of A118G for opioid response. As yet the role of A118G in translation and post translational processing remains undetermined.

Ross *et al.* (2005) conducted a similar study to that of Lötsch *et al.* (2002) and Klepstad *et al.* (2004) focusing on patients who demonstrated morphine intolerance. Two groups were assigned, the first group comprised 138 people as controls that had been using morphine for over a month with clinical benefit, and the second group consisted of 48 switchers that had not achieved analgesic control instead experiencing intolerable side effects. Four genes pertinent to morphine action *in vivo* were examined by the group. They were *UGT2B7*, *OPRM1*, *βarrestin2*, and *stat6*. Since the *βarrestin2* gene was involved in the signalling process for μ receptor desensitisation (Bohn *et al.* 2002) it was also included to the study. The transcription factor *stat6* is

known to be involved in *OPRM1* expression (Kraus *et al.* 2001). Ross *et al.* (2005) were the first group for the identification of a significant correlation between *βarrestin2* and analgesic response in humans. There was a higher prevalence of T8622C in subjects unresponsive to morphine treatment, indicating that T8622C may be a susceptibility polymorphism. This variation is a synonymous SNP (located in exon 11) so such a functional response was unexpected. However, it was postulated that T8622C could be acting in combination with a non synonymous SNP within the *OPRM1* gene. In disagreement with Lötsch *et al.* (2002), no significant relationship between morphine response and the A118G SNP was identified by Ross *et al.* (2005). Indicating that A118G contribution to drug response is highly controversial. For five of the studies described here A118G had associated with addiction, increased morphine requirements, *OPRM1* expression modifications and protection from M6G toxicity (Lötsch *et al.* 2002; Klepstad *et al.* 2004; Zhang *et al.* 2005). However, it had also been reported that *OPRM1* receptor densities as a result of A118G were not significantly different in subjects unresponsive to morphine treatment (Befort *et al.* 2001; Ross *et al.* 2005).

In the same year however Ide *et al.* (2005) moved away from the A118G variant focusing instead on the 3' untranslated region of the *OPRM1* gene. In humans more than 50 polymorphisms have been discovered within the 3' downstream region, and Ide *et al.* (2005) noted that many of these are in significant linkage disequilibrium, effectively making it possible to group humans according to their polymorphic patterns. The group continued to examine *OPRM1* for an association between gene polymorphisms and methamphetamine dependence and psychosis in 2006 (Ide *et al.* 2006). However no significant link could be established between A118G and methamphetamine dependence, contrastingly a significant association between the 1VS2 + G691C SNP in intron 2 and methamphetamine dependence was noted by the

group (Ide *et al.* 2006). Further research on polymorphisms located in intronic and the 3' untranslated region of the *OPRM1* gene is required.

Similarly to the work of Zhang *et al.* (2005) Bayerer *et al.* (2005) examined the effects of *cis*-acting elements on *OPRM1* promoter activity. *Cis*-acting elements are involved with transcription factor binding and gene promoter activity. The *OPRM1* promoter region possesses binding sites for a host of *cis* acting elements NFkB, STAT6, SP1, AP1, GRE and CRE, and variations close to or within the site for one of these elements were postulated to alter promoter activity (Wendel & Hoehe, 1998; Kraus *et al.* 2001, 2003). Bayerer *et al.* (2005) used *in vitro* mutagenesis to examine the effects of 8 promoter mutations at positions -172, -236, -554, -995, -1045, -1320, -1699, and -1748 on gene expression regulation using the luciferase assay. In addition to this *in vitro* work the group also genotyped 700 Caucasian individuals for -554 and -1320 to characterise variation presence within the population. The G554A polymorphism was found to exist within a *cis*-acting element significantly reducing promoter activity. The polymorphism was not however identified within the Caucasian population genotyped. The A1320G variant also showed a significant change in promoter activity, however it is not known whether this polymorphism is located in, or near, a transcription factor binding site. The genotyping results showed one individual to be homozygous for 1320G with another individual demonstrating heterozygosity. The group concluded that out of the eight SNPs studied, two (G554A & A1320G) are likely to affect transcriptional regulation and therefore the *OPRM1* expression. Individuals with these mutations may therefore react differently to opioid administration (Bayerer *et al.* 2005).

Reyes-Gibby *et al.* (2007) continued with the work started by Lötsch *et al.* (2002) and Klepstad *et al.* (2004) by examining the effect of genetic variability on morphine efficacy. The data used was from the study conducted by Klepstad *et al.*

(2004) with genotyping information recorded for a total of 207 patients undergoing morphine therapy for cancer pain. Reyes-Gibby *et al.* (2007) explored the joint effects of *OPRM1* and *COMT* (catechol-*O*-methyl transferase) variations on morphine response. *COMT* is responsible for metabolising the catecholamines including, dopamine, epinephrine and norepinephrine and is known to display wide variations in enzymatic activity that could be underlined by the Val158Met functional polymorphism (Klepstad *et al.* 2005). This particular variation can alter enzymatic activity by up to four-fold difference (Montagna, 2007). Additionally when Rakvag *et al.* (2005) studied this variation in a group of cancer patients being treated with morphine it was noticed that patients homozygous for valine at 58 required higher doses of morphine compared to heterozygous and homozygous methionine. Reyes-Gibby *et al.* (2007) demonstrated a key relationship between *OPRM1* and *COMT* with regards to morphine efficacy noting that patients homozygous for Met/Met (or AA genotype) at 58 in the *COMT* gene and *OPRM1* respectively required lower morphine doses for optimal analgesia (Reyes-Gibby *et al.* 2007). This finding demonstrates the importance of gene-gene interactions as the nature of pharmacogenomic research heralds a new dimension in the studies of genetic linked analgesia.

More recently Yamamoto *et al.* (2008) examined the relationship between *OPRM1* expression and bone cancer pain. The group used a murine model to examine the effects of chronic morphine exposure on *OPRM1* expression and distribution in response to bone cancer pain, revealing that differences in morphine sensitivity correlated with changes in *OPRM1* expression. Additionally reductions in *OPRM1* expression correlated with the sarcoma-implanted mice (Befort *et al.* 2001; Zhang *et al.* 2005; Bayerer *et al.* 2005). SNPs affecting gene expression are therefore critical to the final clinical effect of a drug such as morphine.

In viewing all the research on *OPRM1* to date, it is clear that further examination of A118G relevance to morphine and other illicit drugs is necessary, especially from a forensic context. Additionally joint-effects such as the relationship between *OPRM1* and *COMT* highlighted by Reyes-Gibby *et al.* (2007) may be important.

1.7 Summary

The aim of this review was to explore methadone pharmacogenomics identifying how this information can be used to advance toxicological interpretation. Of the studies reviewed here, only one was conducted from a forensic perspective demonstrating the need for progression in this field. Wong *et al.* 2003 have begun to explore pharmacogenomic relevance for forensic toxicology however there is still much more work required. Areas that required future research have been identified, namely the association between *CYP2B6* and *OPRM1* variations for methadone action and this study will explore this further. Existing knowledge on methadone-related overdoses is mostly based on quantitative data collected retrospectively from coroners' records and drug death statistics (Shields *et al.* 2007). Whilst reports of this nature provide crucial insights into the incidence of methadone-attributed fatalities, the research is less amenable to exploring how, why, and in which situations individual drug users die because of consuming methadone (Shields *et al.* 2007).

Studies on methadone pharmacogenomics have mainly concentrated on metabolising enzymes instead of exploring the role of opioid receptor variations for methadone. The role of the A118G variant for methadone action remains unclear and requires clarification. Studies that have examined the impacts of *CYP2B6* metaboliser status have done so in living subjects. The role of *CYP2B6* in methadone

susceptibility needs to be determined and this can be achieved by examining SNP prevalence in methadone-attributed deaths. This would identify target variations that can be used as molecular autopsy to aid toxicological interpretations. This will benefit many aspects of forensic casework, for example, individuals driving under the influence of drugs (DUID) or for the interpretation of post-mortem drug concentrations. It is hoped that screening protocols for methadone maintenance users could be implemented as a risk management tool to identify susceptible individuals prior to treatment.

CHAPTER 2
METHODOLOGY

2.1 Method Optimisation

2.1.1 DNA Collection and Extraction

2.1.1.1 DNA extraction from buccal swabs

Genomic DNA was collected by rubbing each of the three swabs against the buccal (cheek) surface of six different subjects. Following collection the DNA was extracted in 220 μ l of MasterAmp™ buccal extraction fluid (Epicentre Biotechnologies, USA) following the manufacturers protocol. Each of the swabs were thoroughly submerged and mixed with the extraction fluid to remove the DNA from the swab to the fluid. The samples were vortexed before incubation at 65°C for two minutes. Following this the samples were vortexed again before being incubated at 98°C for three minutes. A final vortex step completed the extraction process. The samples were left to cool at room temperature before being stored at -20°C.

Table 2: DNA sample identification for the buccal extractions.

Samples	Isohelix SK-1	Catch-All Swab	MasterAmp™ Brush
E	E1	E2	E3
L	L1	L2	L3
P	P1	P2	P3
A	A1	A2	A3
Ky	Ky1	Ky2	Ky3
R	R1	R2	R3

2.1.1.1.1 Buccal DNA quantification

To determine which of the three collection swabs was the most suitable for use in this project the extracted DNA samples were quantified. This was conducted using the Human Quantifiler® Kit (Applied Biosystems, UK) and the StepOne™ real-time PCR machine (Applied Biosystems, UK). The buccal samples were run twice to ensure experimental reproducibility.

2.1.1.1.2 Quantifiler® Software Setup

The human Quantifiler® kit quantifies the amount of amplifiable human DNA that is present in a sample from 0.023 ng/L to >50 ng/L. The gene target for the human Quantifiler® kit is the human telomerase reverse transcriptase gene (hTERT). A Quantifiler® programme “buccal extraction run 1” was created using the StepOne Experiment Wizard according to the manufacturer’s instructions for the following samples:

E1, E2, E3, L1, L2, L3, P1, P2, and P3.

A Quantifiler® programme “buccal extraction run 2” was created using the StepOne Experiment Wizard for the following samples:

A1, A2, A3, Ky1, Ky2, Ky3, R1, R2 and R3.

The standard curve quantitation parameter for genomic DNA (gDNA) was selected. A 2 hour run time (standard) was selected for both experimental runs. Each of the samples was run in triplicate, with the Quantifiler® standards run in duplicate in a total well volume of 10µl.

2.1.1.1.3 Sample Preparation

A standard dilution series for the experiment was conducted (Table 3), using the 200 ng purified DNA standard provided. The dilutions were prepared with a 3:1 serial factor. A sample at the lowest concentration contains about 14 to 16 copies of a diploid single-copy locus and 7 to 8 copies of a haploid single-copy locus.

Table 3: Standard dilution series of the 200 ng purified DNA standard for quantification.

Dilution Point	Source	Source Volume (μ l)	Diluent Volume $T_{10}E_{0.1}$ (μ l)	Total Volume (μ l)	Standard Concentration (ng/ μ l)
1	Stock	2.5	7.5	10.0	50.00
2	Dilution 1	3.34	6.66	10.0	16.7
3	Dilution 2	3.34	6.66	10.0	5.56
4	Dilution 3	3.34	6.66	10.0	1.85
5	Dilution 4	3.34	6.66	10.0	0.62
6	Dilution 5	3.34	6.66	10.0	0.21
7	Dilution 6	3.34	6.66	10.0	0.068
8	Dilution 7	3.34	6.66	10.0	0.023

Table 4: Quantifiler® Reaction Mix Components.

Components	Per well (μ l)
Quantifiler Reaction mix	5.0
Quantifiler Primer mix	4.2
Samples (0.1ng/ μ l)/Standards	0.8
Total reaction volume	10

The required Quantifiler® reaction mix and Quantifiler® primer mix (Table 4) for each experimental run (including an extra 10% for excess) was calculated and a master mix created. Then 9.2 μ l of the prepared master mix was added to each well of a 48-well optical plate. For the negative controls 10 μ l of reaction mix was added. Following the plate layout (generated when setting up the StepOne™ quantification experiment) 0.8 μ l of the appropriate samples/standards were added to each well. For results see section *3.1.1.1 DNA extraction from buccal swabs*.

2.1.1.2 DNA extraction from whole blood

Two commercial DNA extraction kits were tested to determine which should be used for the extraction of DNA from post-mortem whole blood samples. The Promega Wizard Purification Kit routinely used for DNA extraction (Wang *et al.* 2007) and the Qiagen DNeasy Blood and Tissue Kit. In addition to determining the optimum kit for

experimental use, the effects of three commonly used preservatives lithium heparin, EDTA, and potassium oxalate on DNA yield were examined during each extraction.

2.1.1.2.1 DNA extraction using the Promega Wizard Purification Kit

Samples of whole blood preserved in EDTA, lithium heparin and potassium oxalate were extracted using the Promega Wizard Purification Kit as per the manufacturers instructions (Table 5). Each sample was extracted in triplicate to ensure experimental efficiency and reproducibility.

Table 5: Promega Wizard Purification Extraction components and volumes.

Sample size	Cell lysis solution	Nuclei lysis solution	Protein precipitation solution	Isopropanol	Ethanol (70%)	DNA rehydration solution
300 µl	900 µl	300 µl	100 µl	300 µl	300 µl	100 µl

2.1.1.2.2 DNA extraction using the Qiagen DNeasy Blood and Tissue kit

Samples of whole blood preserved in EDTA, lithium heparin, and potassium oxalate were extracted using the DNeasy Blood Extraction Kit as per the manufacturer's instructions (Table 6). This method utilises spin column technology to selectively bind the DNA to a silica membrane. Each sample was extracted in triplicate to check method efficiency and reproducibility.

Table 6: Qiagen DNeasy Extraction Components and Volumes.

Sample size	Proteinase K	PBS (7.2 pH)	Buffer AL	Ethanol (100%)	Buffer AW1	Buffer AW2	Buffer AE
100 µl	20 µl	100 µl	200 µl	200 µl	500 µl	500 µl	200 µl

2.1.1.2.3 Quantification of DNA from whole blood

The samples extracted for both the Promega Wizard Purification Kit and the Qiagen DNeasy Blood and Tissue Kit were quantified using the Human Quantifiler® Kit (Applied Biosystems, UK) on the StepOne™ real-time machine (Applied Biosystems, UK). Programmes were titled “Quantification of Promega Samples” and “Qiagen Extraction Run”. Each programme used the standard curve quantitation setting for gDNA. The experiment run time was 2 hours and the samples (9 total for each extraction) were run in triplicate with the quantifiler® standards run in duplicate. The reaction plate was set up as described in section 2.1.1.1.3 *Sample preparation*. For results see section 3.1.1.2 *DNA extraction from whole blood*.

2.1.2 PCR Amplification of SNP regions of *OPRM1* gene

The μ opioid receptor gene (*OPRM1*) is one of the molecular targets for this research project. Amplification of specific gene regions (promoter, exon 1, exon 2, and exon 3) through the polymerase chain reaction (PCR) will identify gene variations (SNPs). These can then be used as positive controls for the real-time SNP genotyping assays conducted on the StepOne™ real-time machine. Complementary oligonucleotide primers were designed using the flanking sequence regions in order to effectively amplify these target regions.

2.1.2.1 Primer design and Rehydration

Sequences from the promoter and coding regions of the human *OPRM1* gene were used to design primers for use in PCR amplification (see appendix). PCR primers were synthesised for three of the four coding regions of the gene, exons 1, 2 and 3

(see appendix). PCR primers were also synthesised for the proximal promoter region of the gene. The following primers PRO554_HB, PRO995_HB, EX1_HB, EX2_HB and EX3_HB were hydrated with T₁₀ buffer according to their molecular weight (Table 7; see Table 8 for primer sequence information). Primers were left for 20 minutes at room temperature to dissolve before being stored at –20°C until used.

Table 7: *OPRM1* Primer rehydration volumes.

PRIMERS	Volume of T ₁₀ required for a concentration of 100 pmol/μL.
PRO995F_HB	186 μL
PRO995R_HB	222 μL
PRO554F_HB	210 μL
PRO554R_HB	224 μL
EX1F_HB	214 μL
EX1R_HB	208 μL
EX2F_HB	215 μL
EX2R_HB	250 μL
EX3F_HB	209 μL
EX3R_HB	194 μL

2.1.2.2 Primer validation

The proximal promoter region including –1045A > G, –995C > A, and –554G > A, the region of exon 1 including –118A >G, and –17C > T, the region of exon 2 including –440C > G, and –454A > G, and the region of exon 3 including –779G > A, –793C > T, –820G > A, –877G > A, and –942G > A were amplified by PCR. The primers used were 19-24 mer oligonucleotides (Table 8). These were synthesised by COGENICS The Sequencing Company (Essex, UK). The sequence of each primer pair, the position in the *OPRM1* gene, and the size of each of the amplicons amplified with PCR are shown in Table 8.

Table 8: *OPRM1* primer sequence information.

Gene and Polymorphism	Amplified Region	Primer sequence	Annealing temperature °C	Amplicon size (bp)
<i>OPRM1</i> A1045G	Promoter region	Forward TAGAAGCACTGGACTTAG Reverse CCTACCCACTGAAACAAAATC	59.5	350
<i>OPRM1</i> C995A	Promoter region	Forward TAGAAGCACTGGACTTAG Reverse CCTACCCACTGAAACAAAATC	59.5	350
<i>OPRM1</i> G554A	Promoter region	Forward CTGCACAAAAGTTTATTTGTTTCTC Reverse CACTGCTACCAAAGACTAACT	59.5	338
<i>OPRM1</i> A118G	Exon 1	Forward ATGCCTTGGCGTACTCAAGTTG Reverse CTAACTCCCAAGGCTCAATGTTG	65.3	333
<i>OPRM1</i> C17T	Exon 1	Forward ATGCCTTGGCGTACTCAAGTTG Reverse CTAACTCCCAAGGCTCAATGTTG	65.3	333
<i>OPRM1</i> C440G	Exon 2	Forward TCCAGAGTGAATTACCTAATG Reverse CAAGGTGAGTGATGTTACCAG	63.2	287
<i>OPRM1</i> A454G	Exon 2	Forward TCCAGAGTGAATTACCTAATG Reverse CAAGGTGAGTGATGTTACCAG	63.2	287
<i>OPRM1</i> G779A	Exon 3	Forward ATTCTCTCATCCAACCTGGTAC Reverse CTCAACCCAGTCCTTTATGCAT	64.7	353
<i>OPRM1</i> C793T	Exon 3	Forward ATTCTCTCATCCAACCTGGTAC Reverse CTCAACCCAGTCCTTTATGCAT	64.7	353
<i>OPRM1</i> G820A	Exon 3	Forward ATTCTCTCATCCAACCTGGTAC Reverse CTCAACCCAGTCCTTTATGCAT	64.7	353
<i>OPRM1</i> G877A	Exon 3	Forward ATTCTCTCATCCAACCTGGTAC Reverse CTCAACCCAGTCCTTTATGCAT	64.7	353
<i>OPRM1</i> G942A	Exon 3	Forward ATTCTCTCATCCAACCTGGTAC Reverse CTCAACCCAGTCCTTTATGCAT	64.7	353

PCRs were performed with a reaction volume of 50 µl, including 27 µl PCR grade water (Sigma), 10 µl of 5x GoTaq™ buffer (Promega, UK), 2 µl MgCl₂, 5 µl of 2.5 mM deoxynucleoside triphosphates (dNTPs) (Roche, UK) (final concentration of 0.25 mM), 1 µl Forward and Reverse primers, 3 µl DNA and 0.3 µl GoTaq™ DNA polymerase (Promega, UK). The cycling conditions were as follows: initial denaturation at 95°C for 5 minutes; subsequent denaturation at 95°C for 1 minute; annealing at 60-62°C for 30 seconds; primer extension at 72°C for 2 minutes, repeated for 30 cycles, followed by final extension at 72°C for 5 minutes. The PCR products were confirmed by electrophoresis with a 2 % Cyber Green-agarose gel on blue light. PCR reactions were performed with a Primus 96 advanced machine (Alpha Laboratories, UK).

2.1.2.3 PCR Development

2.1.2.3.1 $MgCl_2$

Different $MgCl_2$ concentrations were tested in an effort to determine the most effective concentration required to produce optimal DNA amplification. The primer set PRO554_HB was used. The reaction volume was 50 μ l (Table 9). The cycling conditions were as follows: initial denaturation at 95°C for 5 minutes; subsequent denaturation at 95°C for 1 minute; annealing at 62°C for 30 seconds; primer extension at 72°C for 2 minutes, repeated for 30 cycles, followed by final extension at 72 °C for 5 minutes. The PCR products were confirmed by electrophoresis with a 2 % Cyber Green-agarose gel on blue light. PCR reactions were performed with a Primus 96 advanced machine (Alpha Laboratories). For results see section 3.1.2.1 $MgCl_2$.

Table 9: Reaction components for $MgCl_2$ optimisation.

Reaction components	1 μ l $MgCl_2$	1.5 μ l $MgCl_2$	2 μ l $MgCl_2$	2.5 μ l $MgCl_2$	3 μ l $MgCl_2$	3.5 μ l $MgCl_2$	4 μ l $MgCl_2$
H ₂ O	28 μ l	27.5 μ l	27 μ l	26.5 μ l	26 μ l	25.5 μ l	25 μ l
5x GoTaq™ Flexi Buffer	10 μ l	10 μ l	10 μ l	10 μ l	10 μ l	10 μ l	10 μ l
$MgCl_2$	1 μ l	1.5 μ l	2 μ l	2.5 μ l	3 μ l	3.5 μ l	4 μ l
dNTPs (2.5mM)	5 μ l	5 μ l	5 μ l	5 μ l	5 μ l	5 μ l	5 μ l
Forward primer	1 μ l	1 μ l	1 μ l	1 μ l	1 μ l	1 μ l	1 μ l
Reverse primer	1 μ l	1 μ l	1 μ l	1 μ l	1 μ l	1 μ l	1 μ l
DNA	3 μ l	3 μ l	3 μ l	3 μ l	3 μ l	3 μ l	3 μ l
GoTaq™ polymerase	0.3 μ l	0.3 μ l	0.3 μ l	0.3 μ l	0.3 μ l	0.3 μ l	0.3 μ l

2.1.2.3.2 Temperature

Temperature gradients

Temperature gradient reactions were conducted to determine optimal primer annealing temperatures. Primer sets PRO995_HB and PRO554_HB were used. The reaction volume was 50 μ l including 27 μ l PCR grade water, 10 μ l of 5x GoTaq™ buffer, 2 μ l MgCl₂, 5 μ l of 2.5 mM dNTPs (final concentration of 0.25 mM), 1 μ l Forward and Reverse primers, 3 μ l DNA and 0.3 μ l GoTaq™ DNA polymerase. The cycling conditions were as follows: initial denaturation at 95°C for 5 minutes; subsequent denaturation at 95°C for 1 minute; temperature gradient set at 62°C \pm 3°C for 30 seconds; primer extension at 72°C for 2 minutes, repeated for 30 cycles, followed by final extension at 72°C for 5 minutes. The median temperature point was set at the calculated annealing temperature of 62°C for the primer sets. The PCR products were visualised by electrophoresis with a 2 % Cyber Green-agarose gel on blue light. PCR reactions were performed with a Primus 96 advanced machine (Alpha Laboratories). For results see section 3.1.2.2 *Temperature*.

Temperatures selected from gradient PCR reactions

Three temperatures were selected from the gradient reaction to test with PRO554_HB and PRO995_HB. The reaction volume was maintained at 50 μ l and included 28.5 μ l PCR grade water, 10 μ l of 5x GoTaq™ Flexi Buffer, 5 μ l of MgCl₂, 1 μ l of 10mM dNTPs (final concentration of 0.25mM), 1 μ l of forward and reverse primers, 3 μ l DNA, and 0.5 μ l GoTaq™ DNA polymerase. The cycling conditions were as follows: initial denaturation at 95°C for 5 minutes; subsequent denaturation at 95°C for 1 minute; annealing temperature points of 60.1°C, 61.2 °C, and 62.2°C for 30 seconds; primer extension at 72°C for 2 minutes, repeated for 30 cycles, followed by

final extension at 72°C for 5 minutes. The median temperature point was set at the calculated annealing temperature of 62°C for the primer sets. The PCR products were confirmed by electrophoresis with a 2 % Cyber Green-agarose gel on blue light. PCR reactions were performed with a Primus 96 Advanced machine (Alpha Laboratories). For results see section *3.1.2.2 Temperature*.

Temperature alterations to increase specificity

The annealing temperatures for PRO554_HB, PRO995_HB, EX1_HB, and EX2_HH were decreased to increase banding specificity and decrease DNA smearing. The annealing temperature for EX3_HB was increased from 64.4°C to 64.7 °C and to 65.3°C. The reaction volume was 50 µl and included 29.5 µl PCR grade water, 10 µl of 5x GoTaq™ Flexi Buffer, 4 µl of MgCl₂, 1 µl of 10mM dNTPs (final concentration of 0.25mM), 1 µl of forward and reverse primers, 3 µl DNA, and 0.5 µl GoTaq™ DNA polymerase. The cycling conditions were as follows: initial denaturation at 95°C for 5 minutes; subsequent denaturation at 95°C for 1 minute; temperature gradient set at 62.2°C ± 4°C for 30 seconds; primer extension at 72°C for 2 minutes, repeated for 30 cycles, followed by final extension at 72°C for 5 minutes. The median temperature point was set at the calculated annealing temperature of 62°C for the primer sets. The PCR products were processed by electrophoresis with a 2 % cyber green-agarose gel, and amplification by PCR was confirmed. PCR reactions were performed with a Primus 96 Advanced (Alpha Laboratories) machine. For results see section *3.1.2.2 Temperature*.

2.1.2.4 PCR Validation

The results for the PCR reactions were validated through DNA sequencing, examining the sequencing results obtained against the consensus *OPRM1* sequence (see appendix). For this target PCR products were purified using the QIAquick PCR Purification Kit (Qiagen, UK) according to the manufacturer's protocol. The purified PCR products were then sent to COGENICS to be sequenced. For results see section *3.1.2.2.4 SNPs revealed by DNA sequencing results*.

2.1.2.5 A118G identification

Of the *OPRM1* regions studied only one yielded a SNP with possible significance for methadone susceptibility, the exon 1 A118G SNP. A positive control was required for SNP genotyping so using EX1_HB this region was amplified for 20 control subjects. PCRs were performed with a reaction volume of 50 µl, including 27.5 µl PCR grade water, 10 µl of 5x GoTaq™ buffer, 6 µl MgCl₂, 1 µl of 10 mM deoxynucleoside triphosphates (dNTPs) (final concentration of 0.25 mM), 1 µl Forward and Reverse primers, 3 µl DNA and 0.5 µl GoTaq™ DNA polymerase. The cycling conditions were as follows: initial denaturation at 95°C for 5 minutes; subsequent denaturation at 95°C for 1 minute; annealing at 65.3°C for 30 seconds; primer extension at 72°C for 2 minutes, repeated for 30 cycles, followed by final extension at 72°C for 5 minutes. The PCR products were visualised by electrophoresis with a 2 % Cyber Green-agarose gel on blue light. PCR reactions were performed with a Primus 96 advanced machine (Alpha Laboratories, UK). The PCR products were purified using the QIAquick PCR Purification Kit (Qiagen, UK) and sequencing was conducted by COGENICS. For results see section *3.1.2.3 A118G identification* and for a discussion of the results see chapters 4, 5 and 6.

2.1.3 PCR Amplification of SNP regions of *CYP2B6* gene

CYP2B6 is responsible for methadone metabolism and together with *OPRM1* is the focus of this study. Amplification of specific gene regions (promoter, exon 4 and exon 5) through PCR will identify *CYP2B6* SNPs. These can then be used as positive controls for the real-time SNP genotyping assays conducted on the StepOne™ real-time machine.

2.1.3.1 Primer design and Rehydration

Sequences from the promoter and coding regions of the human *CYP2B6* gene were used to design primers for use in PCR amplification. PCR primers were synthesised for two of the nine coding regions of the gene, exons 4 and 5 (see appendix *CYP2B6 Sequence Information*). PCR primers were also synthesised for the proximal promoter region of the gene (Table 10). The following primers C2B6E4, C2B6E5 and C2B6Pr (see Table 11 for primer sequence information) were hydrated in T₁₀ buffer according to their molecular weight (Table 10). Primers were left for 20 minutes at room temperature to dissolve before being stored at -20°C until used.

Table 10: *CYP2B6* Primer rehydration volumes.

PRIMERS	Volume of T ₁₀ required for a concentration of 100 pmol/μL.
C2B6E4F	172 μL
C2B6E4R	152 μL
C2B6E5F	130 μL
C2B6E5R	180 μL
C2B6PrF	206 μL
C2B6PrR	169 μL

2.1.3.2 Primer validation

The *CYP2B6* primers target 750 T > C in the proximal promoter region, 516 G > T in exon 4 and 785 A > G in exon 5. Each SNP has been implicated with modifications to enzyme efficiency, with 516 G > T resulting in a reduction of enzymatic efficiency *in vivo*, 785 A > G increasing enzyme efficiency *in vivo* and 750 T > C affecting overall gene expression. The sequence of each primer pair, the position in the *CYP2B6* gene, and the size of each of the amplicons amplified with PCR are shown in Table 11.

Table 11: *CYP2B6* primer sequence information.

Gene and Polymorphism	Amplified Region	Primer sequence	Annealing temperature °C	Amplicon size (bp)
<i>CYP2B6</i> T750C	Promoter region	C2B6PrF CAGGTTCAAGTGATTCTCTTG C2B6PrR CATGTTCAAACTGAGAGGCT	59.5	229
<i>CYP2B6</i> G516T	Exon 4	C2B6E4F GTACATAATTAGCTGTTACGG C2B6E4R AAGTCTGGTAGAACAAGTTCA	59.5	268
<i>CYP2B6</i> A785G	Exon 5	C2B6E5F AGGAGATATAGAGTCAGTGAG C2B6E5R AGTTCCTCCTCCCTATTTTCT	62.3	536

PCRs were performed with a reaction volume of 50 µl, including 27.5 µl PCR grade water (Sigma), 10 µl of 5x GoTaq™ buffer (Promega, UK), 6 µl MgCl₂, 1µl of 10 mM deoxynucleoside triphosphates (dNTPs) (Roche, UK) (final concentration of 0.25 mM), 1 µl Forward and Reverse primers, 3 µl DNA and 0.5 µl GoTaq™ DNA polymerase (Promega, UK). The cycling conditions were as follows: initial denaturation at 95°C for 5 minutes; subsequent denaturation at 95°C for 1 minute; annealing at 56-62.5°C for 30 seconds; primer extension at 72°C for 2 minutes, repeated for 30 cycles, followed by final extension at 72°C for 5 minutes. The PCR products were confirmed by electrophoresis with a 2 % Cyber Green-agarose gel on blue light. PCR reactions were performed with a Primus 96 advanced machine (Alpha Laboratories, UK). For results see *section 3.1.3.1 Primer Validation*.

2.1.3.3 T750C PCR Validation

2.1.3.3.1 Temperature

Temperature gradient reactions were conducted to determine optimal primer annealing temperatures. The reaction volume was 50 µl including 27 µl PCR grade water, 10 µl of 5x GoTaq™ buffer, 6 µl MgCl₂, 1 µl of 10 mM dNTPs (final concentration of 0.25 mM), 1 µl Forward and Reverse primers, 3 µl DNA and 0.5 µl GoTaq™ DNA polymerase. The cycling conditions were as follows: initial denaturation at 95°C for 5 minutes; subsequent denaturation at 95°C for 1 minute; temperature gradient set at 62°C ± 3°C for 30 seconds; primer extension at 72°C for 2 minutes, repeated for 30 cycles, followed by final extension at 72°C for 5 minutes. The median temperature point was set at the calculated annealing temperature for the primer sets (62°C). The PCR products were visualised by electrophoresis with a 2 % Cyber Green-agarose gel on blue light. PCR reactions were performed with a Primus 96 advanced machine (Alpha Laboratories). For results see *section 3.1.3.2.1 Temperature*.

2.1.3.3.2 MgCl₂

A reduction in MgCl₂ concentration was tested in an effort to determine the optimal concentration required for efficient DNA amplification. The reaction volume was 50 µl including 29.5 µl PCR grade water, 10 µl of 5x GoTaq™ buffer, 4 µl MgCl₂, 1 µl of 10 mM dNTPs (final concentration of 0.25 mM), 1 µl Forward and Reverse primers, 3 µl DNA and 0.5 µl GoTaq™ DNA polymerase. The cycling conditions were as follows: initial denaturation at 95°C for 5 minutes; subsequent denaturation at 95°C for 1 minute; annealing at 62.1°C for 30 seconds; primer extension at 72°C for 2 minutes, repeated for 30 cycles, followed by final extension at 72 °C for 5 minutes.

The PCR products were confirmed by electrophoresis with a 2 % Cyber Green-agarose gel on blue light. PCR reactions were performed with a Primus 96 advanced machine (Alpha Laboratories). For results see section 3.1.3.2.2 *MgCl₂*.

2.1.3.4 T750C Identification

Following method optimisation for T750C amplification PCRs were performed to identify positive controls for SNP genotyping. The PCR volume was 50 µl, including 29.5 µl PCR grade water, 10 µl of 5x GoTaq™ buffer, 4 µl MgCl₂, 1 µl of 10 mM deoxynucleoside triphosphates (dNTPs) (final concentration of 0.25 mM), 1 µl Forward and Reverse primers, 3 µl DNA and 0.5 µl GoTaq™ DNA polymerase. The cycling conditions were as follows: initial denaturation at 95°C for 5 minutes; subsequent denaturation at 95°C for 1 minute; annealing at 65.0°C for 30 seconds; primer extension at 72°C for 2 minutes, repeated for 30 cycles, followed by final extension at 72°C for 5 minutes. The PCR products were visualised by electrophoresis with a 2 % Cyber Green-agarose gel on blue light. PCR reactions were performed with a Primus 96 advanced machine (Alpha Laboratories, UK). The PCR products were purified using the QIAquick PCR Purification Kit (Qiagen, UK) and sequencing was conducted by COGENICS. For results see *section 3.1.3.3.1 T750C Sequencing Results*.

2.1.3.5 G516T PCR Validation

2.1.3.5.1 Temperature

Temperature Gradients

A temperature gradient reaction was conducted to determine optimal C2B6E4 primer annealing temperature. The temperatures tested were as follows: 58.0 °C, 58.8 °C,

59.5 °C, 60.2 °C, 61.0 °C, 61.7 °C, 62.3 °C, 63.0 °C, 63.8 °C, X °C, and 65.2 °C. The reaction volume was 50 µl including 27.5 µl PCR grade water, 10 µl of 5x GoTaq™ buffer, 6 µl MgCl₂, 1 µl of 10 mM dNTPs (final concentration of 0.25 mM), 1 µl Forward and Reverse primers, 3 µl DNA and 0.5 µl GoTaq™ DNA polymerase. The cycling conditions were as follows: initial denaturation at 95°C for 5 minutes; subsequent denaturation at 95°C for 1 minute; temperature gradient set at 62°C ± 4°C for 30 seconds; primer extension at 72°C for 2 minutes, repeated for 30 cycles, followed by final extension at 72°C for 5 minutes. The PCR products were visualised by electrophoresis with a 2 % Cyber Green-agarose gel on blue light. PCR reactions were performed with a Primus 96 advanced machine (Alpha Laboratories). For results see *section 3.1.3.4.1 Temperature*.

Temperatures selected from gradient PCR reactions

The gradient reaction demonstrated that the lower annealing temperatures yielded the most specific DNA bands. From this a further gradient reaction was conducted focusing on lower annealing temperatures: 56.0 °C, 56.8 °C, 57.5 °C, 58.2 °C and 59.0 °C. The reaction volume was 50 µl including 27.5 µl PCR grade water, 10 µl of 5x GoTaq™ buffer, 6 µl MgCl₂, 1 µl of 10 mM dNTPs (final concentration of 0.25 mM), 1 µl Forward and Reverse primers, 3 µl DNA and 0.5 µl GoTaq™ DNA polymerase. The cycling conditions were as follows: initial denaturation at 95°C for 5 minutes; subsequent denaturation at 95°C for 1 minute; temperature gradient set at 60°C ± 4°C for 30 seconds; primer extension at 72°C for 2 minutes, repeated for 30 cycles, followed by final extension at 72°C for 5 minutes. The PCR products were visualised by electrophoresis with a 2 % Cyber Green-agarose gel on blue light. PCR reactions

were performed with a Primus 96 advanced machine (Alpha Laboratories). For results see *section 3.1.3.4.1 Temperature*.

2.1.3.5.2 MgCl₂

Different MgCl₂ concentrations were tested in an effort to determine the most effective concentration required to produce optimal DNA amplification. The reaction volume was 50 µl (Table 12). The cycling conditions were as follows: initial denaturation at 95°C for 5 minutes; subsequent denaturation at 95°C for 1 minute; annealing at 59.5°C for 30 seconds; primer extension at 72°C for 2 minutes, repeated for 30 cycles, followed by final extension at 72 °C for 5 minutes. The PCR products were confirmed by electrophoresis with a 2 % Cyber Green-agarose gel on blue light. PCR reactions were performed with a Primus 96 advanced machine (Alpha Laboratories). For results see *section 3.1.3.4.2 MgCl₂*.

Table 12: Reaction components for MgCl₂ optimisation protocol.

Reaction components	4 µl MgCl ₂	5 µl MgCl ₂	6 µl MgCl ₂	7 µl MgCl ₂	8 µl MgCl ₂	9 µl MgCl ₂
H ₂ O	29.5 µl	28.5 µl	27.5 µl	26.5 µl	25.5 µl	24.5 µl
5x GoTaq™ Flexi Buffer	10 µl	10 µl	10 µl	10 µl	10 µl	10 µl
MgCl ₂	4 µl	5 µl	6 µl	7 µl	8 µl	9 µl
dNTPs (10mM)	1 µl	1 µl	1 µl	1 µl	1 µl	1 µl
Forward primer	1 µl	1 µl	1 µl	1 µl	1 µl	1 µl
Reverse primer	1 µl	1 µl	1 µl	1 µl	1 µl	1 µl
DNA	3 µl	3 µl	3 µl	3 µl	3 µl	3 µl
GoTaq™ polymerase	0.5 µl	0.5 µl	0.5 µl	0.5 µl	0.5 µl	0.5 µl

2.1.3.6 G516T Identification

Following method optimisation for G516T amplification PCRs were performed to identify positive controls for SNP genotyping. The PCR volume was 50 µl, including 27.5 µl PCR grade water, 10 µl of 5x GoTaq™ buffer, 7 µl MgCl₂, 1 µl of 10 mM

deoxynucleoside triphosphates (dNTPs) (final concentration of 0.25 mM), 1 µl Forward and Reverse primers, 2 µl DNA and 0.5 µl GoTaq™ DNA polymerase. The cycling conditions were as follows: initial denaturation at 95°C for 5 minutes; subsequent denaturation at 95°C for 1 minute; annealing at 59.5°C for 30 seconds; primer extension at 72°C for 2 minutes, repeated for 30 cycles, followed by final extension at 72°C for 5 minutes. The PCR products were visualised by electrophoresis with a 2 % Cyber Green-agarose gel on blue light. PCR reactions were performed with a Primus 96 advanced machine (Alpha Laboratories, UK). The PCR products were purified using the QIAquick PCR Purification Kit (Qiagen, UK) according to the manufacturer's protocol. The purified PCR products were then sent to COGENICS to be sequenced. For results see *section 3.1.3.5 G516T Identification*.

2.1.3.7 A785G PCR Validation

2.1.3.7.1 Temperature

The banding yielded during C2B6E5 primer validation (Section 2.1.3.2 *Primer validation*) was unselective with possible non-specific amplification. To improve this result an increase in annealing temperature was conducted. The annealing temperatures from the preliminary reaction were: 58.0 °C, 59.5 °C and 61.0 °C. These temperatures were increased to 61.5 °C, 62.1°C, and 63.2°C. The reaction volume was 50 µl including 27.5 µl PCR grade water, 10 µl of 5x GoTaq™ buffer, 6 µl MgCl₂, 1 µl of 10 mM dNTPs (final concentration of 0.25 mM), 1 µl Forward and Reverse primers, 3 µl DNA and 0.5 µl GoTaq™ DNA polymerase. The cycling conditions were as follows: initial denaturation at 95°C for 5 minutes; subsequent denaturation at 95°C for 1 minute; temperature gradient set at 64.5°C ± 3°C for 30 seconds; primer extension at 72°C for 4 minutes, repeated for 30 cycles, followed by final extension at

72°C for 5 minutes. The PCR products were visualised by electrophoresis with a 2 % Cyber Green-agarose gel on blue light. PCR reactions were performed with a Primus 96 advanced machine (Alpha Laboratories). For results see *section 3.1.3.6.1*

Temperature.

2.1.3.8 A785G Identification

Following method optimisation for A785G amplification PCRs were performed to identify positive controls for SNP genotyping. The PCR volume was 50 µl, including 27.5 µl PCR grade water, 10 µl of 5x GoTaq™ buffer, 6 µl MgCl₂, 1 µl of 10 mM deoxynucleoside triphosphates (dNTPs) (final concentration of 0.25 mM), 1 µl Forward and Reverse primers, 3 µl DNA and 0.5 µl GoTaq™ DNA polymerase. The cycling conditions were as follows: initial denaturation at 95°C for 5 minutes; subsequent denaturation at 95°C for 1 minute; annealing at 62.1°C for 30 seconds; primer extension at 72°C for 4 minutes, repeated for 30 cycles, followed by final extension at 72°C for 5 minutes. The PCR products were visualised by electrophoresis with a 2 % Cyber Green-agarose gel on blue light. PCR reactions were performed with a Primus 96 advanced machine (Alpha Laboratories, UK). The PCR products were purified using the QIAquick PCR Purification Kit (Qiagen, UK) according to the manufacturer's protocol. The purified PCR products were then sent to COGENICS to be sequenced. For results see *section 3.1.3.7 A785G Identification.*

2.2 Post-mortem Sample Examination

2.2.1 DNA extraction from whole blood

DNA was extracted from whole blood samples for 84 subjects whose deaths were associated with methadone (Tayside, Fife and Central regions of Scotland). The samples were preserved in fluoride/oxalate. The extraction was performed using the DNeasy Blood and Tissue Kit as described above in *section 2.1.1.2.2 DNA extraction using the Qiagen DNeasy Blood and Tissue kit*.

2.2.2 Quantification of DNA from post-mortem blood

The post-mortem DNA samples were quantified using the Quantifiler® Kit (Applied Biosystems, UK) on the StepOne™ real-time machine (Applied Biosystems, UK). Programmes were titled Dundee Run 1, Dundee Run 2, and Dundee Run 3. Each programme used the standard curve quantitation setting for gDNA. The experiment run time was standard (2 hours) and the quantifiler® standards run in duplicate. The reaction plate was set up as described in *section 2.1.1.1.3 Sample preparation*. For results see *section 3.2.1.1 Quantification of DNA from post-mortem blood*.

2.2.3 A118G SNP Genotyping

After DNA quantification the samples were genotyped for the *OPRM1* A118G variation using the validated Taqman™ assay (product no. 4351379, Applied Biosystems, UK).

2.2.3.1 Software set-up

A Taqman™ SNP genotyping programme “A118G typing Dundee 1” was created using the StepOne Advanced Experiment Design programme according to the manufacturer’s instructions for the following samples:

DC1, DC2, DC3, DC4, DC5, DC6, DC7, DC8, DC9, DC10, DC11, DC12, DC13, DC14, DC15, DC16, DC17, DC18, DC19, DC20, DC21, DC22, DC23, DC24, DC25, DC26, DC27, DC28, DC29, DC30, DC31, DC32, DC33, DC34, DC35, DC36, DC37, DC38, DC39, DC40.

A Taqman™ SNP genotyping programme “A118G typing Dundee 2” was created using the StepOne Advanced Experiment Design programme for the following samples:

DC1, DC2, DC3, DC4, DC5, DC6, DC7, DC8, DC9, DC10, DC11, DC12, DC13, DC14, DC15, DC16, DC17, DC18, DC19, DC20, DC21, DC22, DC23, DC24, DC25, DC26, DC27, DC28, DC29, DC30, DC31, DC32, DC33, DC34, DC35, DC36, DC37, DC38, DC39, DC40.

A Taqman™ SNP genotyping programme “A118G typing Dundee 3” was created using the StepOne Advanced Experiment Design programme for the following samples:

DC41, DC41, DC42, DC42, DC43, DC43, DC44, DC44, DC45, DC45, DC46, DC46, DC47, DC47, DC48, DC48, DC49, DC49, DC50, DC50, DC51, DC51, DC52, DC52, DC53, DC53, DC54, DC54, DC55, DC55.

A Taqman™ SNP genotyping programme “A118G typing Dundee 4” was created using the StepOne Advanced Experiment Design programme for the following samples:

DC56, DC57, DC58, DC59, DC60, DC61, DC62, DC63, DC64, DC65, DC66, DC67, DC68, DC69, DC70, DC71, DC72, DC73, DC74, DC75, DC76, DC77, DC78, DC79, DC80, DC81, DC82, DC83, DC84.

A Taqman™ SNP genotyping programme “A118G typing Dundee 5” was created using the StepOne Advanced Experiment Design programme for the following samples:

DC56, DC57, DC58, DC59, DC60, DC61, DC62, DC63, DC64, DC65, DC66, DC67, DC68, DC69, DC70, DC71, DC72, DC73, DC74, DC75, DC76, DC77, DC78, DC79, DC80, DC81, DC82, DC83, DC84.

The standard run time (2 hours) was selected for all of the experimental runs, with 50 cycles of 92 °C for 30 seconds and 65° for 1.30 minutes. Two negative controls and three positive controls were run for all experiments. Positive controls were allocated accordingly:

Allele1/ Allele 1 (AA) DC1

Allele 1/ Allele 2 (AG) DC19

Allele 2/ Allele 2 (GG) DC15

For all controls and samples a total well volume of 10µl was used.

2.2.3.2 Sample preparation

The Taqman™ mastermix, SNP assay mix, and DNase free H₂O (Table 13) for each experimental run (including an extra 10% for excess) was calculated and a mastermix created. Then 9µl of the prepared master mix was added into each well of a 48-well optical plate. For the negative control wells 10µl of reaction mix was added. Finally 1µl of the appropriate samples/positive controls were added to each well; following the plate layout generated when setting up the StepOne™ quantification experiment.

For results see *section 3.2.1.2 A118G SNP Genotyping*, for a discussion of the results see Chapters 4, 5, & 6.

Table 13: Taqman™ SNP Genotyping Reaction Mix Components.

Components	Per well (µl)
Taqman™ mastermix	5µl
SNP Assay mix (x20)	0.5µl
H ₂ O, DNase-free	3.5µl
DNA (0.1ng/µl)/Controls	1µl
Total reaction volume	10µl

2.2.4 T750C SNP Genotyping

The post-mortem samples were genotyped for the *CYP2B6* T750C variation using a validated Taqman™ assay (product no. 4362691, Applied Biosystems, UK).

2.2.4.1. Software set-up

A Taqman™ SNP genotyping programme “T750C SNP 1” was created using the StepOne Advanced Experiment Design programme according to the manufacturer’s instructions for the following samples:

DC1, DC2, DC3, DC4, DC5, DC6, DC7, DC8, DC9, DC10, DC11, DC12, DC13, DC14, DC15, DC16, DC17, DC18, DC19, DC20, DC21, DC22, DC23, DC24, DC25, DC26, DC27, DC28, DC29, DC30, DC31, DC32, DC33, DC34, DC35, DC36, DC37, DC38, DC39, DC40.

A Taqman™ SNP genotyping programme “T750C SNP 2” was created using the StepOne Advanced Experiment Design programme for the repeat SNP genotyping of:

DC1, DC2, DC3, DC4, DC5, DC6, DC7, DC8, DC9, DC10, DC11, DC12, DC13, DC14, DC15, DC16, DC17, DC18, DC19, DC20, DC21, DC22, DC23, DC24, DC25,

DC26, DC27, DC28, DC29, DC30, DC31, DC32, DC33, DC34, DC35, DC36, DC37, DC38, DC39, DC40.

A Taqman™ SNP genotyping programme “T750C SNP 3” was created using the

StepOne Advanced Experiment Design programme for the following samples:

DC41, DC41, DC42, DC42, DC43, DC43, DC44, DC44, DC45, DC45, DC46, DC46, DC47, DC47, DC48, DC48, DC49, DC49, DC50, DC50, DC51, DC51, DC52, DC52, DC53, DC53, DC54, DC54, DC55, DC55

A Taqman™ SNP genotyping programme “T750C SNP 4” was created using the

StepOne Advanced Experiment Design programme for the following samples:

DC56, DC57, DC58, DC59, DC60, DC61, DC62, DC63, DC64, DC65, DC66, DC67, DC68, DC69, DC70, DC71, DC72, DC73, DC74, DC75, DC76, DC77, DC78, DC79, DC80, DC81, DC82, DC83, DC84

A Taqman™ SNP genotyping programme “T750C SNP 5” was created using the

StepOne Advanced Experiment Design programme for the following samples:

DC56, DC57, DC58, DC59, DC60, DC61, DC62, DC63, DC64, DC65, DC66, DC67, DC68, DC69, DC70, DC71, DC72, DC73, DC74, DC75, DC76, DC77, DC78, DC79, DC80, DC81, DC82, DC83, DC84

The standard run time (2 hours) was selected for all of the experimental runs, with 50 cycles of 92 °C for 30 seconds and 65° for 1.30 minutes. Two negative controls and three positive controls were run for all experiments. Positive controls were allocated accordingly:

Allele1/ Allele 1 (TT) DC2

Allele 1/ Allele 2 (TC) DC1

Allele 2/ Allele 2 (CC) DC13

For all controls and samples a total well volume of 10µl was used.

2.2.4.2 Sample preparation

Sample preparation was as described above (*section 2.2.3.2*). For results see *section 3.2.1.3 T750C SNP Genotyping*, for a discussion of the results see Chapters 4, 5, & 6.

2.2.5 G516T SNP Genotyping

The post-mortem samples were genotyped for the *CYP2B6* G516T variation using a validated Taqman™ assay (product no. 4362691, Applied Biosystems, UK).

2.2.5.1 Software set-up

A Taqman™ SNP genotyping programme “G516T SNP 1” was created using the StepOne Advanced Experiment Design programme according to the manufacturer’s instructions for the following samples:

DC1, DC2, DC3, DC4, DC5, DC6, DC7, DC8, DC9, DC10, DC11, DC12, DC13, DC14, DC15, DC16, DC17, DC18, DC19, DC20, DC21, DC22, DC23, DC24, DC25, DC26, DC27, DC28, DC29, DC30, DC31, DC32, DC33, DC34, DC35, DC36, DC37, DC38, DC39, DC40.

A Taqman™ SNP genotyping programme “G516T SNP 2” was created using the StepOne Advanced Experiment Design programme for the repeat SNP genotyping of:

DC1, DC2, DC3, DC4, DC5, DC6, DC7, DC8, DC9, DC10, DC11, DC12, DC13, DC14, DC15, DC16, DC17, DC18, DC19, DC20, DC21, DC22, DC23, DC24, DC25, DC26, DC27, DC28, DC29, DC30, DC31, DC32, DC33, DC34, DC35, DC36, DC37, DC38, DC39, DC40.

A Taqman™ SNP genotyping programme “G516T SNP 3” was created using the StepOne Advanced Experiment Design programme for the following samples:

DC41, DC41, DC42, DC42, DC43, DC43, DC44, DC44, DC45, DC45, DC46, DC46, DC47, DC47, DC48, DC48, DC49, DC49, DC50, DC50, DC51, DC51, DC52, DC52, DC53, DC53, DC54, DC54, DC55, DC55.

A Taqman™ SNP genotyping programme “G516T SNP 4” was created using the StepOne Advanced Experiment Design programme for the following samples:

DC56, DC57, DC58, DC59, DC60, DC61, DC62, DC63, DC64, DC65, DC66, DC67, DC68, DC69, DC70, DC71, DC72, DC73, DC74, DC75, DC76, DC77, DC78, DC79, DC80, DC81, DC82, DC83, DC84

A Taqman™ SNP genotyping programme “G516T SNP 5” was created using the StepOne Advanced Experiment Design programme for the following samples:

DC56, DC57, DC58, DC59, DC60, DC61, DC62, DC63, DC64, DC65, DC66, DC67, DC68, DC69, DC70, DC71, DC72, DC73, DC74, DC75, DC76, DC77, DC78, DC79, DC80, DC81, DC82, DC83, DC84

The standard run time (2 hours) was selected for all of the experimental runs, with 50 cycles of 92 °C for 30 seconds and 65° for 1.30 minutes. Two negative controls and three positive controls were run for all experiments. Positive controls were allocated accordingly:

Allele1/ Allele 1 (GG) DC13

Allele 1/ Allele 2 (GT) DC1

Allele 2/ Allele 2 (TT) DC38

For all controls and samples a total well volume of 10µl was used.

2.2.5.2 Sample preparation

Sample preparation was as described above (*section 2.2.3.2*). For results see *section 3.2.1.4 G516T SNP Genotyping*, for a discussion of the results see Chapters 4, 5, & 6.

2.2.6 A785G SNP Genotyping

The post-mortem samples were genotyped for the *CYP2B6* A785G variation using a custom-designed Taqman™ assay (product no. 4331349, Applied Biosystems, UK).

2.2.6.1 Software set-up

A Taqman™ SNP genotyping programme “A785G SNP 1” was created using the StepOne Advanced Experiment Design programme according to the manufacturer’s instructions for the following samples:

DC1, DC2, DC3, DC4, DC5, DC6, DC7, DC8, DC9, DC10, DC11, DC12, DC13, DC14, DC15, DC16, DC17, DC18, DC19, DC20, DC21, DC22, DC23, DC24, DC25, DC26, DC27, DC28, DC29, DC30, DC31, DC32, DC33, DC34, DC35, DC36, DC37, DC38, DC39, DC40.

A Taqman™ SNP genotyping programme “A785G SNP 2” was created using the StepOne Advanced Experiment Design programme for the repeat SNP genotyping of:

DC1, DC2, DC3, DC4, DC5, DC6, DC7, DC8, DC9, DC10, DC11, DC12, DC13, DC14, DC15, DC16, DC17, DC18, DC19, DC20, DC21, DC22, DC23, DC24, DC25, DC26, DC27, DC28, DC29, DC30, DC31, DC32, DC33, DC34, DC35, DC36, DC37, DC38, DC39, DC40.

A Taqman™ SNP genotyping programme “A785G SNP 3” was created using the StepOne Advanced Experiment Design programme for the following samples:

DC41, DC41, DC42, DC42, DC43, DC43, DC44, DC44, DC45, DC45, DC46, DC46, DC47, DC47, DC48, DC48, DC49, DC49, DC50, DC50, DC51, DC51, DC52, DC52, DC53, DC53, DC54, DC54, DC55, DC55.

A Taqman™ SNP genotyping programme “A785G SNP 4” was created using the StepOne Advanced Experiment Design programme for the following samples:

DC56, DC57, DC58, DC59, DC60, DC61, DC62, DC63, DC64, DC65, DC66, DC67, DC68, DC69, DC70, DC71, DC72, DC73, DC74, DC75, DC76, DC77, DC78, DC79, DC80, DC81, DC82, DC83, DC84

A Taqman™ SNP genotyping programme “A785G SNP 5” was created using the StepOne Advanced Experiment Design programme for the following samples:

DC56, DC57, DC58, DC59, DC60, DC61, DC62, DC63, DC64, DC65, DC66, DC67, DC68, DC69, DC70, DC71, DC72, DC73, DC74, DC75, DC76, DC77, DC78, DC79, DC80, DC81, DC82, DC83, DC84

The standard run time (2 hours) was selected for all of the experimental runs, with 50 cycles of 92 °C for 30 seconds and 65° for 1.30 minutes. Two negative controls and three positive controls were run for all experiments. Positive controls were allocated accordingly:

Allele1/ Allele 1 (AA) DC5

Allele 1/ Allele 2 (AG) DC15

Allele 2/ Allele 2 (GG) DC38

For all controls and samples a total well volume of 10µl was used.

2.2.6.2 Sample preparation

Sample preparation was as described above (*section 2.2.3.2*). For results see *section 3.2.1.5 A785G SNP Genotyping*, for a discussion of the results see Chapters 4, 5 & 6.

2.3 Control Sample Examination

2.3.1 DNA Extraction from buccal swabs

A non-methadone using control population of staff and student volunteers from Bournemouth University was sampled. This consisted of 45 men and 55 women. The mean age was 24 ± 0.72 (18-55 range). DNA was extracted from 100 buccal samples. The extraction was performed using 150 μ l of MasterAmp™ buccal extraction fluid (Epicentre Biotechnologies, USA) as described in section *2.1.1.1 DNA extraction from buccal swabs*.

2.3.2 Buccal DNA Quantification

The control samples extracted were quantified using the Quantifiler® Kit (Applied Biosystems, UK) on the StepOne™ real-time machine (Applied Biosystems, UK). Programmes were titled Control Run 1, Control Run 2, Control Run 3, and Control Run 4. Each programme used the standard curve quantitation setting for gDNA. The experiment run time was standard (2 hours) and the quantifiler® standards run in duplicate. The reaction plate was set up as described in section *2.1.1.1.3 Sample preparation*. For results see section *3.3.2 Buccal DNA Quantification* and for a discussion of the results see Chapter 5.

2.3.3 A118G Genotyping

Following DNA quantification the 100 control samples were genotyped for the *OPRM1* A118G variation using the validated Taqman™ assay (product no. 4351379, Applied Biosystems, UK).

2.3.3.1 Software set-up

A Taqman™ SNP genotyping programme “A118G Control SNP 1” was created using the StepOne Advanced Experiment Design programme according to the manufacturer’s instructions for the following samples:

CC1, CC2, CC3, CC4, CC5, CC6, CC7, CC8, CC9, CC10, CC11, CC12, CC13, CC14, CC15, CC16, CC17, CC18, CC19, CC20, CC21, CC22, CC23, CC24, CC25, CC26, CC27, CC28, CC29, CC30, CC31, CC32, CC33, CC34, CC35, CC36, CC37, CC38, CC39, CC40, CC41, CC42, CC43.

A Taqman™ SNP genotyping programme “A118G Control SNP 2” was created using the StepOne Advanced Experiment Design programme for the repeat SNP genotyping of:

CC1, CC2, CC3, CC4, CC5, CC6, CC7, CC8, CC9, CC10, CC11, CC12, CC13, CC14, CC15, CC16, CC17, CC18, CC19, CC20, CC21, CC22, CC23, CC24, CC25, CC26, CC27, CC28, CC29, CC30, CC31, CC32, CC33, CC34, CC35, CC36, CC37, CC38, CC39, CC40, CC41, CC42, CC43.

A Taqman™ SNP genotyping programme “A118G Control SNP 3” was created using the StepOne Advanced Experiment Design programme for the following samples:

CC44, CC45, CC46, CC47, CC48, CC49, CC50, CC51, CC52, CC53, CC54, CC55, CC56, CC57, CC58, CC59, CC60, CC61, CC62, CC63, CC64, CC65, CC66, CC67, CC68, CC69, CC70, CC71, CC72, CC73, CC74, CC75, CC76, CC77, CC78, CC79, CC80, CC81, CC82, CC83, CC84, CC85, CC86, CC87.

A Taqman™ SNP genotyping programme “A118G Control SNP 4” was created using the StepOne Advanced Experiment Design programme for the following samples:

CC44, CC45, CC46, CC47, CC48, CC49, CC50, CC51, CC52, CC53, CC54, CC55, CC56, CC57, CC58, CC59, CC60, CC61, CC62, CC63, CC64, CC65, CC66, CC67, CC68, CC69, CC70, CC71, CC72, CC73, CC74, CC75, CC76, CC77, CC78, CC79, CC80, CC81, CC82, CC83, CC84, CC85, CC86, CC87.

A Taqman™ SNP genotyping programme “A118G Control SNP 5” was created using the StepOne Advanced Experiment Design programme for the following samples:

CC88, CC88, CC89, CC89, CC90, CC90, CC91, CC91, CC92, CC92, CC93, CC93, CC94, CC94, CC95, CC95, CC96, CC96, CC97, CC97, CC98, CC98, CC99, CC99, CC100, CC100

The standard run time (2 hours) was selected for all of the experimental runs, with 50 cycles of 92 °C for 30 seconds and 65° for 1.30 minutes. Two negative controls and three positive controls were run for all experiments. Positive controls were allocated accordingly:

Allele1/ Allele 1 (AA) DC1

Allele 1/ Allele 2 (AG) DC19

Allele 2/ Allele 2 (GG) DC15

For all controls and samples a total well volume of 10µl was used.

2.3.3.2 Sample preparation

Sample preparation was as described above (*section 2.2.3.2*). For results see *section 3.3.3 A118G SNP Genotyping*, for a discussion of the results see Chapter 6.

2.3.4 T750C Genotyping

Following DNA quantification the 100 control samples were genotyped for the *CYP2B6* T750C variation using the validated Taqman™ assay (product no. 4362691, Applied Biosystems, UK).

2.3.4.1 Software set-up

A Taqman™ SNP genotyping programme “T750C Control SNP 1” was created using the StepOne Advanced Experiment Design programme according to the manufacturer’s instructions for the following samples:

CC1, CC2, CC3, CC4, CC5, CC6, CC7, CC8, CC9, CC10, CC11, CC12, CC13, CC14, CC15, CC16, CC17, CC18, CC19, CC20, CC21, CC22, CC23, CC24, CC25, CC26, CC27, CC28, CC29, CC30, CC31, CC32, CC33, CC34, CC35, CC36, CC37, CC38, CC39, CC40, CC41, CC42, CC43.

A Taqman™ SNP genotyping programme “T750C Control SNP 2” was created using the StepOne Advanced Experiment Design programme for the repeat SNP genotyping of:

CC1, CC2, CC3, CC4, CC5, CC6, CC7, CC8, CC9, CC10, CC11, CC12, CC13, CC14, CC15, CC16, CC17, CC18, CC19, CC20, CC21, CC22, CC23, CC24, CC25, CC26, CC27, CC28, CC29, CC30, CC31, CC32, CC33, CC34, CC35, CC36, CC37, CC38, CC39, CC40, CC41, CC42, CC43.

A Taqman™ SNP genotyping programme “T750C Control SNP 3” was created using the StepOne Advanced Experiment Design programme for the following samples:

CC44, CC45, CC46, CC47, CC48, CC49, CC50, CC51, CC52, CC53, CC54, CC55, CC56, CC57, CC58, CC59, CC60, CC61, CC62, CC63, CC64, CC65, CC66, CC67, CC68, CC69, CC70, CC71, CC72, CC73, CC74, CC75, CC76, CC77, CC78, CC79, CC80, CC81, CC82, CC83, CC84, CC85, CC86, CC87.

A Taqman™ SNP genotyping programme “T750C Control SNP 4” was created using the StepOne Advanced Experiment Design programme for the following samples:

CC44, CC45, CC46, CC47, CC48, CC49, CC50, CC51, CC52, CC53, CC54, CC55, CC56, CC57, CC58, CC59, CC60, CC61, CC62, CC63, CC64, CC65, CC66, CC67, CC68, CC69, CC70, CC71, CC72, CC73, CC74, CC75, CC76, CC77, CC78, CC79, CC80, CC81, CC82, CC83, CC84, CC85, CC86, CC87.

A Taqman™ SNP genotyping programme “T750C Control SNP 5” was created using the StepOne Advanced Experiment Design programme for the following samples:

CC88, CC88, CC89, CC89, CC90, CC90, CC91, CC91, CC92, CC92, CC93, CC93, CC94, CC94, CC95, CC95, CC96, CC96, CC97, CC97, CC98, CC98, CC99, CC99, CC100, CC100

The standard run time (2 hours) was selected for all of the experimental runs, with 50 cycles of 92 °C for 30 seconds and 65° for 1.30 minutes. Two negative controls and three positive controls were run for all experiments. Positive controls were allocated accordingly:

Allele1/ Allele 1 (TT) DC2

Allele 1/ Allele 2 (TC) DC1

Allele 2/ Allele 2 (CC) DC13

For all controls and samples a total well volume of 10µl was used.

2.3.4.2 Sample preparation

Sample preparation was as described above (*section 2.2.3.2*). For results see *section 3.3.4 T750C SNP Genotyping*, for a discussion of the results see Chapter 6.

2.3.5 G516T Genotyping

Following DNA quantification the 100 control samples were genotyped for the *CYP2B6* G516T variation using the custom designed Taqman™ assay (product no. 4362691, Applied Biosystems, UK).

2.3.5.1 Software set-up

A Taqman™ SNP genotyping programme “G516T Control SNP 1” was created using the StepOne Advanced Experiment Design programme according to the manufacturer’s instructions for the following samples:

CC1, CC2, CC3, CC4, CC5, CC6, CC7, CC8, CC9, CC10, CC11, CC12, CC13, CC14, CC15, CC16, CC17, CC18, CC19, CC20, CC21, CC22, CC23, CC24, CC25, CC26, CC27, CC28, CC29, CC30, CC31, CC32, CC33, CC34, CC35, CC36, CC37, CC38, CC39, CC40, CC41, CC42, CC43.

A Taqman™ SNP genotyping programme “G516T Control SNP 2” was created using the StepOne Advanced Experiment Design programme for the repeat SNP genotyping of:

CC1, CC2, CC3, CC4, CC5, CC6, CC7, CC8, CC9, CC10, CC11, CC12, CC13, CC14, CC15, CC16, CC17, CC18, CC19, CC20, CC21, CC22, CC23, CC24, CC25, CC26, CC27, CC28, CC29, CC30, CC31, CC32, CC33, CC34, CC35, CC36, CC37, CC38, CC39, CC40, CC41, CC42, CC43.

A Taqman™ SNP genotyping programme “G516T Control SNP 3” was created using the StepOne Advanced Experiment Design programme for the following samples:

CC44, CC45, CC46, CC47, CC48, CC49, CC50, CC51, CC52, CC53, CC54, CC55, CC56, CC57, CC58, CC59, CC60, CC61, CC62, CC63, CC64, CC65, CC66, CC67, CC68, CC69, CC70, CC71, CC72, CC73, CC74, CC75, CC76, CC77, CC78, CC79, CC80, CC81, CC82, CC83, CC84, CC85, CC86, CC87.

A Taqman™ SNP genotyping programme “G516T Control SNP 4” was created using the StepOne Advanced Experiment Design programme for the following samples:

CC44, CC45, CC46, CC47, CC48, CC49, CC50, CC51, CC52, CC53, CC54, CC55, CC56, CC57, CC58, CC59, CC60, CC61, CC62, CC63, CC64, CC65, CC66, CC67, CC68, CC69, CC70, CC71, CC72, CC73, CC74, CC75, CC76, CC77, CC78, CC79, CC80, CC81, CC82, CC83, CC84, CC85, CC86, CC87.

A Taqman™ SNP genotyping programme “G516T Control SNP 5” was created using the StepOne Advanced Experiment Design programme for the following samples:

CC88, CC88, CC89, CC89, CC90, CC90, CC91, CC91, CC92, CC92, CC93, CC93, CC94, CC94, CC95, CC95, CC96, CC96, CC97, CC97, CC98, CC98, CC99, CC99, CC100, CC100

The standard run time (2 hours) was selected for all of the experimental runs, with 50 cycles of 92 °C for 30 seconds and 65° for 1.30 minutes. Two negative controls and three positive controls were run for all experiments. Positive controls were allocated accordingly:

Allele1/ Allele 1 (GG) DC13

Allele 1/ Allele 2 (GT) DC1

Allele 2/ Allele 2 (TT) DC38

For all controls and samples a total well volume of 10µl was used.

2.3.5.2 Sample preparation

Sample preparation was as described above (*section 2.2.3.2*). For results see *section 3.3.5 G516T SNP Genotyping*, for a discussion of the results see Chapter 6.

2.3.6 A785G Genotyping

Following DNA quantification the 100 control samples were genotyped for the *CYP2B6* A785G variation using the validated Taqman™ assay (product no. 4331349, Applied Biosystems, UK).

2.3.6.1 Software set-up

A Taqman™ SNP genotyping programme “A785G Control SNP 1” was created using the StepOne Advanced Experiment Design programme according to the manufacturer’s instructions for the following samples:

CC1, CC2, CC3, CC4, CC5, CC6, CC7, CC8, CC9, CC10, CC11, CC12, CC13, CC14, CC15, CC16, CC17, CC18, CC19, CC20, CC21, CC22, CC23, CC24, CC25, CC26, CC27, CC28, CC29, CC30, CC31, CC32, CC33, CC34, CC35, CC36, CC37, CC38, CC39, CC40, CC41, CC42, CC43.

A Taqman™ SNP genotyping programme “A785G Control SNP 2” was created using the StepOne Advanced Experiment Design programme for the repeat SNP genotyping of:

CC1, CC2, CC3, CC4, CC5, CC6, CC7, CC8, CC9, CC10, CC11, CC12, CC13, CC14, CC15, CC16, CC17, CC18, CC19, CC20, CC21, CC22, CC23, CC24, CC25, CC26, CC27, CC28, CC29, CC30, CC31, CC32, CC33, CC34, CC35, CC36, CC37, CC38, CC39, CC40, CC41, CC42, CC43.

A Taqman™ SNP genotyping programme “A785G Control SNP 3” was created using the StepOne Advanced Experiment Design programme for the following samples:

CC44, CC45, CC46, CC47, CC48, CC49, CC50, CC51, CC52, CC53, CC54, CC55, CC56, CC57, CC58, CC59, CC60, CC61, CC62, CC63, CC64, CC65, CC66, CC67, CC68, CC69, CC70, CC71, CC72, CC73, CC74, CC75, CC76, CC77, CC78, CC79, CC80, CC81, CC82, CC83, CC84, CC85, CC86, CC87.

A Taqman™ SNP genotyping programme “A758G Control SNP 4” was created using the StepOne Advanced Experiment Design programme for the following samples:

CC44, CC45, CC46, CC47, CC48, CC49, CC50, CC51, CC52, CC53, CC54, CC55, CC56, CC57, CC58, CC59, CC60, CC61, CC62, CC63, CC64, CC65, CC66, CC67, CC68, CC69, CC70, CC71, CC72, CC73, CC74, CC75, CC76, CC77, CC78, CC79, CC80, CC81, CC82, CC83, CC84, CC85, CC86, CC87.

A Taqman™ SNP genotyping programme “A758G Control SNP 5” was created using the StepOne Advanced Experiment Design programme for the following samples:

CC88, CC88, CC89, CC89, CC90, CC90, CC91, CC91, CC92, CC92, CC93, CC93, CC94, CC94, CC95, CC95, CC96, CC96, CC97, CC97, CC98, CC98, CC99, CC99, CC100, CC100

The standard run time (2 hours) was selected for all of the experimental runs, with 50 cycles of 92 °C for 30 seconds and 65° for 1.30 minutes. Two negative controls and three positive controls were run for all experiments. Positive controls were allocated accordingly:

Allele1/ Allele 1 (AA) DC5

Allele 1/ Allele 2 (AG) DC15

Allele 2/ Allele 2 (GG) DC38

For all controls and samples a total well volume of 10µl was used.

2.3.6.2 Sample preparation

Sample preparation was as described above (*section 2.2.3.2*). For results see *section*

3.3.6 A785G SNP Genotyping, for a discussion of the results see Chapter 6.

2.4 *CYP2B6* cloning

2.4.1 Primary Cloning strategy

The sequence information for the *CYP2B6* promoter regions was analysed, identifying the stages of cloning using Redasoft software. The cloning strategies are highlighted in Figure 4.

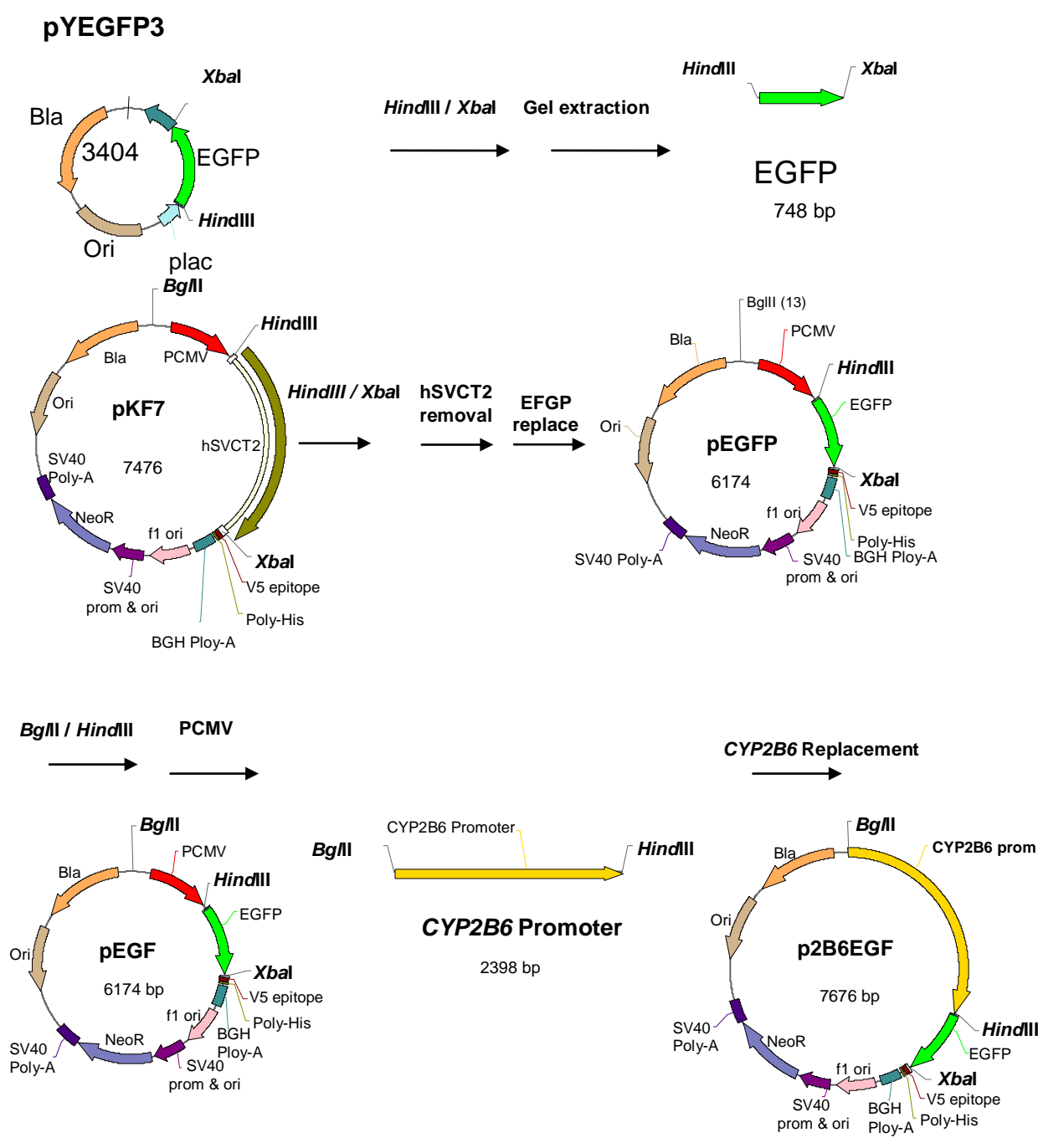


Figure 4: Molecular cloning strategy for *CYP2B6* promoter region.

2.4.2 Plasmid DNA preparation

E. coli strains harbouring the hSVC2 and EGFP plasmids were cultured on LB ampicillin agar plates overnight at 37° C. Plasmid DNA was extracted using the Quicklyse Miniprep kit (Qiagen, UK) according to the manufacturer's protocol.

2.4.3 *HindIII* & *XbaI* digest

Restriction digests for the hSVCT2 and EFGP plasmid DNA were conducted using the *HindIII*, *BamHI*, and *XbaI* restriction enzymes. The digests were conducted with a total volume of 50µl, including 37.5µl PCR grade water, 5µl buffer 2 (x10) (New England Biolabs), 5µl DNA, 1µl BSA (New England Biolabs), 0.5µl *HindIII*, 0.5µl *BamHI* and 0.5µl *XbaI* (New England Biolabs). The samples were left to incubate for 3 hours at 37° C before the reaction was terminated with 10µl 6x blue dye (New England Biolabs). The results were confirmed by gel electrophoresis (1.6 % Agarose & Cyber Green gel) and visualised using blue light (Figure 50). Uncut DNA (1µl) with 4µl TE buffer and 6 x blue dye was used as a control. For results see section *3.4.1.1 Examination of the plasmid by HindIII & XbaI Digest.*

2.4.4 Gel Extraction of EGFP Gene

The EGFP inserts were cut from the gel and extracted using the QIAquick gel extraction kit (Qiagen, UK) in accordance with the manufacturer's instructions. The extraction was confirmed by gel electrophoresis (2 % Agarose & Cyber Green gel) and visualised under blue light (Figures 51, 52).

2.4.5 Gel Extraction of hSVCT2 Gene

The hSVCT2 inserts were cut from the gel and extracted using the QIAquick gel extraction kit (Qiagen, UK) in accordance with the manufacturer's instructions. The extraction was confirmed by gel electrophoresis (2 % Agarose & Cyber Green gel) and visualised under blue light (Figures 53, 54).

2.4.6 DNA ligation of EGFP into hSVCT2 vector

A 1:1 ratio between the hSVCT2 vector and the EGFP insert was determined, equal to 1 μ l of hSVCT2: 8 μ l of EGFP. A series of different vector: insert ratios was tested (Table 14) to determine the optimal ligation ratio for transformation. Reactions A (0/1) and G (1/0) acted as negative controls to test enzymatic efficiency. Additionally, a single cut vector was used in the reaction both with DNA ligase (DDL) and without DNA ligase (DDM) to test reaction efficiency. Finally a positive control (LDH) for the ligation was conducted using a Lamda-HindIII control sample (New England Biolabs, UK).

Table 14: Reaction components for the DNA ligation of EGFP into the hSVCT2 vector.

Reaction components	A 0/1	B 1/3	C 1/2	D 1/1	E 2/1	F 3/1	G 1/0	DDL	DDM	LHD
Water (μ l)	8.5	1.5	0	7.5	6.5	5.5	15.5	15.5	16	14.5
Vector (μ l)	0	1	1	1	2	3	1	1	1	2
Insert (μ l)	8	24	16	8	8	8	0	0	0	0
Buffer (μ l)	3	3	3	3	3	3	3	3	3	3
T4 DNA ligase (μ l)	0.5	0.5	0.5	0.5	0.5	0.5	0.5	0.5	0	0.5
Final Volume (μ l)	20	30	20.5	20	20	20	20	20	20	20

The reactions were set up according to the manufacturer's instructions (Table 14) and left to incubate at room temperature for 30 minutes. The ligation was confirmed by gel electrophoresis (2 % Agarose & Cyber Green gel) of LDH and visualisation under blue light (Figure 55).

2.4.7 Transformation of EGFP clone into JM109 cells

The ligated hSVCT2-EGFP vector was transformed into JM109 competent cells (Promega, UK) according to the manufacturer's instructions. Briefly, on ice, 5µl of ligated product was added to 100µl of competent cells and incubated for ten minutes. The reactions were heated at 42 °C for 45 seconds before being returned to ice for two minutes. After this 900µl of SOC media was added and the reactions were incubated at 37 °C for 6 minutes before being streaked onto LB-ampicillin plates. The plates were incubated at 37 °C for 15 hours. The resulting colonies were verified by conducting *NdeI* restriction digests (Figures 56, 57, 58, 59).

2.4.8 PCR amplification of *CYP2B6* promoter region

2.4.8.1 Primer design and Rehydration

CYP2B6 promoter sequence information was used to design three sets of primers for the amplification of the gene promoter region for the cloning experiment (Table 15). The following primers C2B6F1 *Bgl*II, C2B6F2, CSB6F3, C2B6R1 *Hind*III, C2B6R2, and C2B6R3 were hydrated with appropriate amounts of T₁₀ buffer according to their molecular weight (Table 16). Primers were left for 20 minutes at room temperature to dissolve before being stored at -20°C until used.

Table 15: *CYP2B6* promoter primer sequences.

Primer	<i>CYP2B6</i> Amplified Region	Primer sequence	Annealing temperature °C
C2B6F1 <i>Bgl</i> II *	Promoter region	ata AGATC TTTCTGGTTTTACGGCTCAG	62.2
C2B6F2	Promoter region	GTTACTGTGTGTAAAGCACTT	54.0
C2B6F3	Promoter region	GCTATGCTACAAAGGCAGT	54.5
C2B6R1 <i>Hind</i> III **	Promoter region	att AAGCTT CATCATCCAGGAGCATTAGCTT	61.9
C2B6R2	Promoter region	ACTGCCTTTGTAGCATAGC	54.4
C2B6R3	Promoter region	AAGTGCTTTACACACAGTAAC	54.0

* F denotes forward primer ** R denotes reverse primer

Table 16: *CYP2B6* promoter primer rehydration volumes.

PRIMERS	Volume of T ₁₀ required for a concentration of 100 pmol/μl.
C2B6F1 <i>Bgl</i> II *	232μl
C2B6F2	173μl
C2B6F3	175μl
C2B6R1 <i>Hind</i> III **	187μl
C2B6R2	273μl
C2B6R3	248μl

* F denotes forward primer ** R denotes reverse primer

2.4.8.2 Primer validation

The proximal promoter region including –750 T > C was amplified by PCR. The primers used were 19-24 mer oligonucleotides (Table 15). These were synthesised by COGENICS (UK). The sequence of each primer pair, the position in the *CYP2B6* gene, and the calculated annealing temperatures are shown in Table 15. PCRs were performed with a reaction volume of 50 μl, including 27.5 μl PCR grade water (Sigma), 10 μl of 5x GoTaq™ buffer (Promega, UK), 6 μl MgCl₂, 1 μl of 10 mM deoxynucleoside triphosphates (dNTPs) (Roche, UK) (final concentration of 0.25 mM), 1 μl Forward and Reverse primers, 3 μl DNA and 0.5 μl GoTaq™ DNA polymerase (Promega, UK). The cycling conditions were as follows: initial denaturation at 95°C for 5 minutes; subsequent denaturation at 95°C for 1 minute;

annealing at 60-62°C for 30 seconds; primer extension at 72°C for 2 minutes, repeated for 30 cycles, followed by final extension at 72°C for 5 minutes. The PCR products were confirmed by electrophoresis with a 2 % Cyber Green-agarose gel on blue light (Figure 60). PCR reactions were performed with a Primus 96 advanced machine.

2.4.8.3 PCR temperature development

In order to determine the optimal annealing temperature for C2B6F1 *Bgl*I and C2B6R1 *Hind*III a gradient PCR was conducted. Additionally to reduce smearing the MgCl₂ concentration was reduced. PCRs were performed with a reaction volume of 50 µl, including 28.5 µl PCR grade water (Sigma), 10 µl of 5x GoTaq™ buffer (Promega, UK), 5 µl MgCl₂, 1 µl of 10 mM deoxynucleoside triphosphates (dNTPs) (Roche, UK) (final concentration of 0.25 mM), 1 µl Forward and Reverse primers, 3 µl DNA and 0.5 µl GoTaq™ DNA polymerase (Promega, UK). The cycling conditions were as follows: initial denaturation at 95°C for 5 minutes; subsequent denaturation at 95°C for 1 minute; gradient reaction for annealing 58.0-65.2°C for 30 seconds; primer extension at 72°C for 2 minutes, repeated for 30 cycles, followed by final extension at 72°C for 5 minutes. The PCR products were confirmed by electrophoresis with a 2 % Cyber Green-agarose gel on blue light (Figure 61). PCR reactions were performed with a Primus 96 advanced machine (Alpha Laboratories, UK).

2.4.8.4 Amplification of *CYP2B6* promoter region.

The *CYP2B6* promoter regions for T750C heterozygous, homozygous wild type and homozygous variant subjects were amplified using the 60.2 ° C annealing temperature parameter from the gradient reaction. PCRs were performed with a reaction volume of

50 µl, including 28.5 µl PCR grade water (Sigma), 10 µl of 5x GoTaq™ buffer (Promega, UK), 5 µl MgCl₂, 1 µl of 10 mM deoxynucleoside triphosphates (dNTPs) (Roche, UK) (final concentration of 0.25 mM), 1 µl Forward and Reverse primers, 3 µl DNA and 0.5 µl GoTaq™ DNA polymerase (Promega, UK). The cycling conditions were as follows: initial denaturation at 95°C for 5 minutes; subsequent denaturation at 95°C for 1 minute; gradient reaction for annealing 60.2 °C for 30 seconds; primer extension at 72°C for 2 minutes, repeated for 30 cycles, followed by final extension at 72°C for 5 minutes. The PCR products were confirmed by electrophoresis with a 2 % Cyber Green-agarose gel on blue light (Figure 62). PCR reactions were performed with a Primus 96 advanced machine.

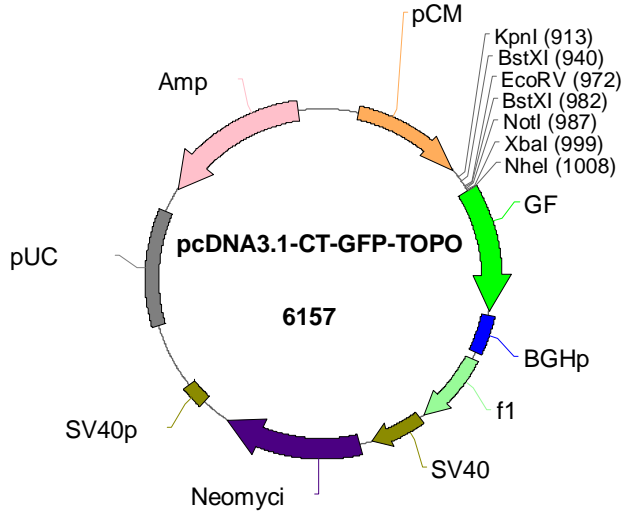
2.4.8.5 Gel Extraction of CYP2B6 promoter region

The *CYP2B6* wild type, heterozygous and homozygous variant amplified promoters were cut from the gel and extracted using the QIAquick gel extraction kit (Qiagen, UK) in accordance with the manufacturer's instructions. After this a dATP extension was conducted to ensure (a) overhangs for ligation into the vector. For this 5 µl of Flexi Buffer (10 x), 1 µl of dATP and 0.5 µl of GoTaq™ was added to the gel extracted *CYP2B6* promoters. This was followed by a 15 minute incubation at 72 °C. The extraction was confirmed by gel electrophoresis (2 % Agarose & Cyber Green gel) and visualised under blue light.

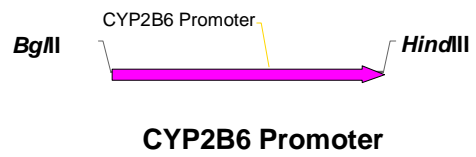
2.4.9 Alternative Cloning strategy

The cloning strategy for inserting the *CYP2B6* promoter regions into the pcDNA3.1/CT-GFP-TOPO® vector (Invitrogen) was conducted, using Redasoft software. The cloning strategies are highlighted in Figure 5.

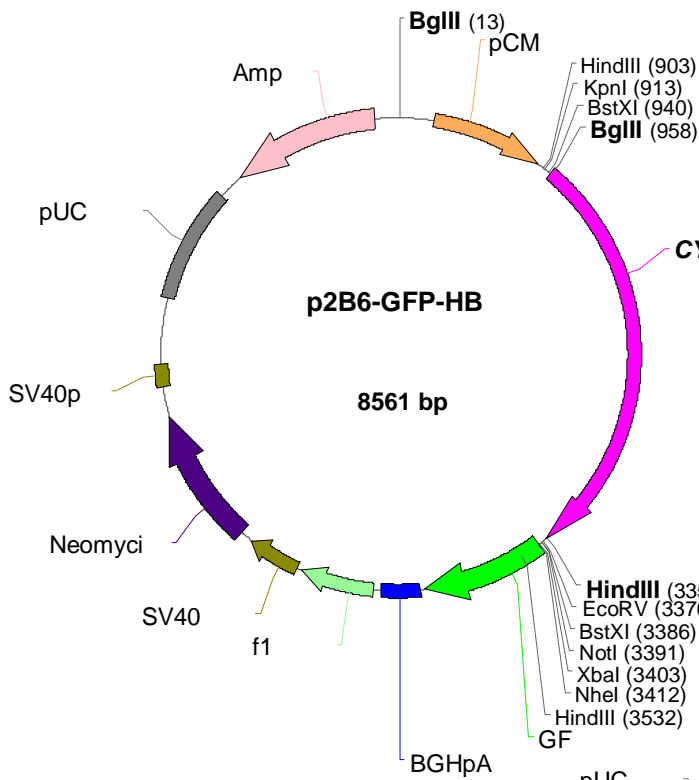
PcDNA3.1-CT-GFP-TOPO Vector



Amplification of *CYP2B6* promoter regions



Insertion of *CYP2B6* promoter regions for 750TT, 750TC, & 750CC.



← Required *CYP2B6* orientation

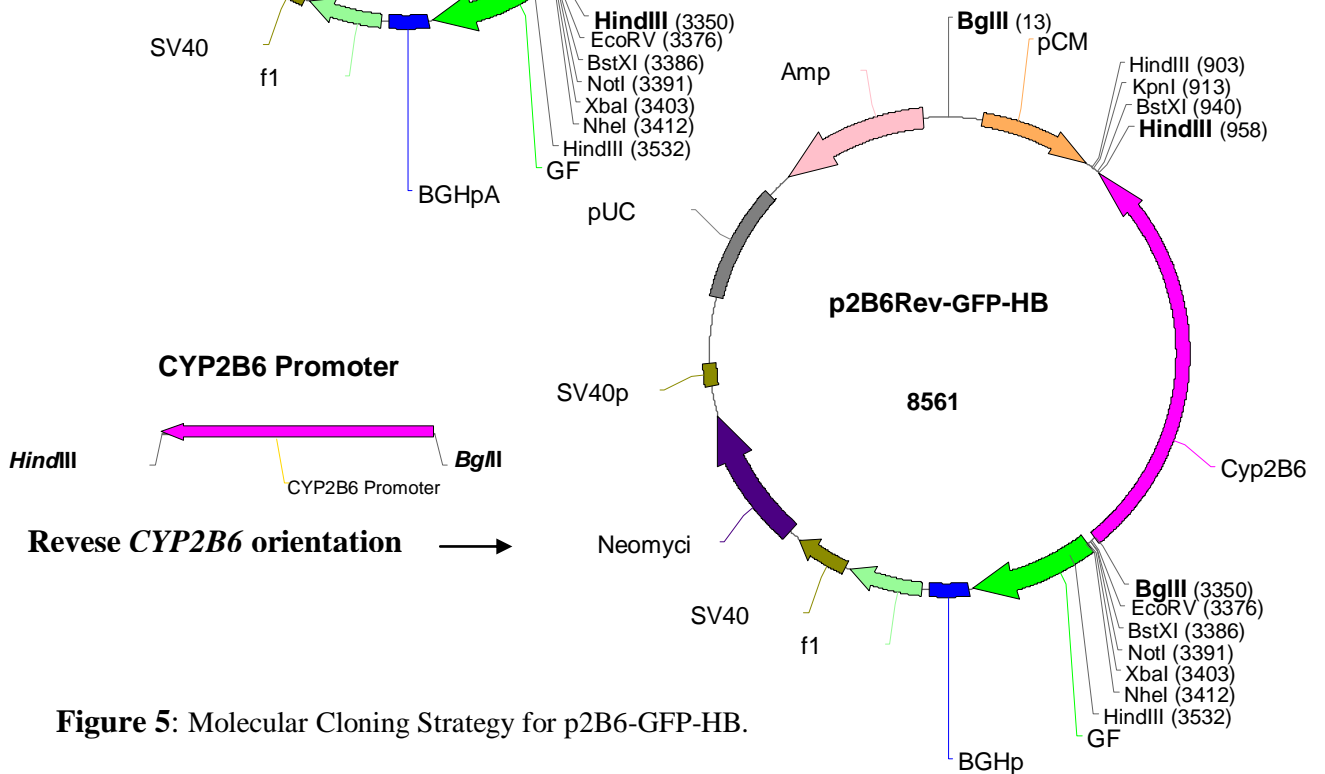


Figure 5: Molecular Cloning Strategy for p2B6-GFP-HB.

2.4.10 *CYP2B6* promoter insertion into pcDNA3.1/CT-GFP-TOPO® vector

2.4.10.1 DNA ligation of *CYP2B6* into pcDNA3.1/CT-GFP-TOPO® vector

The *CYP2B6* promoter regions were ligated into the pcDNA3.1/CT-GFP-TOPO® (Invitrogen, UK) vector according to the manufacturers instructions (Table 17).

Table 17: Reaction components for the DNA ligation of *CYP2B6* into the pcDNA3.1/CT-GFP-TOPO® vector.

<i>CYP2B6</i> Reaction		Control Reaction	
Reagent	Volume	Reagent	Volume
Fresh PCR product	4 µl	Control PCR product	1 µl
Salt Solution	1µl	Salt Solution	1µl
Sterile Water	1µl	Sterile Water	3µl
TOPO Vector	1µl	TOPO Vector	1µl
Total Volume	7µl	Total Volume	6µl

In order to test ligation efficiency a control PCR reaction was also conducted. The samples were incubated at room temperature for 30 minutes.

2.4.10.2 Transformation of p2B6-GFP-HB clones into OneShot® TOP10 *E. coli*

The homozygous wild type, heterozygous and homozygous variant p2B6-GFP-HB clones were transformed into OneShot® TOP10 chemically competent *E. coli* following the manufacturer's protocol. Briefly 2 µl of each TOPO® Cloning reaction (including the control reaction) was added into a vial of OneShot® TOP10 chemically competent *E. coli* and mixed gently. The vials were then incubated on ice for five minutes. The cells were then heat-shocked at 42 °C, before being immediately transferred back to ice. After this 250 µl of room temperature SOC medium was added and the vials were capped tightly and shook (horizontally) at 200 rpm at 37 °C for 1 hour. Then 125 µl from each transformation was spread onto a prewarmed LB ampicillin plate. Two plates for each transformation were prepared these were then

incubated for 16 hours at 37 °C. The resulting colonies were verified by conducting a *Bgl*III & *Hind*III double restriction digest and a *Bgl*III single digest to check *CYP2B6* orientation (Figures 63, 64, 65).

2.4.10.3 p2B6-GFP-HB Clone Sequencing

Each p2B6-GFP-HB clone was sent off for sequencing to COGENICS to confirm the successful transformation of the *CYP2B6* promoter region into the TOPO® TA vector.

2.5 A118G Methadone Binding Study

2.5.1 B-Cell line DNA extraction

A total of 44 chronic lymphoid leukaemia (CLL) primary B-cell lines were extracted using the DNeasy Blood Extraction Kit as per the manufacturer's instructions (Table 18) to identify 118 AG/GG subjects.

Table 18: Qiagen DNeasy Extraction Components and Volumes.

Sample size	Proteinase K	PBS (7.2 pH)	Buffer AL	Ethanol (100%)	Buffer AW1	Buffer AW2	Buffer AE
100 µl	20 µl	200 µl	200 µl	200 µl	500 µl	500 µl	200 µl

2.5.2 Quantification of DNA from post-mortem blood

The B-cell CLL DNA samples were quantified using the Nanodrop (Thermo Scientific, Wilmington, USA). For results *Section 3.5.1 B-cell line DNA Quantification*.

2.5.3 A118G SNP Genotyping

After DNA quantification the samples were genotyped for the *OPRM1* A118G variation using the validated Taqman™ assay (product no. 4351379, Applied Biosystems, UK).

2.5.3.1 Software set-up

A Taqman™ SNP genotyping programme “CLL A118G typing 1” was created using the StepOne Advanced Experiment Design programme according to the manufacturer's instructions for the following samples:

CL1, CL1, CL2, CL2, CL3, CL3, CL4, CL4, CL5, CL5, CL6, CL6, CL7, CL7, CL8, CL8, CL9, CL9, CL10, CL10, CL11, CL11, CL12, CL12, CL13, CL13, CL14, CL14, CL15, CL15, CL16, CL16, CL17, CL17, CL18, CL18, CL19, CL19, CL20, CL20, CL21, CL21, CL22, CL22.

The standard run time (2 hours) was selected, with 50 cycles of 92 °C for 30 seconds and 65° for 1.30 minutes. Two negative controls and two positive controls were run for all experiments. Positive controls were allocated accordingly:

Allele1/ Allele 1 (AA) CC1

Allele 1/ Allele 2 (AG) CC3

For all controls and samples a total well volume of 10µl was used.

A Taqman™ SNP genotyping programme “CLL A118G typing 2” was created using the StepOne Advanced Experiment Design programme according to the manufacturer’s instructions for the following samples:

CL23, CL23, CL24, CL24, CL25, CL25, CL26, CL26, CL27, CL27, CL28, CL28, CL29, CL29, CL30, CL30, CL31, CL31, CL32, CL32, CL33, CL33, CL34, CL34, CL35, CL35, CL36, CL36, CL37, CL37, CL38, CL38, CL39, CL39, CL40, CL40, CL41, CL41, CL42, CL42, CL43, CL43, CL44, CL44.

The standard run time (2 hours) was selected, with 50 cycles of 92 °C for 30 seconds and 65° for 1.30 minutes. Two negative controls and two positive controls were run for all experiments. Positive controls were allocated accordingly:

Allele1/ Allele 1 (AA) CC1

Allele 1/ Allele 2 (AG) CC3

For all controls and samples a total well volume of 10µl was used.

2.5.3.2 Sample preparation

The Taqman™ mastermix, SNP assay mix, and DNase free H₂O (Table 13) for each experimental run (including an extra 10% for excess) was calculated and a mastermix created. Then 9µl of the prepared master mix was added into each well of a 48-well optical plate. For the negative control wells 10µl of reaction mix was added. Finally 1µl of the appropriate samples/positive controls were added to each well; following the plate layout generated when setting up the StepOne™ quantification experiment. For results see *Section 3.5.2 A118G SNP Genotyping*, for a discussion of the results see Chapter 8.

2.5.4 Receptor Internalisation

2.5.4.1 Primary anti-µ and secondary anti-rabbit IgGFITC Optimisation

Using a whole blood sample from a CLL subject (stored at room temperature for 4 days) an assay was conducted to determine the optimal primary and secondary antibody concentrations for µ receptor binding. The rabbit monoclonal [EP1470Y] to µ opioid receptor (Abcam, Cambridge, UK) acted as the primary antibody and the goat polyclonal to rabbit IgG – H&L (Fluorescein isothiocyanate, FITC) (Abcam, UK) acted as the secondary antibody. For both the primary and secondary antibodies 1:10, 1:20, and 1:50 concentrations were tested according to the strategy outlined in Table 19. A positive control using the kappa and lambda antibodies with the secondary rabbit IgG was performed.

Table 19: Reaction strategy 1 to determine optimal antibody concentration.

Tube	Reaction	Primary antibody	Secondary antibody
1	Negative Control	1:10 anti- μ (2 μ l)	
2	Negative Control		1:10 anti-rabbit IgG (2 μ l)
3	Positive Control	anti Kappa(2 μ l) anti-Lambda (2 μ l)	1:10 anti-rabbit IgG (2 μ l)
4	Test Reaction	1:10 anti- μ (2 μ l)	1:10 anti-rabbit IgG (2 μ l)
5	Test Reaction	1:10 anti- μ (2 μ l)	1:20 anti-rabbit IgG (2 μ l)
6	Test Reaction	1:10 anti- μ (2 μ l)	1:50 anti-rabbit IgG (2 μ l)
7	Test Reaction	1:20 anti- μ (2 μ l)	1:10 anti-rabbit IgG (2 μ l)
8	Test Reaction	1:20 anti- μ (2 μ l)	1:20 anti-rabbit IgG (2 μ l)
9	Test Reaction	1:20 anti- μ (2 μ l)	1:50 anti-rabbit IgG (2 μ l)
10	Test Reaction	1:50 anti- μ (2 μ l)	1:10 anti-rabbit IgG (2 μ l)
11	Test Reaction	1:50 anti- μ (2 μ l)	1:20 anti-rabbit IgG (2 μ l)
12	Test Reaction	1:50 anti- μ (2 μ l)	1:50 anti-rabbit IgG (2 μ l)

A blood cell count was conducted on the whole blood sample with a white blood cell (WBC) cell count of 40×10^6 cells/ml. For the assay a million cells per reaction was required = 25 μ l of whole blood per reaction, which was transferred into 12 labelled flow tubes. Next 75 μ l of FACSFlow (BD Biosciences, UK) solution was added to the blood. Using the strategy outlined in Table 19 2 μ l of the relevant primary antibody concentration was added to the reactions and incubated at 4°C for 30 minutes.

Following this the samples were washed with FACSFlow centrifuged at 13,000 rpm for 5 minutes. The supernatant was discarded leaving a pellet and approximately 100 μ l of solution in the flow tubes. Next 2 μ l of the secondary antibody was added and the reactions incubated at 4°C for 30 minutes. After incubation 1 ml of FACSLyse (BD Biosciences, UK) was added to the reactions and vortexed to lyse the red blood cells. The reactions were incubated at room temperature for 5 minutes before centrifugation at 13,000 rpm for 5 minutes. The supernatant was discarded and the pellet re-suspended in 100 μ l of FACSFlow. Each reaction was tested with a flow cytometer which was set to record 10,000 events at 700 volts. The data was analysed by examining forward scatter, side scatter and anti- μ + anti-rabbit IgGFITC.

Following gating of the lymphocyte cell population histograms were generated and the geometric means for each reaction were deduced.

2.5.4.2 Blockage of Fc receptors to improve Antibody-Receptor Binding

Using a whole blood sample from a CLL subject (collected that day) an assay was conducted to test the effects of human AB (HAB) serum on blocking Fc receptors (thought to be influencing the high baseline for the secondary antibody). A positive control using the kappa and lambda antibodies with the secondary rabbit IgG was performed. The reaction strategy used was as outlined above in Table 19. The white blood cell (WBC) cell count was 20×10^6 cells/ml. For the assay 100 μ l of HAB serum was added to 100 μ l of whole blood and incubated at room temperature for 5 minutes to block the interfering Fc receptors. After this the experiment was performed as discussed earlier. Each reaction was tested with a flow cytometer which was set to record 10,000 events at 700 volts. The data was analysed by examining forward scatter, side scatter and anti- μ + anti-rabbit IgGFITC. Following gating of the lymphocyte cell population histograms were generated and the geometric means for each reaction were deduced.

2.5.4.3 Primary anti- μ and secondary anti-rabbit IgGPE Optimisation

Using a whole blood sample from a CLL subject (stored at 4°C for 2 days) an assay was conducted to test a new monoclonal secondary antibody. The rabbit monoclonal [EP1470Y] to μ opioid receptor (Abcam, Cambridge, UK) acted as the primary antibody and the mouse monoclonal to rabbit IgG – R-Phycoerythrin (PE) (Acris Antibodies, Herford, Germany) acted as the secondary antibody.

A positive control using the kappa and lambda antibodies with the secondary rabbit IgG was performed. Additionally the polyclonal rabbit IgG-FITC (Abcam, UK) antibody was tested as a control for binding to the primary antibody (Table 20).

Table 20: Reaction strategy 2 to determine optimal antibody concentration.

Tube	Reaction	Primary antibody	Secondary antibody - PE	Secondary antibody - FITC
1	Negative Control	1:20 anti- μ		
2	Negative Control		1:10 anti-rabbit IgG	
3	Test Reaction	1:10 anti- μ	1:10 anti-rabbit IgG	
4	Test Reaction	1:10 anti- μ	1:20 anti-rabbit IgG	
5	Test Reaction	1:10 anti- μ	1:50 anti-rabbit IgG	
6	Test Reaction	1:20 anti- μ	1:10 anti-rabbit IgG	
7	Test Reaction	1:20 anti- μ	1:20 anti-rabbit IgG	
8	Test Reaction	1:20 anti- μ	1:50 anti-rabbit IgG	
9	Test Reaction	1:50 anti- μ	1:10 anti-rabbit IgG	
10	Test Reaction	1:50 anti- μ	1:20 anti-rabbit IgG	
11	Test Reaction	1:50 anti- μ	1:50 anti-rabbit IgG	
12	Test Reaction			1.10 anti-rabbit IgG
13	Test Reaction	1:20 anti- μ		1.10 anti-rabbit IgG
14	Positive Control	anti Kappa anti-Lambda	1:10 anti-rabbit IgG	

The white blood cell (WBC) cell count was 20×10^6 cells/ml. Using the strategy outlined in Table 20 the experiment was conducted as previously described. Each reaction was tested with a flow cytometer which was set to record 10,000 events at 700 volts. The data was analysed by examining forward scatter, side scatter and anti- μ + anti-rabbit IgG PE and anti- μ + anti-rabbit FITC. Following gating of the lymphocyte cell population histograms were generated and the geometric means for each reaction were deduced.

2.5.4.4 Primary anti- μ and secondary anti-rabbit IgGFITC Optimisation

Using a whole blood sample from a CLL subject (stored at 4°C for 2 days) an assay was conducted to determine the optimal primary and secondary antibody concentrations for the rabbit polyclonal to μ opioid receptor (ab10275, Abcam, Cambridge, UK) and the goat polyclonal to rabbit IgG – H&L (Fluorescein isothiocyanate, FITC) (Abcam, UK), and mouse monoclonal to rabbit IgG – R-Phycoerythrin (PE) (Acris Antibodies, Herford, Germany) secondary antibodies. For both the primary and secondary antibodies 1:10, 1:100, and 1:1000 concentrations were tested according to the strategy outlined in Table 21. A positive control using the kappa and lambda antibodies with the secondary rabbit IgG was performed.

Table 21: Reaction strategy 3 to determine optimal antibody concentration.

Tube	Reaction	Primary antibody	Secondary antibody - PE	Secondary antibody - FITC
1	Negative Control	1:10 anti- μ		
2	Negative Control			1:10 anti-rabbit IgG
3	Negative Control		1:10 anti-rabbit IgG	
4	Test Reaction	1:10 anti- μ		1:10 anti-rabbit IgG
5	Test Reaction	1:10 anti- μ		1:100 anti-rabbit IgG
6	Test Reaction	1:10 anti- μ		1:1000 anti-rabbit IgG
7	Test Reaction	1:100 anti- μ		1:10 anti-rabbit IgG
8	Test Reaction	1:100 anti- μ		1:100 anti-rabbit IgG
9	Test Reaction	1:100 anti- μ		1:1000 anti-rabbit IgG
10	Test Reaction	1:1000 anti- μ		1:10 anti-rabbit IgG
11	Test Reaction	1:1000 anti- μ		1:100 anti-rabbit IgG
12	Test Reaction	1:1000 anti- μ		1:1000 anti-rabbit IgG
13	Test Reaction	1:10 anti- μ	1:10 anti-rabbit IgG	
14	Test Reaction	1:10 anti- μ	1:100 anti-rabbit IgG	
15	Test Reaction	1:10 anti- μ	1:1000 anti-rabbit IgG	
16	Test Reaction	1:100 anti- μ	1:10 anti-rabbit IgG	
17	Test Reaction	1:100 anti- μ	1:100 anti-rabbit IgG	
18	Test Reaction	1:100 anti- μ	1:1000 anti-rabbit IgG	
19	Test Reaction	1:1000 anti- μ	1:10 anti-rabbit IgG	
20	Test Reaction	1:1000 anti- μ	1:100 anti-rabbit IgG	
21	Test Reaction	1:1000 anti- μ	1:1000 anti-rabbit IgG	
22	Positive Control	anti Kappa anti-Lambda	1:10 anti-rabbit IgG	

The white blood cell (WBC) cell count was 20×10^6 cells/ml. Using the strategy outlined in Table 21 the experiment was conducted as previously described. Each reaction was tested with a flow cytometer which was set to record 10,000 events at 700 volts. The data was analysed by examining forward scatter, side scatter and anti- μ + anti-rabbit IgG PE and anti- μ + anti-rabbit FITC. Following gating of the lymphocyte cell population histograms were generated and the geometric means for each reaction were deduced.

2.5.5 Racemic Methadone Binding Study

2.5.5.1 The effects of cell culture incubation interval on cell apoptosis

A total of 4 CLL primary B-cell lines were selected for cell culture to determine the effects of cell culture incubation interval on cellular apoptosis. The cells were rapidly thawed in a water bath at 37°C before being resuspended in 10 ml of culture media. The samples were then centrifuged at 1,500 rpm for 5 minutes, the supernatant was discarded and the pelleted cells were resuspended in 3 ml of fresh culture media. Into a 4 x 6 culture plate, 500 μ l of each cell sample was transferred into a total of 6 wells. Following this 500 μ l of culture media was added and the samples were incubated at 37°C for 30 minutes, 1 hour, 1.3 hours, 2 hours and 2.3 hours.

2.5.5.2 Cell apoptosis Trial

To determine the effects of freezing and rapid thawing on cell survival the Annexin V-FITC Apoptosis Detection Kit (Sigma, Dorset, UK) was used. Following each incubation interval the cells were transferred into flow tubes and washed in phosphate buffered saline (PBS) solution by centrifuging at 13,000 rpm for 5 minutes. The supernatant was discarded and the cells were resuspended in 100 μ l of PBS. To this 1

μ l of Annexin V-FITC conjugate and 2 μ l of propidium iodide was added and the samples were incubated at room temperature for 10 minutes, in the dark. Each reaction was tested with a flow cytometer which was set to record 10,000 events at 700 volts. The data was analysed by examining forward scatter, side scatter, Annexin V-FITC, and propidium Iodide. Following gating of the lymphocyte cell population histograms were generated and the geometric means for each reaction were deduced. For Annexin V the cell sample was divided into Annexin positive and Annexin negative cells. For propidium iodide the cell sample was divided into live cells (propidium iodide negative), permeabilised cells and fragmented cells.

2.5.5.3 Cell Culture of B-lymphocytes in methadone

A total of 12 CLL primary B-cell lines were selected for cell culture including six homozygous for the A allele (CLL44, CLL43, CLL39, CLL38, CLL37, CLL34), 5 heterozygous for the G allele and 1 homozygous for the G allele (CLL42, CLL41, CLL40, CLL36, CLL19, CLL18). The cells were rapidly thawed in a water bath at 37 °C before being resuspended in 10 ml of culture media. The samples were then centrifuged at 1,500 rpm for 5 minutes, the supernatant discarded and the pelleted cells were resuspended in 3 ml of fresh culture media. Into a 4 x 6 culture plate, 500 μ l of each cell sample was transferred into a total of 6 wells. Following the strategy outlined in Table 22 methadone spiked culture media (stock concentration of 200 μ M) and unspiked culture media was added to each of the wells to ensure 6 treatments (Control, 100 μ M, 20 μ M, 10 μ M, 5 μ M, 1 μ M methadone). The samples were then incubated at 37°C for 1 hour.

Table 22: Reaction strategy for sample cell culture in methadone.

	Control (μ l)	100 μ M (μ l)	20 μ M (μ l)	10 μ M (μ l)	5 μ M (μ l)	1 μ M (μ l)
Cells	500	500	500	500	500	500
Media	500	0	400	450	475	495
Methadone	0	500	100	50	25	5

2.5.5.4 Cell apoptosis Trial

After incubation with methadone 500 μ l of cells from each treatment were transferred into flow tubes and washed in phosphate buffered saline (PBS) solution by centrifuging at 13,000 rpm for 5 minutes. The supernatant was discarded and the cells were resuspended in 100 μ l of PBS. To this 1 μ l of Annexin V-FITC conjugate and 2 μ l of propidium iodide was added and the samples were incubated at room temperature for 10 minutes, in the dark. Each of the reactions was tested with a flow cytometer which was set to record 10,000 events at 700 volts. The data was analysed by examining forward scatter, side scatter, Annexin V-FITC, and propidium Iodide. Following gating of the lymphocyte cell population histograms were generated and the geometric means for each reaction were deduced. For Annexin V the cell sample was divided into Annexin positive and Annexin negative cells. For propidium iodide the cell sample was divided into live cells (propidium iodide negative), permeabilised cells and fragmented cells.

2.5.5.5 μ receptor Internalisation

The extent of μ -opioid receptor internalisation following methadone treatment was analysed using the μ opioid receptor (ab10275) primary antibody (Abcam, UK) and the goat polyclonal to rabbit IgG – H&L (Fluorescein isothiocyanate, FITC) (Abcam, UK). Having been cultured in methadone 500 μ l of cells for each treatment were

transferred into flow tubes and washed in FACSFlow by centrifuging at 13,000 rpm for 5 minutes. The supernatant was discarded and the cells were resuspended in 100 μ l of FACSFlow. To this 2 μ l of the primary antibody in a 1:10 concentration was added and the samples were incubated at 4°C for 30 minutes. Following this the samples were washed by adding FACSFlow and centrifuging at 13,000 rpm for 5 minutes. The supernatant was discarded leaving a pellet and approximately 100 μ l of solution in the flow tubes. Then 2 μ l of the secondary antibody (1:10) was added and the reactions were incubated at 4°C for 30 minutes. The reactions were washed in FACSFlow through centrifugation at 13,000 rpm for 5 minutes. The supernatant was discarded and the pellet was re-suspended in 100 μ l of FACSFlow. Each reaction was tested with a flow cytometer which was set to record 10,000 events at 700 volts. The data was analysed by examining forward scatter, side scatter and anti- μ + anti-rabbit FITC. Following gating of the lymphocyte cell population histograms were generated and the geometric means for each reaction were deduced.

2.6 Statistical Analysis

2.6.1 Data Normalisation

All data was tested for normality by conducting data frequency analysis, examining comparative and descriptive statistics including mean, standard error and data outliers using SPSS 14.0 software.

2.6.2 Post-mortem drug-drug correlations

As a number of the post-mortem subjects studied were engaged in polydrug use the association between methadone and other drugs identified in the toxicology screen was examined. The drugs found together with methadone included:

- Opioids – morphine, dihydrocodeine, codeine.
- Benzodiazepines – diazepam, oxazepam.
- Ethanol.
- Selective Serotonin Reuptake Inhibitors (SSRI's) – citalopram, fluoxetine, paroxetine, sertraline.
- Serotonin-Norepinephrine Reuptake Inhibitors (SNRI's) – venlafaxine.
- Tricyclic antidepressants – amitriptyline, dothiepin.
- Tetracyclic antidepressants – mirtazapine.
- Antipsychotics – quetiapine.

2.6.2.1. Post-mortem drug concentrations

Bivariate correlations using Pearson's two-tailed significance were used to evaluate the relationship between each of the drugs identified post-mortem. In addition to this simple scatter plots were created to identify positive or negative correlations. This was conducted using SPSS 14.0 software.

2.6.3 Independent T-test

This study used the Independent T-test to identify significant associations between *CYP2B6* and *OPRM1* SNPs and post-mortem methadone concentration. The Independent T-test is used to test for a difference between two independent groups (wild type allele and variant alleles) on the means of a continuous variable (post-mortem methadone concentration).

2.6.4 Hardy Weinberg equilibrium

The Hardy-Weinberg Equilibrium or Hardy-Weinberg Law is a concept of population genetics, which states that both allele and genotype frequencies in a population will remain constant, hence be in equilibrium, unless disturbing influences are introduced. These can include mutations, selection, non-random breeding, limited population's size, random genetic drift and gene flow. In nature one or more of these disturbing influences will always be active; therefore it is impossible to achieve Hardy-Weinberg Equilibrium in nature. In this study the Hardy-Weinberg Equilibrium has been used as a baseline that *CYP2B6* and *OPRM1* genetic change can be measured against for the post-mortem and control populations sampled.

Hardy-Weinberg Equilibrium

$$p^2 + 2 pq + q^2 = 1.$$

Where p^2 represents the wild type genotype, pq is the heterozygous genotype and q^2 stands for the homozygous variant genotype.

For *CYP2B6*, T750C, G516T, A785G and *OPRM1* A118G Hardy Weinberg Equilibrium was tested for both the post-mortem and control populations using Chang Bioscience software.

2.6.5 *CYP2B6* & *OPRM1* SNP-SNP Correlations

Linkage between gene variants for both *CYP2B6* and *OPRM1* was determined using Pearson's Chi-square test and Spearman's rank correlation. This was conducted for both the post-mortem and control populations. A P value of ≤ 0.05 was considered to indicate statistical significance.

2.6.6 Comparing the prevalence of *CYP2B6* and *OPRM1* variations in a post-mortem and a control population

This study examined two populations, a post-mortem population where the deaths had been attributed to methadone and a healthy living control population in order to determine whether methadone susceptibility could be identified through SNP prevalence. Differences in genotype frequencies for T750C, G516T, A785G, and A118G between populations were examined using T-Test and Fisher's exact test.

2.6.7 The influence of Age, Gender and Involvement in Methadone Maintenance

The influence of age and gender for the *CYP2B6* and *OPRM1* gene variations was examined using a binary logistic regression model. The dependent variable used was population, and the cofactors examined were age, gender and race. The influence of subject participation in methadone maintenance for methadone susceptibility was examined using the Independent T-test.

3.0 RESULTS

3.1 Method Optimisation

3.1.1 DNA Extraction

3.1.1.1 DNA extraction from buccal swabs

Three different swabs were tested to identify which yielded the greatest DNA concentration. The swabs comprised:

- The Isohelix SK-1 swab-which uses a reduced liquid absorbancy matrix together with a quick release surface to increase DNA uptake and yield.
- The Epicentre Catch-All Collection swab- which utilises a porous spongy swab, said to increase collection due to greater DNA retention.
- The Epicentre MasterAmp™ Buccal Swab Brush-which uses soft bristles to collect DNA from the buccal surface.

The DNA quantification results for the three different swabs demonstrate that the Epicentre Catch-All Collection swab yields the highest DNA concentration with an average of 1.14 ng/μl (Table 23). The lowest DNA yield was collected by the Isohelix SK-1 swab with an average of 0.86 ng/μl.

Table 23: Mean DNA yield for the three buccal swabs.

DNA Swab	Mean (ng/μl)	Std. deviation
Isohelix SK-1	0.86	± 0.89
Epicentre Catch-All Collection swab	1.14	± 0.49
Epicentre MasterAmp™ Buccal Swab Brush	1.04	± 0.19

Significance was tested using the Kruskal Wallis test. There was no significant difference (P 0.101).

The Quantifiler® standard curves are displayed below (Figures 6 & 7). The R₂ value for buccal extraction run 1 is lower than expected perhaps reflecting poor mixing of the assay mix prior to use.

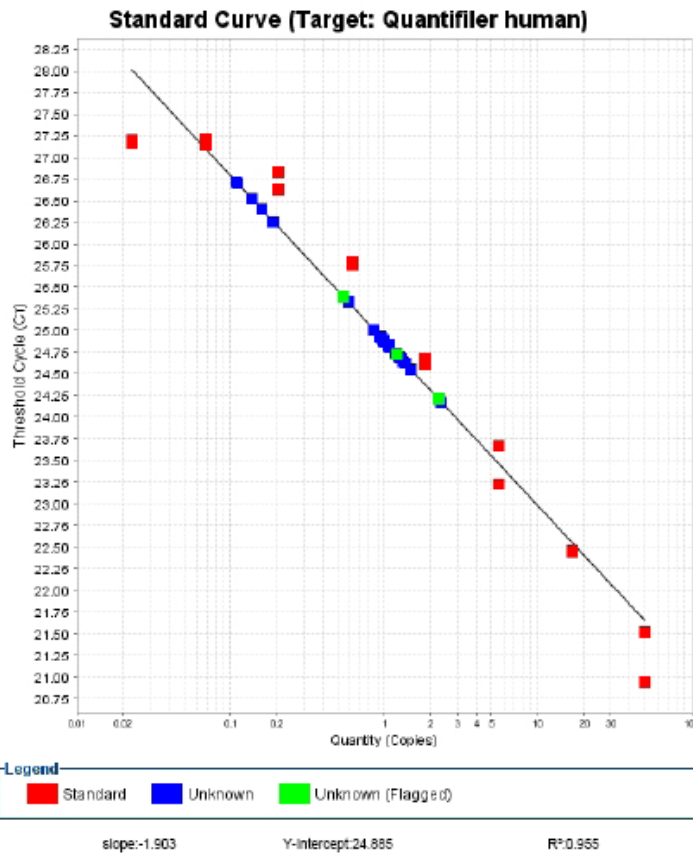


Figure 6: Standard curve for buccal extraction run 1.

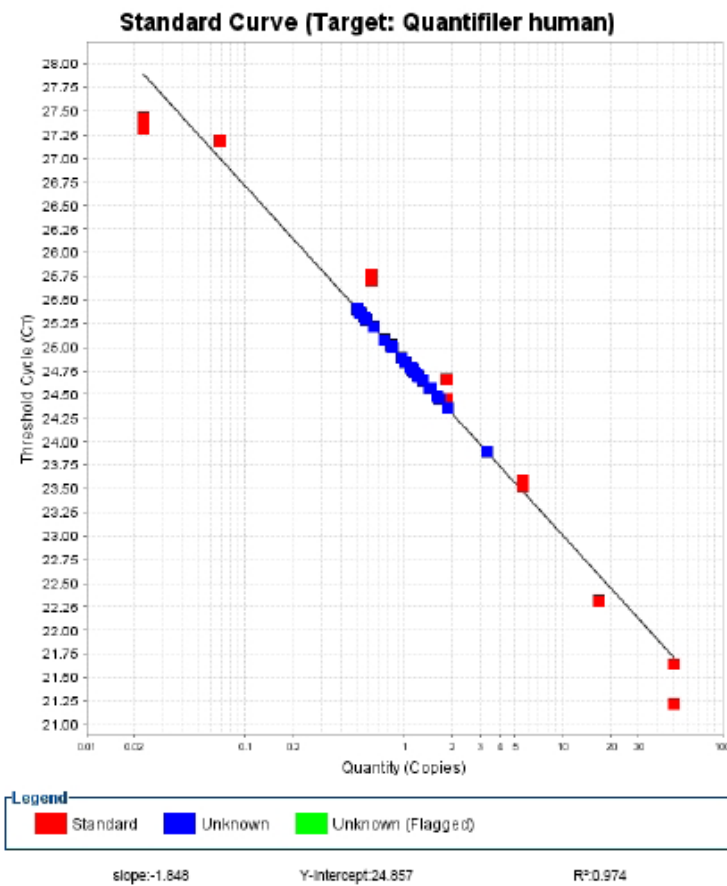


Figure 7: Standard curve for buccal extraction run 2.

3.1.1.2 DNA extraction from whole blood

The DNA extractions from blood yielded a much higher concentration of DNA compared with the buccal swab extraction protocol. This finding is expected and has been well documented. The quantification study revealed that the Qiagen DNeasy Blood and Tissue Kit yielded significantly more DNA than the Promega Wizard Purification Kit (Figures 8 & 9, Table 24). Both kits have been commercially validated and are suitable for use in molecular research. However for the purpose of this study the Quantifiler® results recommend the Qiagen kit for further use. Additionally the effects of different preservatives on DNA yield were examined with EDTA yielding the highest DNA concentrations for both the Qiagen and Promega kits and potassium oxalate yielding the lowest DNA concentrations (Table 25).

Table 24: Mean DNA yield for the Promega and Qiagen extraction kits examined.

Whole Blood DNA Extraction Kit	Mean (ng/μl)	Std. deviation
Promega Wizard Purification Kit	0.28	± 0.25
Qiagen Dneasy Blood and Tissue Kit	20.8	± 12.3

Significance was tested using the non parametric Mann Whitney test as the data was not normally distributed ($P > 0.001$).

Table 25: The effects of different whole blood preservatives on DNA yield.

Blood preservative	DNA yield (Mean ng/μl)	Std. deviation
EDTA	15.9	± 16.8
Lithium heparin	12.4	± 13.5
Potassium oxalate	3.4	± 4.0

Significance was tested using the Kruskal Wallis test as the data distribution was not normal. There was a significant difference between the three different blood preservatives with a P value of 0.036

From these results it is clear that EDTA is the optimal preservative out of the three examined for maintaining DNA stability. However it must be mentioned that all of the preservatives yielded appropriate DNA quantities for molecular analysis. This is particularly useful as post-mortem samples are routinely stored in sodium fluoride potassium oxalate tubes which yielded the lowest quantity of DNA here. As anticoagulants such as sodium fluoride potassium oxalate might inhibit PCR (de Vries *et al.* 2001) it may be that during the washing process EDTA and Lithium Heparin are more extensively removed influencing the Quantifiler result.

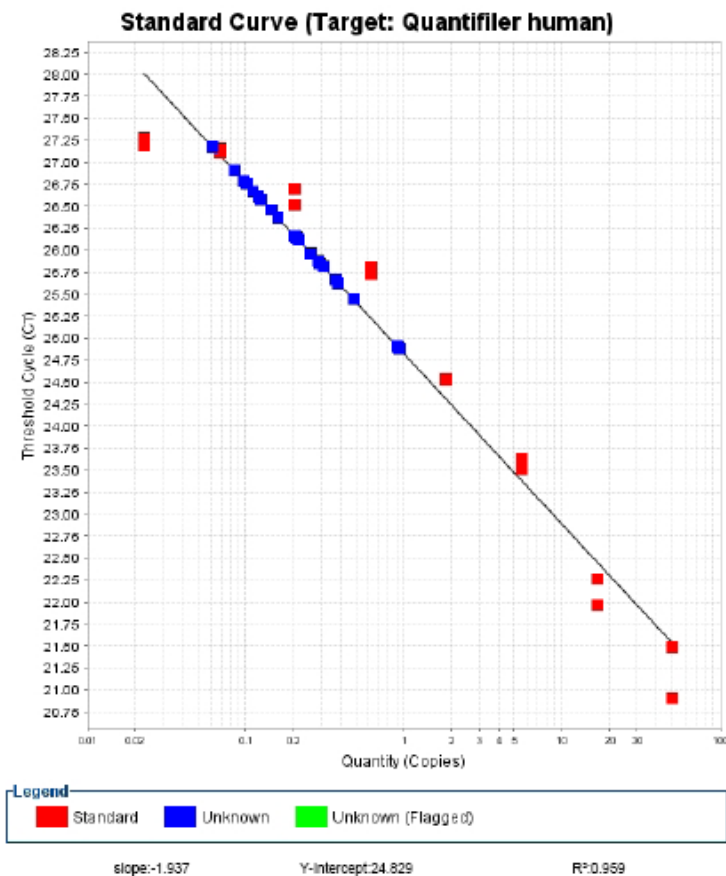


Figure 8: Standard curve for Quantification of Promega Samples.

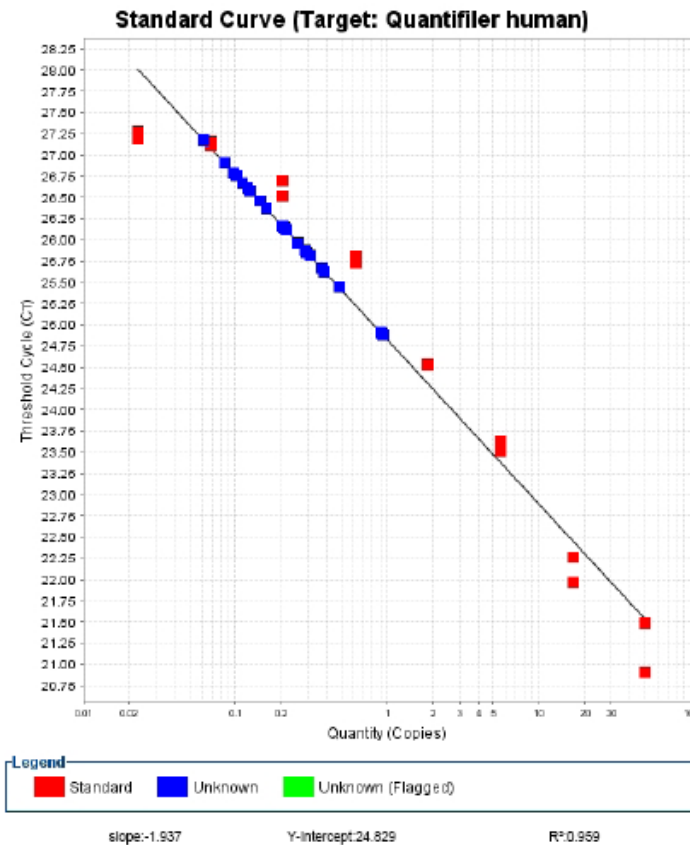


Figure 9: Standard curve for Quantification of Qiagen Samples.

3.1.2 PCR Amplification of SNP regions of the human *OPRM1* gene

Polymerase chain reactions (PCRs) were performed following buccal DNA extraction to determine the validity of several primers designed to amplify targeted regions of *OPRM1*. As demonstrated in the methodology this protocol required development in order to effectively produce specific primer-template binding.

3.1.2.1 MgCl₂

The aim of this experiment was to demonstrate the effect of MgCl₂ on PCR efficiency, whilst identifying a concentration range to consider for further work.

Of the seven MgCl₂ volumes only four (1µl, 1.5µl, 2µl and 2.5µl) performed efficiently producing adequate DNA banding (Figure 10). The higher MgCl₂ volumes

resulted no banding (3µl, 3.5µl and 4µl). This is not wholly unexpected, it was commented on in the methodology that changes in MgCl₂ can affect PCR efficiency (Wolff *et al.* 1993). As demonstrated in Figure 10 the DNA bands for 1.5µl, 2µl and 3µl are the brightest suggesting an optimal MgCl₂ concentration within this concentration range. The 1µl band is not as bright possibly reflecting suboptimal binding.

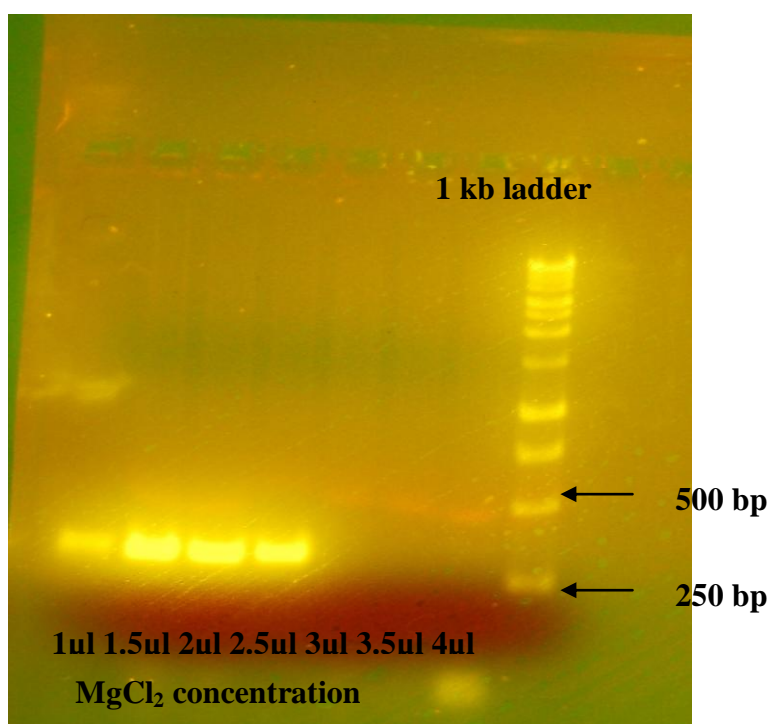


Figure 10: The effect of MgCl₂ on PCR success.

Agarose gel (1.6 %), run at 70 volts. MgCl₂ volumes >3µl resulted in no DNA banding.

3.1.2.2 Temperature

3.1.2.2.1 Gradient PCR reaction

The initial stage in testing the effects of temperature as discussed in the methodology was to conduct a gradient PCR. The results from this experiment however were poor and this was somewhat unexpected (Figure 11). Clear banding is only present for 60.1°C PRO554 and 62.2°C PRO995. Smearing can be identified for 60.7°C PRO554

and 60.1°C PRO995 reflecting non-specific primer annealing. Faint banding can also be seen for 61.8°C and 63.3°C PRO554.

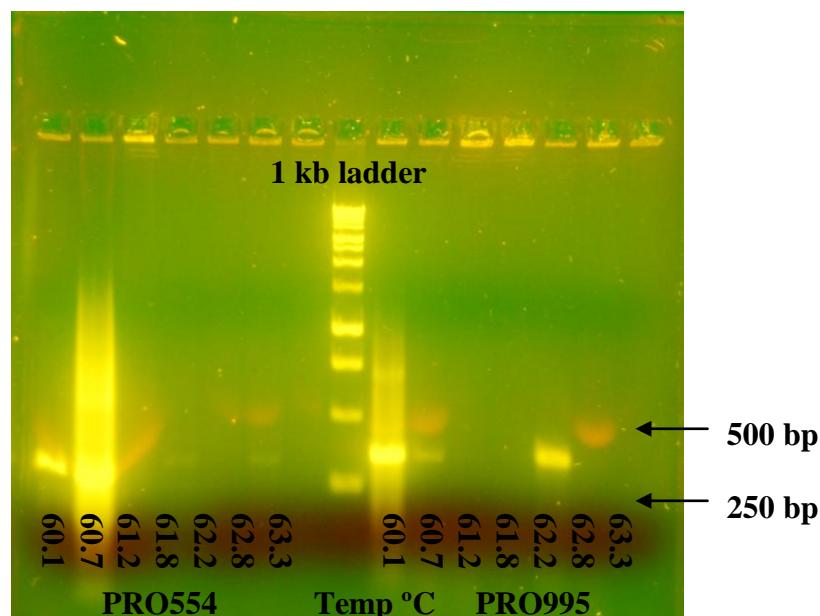


Figure 11: Gradient PCR reaction for PRO554 and PRO995 primers.

Agarose gel (1.6 %), run at 70 volts. The gel shows non-specific primer annealing.

In response to the poor banding demonstrated in Figure 11 a new dNTP stock was used together with an increase in $MgCl_2$ amount to 5 μ l.

3.1.2.2.2 Temperatures selected from the Gradient Reaction

The effects of three temperatures (60.1°C, 61.2°C, and 62.2°C) selected from the previous gradient reaction on PRO554 and PRO995 primer banding are displayed in Figure 12. Banding is clear however there is still smearing indicating too much $MgCl_2$ which correlates with the results demonstrated in Figure 10 where the optimum $MgCl_2$ concentration range was between 1.5 and 3 μ l.

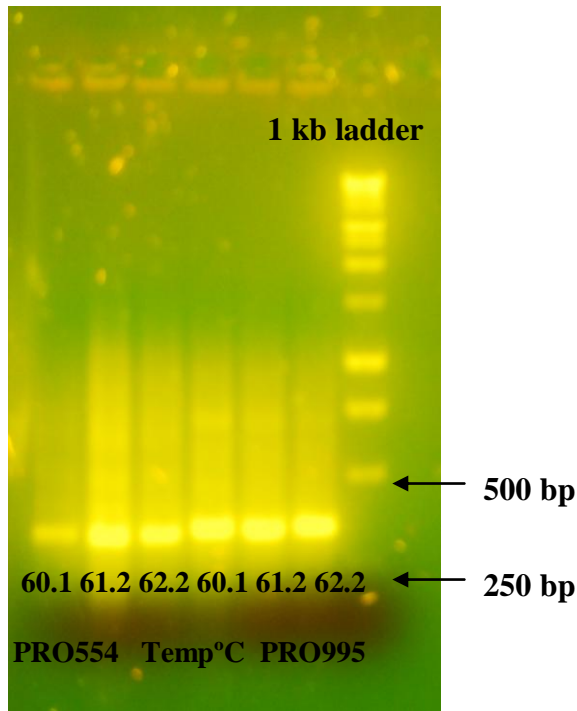


Figure 12: Temperature reaction for PRO554 and PRO995 primers.

Agarose gel (1.6 %), run at 70 volts. Smearing indicates a high concentration of $MgCl_2$.

3.1.2.2.3 Temperature optimisation to increase specificity

Further temperature optimisation was required to produce DNA banding suitable for DNA sequencing. As described in *Section 2.1.2.3.2 Temperature* this involved a decrease in temperature for PRO55, PR0995, EX1 and EX2. The annealing temperature for EX3 was increased and as Figure 13 demonstrates this greatly improved the PCR results.

Clear bands were identified for EX1, EX2 and EX3 allowing the sequencing of these samples, the promoter regions did not amplify efficiently with smearing present. As a result the temperatures for PRO554 and PRO995 were decreased further (Figures 14 & 15).

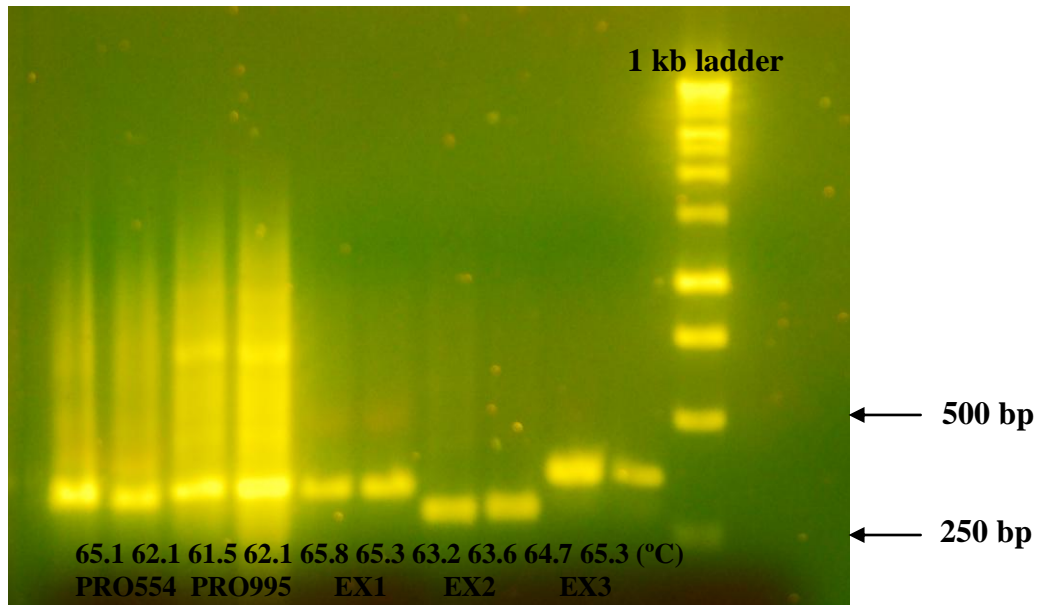


Figure 13: Improved banding efficiency following annealing temperature optimisation.

Agarose gel (1.6 %), run at 70 volts. Clear DNA banding for the PCR amplified exon 1 region.

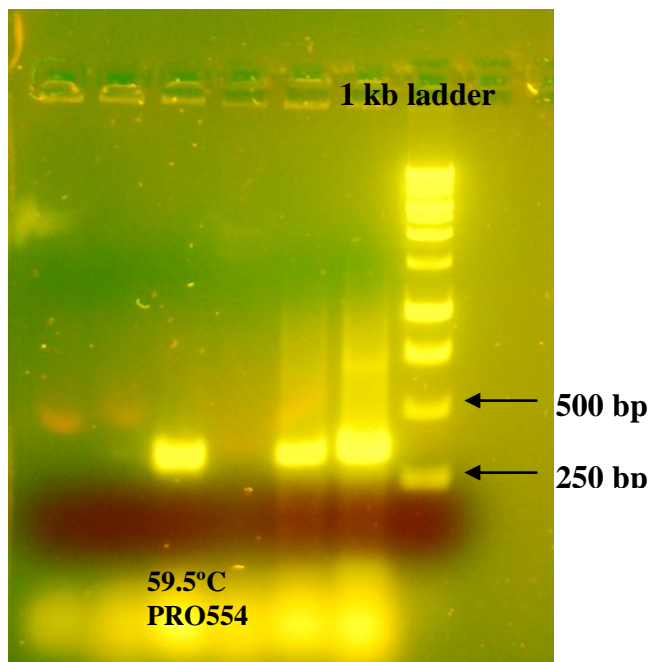


Figure 14: Improved PRO554 annealing following a decrease in temperature.

Agarose gel (1.6 %), run at 70 volts. Clear DNA banding for the promoter region containing G554A.

As demonstrated by Figure 14 a decrease in temperature improved the specificity of the reaction producing a band suitable for subsequent DNA processing sequencing of the promoter region PRO554 primer set.

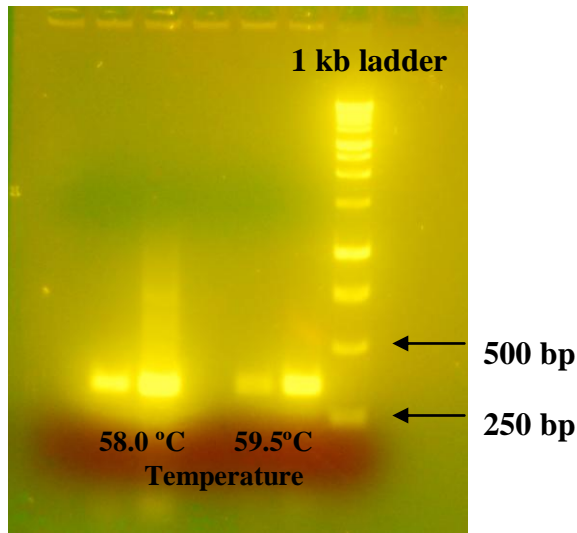


Figure 15: Improved PR0995 annealing following an increase in temperature.

Agarose gel (1.6 %), run at 70 volts. Clear DNA banding for the promoter region containing C995A.

3.1.2.2.4 SNPs revealed by DNA sequencing results

Following PCR development the samples were sent for sequencing to validate primer efficiency. Each of the primer sets (PRO554, PRO995, EX1, EX2, and EX3) amplified the required target regions of *OPRM1*. From this it can be deduced that the primers used during method development are suitable to screen for specific *OPRM1* SNPs. The DNA sample processed for the promoter and exonic regions of *OPRM1* did not demonstrate any variations and can therefore be used as negative controls in the real-time genotyping experiments.

In Figure 16 the highlighted base (51) denotes the position of the A118G SNP discussed in the literature review earlier. The wild type allele AA is present for this sample. The variant allele would be present either as a heterozygous (AG) or as a homozygous (GG) allele change. This variation is a functional variation causing an amino acid change from asparagine to aspartic acid. As discussed in *Section 1.6.3 Pharmacogenomic influences on methadone-receptor binding and response* the fundamental role of this mutation is unclear and requires further investigation.

Exon 1

A A C T T G T C C A C T T A G A T G G C A A C C T G T C C G A C C C A T G

40 50 60

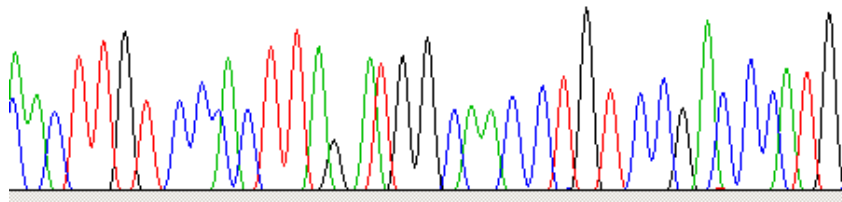
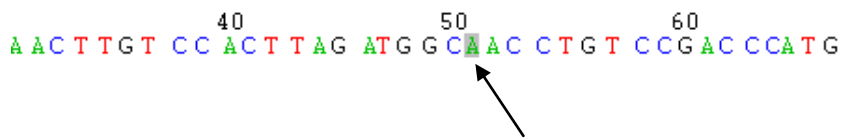


Figure 16: DNA sequencing results for EX1_HB primer amplification of *OPRM1* A118G SNP.

The arrow indicates the base position of the A118G SNP.

G A C C G G C A G T C C C T C A T G A T C A C G G C

120 130 140

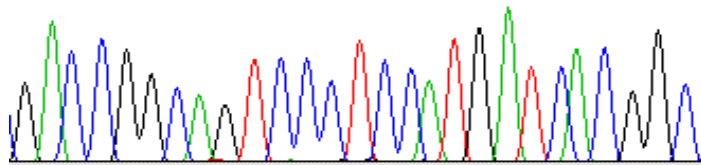
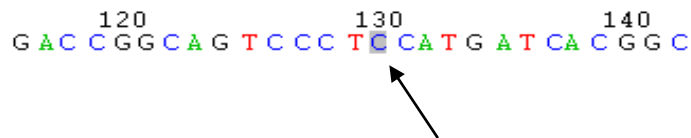


Figure 17: DNA sequencing results for EX1_HB primer amplification of the *OPRM1* C17T SNP.

The arrow indicates the base position of the C17T SNP.

The highlighted base above (Figure 17) demonstrates the position of the C17T SNP, the base seen is the ancestral allele CC, the variant allele would be TT. This missense mutation induces an amino acid change from serine to phenylalanine.

Exon 2

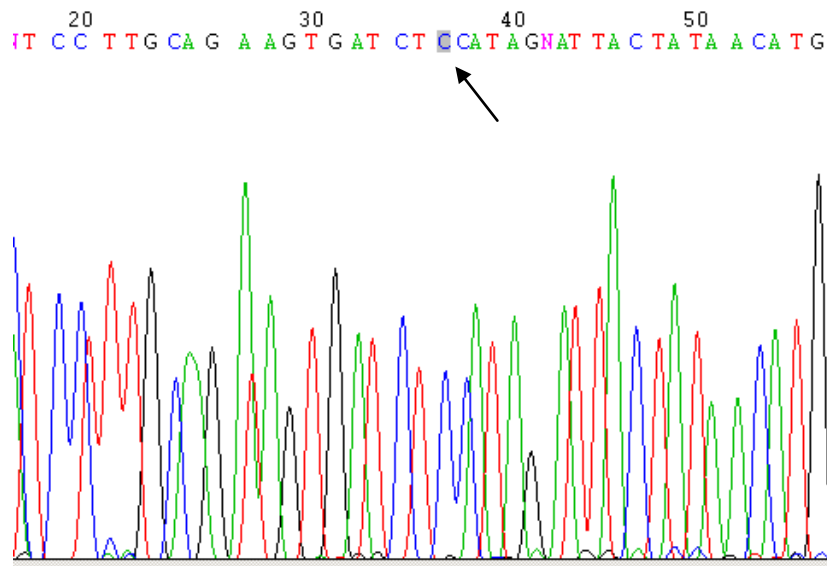


Figure 18: DNA sequencing results for EX2_HB primer amplification of *OPRM1* C440G SNP.

The arrow indicates the base position of the C440G SNP.

The highlighted base above (Figure 18) refers to the *OPRM1* C440G SNP, the ancestral base C is present. This DNA sample can therefore be used as a negative control if SNP genotyping is conducted for this variant. This variant is a non synonymous mutation inducing an amino acid change from serine to cysteine.

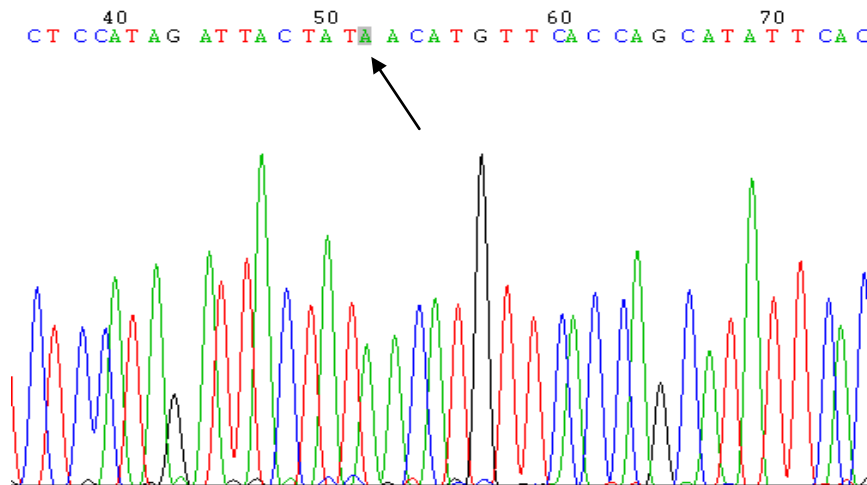


Figure 19: DNA sequencing results for EX2_HB primer amplification of *OPRM1* A454G SNP.

The arrow indicates the base position of the A454G SNP.

The wild type allele AA is shown in Figure 19 by the highlighted A nucleotide base.

The variant allele GG for this SNP induces an amino acid change from asparagine to aspartic acid. The results for the exon 2 SNPs validate the EX2_HB primer set.

Exon 3

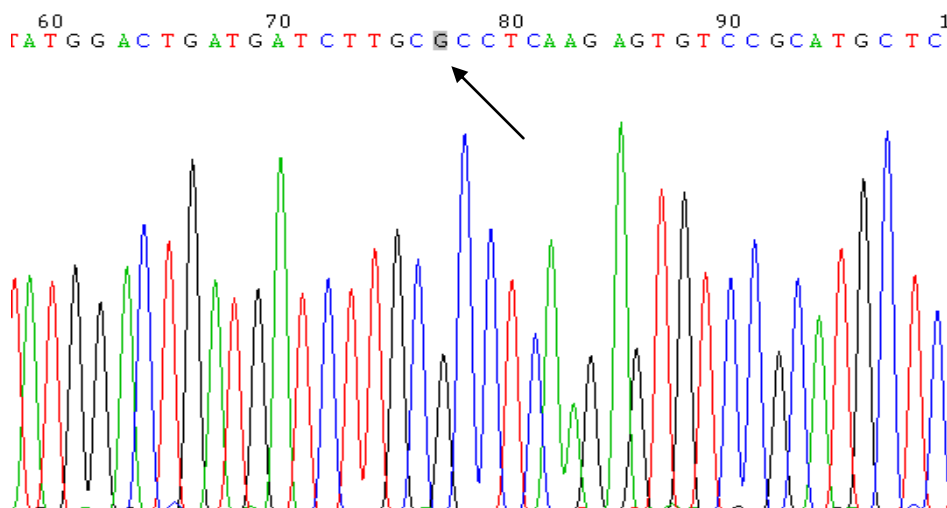


Figure 20: DNA sequencing results for EX3_HB primer amplification of *OPRM1* G779A SNP.

The arrow indicates the base position of the G779A SNP.

The highlighted base above (Figure 20) denotes the ancestral allele GG the variant would be present as either GA or AA and induces an amino acid change from arginine to histidine.

The wild type allele CC for the C793T SNP is present in Figure 21. This is a functional non synonymous SNP inducing an amino acid change from arginine to cysteine

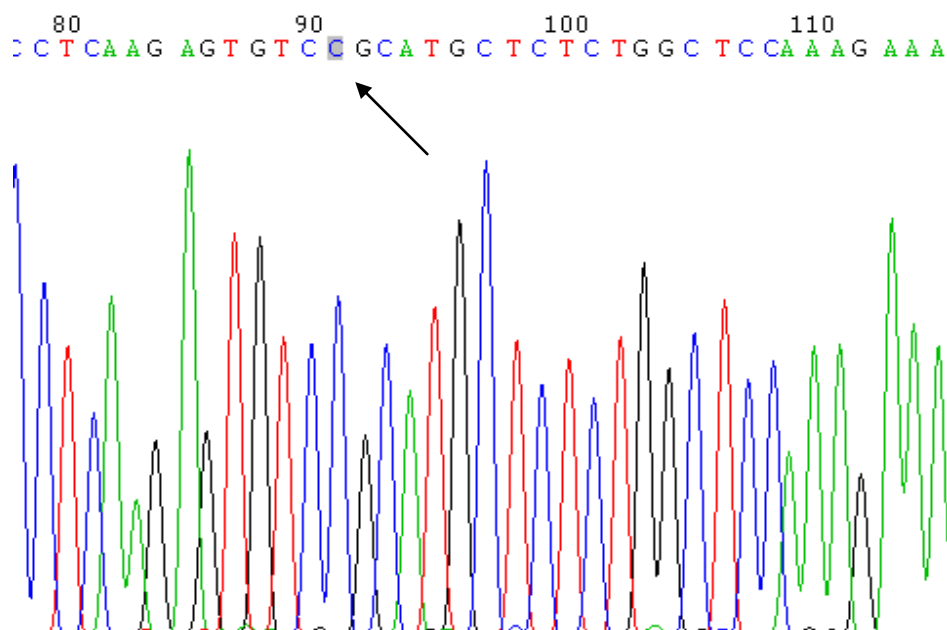


Figure 21: DNA sequencing results for EX3_HB primer amplification of *OPRM1* C793T SNP.

The arrow indicates the base position of the C793T SNP.

The ancestral allele (GG) was identified for the third SNP examined (Figure 22) within the exon 3 region. The variant would be present as either the heterozygous GA or the homozygous AA allele inducing an amino acid change from aspartic acid to asparagine.

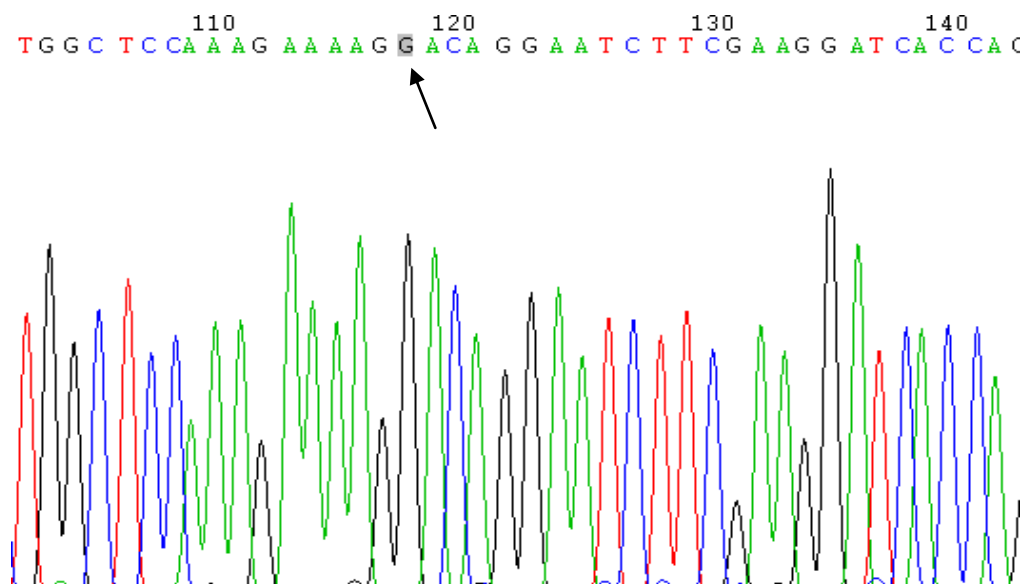


Figure 22: DNA sequencing results for EX3_HB primer amplification of *OPRM1* G820A SNP.

The arrow indicates the base position of the G820A SNP.

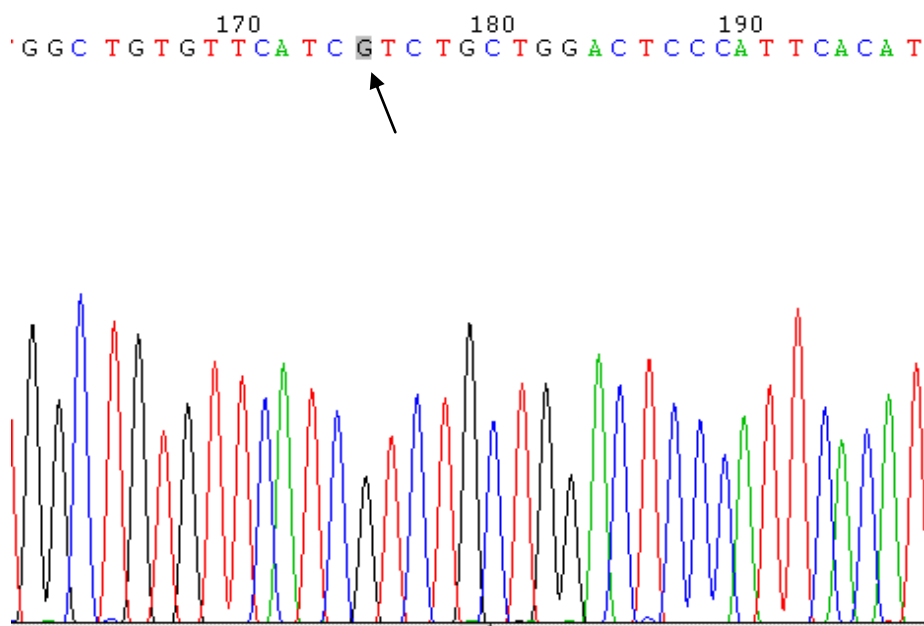


Figure 23: DNA sequencing results for EX3_HB primer amplification of *OPRM1* G877A SNP.

The arrow indicates the base position of the G877A SNP.

Figure 23 shows the ancestral allele GG for the G877A SNP screened for. The variant would be present as either GA, or AA and would induce an amino acid change from valine to isoleucine.

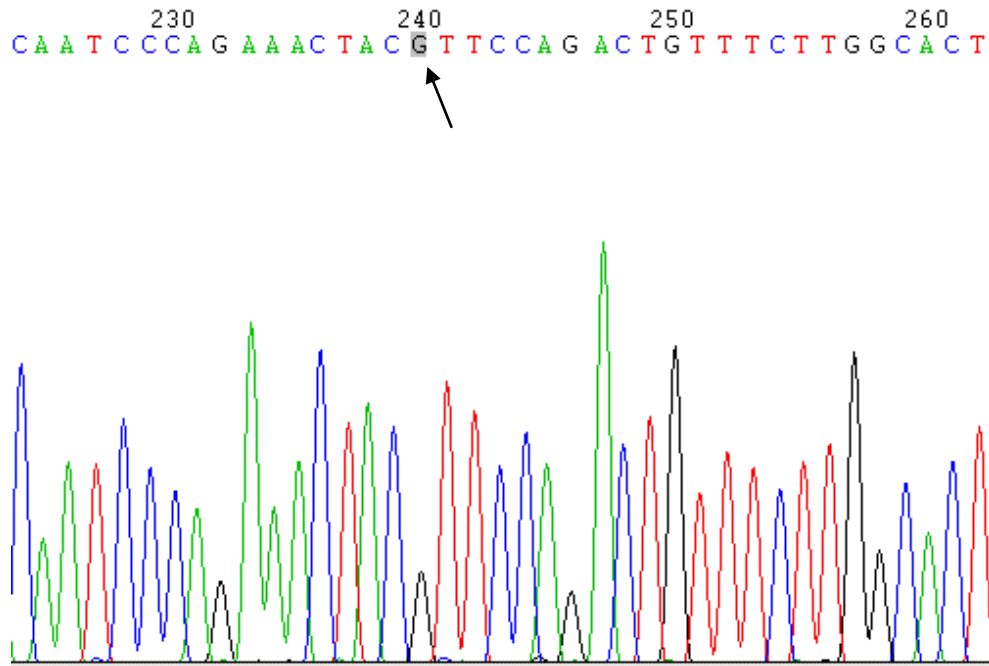


Figure 24: DNA sequencing results for EX3_HB primer amplification of *OPRM1* G942A SNP.

The arrow indicates the base position of the G942A SNP.

The final exon 3 SNP screened for was the G942A SNP, as shown in Figure 24 the ancestral allele is present GG. This variation is a synonymous or silent mutation which does not affect the amino acid sequence. Synonymous variations as discussed in the previously have been linked with alterations in gene expression.

The *OPRM1* Promoter region

The PRO554 mutation is located within a *cis*-element in the *OPRM1* promoter region and may therefore be involved with gene expression modifications. The wild type allele GG is depicted in Figure 25, the variant would be present as either GA or AA.

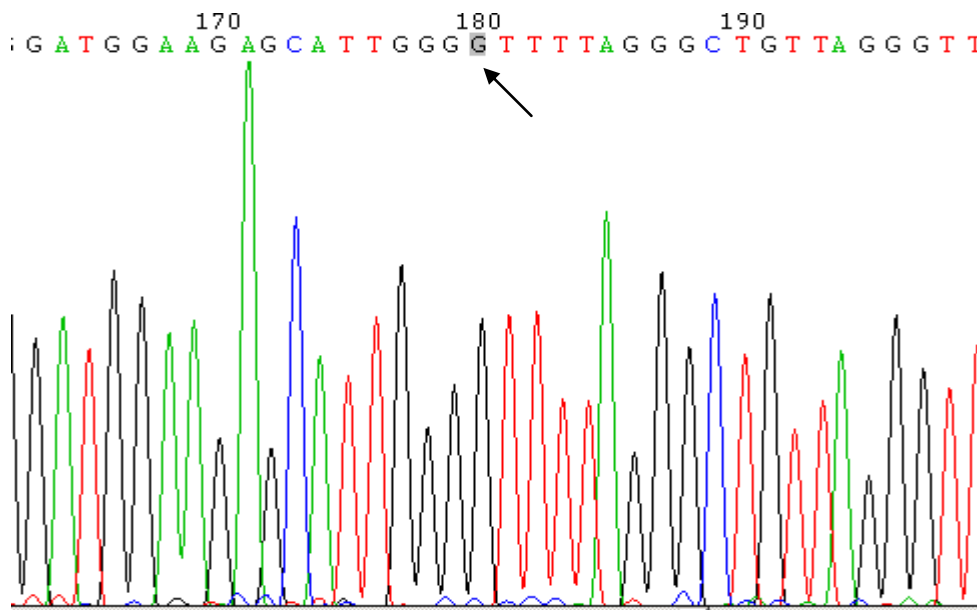


Figure 25: DNA sequencing for PR0554_HB primer amplification.

The arrow indicates the base position of the G554A SNP.

The PRO995 variant displayed in Figure 26 similarly to PRO554 is located within a *cis*-element and is therefore likely to be involved in gene expression. The wild type allele CC is demonstrated, the variant would be present either as CA or AA.

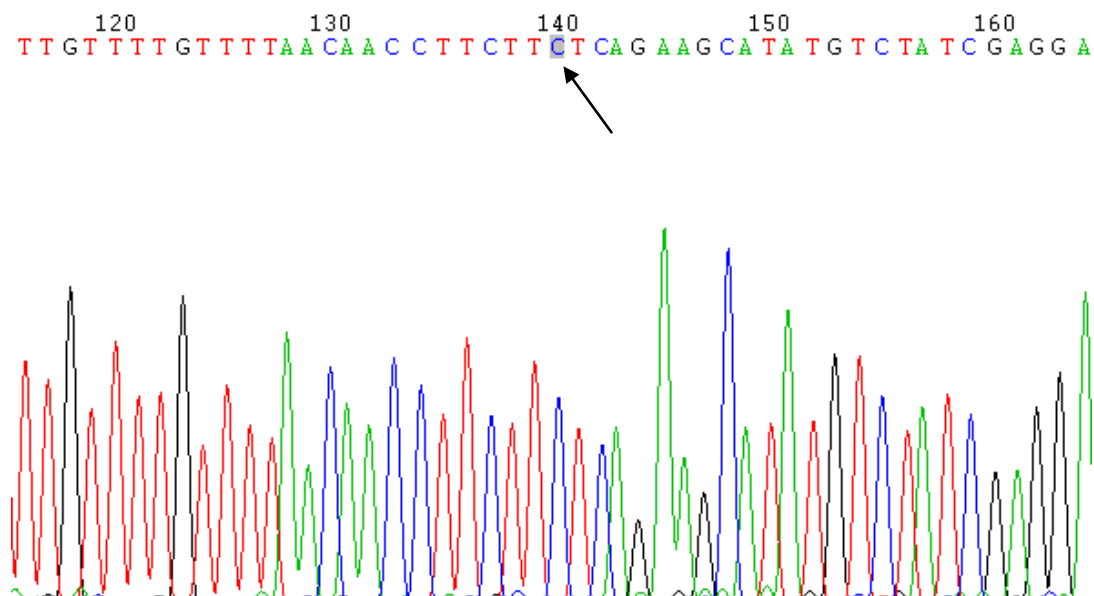


Figure 26: DNA sequencing for PRO995_HB primer amplification.

The arrow indicates the base position of the C995A SNP.

3.1.2.3 A118G identification

Of the *OPRM1* SNPs examined thus far only one is a likely candidate for further research, the A118G SNP. As discussed in *Section 1.6.3 Pharmacogenomic influences on methadone-receptor binding and response* A118G may be linked with inter-individual responses to opioids (specifically morphine). However only one study has discussed this variation with regards to methadone response and there are no studies that have examined this SNP for molecular autopsy. A real-time Taqman® SNP genotyping assay will be used to examine allelic discrimination in multiple samples (post-mortem and healthy living controls). This method requires both negative (wild type allele) and positive variant allele controls. Earlier work demonstrates that the EX1_HB primer set correctly amplifies the region surrounding A118G. Therefore this primer set was used to screen 20 different subjects to identify an A118G positive control for SNP genotyping. Clear DNA amplification for all 20 samples was achieved (Figures 27 & 28). This result allowed further DNA processing in the form of DNA sequencing to screen for the A118G mutation.

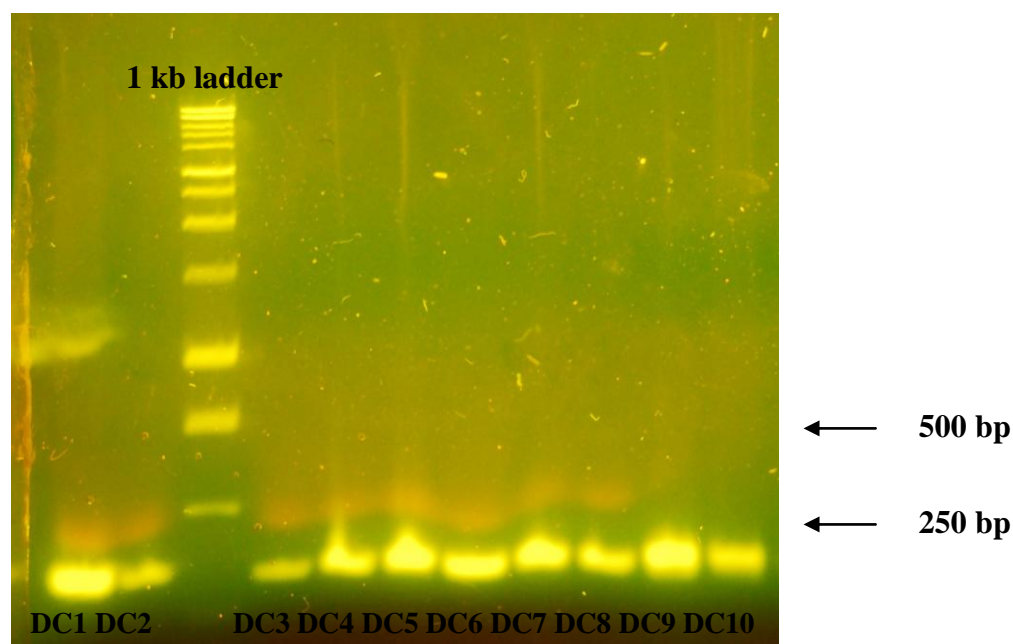


Figure 27: Amplification of *OPRM1* exon 1 region using EX1_HB primers PCR 1.

Agarose gel (1.6 %), run at 70 volts. The exon 1 region was successfully amplified for 10 subjects.

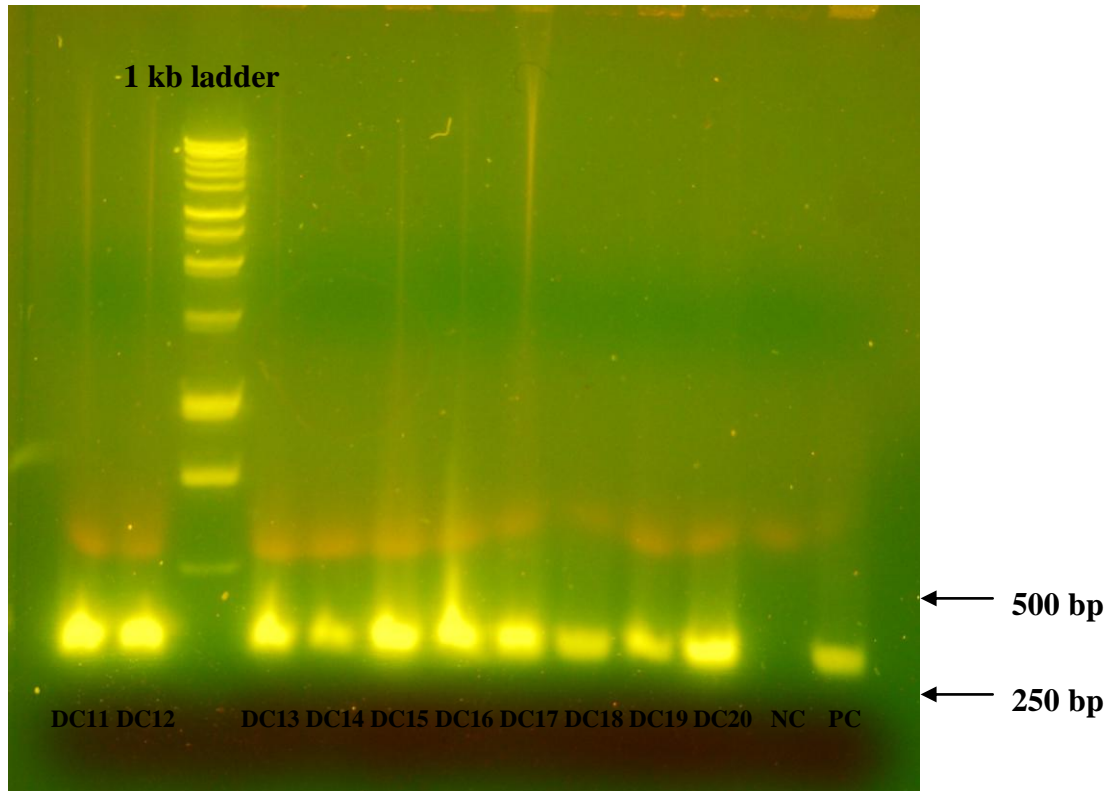


Figure 28: Amplification of *OPRM1* exon 1 region using EX1_HB primers PCR 2.

Agarose gel (1.6 %), run at 70 volts. The exon 1 region was successfully amplified for 10 subjects

3.1.2.3.1 A118G sequencing results

PCR amplified DNA for 20 subjects were sequenced to identify a positive control for A118G. All of the samples sent for sequencing yielded sufficient sequences for analysis.

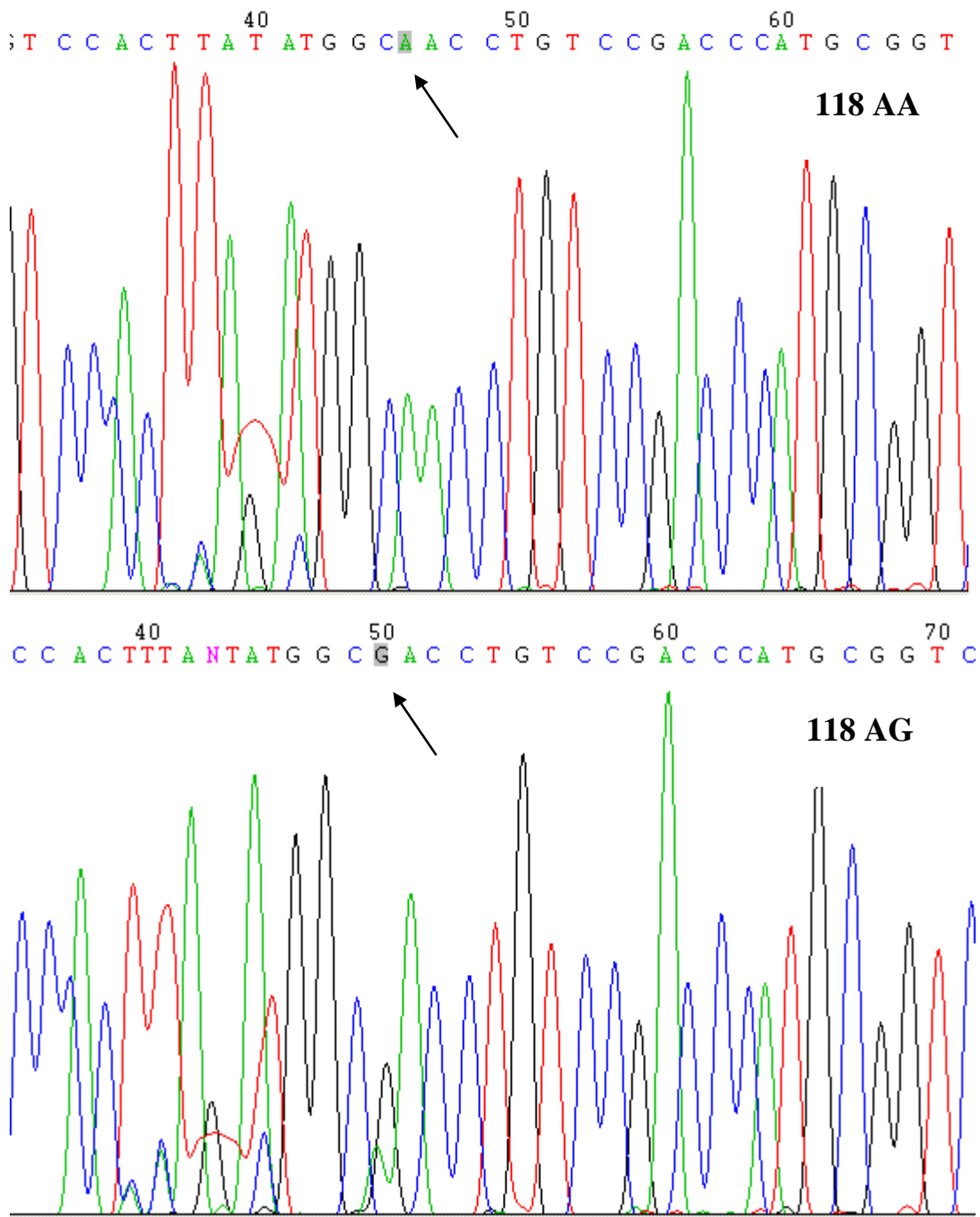


Figure 29: A comparison of two SNP genotypes for the A118G SNP (118 AA & 118 AG).

A typical DNA profile for the *OPRM1* A118G SNP. The arrows indicate the base position of the A118G SNP for the 118 AA and 118 AG genotypes. For the 118 AA genotype there is a single green peak denoting the A allele. For the 118 AG genotype there is a black peak denoting the G allele and below this there is a green peak denoting the A allele. Therefore this is a heterozygous subject.

In total three out of twenty post-mortem samples sequenced were heterozygous for the A118G SNP (DC15, DC12, & DC19).

3.1.3 PCR Amplification of SNP regions of the human *CYP2B6* gene

3.1.3.1 Primer validation

Polymerase chain reactions (PCRs) were performed to test the validity of the C2B6E4, C2B6E5, and C2B6Pr primers which have been designed to amplify targeted regions of *CYP2B6*.

C2B6E4 & C2B6E5

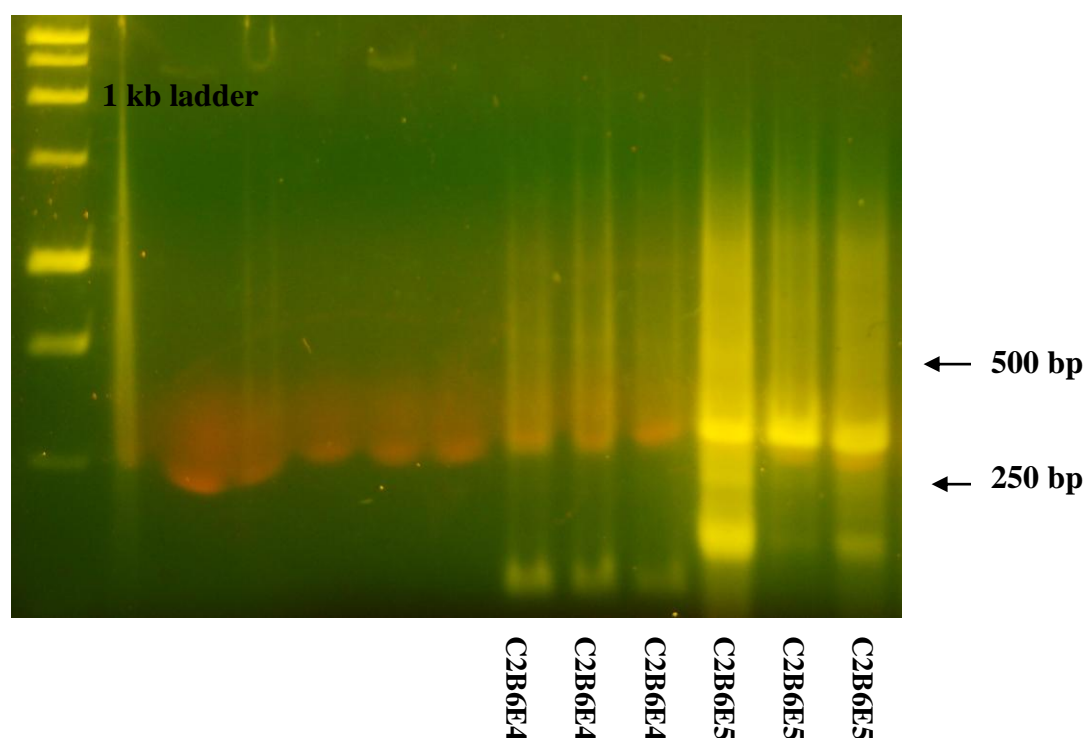


Figure 30: PCR validation for C2B6E4 & C2B6E5 primers.

Agarose gel (1.6 %), run at 70 volts. Method development for the C2B6E4 and C2B6E5 primer sets.

Figure 30 displays the banding yielded for the C2B6E4 and C2B6E5 primers during PCR validation. For the C2B6E5 primer set there is a significant amount of smearing and the presence of non specific amplification with more than one DNA band identified, suggesting poor PCR selectivity. Faint DNA banding is present for the C2B6E4 primer set. This is the initial phase in the method development for C2B6E4 and C2B6E5 and the presence of DNA bands demonstrates adequate primer design.

C2B6Pr

Figure 31 displays a gradient reaction conducted to validate the C2B6Pr primer set. There is significant DNA smearing beginning at the well and continuing throughout the gel suggesting the presence of genomic DNA. In addition multiple DNA bands can be seen highlighting non specific amplification. Further optimisation is required for this primer set.

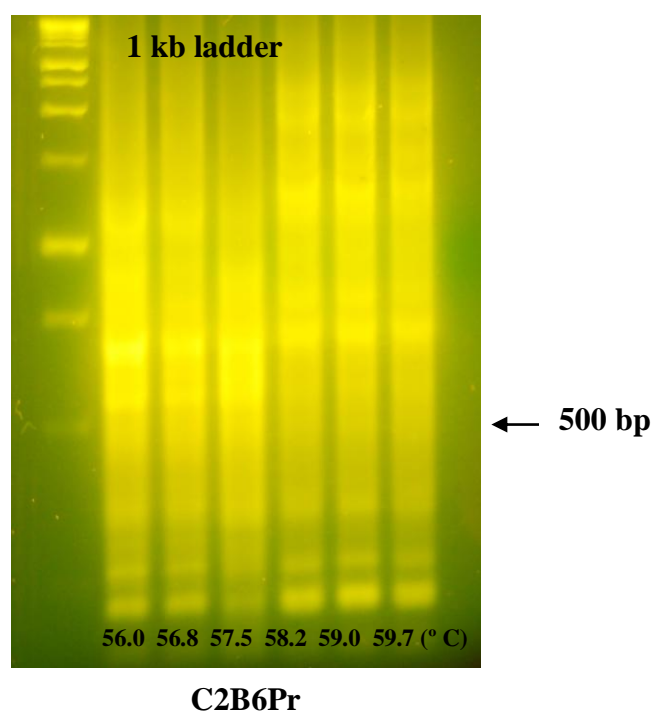


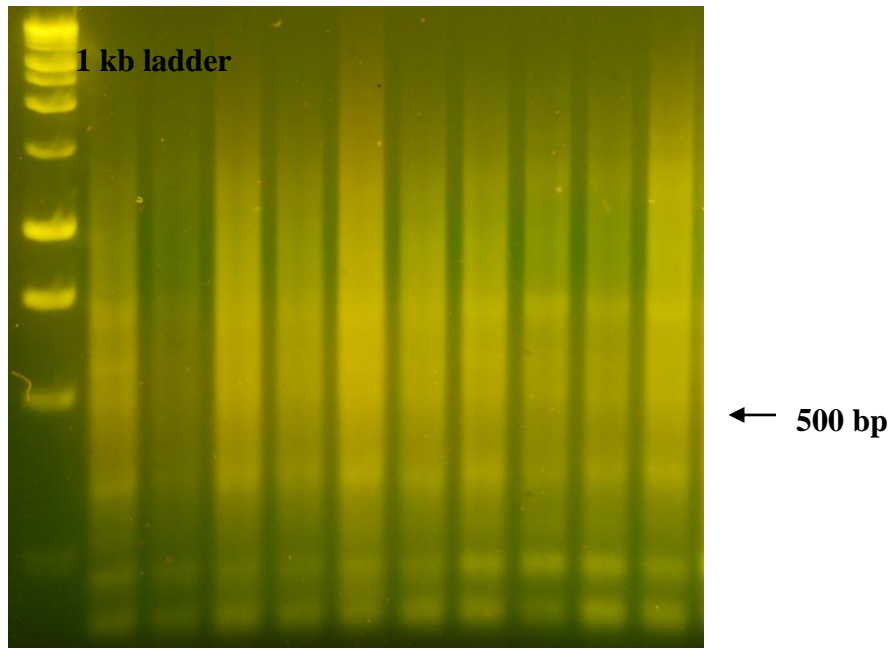
Figure 31: PCR validation for C2B6Pr primers.

Agarose gel (1.6 %), run at 70 volts. Method development for C2B6Pr primer set indicating poor selectivity.

3.1.3.2 T750C PCR validation

3.1.3.2.1 Temperature

Poor selectivity is still apparent in this reaction with multiple bands present throughout the gel (Figure 32).



DC1, DC2, DC3, DC4, DC5, DC6, DC7, DC8, DC9, DC10

Figure 32: PCR temperature optimisation for C2B6Pr.

Agarose gel (1.6 %), run at 70 volts. Temperature gradient set at $62\text{ }^{\circ}\text{C} \pm 3\text{ }^{\circ}\text{C}$.

3.1.3.2.2 MgCl_2

A reduction in MgCl_2 reduced some of the smearing and poor selectivity. However this result is still not sufficient for further processing.

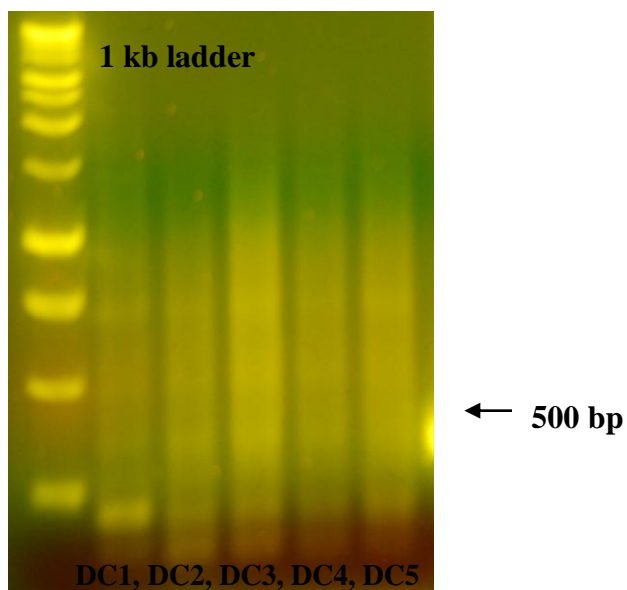


Figure 33: PCR MgCl_2 optimisation for C2B6Pr.

Agarose gel (1.6 %), run at 70 volts. A decrease from $6\text{ }\mu\text{l}$ to $4\text{ }\mu\text{l}$ MgCl_2 did not improve selectivity.

3.1.3.3 T750C Identification

As demonstrated in Figure 34 an increase in annealing temperature (65°C) produced banding suitable for DNA sequencing.

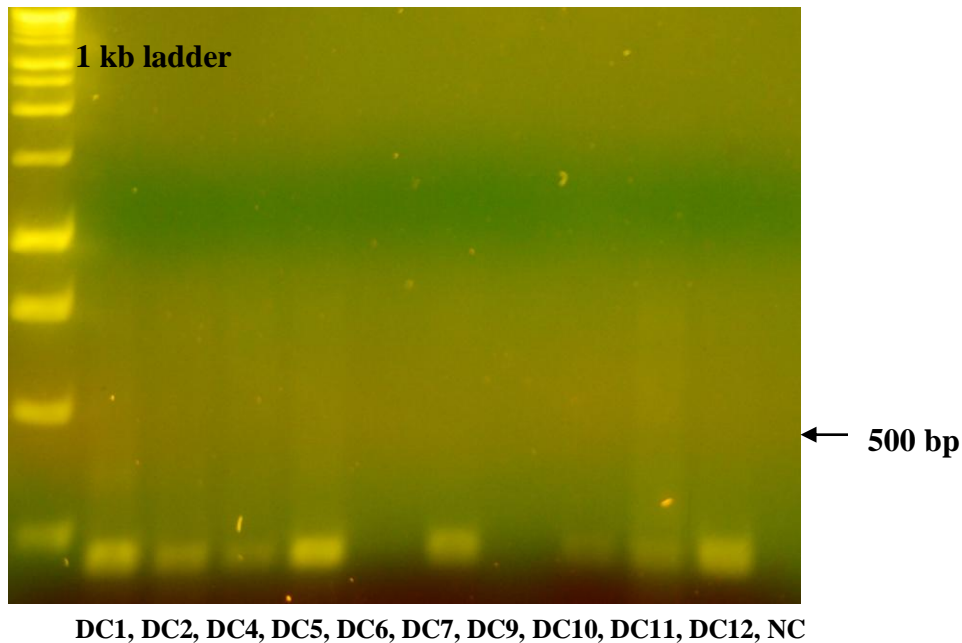


Figure 34: Amplification of *CYP2B6* promoter region using C2B6PR primers.

Agarose gel (1.6 %), run at 70 volts. An increase in temperature from 62.1 °C to 65 °C improved DNA banding for the C2B6Pr primer set.

3.1.3.3.1 T750C sequencing results

PCR amplified DNA for 9 subjects were sequenced to identify a positive control for T750C. All of the samples sent yielded sufficient sequences for analysis.

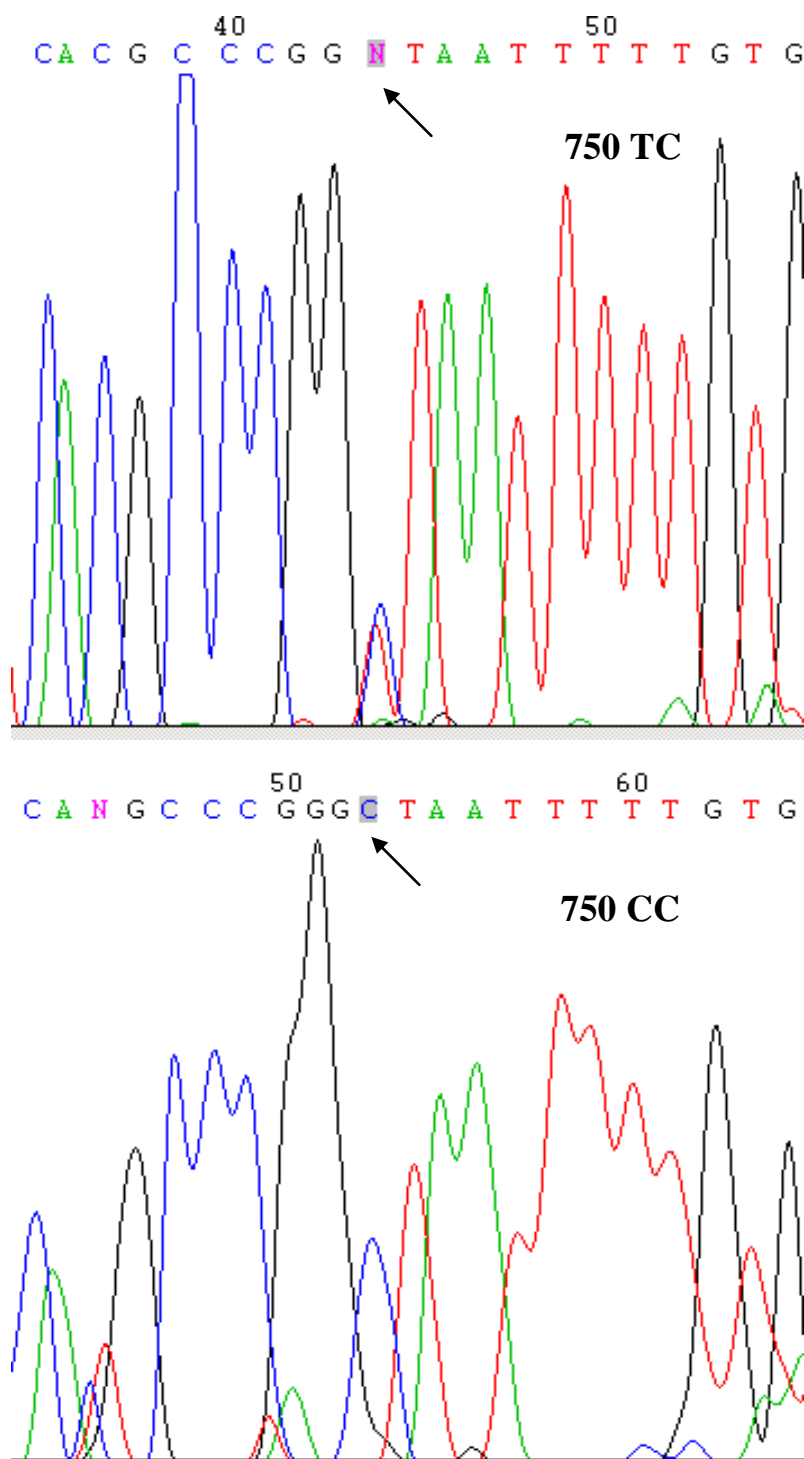


Figure 35: A comparison of two SNP genotypes for the T750C SNP (750 TC & 750 CC).

A typical DNA profile for the *CYP2B6* T750C SNP. The arrows indicate the base position of the T750C SNP for the 750 TC and 750 CC genotypes. For the 750 TC genotype there is a black peak denoting the G allele and below this there is a blue peak denoting the C allele. Therefore this is a heterozygous subject. For the 750 CC genotype there is a single blue peak denoting the C allele.

3.1.3.4 G516T PCR validation

3.1.3.4.1 Temperature

Temperature gradients

A gradient reaction for C2B6E4 was conducted to determine the optimal primer annealing temperature. Temperatures 58.0 °C, 58.8 °C and 59.5 °C yielded the clearest DNA bands. The higher temperatures tested demonstrated poor selectivity with temperatures exceeding 63.0 °C yielding barely visible DNA bands (Figure 36).

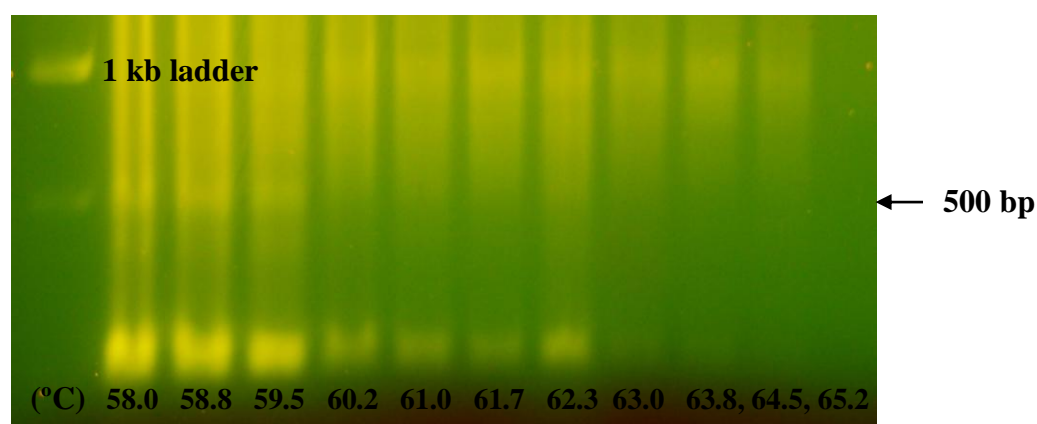


Figure 36: Gradient PCR amplification for C2B6E4.

Agarose gel (1.6 %), run at 70 volts. Temperatures > 63 °C did not produce adequate DNA banding.

Temperatures selected from gradient PCR reactions

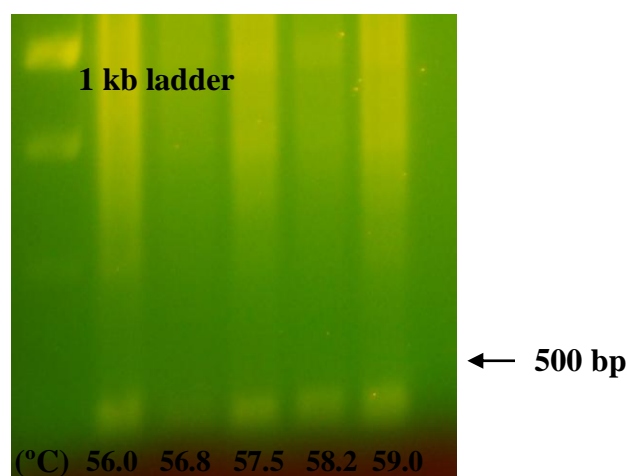


Figure 37: C2B6E4 banding following a decrease in annealing temperature.

Agarose gel (1.6 %), run at 70 volts. The 59.0 °C temperature yielded the best DNA banding.

A decrease in annealing temperature was tested following the gradient reaction results (Figure 37). The best DNA bands were obtained at 58.2 °C and 59.0 °C in agreement with earlier results (Figure 36).

3.1.3.4.2 $MgCl_2$

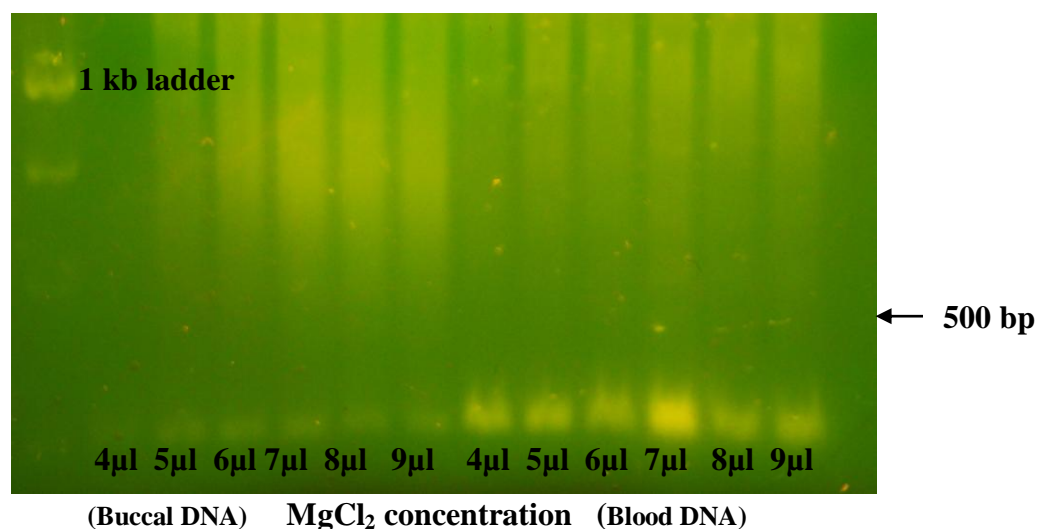


Figure 38: The effect of $MgCl_2$ concentration on C2B6E4 amplification.

Agarose gel (1.6 %), run at 70 volts. DNA extracted from blood yielded clearer DNA banding.

The effect of differing $MgCl_2$ concentrations on PCR success for C2B6E4 primers was tested (Figure 38). The volumes of $MgCl_2$ ranged from 4 to 9 μ l with 7 μ l yielding the clearest DNA banding. Template source was also tested with DNA extracted from blood samples demonstrating much clearer DNA bands than the buccal samples. The results from this study recommend further reactions with C2B6E4 using a $MgCl_2$ volume of 7 μ l.

3.1.3.5 G516T Identification

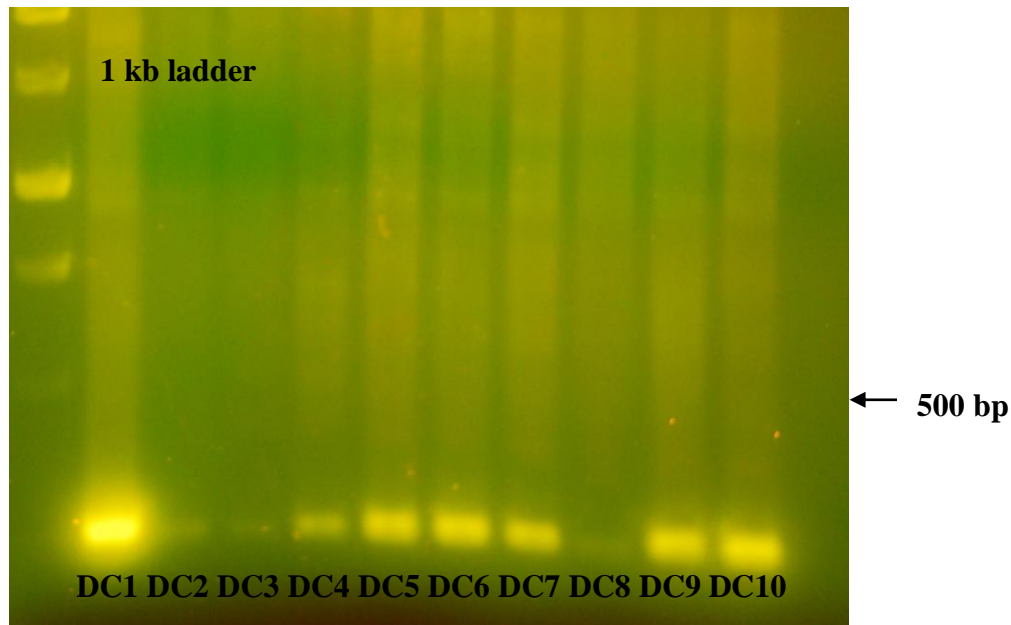


Figure 39: Amplification of *CYP2B6* exon 4 region using C2B6E4 primers run 1.

Agarose gel (1.6 %), run at 70 volts. PCR amplification of C2B6E4 for ten subjects.

Clear DNA amplification for most of the samples was successfully achieved (Figures 39 & 40). Poor amplification was noted for DC2, DC3, and DC8 (Figure 39) which may be a result of template degradation following repeated freeze and thaw cycles. Alternatively the DNA sample may have required further mixing prior to use to ensure a homogenous solution and adequate template collection. All of the other samples amplified yielded clear bands allowing further DNA processing in the form of DNA sequencing to screen for the G516T mutation.

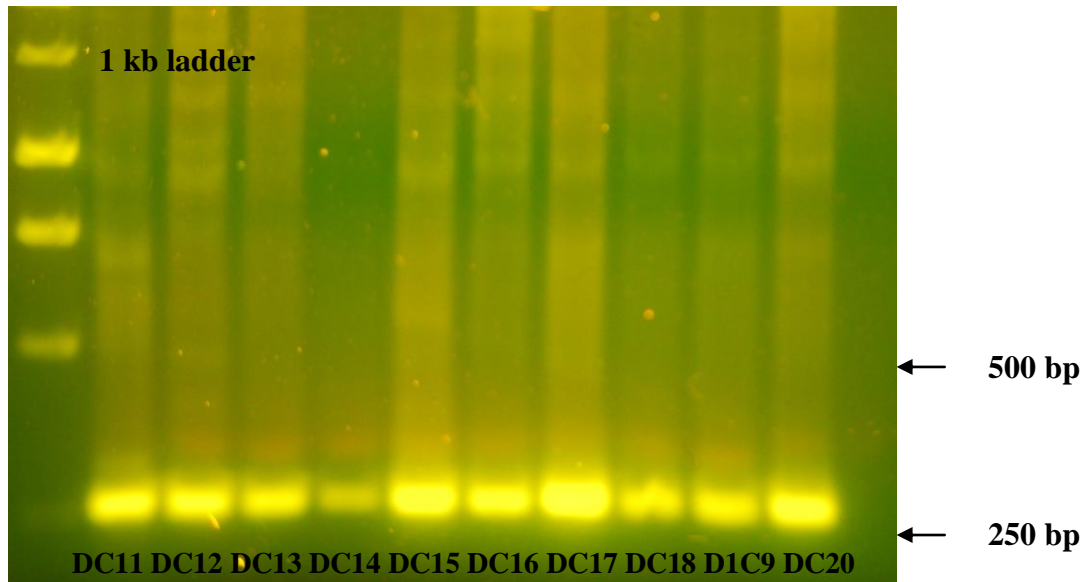


Figure 40: Amplification of *CYP2B6* exon 4 region using C2B6E4 primers run 2.

Agarose gel (1.6 %), run at 70 volts. PCR amplification of C2B6E4 for ten subjects.

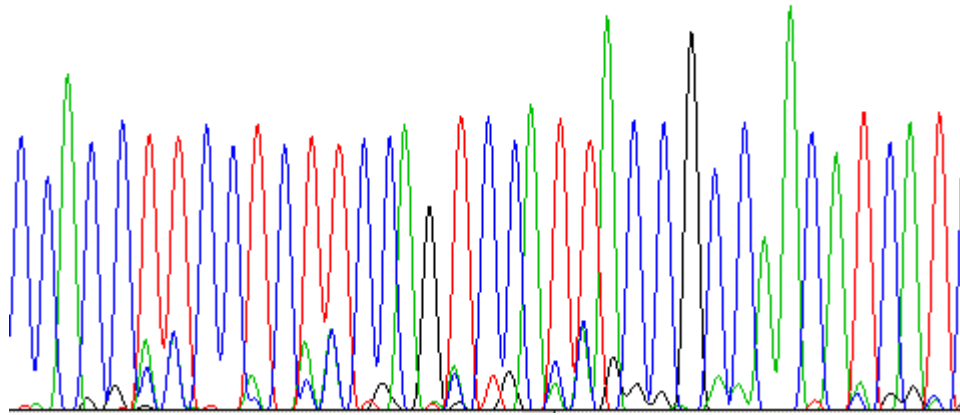
3.1.3.5.1 G516T sequencing results

PCR amplified DNA were sequenced to identify a positive control for G516T. All of the 10 samples sent off for sequencing yielded sufficient sequences for analysis.

140 150 160 170
C C A C C T T C C T C T T C C A G T C C A T T A C C G C C A A C A T C A T C



516 GG



140 150 160
C C A C C T T C C T C T T C C A T T C C A T T A C C G C C A A C A T C A T C



516 GT

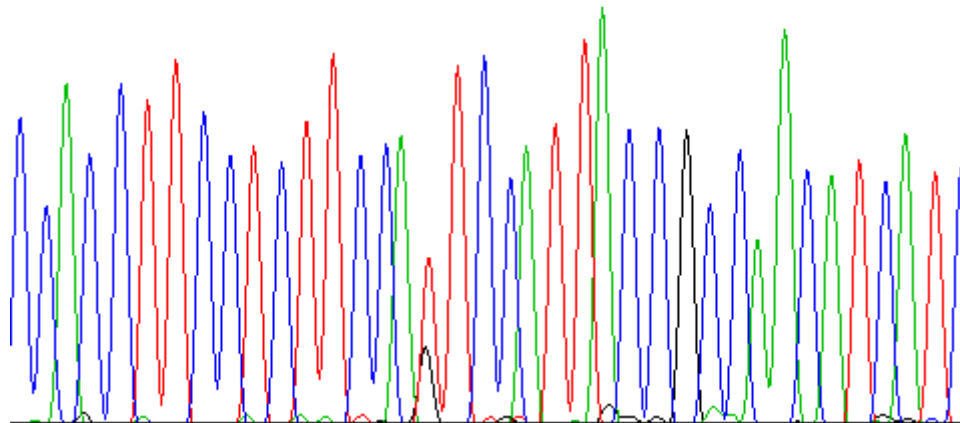


Figure 41: A comparison of two SNP genotypes for the G516T SNP (516 GG & 516 GT).

A typical DNA profile for the *CYP2B6* G516T SNP. The arrows indicate the base position of the G516T SNP for the 516 GG and 516 GT genotypes. For the 516 GG genotype there is a single black peak denoting the G allele. For the 516 GT genotype there is a red peak denoting the T allele and below this there is a black peak denoting the G allele. Therefore this is a heterozygous subject.

3.1.3.6 A785G validation

3.1.3.6.1 Temperature

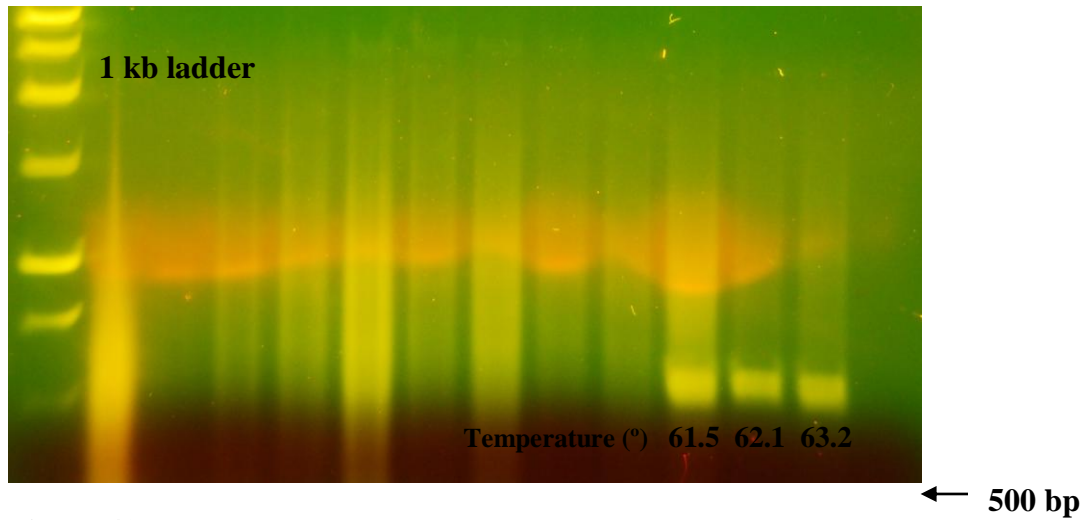


Figure 42: C2B6E5 banding following an increase in annealing temperature.

Agarose gel (1.6 %), run at 70 volts. Temperatures between 61.5 °C and 63.2 °C yielded suitable bands.

The results from the primer validation run for C2B6E5 (Figure 42) highlighted the need for an increase in annealing temperature. Of the three temperatures tested 63.2 °C demonstrated the clearest DNA band, with minimal smearing. Therefore this annealing temperature will be used for further C2B6E5 amplifications.

3.1.3.7 A785G Identification

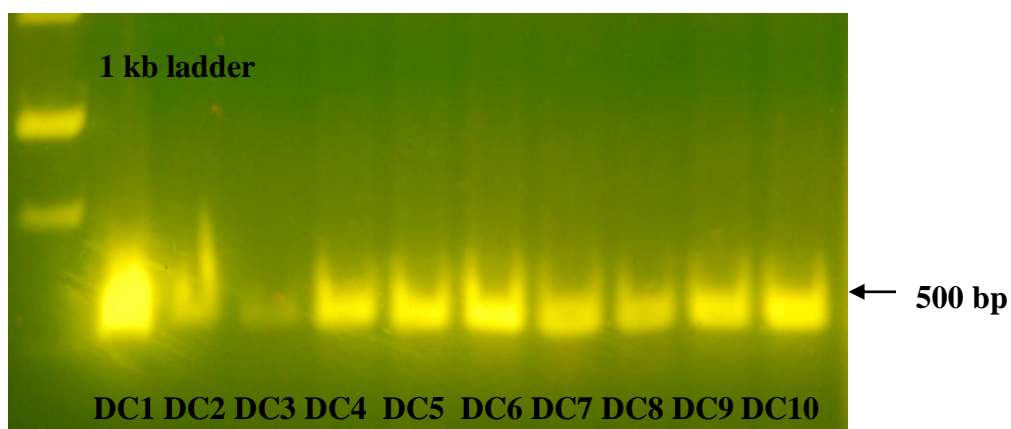


Figure 43: Amplification of *CYP2B6* exon 5 region using C2B6E5 primers run 1.

Agarose gel (1.6 %), run at 70 volts. PCR amplification of C2B6E5 for ten subjects.

Clear DNA amplifications from all but samples DC3 (Figure 43) and DC14 (Figure 44) were successfully achieved (Figures 43 & 44). This result allowed further DNA processing in the form of DNA sequencing to screen for the A785G polymorphism.

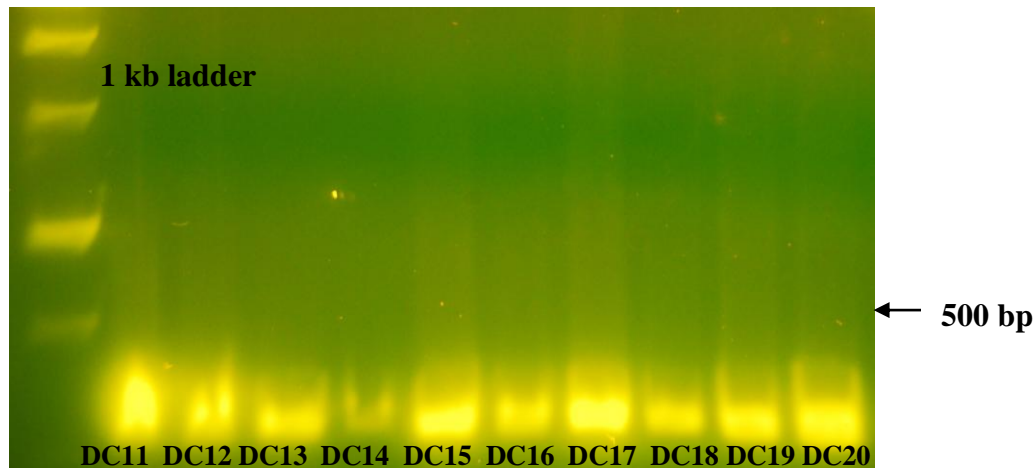


Figure 44: Amplification of CYP2B6 exon 5 region using C2B6E5 primers run 2.

Agarose gel, run at 70 volts. PCR amplification of C2B6E5 for ten subjects.

3.1.3.7.1 A785G sequencing results

PCR amplified DNA were sequenced to identify a positive control for A785G. All of the 10 samples sent off for sequencing yielded sufficient sequences for analysis.

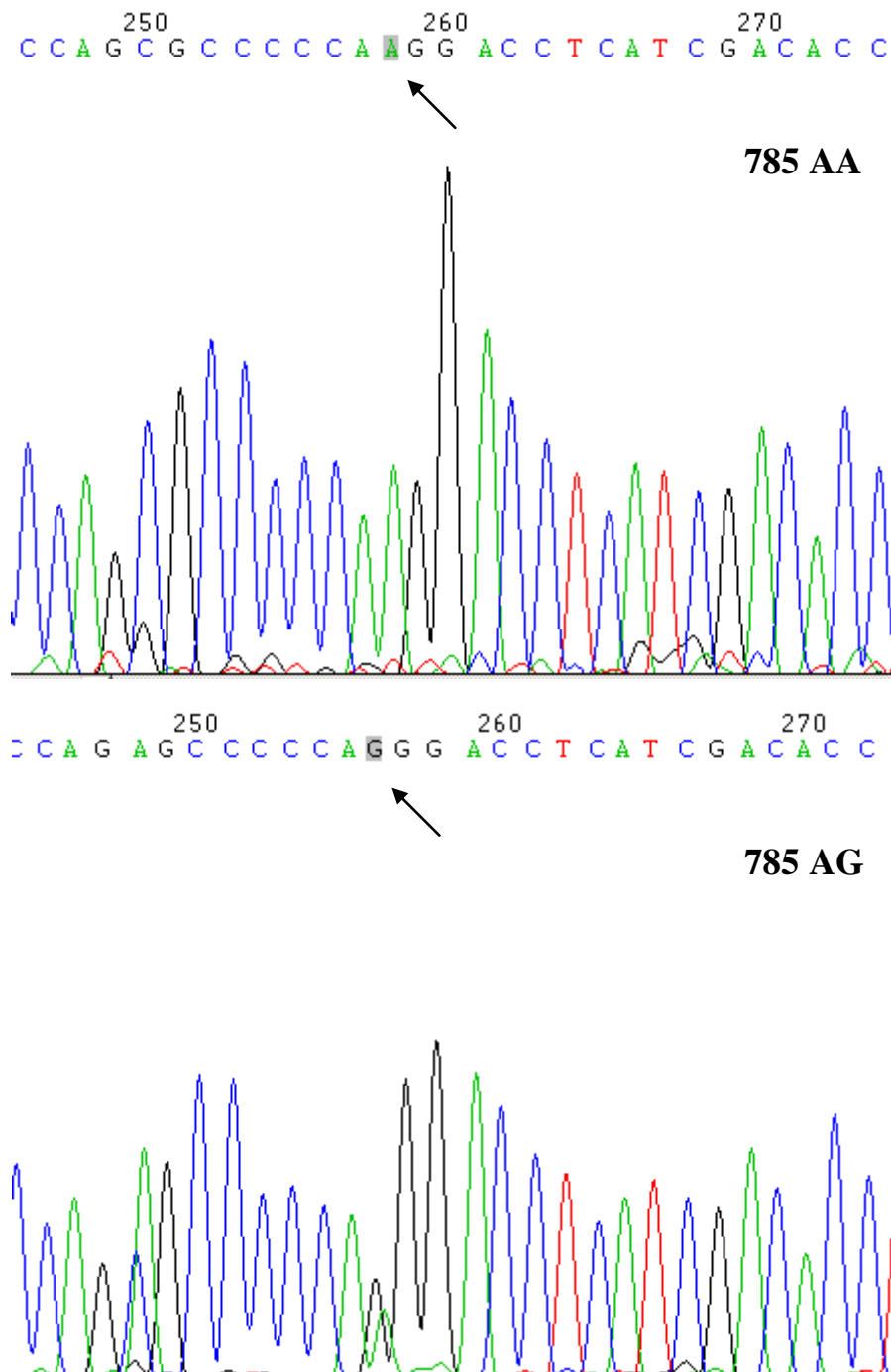


Figure 45: A comparison of two SNP genotypes for the A785G SNP (785 AA & 785 GG).

A typical DNA profile for the *CYP2B6* A785G SNP. The arrows indicate the base position of the A785G SNP for the 785 AA and 785 AG genotypes. For the 785 AA genotype there is a single green peak denoting the A allele. For the 785 AG genotype there is a black peak denoting the G allele and below this there is a green peak denoting the A allele. Therefore this is a heterozygous subject.

3.2 Post-mortem Sample Examination

3.2.1 Postmortem sample study

This section discusses the summary of toxicological findings reported by the Centre of Forensic and Legal Medicine Laboratory, Dundee University for all cases that have been used in this work. In total 84 cases were examined (Table 26), of these 69 were attributed to methadone, determined by the pathologist using case histories (which were not always available for use in this study) and post-mortem findings. Most toxicologists would generally agree that a methadone blood concentration > 0.4 mg/L is fatal and that the death can be attributed to methadone, however due to unknown case histories and polydrug use the cases reported in this study are reliant on the pathologists decision. A preliminary study reported the association between *OPRM1* and *CYP2B6* variations and blood methadone concentrations in 40 post-mortem subjects (Chapter 4). The study was then increased to include 69 methadone-attributed deaths as determined by the pathologist (Chapter 5). A further 15 cases where methadone was involved in the cause of death (death attributed to polydrug use) were then used to examine the difference of *OPRM1* and *CYP2B6* allele frequencies between the post-mortem population and a living control population of non-methadone using subjects. The results from the post-mortem study are reported below and discussed further in Chapters 4, 5, and 6.

Table 26: Drug Toxicology for samples DC1-DC84 where the deaths had been associated with methadone.

Case	Age	Sex	Race	Methadone (mg/l)	Sample	EtOH (mg/100ml)	Drug Toxicology (mg/L)
1	43	M	Caucasian	0.13	Sc	ND	Morphine total 8.3
2	32	M	Caucasian	0.27	Fm	ND	Diazepam 1.2
3	57	F	Caucasian	0.86	Fm	ND	Diazepam 1.3
4	37	F	Caucasian	1.16	Fm	ND	Venlafaxine 3.9
5	36	M	Caucasian	0.30	Fm	ND	Morphine 0.085
6	20	M	Caucasian	1.1	Fm	ND	
7	32	M	Caucasian	0.82	Fm	138	Propranolol 4.09 Mirtazapine 1.2
8	24	M	Caucasian	0.97	Fm	ND	
9	26	M	Caucasian	0.22	Fm	18	Morphine 0.024 Diazepam 0.8 Nordiazepam 1.98
10	33	M	Caucasian	trace	Fm	ND	Morphine 0.13 Diazepam 0.42
11	28	M	Caucasian	0.20	Fm	81	Trazadone 0.18
12	26	M	Caucasian	1.44	Fm	ND	
13	31	M	Caucasian	0.48	Fm	ND	Morphine 0.032 Diazepam 0.84
14	38	M	Caucasian	1.25	Fm	35	Citalopram 0.28 Quetiapine 1.5
15	32	F	Caucasian	1.08	Fm	ND	Morphine 0.028 Diazepam 1.13 Nordiazepam 2.72 Dothiepin 1.19
16	27	M	Caucasian	0.44	Fm	78	Morphine 0.04 Diazepam 1.23 Nordiazepam 0.76
17	44	M	Caucasian	0.58	Fm	ND	Morphine 0.03 Diazepam 0.41
18	30	M	Caucasian	0.44	Sc	ND	Diazepam 0.26 Nordiazepam 0.44
19	20	M	Caucasian	0.33	Fm	ND	Diazepam 2.19 Nordiazepam 1.6 Amfetamine 0.59
20	37	M	Caucasian	0.95	Fm	296	Diazepam 0.81 Nordiazepam 2.72 Fluoxetine 0.5
21	32	M	Caucasian	0.58	Fm	ND	
22	42	M	Caucasian	0.65	Fm	299	Dihydrocodeine 1.8
23	20	M	Caucasian	1.66	Fm	ND	Morphine 0.05 Diazepam 0.30 Nordiazepam 1.10
24	17	F	Caucasian	0.60	Fm	ND	Morphine 0.02
25	41	F	Caucasian	D	Ur	ND	Morphine 0.34 Diazepam 0.57 Nordiazepam 0.49 Citalopram 0.41
26	23	M	Caucasian	1.70	Cd	68	
27	22	M	Caucasian	0.54	Fm	86	Diazepam 0.21 Nordiazepam 0.32 Citalopram 0.39
28	60	F	Caucasian	0.26	Fm	ND	

Case	Age	Sex	Caucasian	Metadone (mg/l)	Sample	EtOH (mg/100ml)	Toxicology (mg/l)
29	45	M	Caucasian	D	Ur	ND	Morphine 0.09 Diazepam 1.13 Nordiazepam 3.29 Mirtazapine 0.17
30	34	M	Caucasian	2.23	Fm	ND	Morphine 0.09
31	36	M	Caucasian	0.39	Fm	14	Morphine 1.00 Dihydrocodeine 0.50
32	18	M	Caucasian	0.25	Fm	51	Diazepam 0.27 Nordiazepam 0.35
33	44	M	Caucasian	0.15	Cd	ND	Amitriptyline 2.5 Venlafaxine 2.3
34	24	M	Caucasian	0.37	Fm	ND	Morphine 0.02 Nordiazepam 0.39
35	21	M	Caucasian	0.22	Fm	110	Diazepam 0.68 Nordiazepam 0.55
36	22	M	Caucasian	0.22	Fm	34	Morphine 0.11 Diazepam 0.24 Nordiazepam 0.34
37	41	M	Caucasian	1.3	Fm	ND	
38	32	M	Caucasian	1.38	Fm	ND	
39	20	M	Caucasian	0.19	Fm	53 (Ur)	Morphine 0.04
40	23	M	Caucasian	D	Ur	ND	Morphine 0.06 MDMA 0.74
41	40	M	Caucasian	0.75	Fm	24	Diazepam 0.45 Nordiazepam 1.11
42	18	M	Caucasian	0.24	Fm	ND	
43	31	M	Caucasian	1.53	Fm	ND	Morphine 0.025 Diazepam 0.64 Nordiazepam 1.02
44	32	M	Caucasian	Tr	Fm	ND	Morphine 0.09
45	46	M	Caucasian	0.56	Fm	16	
46	21	F	Caucasian	D	Ur	ND	Morphine 0.41
47	34	M	Caucasian				
48	29	F	Caucasian				
49	35	M	Caucasian / Asian	0.80	Fm	ND	Morphine 0.02 Diazepam 0.59 Nordiazepam 1.21 Dothiepin 0.45
50	33	M	Caucasian	0.75	Fm	ND	Diazepam 0.78 Nordiazepam 1.64
51	29	M	Caucasian	0.43	Cd	ND	Diazepam 0.29 Nordiazepam 0.53 Dothiepin 0.56 Lamotrigine 0.4
52	26	M	Caucasian	10.1	Cd	ND	
53	44	M	Caucasian	0.72	Fm	ND	Dihydrocodeine 0.90 Nordiazepam 0.26 Chlorodiazepoxide 0.8
54	51	M	Caucasian	D	Ur	ND	Diazepam 0.23 Nordiazepam 0.36 Dihydrocodeine 4.13
55	22	F	Caucasian	0.85	Fm	ND	Morphine 0.016 Diazepam 0.62 Nordiazepam 0.58
56	30	F	Caucasian	0.44	Fm	11	

Case	Age	Sex	Caucasian	Methadone (mg/l)	Sample	EtOH (mg/100ml)	Toxicology (mg/l)
57	56	M	Caucasian	2.99	Fm	ND	
58	44	F	Caucasian	<0.15	Fm	ND	Tramadol 0.39
59	35	M	Caucasian	0.31	Fm	13	Morphine 0.08
60	49	F	Caucasian	0.99	Fm	29	
61	27	F	Iranian	2.48	Fm	ND	
62	26	M	Caucasian	0.021	Fm	ND	Morphine 0.22
63	22	M	Caucasian	0.71	Fm	ND	
64	37	F	Caucasian	2.1	Fm	ND	
65	21	M	Caucasian	0.15	Fm	11	Morphine 0.18
66	32	F	Caucasian	2.59	Fm	ND	Morphine 0.05 Amitriptyline 2.62 Nortriptyline 5.89
67	35	M	Caucasian	0.21	Fm	ND	Amitriptyline 1.58
68	55	F	Caucasian	0.3	Fm	ND	
69	32	M	Caucasian	1.24	Fm	ND	Amitriptyline 0.26 Diazepam 0.78 Nordiazepam 0.68
70	37	F	Caucasian	1.1	Fm	ND	Diazepam 1.3 Nordiazepam 0.98 Citalopram 0.84
71	43	F	Caucasian	1.9	Fm	ND	Diazepam 0.95 Nordiazepam 0.48 Mirtazapine 0.39
72	43	M	Caucasian	2.63	Fm	ND	
73	54	M	Caucasian	0.75	Fm	114	Nordiazepam 0.21
74	20	F	Caucasian	0.3	Fm	ND	Diazepam 0.52
75	34	M	Caucasian / Asian	0.35	Fm	ND	
76	40	M	Caucasian	1.22	Fm	ND	
77	23	M	Caucasian	0.42	Fm	22	Diazepam 1.07 Nordiazepam 0.58
78	28	M	Caucasian	0.66	Fm	11	Diazepam 0.24 Nordiazepam 0.32
79	30	F	Caucasian	0.58	Fm		Diazepam 2.38 Nordiazepam 1.67
80	34	F	Caucasian	0.36	Fm	98	Citalopram 0.84
81	31	M	Caucasian	1.17	Fm	ND	Morphine 1.1
82	49	F	Caucasian	2.11	Fm	ND	Morphine 0.02 Diazepam 1.90 Tramadol 2.95 Amitriptyline 1.05 Carbamazepine 4.05
83	37	M	Caucasian	1.77	Fm	ND	Morphine 0.05 Temazepam 1.03
84	23	M	Caucasian	0.22	Fm	ND	Morphine 0.07 Diazepam 0.43 Nordiazepam 0.43

Note: D equals detected, Fm is femoral, Sc is subclavian, Ur is urine, Cd is cardiac and ND equals undetermined.

The drug toxicology results for the 84 methadone involved deaths samples are displayed above in Table 26. The mean and median age of the post-mortem subjects

was 33.2 and 33 respectively. Sixty two of the subjects were male (74 %) and 98 % were Caucasian. Methadone was detected in all 84 cases however in some cases only trace amounts were identified. Furthermore, for some case subjects the blood sampled was collected from the sub clavian and cardiac regions, not the preferred femoral vein. Therefore for the analysis of SNP effects on methadone concentration and response only femoral and quantifiable samples were analysed (For results see Chapters 4, 5, & 6). Polydrug use was identified for most of the case subjects sampled, with benzodiazepines found in combination with methadone in 47 % of subjects.

3.2.1.1 Quantification of DNA from post-mortem blood

All of the 84 extracted post-mortem samples were successfully quantified using the human quantifiler® kit (Table 27).

Table 27: DNA yield for methadone and morphine associated post-mortem whole blood extractions.

Sample	DNA yield ng/µl	Sample	DNA yield ng/µl	Sample	DNA yield ng/µl	Sample	DNA yield ng/µl	Sample	DNA yield ng/µl
DC1	55.98	DC18	36.06	DC35	43.72	DC52	39.67	DC69	28.36
DC2	11.35	DC19	24.30	DC36	22.87	DC53	89.42	DC70	34.80
DC3	2.88	DC20	28.51	DC37	10.41	DC54	51.07	DC71	19.74
DC4	20.19	DC21	20.64	DC38	106.39	DC55	54.02	DC72	15.81
DC5	48.25	DC22	15.77	DC39	46.13	DC56	59.62	DC73	3.47
DC6	30.69	DC23	72.13	DC40	45.30	DC57	21.77	DC74	34.20
DC7	23.85	DC24	60.69	DC41	114.12	DC58	20.50	DC75	0.13
DC8	4.16	DC25	65.18	DC42	71.24	DC59	20.24	DC76	35.07
DC9	78.98	DC26	103.36	DC43	8.57	DC60	14.76	DC77	9.12
DC10	63.93	DC27	75.01	DC44	74.53	DC61	12.39	DC78	0.92
DC11	60.89	DC28	20.41	DC45	13.06	DC62	20.22	DC79	0.87
DC12	36.52	DC29	41.11	DC46	81.53	DC63	45.33	DC80	57.35
DC13	28.72	DC30	38.72	DC47	1.21	DC64	8.58	DC81	23.98
DC14	16.20	DC31	62.21	DC48	38.84	DC65	21.86	DC82	88.34
DC15	49.77	DC32	86.29	DC49	59.00	DC66	69.60	DC83	21.37
DC16	18.29	DC33	30.22	DC50	34.93	DC67	7.55	DC84	68.07
DC17	78.86	DC34	84.56	DC51	6.08	DC68	37.71		

3.2.1.2 A118G SNP Genotyping

All 84 subjects of the post-mortem group where methadone was associated with the cause of death were successfully genotyped for the *OPRM1* A118G variation (Figure 46; Table 28).

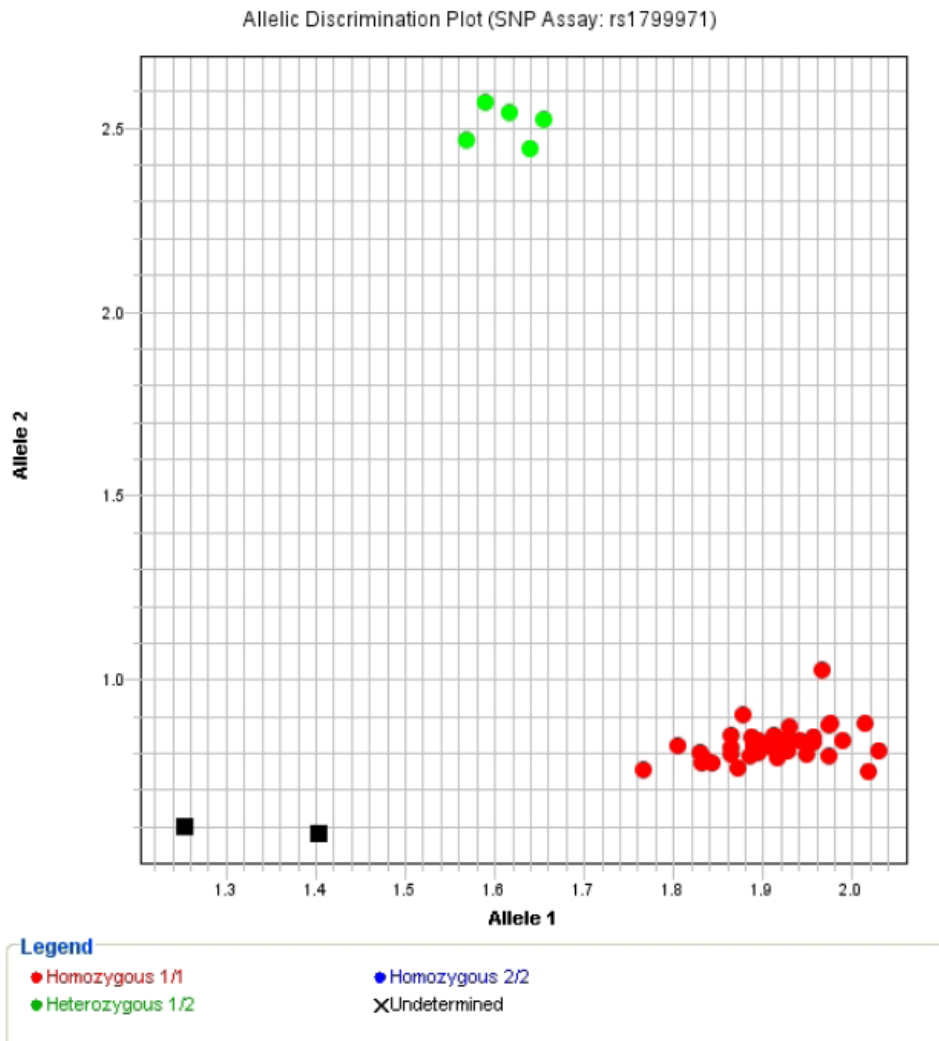


Figure 46: A typical allelic discrimination plot for the A118G SNP.

Where homozygous 1/1 stands for 118 AA subjects, 1/2 stands for 118 AG subjects and homozygous 2/2 represents 118 GG subjects. As shown in the legend undetermined samples are denoted by a X. No post-mortem subjects were undetermined during A118G SNP genotyping. The black square denotes the negative control. All samples were run in duplicate together with positive controls.

Table 28: A118G genotypes for the 84 post-mortem samples.

Sample	A118G genotype	Sample	A118G genotype	Sample	A118G genotype	Sample	A118G genotype
DC1	AA	DC22	AA	DC43	AA	DC64	AA
DC2	AA	DC23	AA	DC44	AA	DC65	AA
DC3	AA	DC24	AA	DC45	AA	DC66	AA
DC4	AA	DC25	AA	DC46	AA	DC67	AA
DC5	AA	DC26	AA	DC47	AA	DC68	AA
DC6	AA	DC27	AA	DC48	AA	DC69	AA
DC7	AA	DC28	AA	DC49	AA	DC70	AA
DC8	AA	DC29	AG	DC50	AA	DC71	AA
DC9	AA	DC30	AA	DC51	AG	DC72	AA
DC10	AA	DC31	AA	DC52	AA	DC73	AG
DC11	AA	DC32	AA	DC53	AG	DC74	AA
DC12	AG	DC33	AA	DC54	AA	DC75	AA
DC13	AA	DC34	AA	DC55	AG	DC76	AA
DC14	AA	DC34	AA	DC56	AA	DC77	AA
DC15	AG	DC36	AA	DC57	AG	DC78	AA
DC16	AA	DC37	AA	DC58	AA	DC79	AA
DC17	AA	DC38	AA	DC59	AA	DC80	AA
DC18	AA	DC39	AA	DC60	AA	DC81	AA
DC19	AG	DC40	AA	DC61	AA	DC82	AG
DC20	AA	DC41	AA	DC62	AA	DC83	AG
DC21	AA	DC42	AA	DC63	AA	DC84	AG

In total 12 of the post-mortem subjects were heterozygous for the A118G SNP and 72 subjects were homozygous for the A allele. No subjects were homozygous for the G allele.

3.2.1.3 T750C SNP Genotyping

All 84 subjects of the post-mortem group where methadone was associated with the cause of death were successfully genotyped for the *CYP2B6* T750C variation (Figure 47, Table 29).

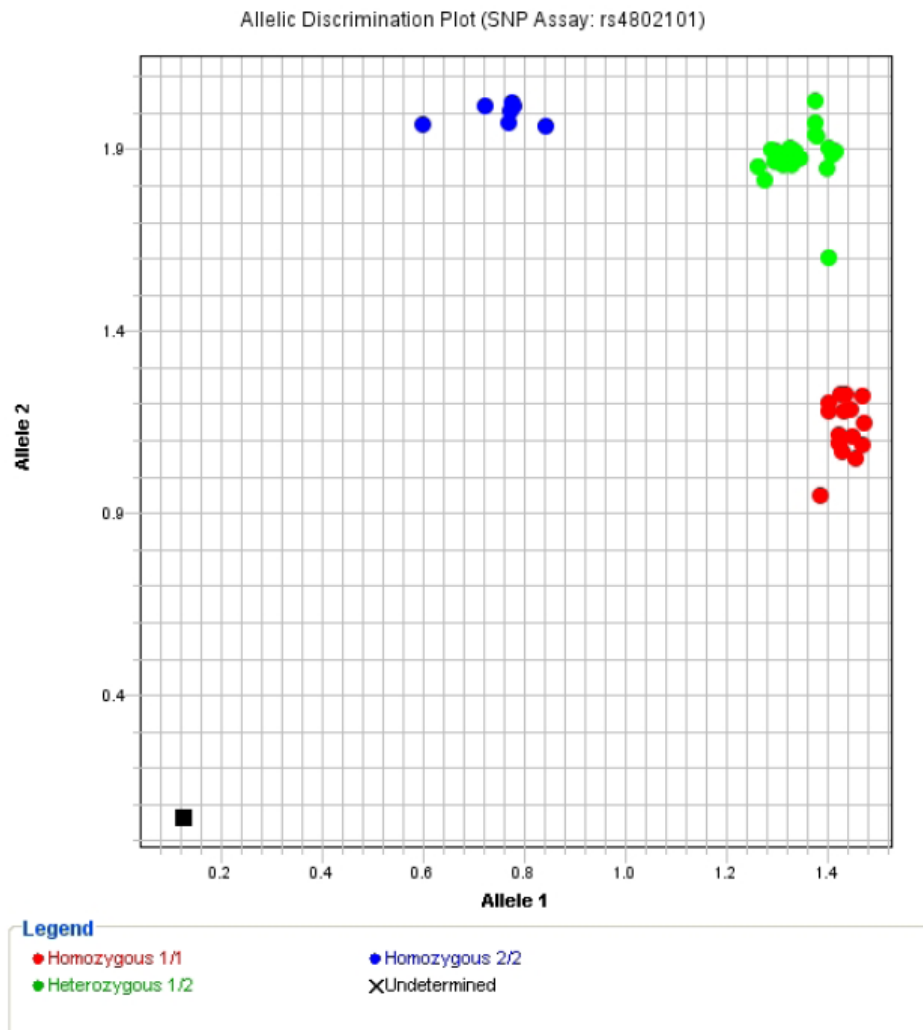


Figure 47: A typical allelic discrimination plot for the T750C SNP.

Where homozygous 1/1 stands for 750 TT subjects, 1/2 stands for 750 TC subjects and homozygous 2/2 represents 750 CC subjects. As shown in the legend undetermined samples are denoted by a X. No post-mortem subjects were undetermined during T750C SNP genotyping. The black square denotes the negative control. All samples were run in duplicate together with positive controls.

Table 29: T750C genotypes for the 84 post-mortem samples.

Sample	T750C genotype	Sample	T750C genotype	Sample	T750C genotype	Sample	T750C genotype
DC1	TC	DC22	CC	DC43	TC	DC64	TT
DC2	TT	DC23	TT	DC44	TC	DC65	CC
DC3	TC	DC24	TT	DC45	TT	DC66	TT
DC4	TT	DC25	TT	DC46	TT	DC67	CC
DC5	TT	DC26	TT	DC47	TT	DC68	TT
DC6	TC	DC27	TC	DC48	TC	DC69	TC
DC7	TT	DC28	TT	DC49	TC	DC70	TC
DC8	TC	DC29	CC	DC50	CC	DC71	TT
DC9	TC	DC30	TT	DC51	CC	DC72	TC
DC10	TC	DC31	TC	DC52	TC	DC73	TC
DC11	TT	DC32	TC	DC53	TC	DC74	TT
DC12	TC	DC33	TC	DC54	TT	DC75	TC
DC13	CC	DC34	CC	DC55	TT	DC76	TC
DC14	TC	DC34	CC	DC56	CC	DC77	TC
DC15	TT	DC36	TC	DC57	CC	DC78	TT
DC16	CC	DC37	TT	DC58	TC	DC79	TC
DC17	TC	DC38	TT	DC59	TC	DC80	CC
DC18	TT	DC39	TC	DC60	TC	DC81	CC
DC19	TC	DC40	TC	DC61	TT	DC82	TT
DC20	TC	DC41	CC	DC62	TT	DC83	TC
DC21	TC	DC42	TT	DC63	CC	DC84	TT

In total 37 of the post-mortem subjects were heterozygous for the T750C SNP, 16 subjects were homozygous for the C allele, and 31 subjects were homozygous for the T allele.

3.2.1.4 G516T SNP Genotyping

All 84 subjects of the post-mortem group where methadone was associated with the cause of death were successfully genotyped for the *CYP2B6* G516T variation (Figure 48, Table 30).

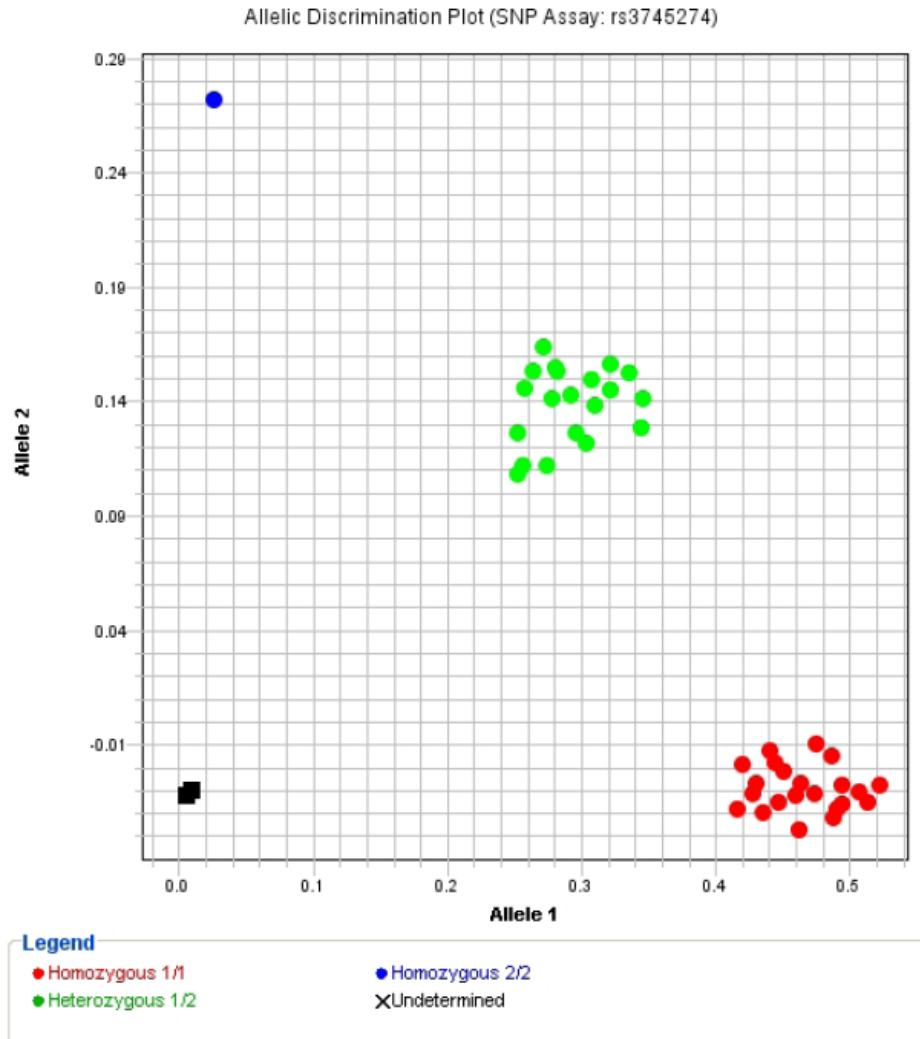


Figure 48: A typical allelic discrimination plot for the G516T SNP.

Where homozygous 1/1 stands for 516 GG subjects, 1/2 stands for 516 GT subjects and homozygous 2/2 represents 516 TT subjects. As shown in the legend undetermined samples are denoted by a X. No post-mortem subjects were undetermined during G516T SNP genotyping. The black square denotes the negative control. All samples were run in duplicate together with positive controls.

Table 30: G516T genotypes for the 84 post-mortem samples.

Sample	G516T genotype	Sample	G516T genotype	Sample	G516T genotype	Sample	G516T genotype
DC1	GT	DC22	GG	DC43	GG	DC64	GG
DC2	GG	DC23	GT	DC44	GT	DC65	GG
DC3	GG	DC24	GG	DC45	GG	DC66	GT
DC4	GT	DC25	GT	DC46	GT	DC67	GG
DC5	GG	DC26	GG	DC47	GT	DC68	GG
DC6	GG	DC27	GT	DC48	GT	DC69	GT
DC7	GT	DC28	GT	DC49	GG	DC70	GG
DC8	GT	DC29	GG	DC50	GG	DC71	GG
DC9	GG	DC30	GT	DC51	GG	DC72	GG
DC10	GT	DC31	GG	DC52	GT	DC73	GT
DC11	GT	DC32	GG	DC53	GG	DC74	GT
DC12	GT	DC33	GT	DC54	GT	DC75	GT
DC13	GG	DC34	GG	DC55	GT	DC76	GT
DC14	GG	DC34	GG	DC56	GG	DC77	GT
DC15	GT	DC36	GG	DC57	GG	DC78	GT
DC16	GG	DC37	GT	DC58	GG	DC79	GT
DC17	GG	DC38	TT	DC59	GG	DC80	GG
DC18	GT	DC39	GG	DC60	GT	DC81	GG
DC19	GT	DC40	GG	DC61	GG	DC82	GT
DC20	GG	DC41	GG	DC62	GG	DC83	GT
DC21	GG	DC42	GG	DC63	TT	DC84	GT

In total 37 of the post-mortem subjects were heterozygous for the G516T SNP, 2 subjects were homozygous for the T allele, and 45 subjects were homozygous for the G allele.

3.2.1.5 A785G SNP Genotyping

All 84 subjects of the post-mortem group where methadone was associated with the cause of death were successfully genotyped for the *CYP2B6* A785G variation (Figure 49, Table 31).

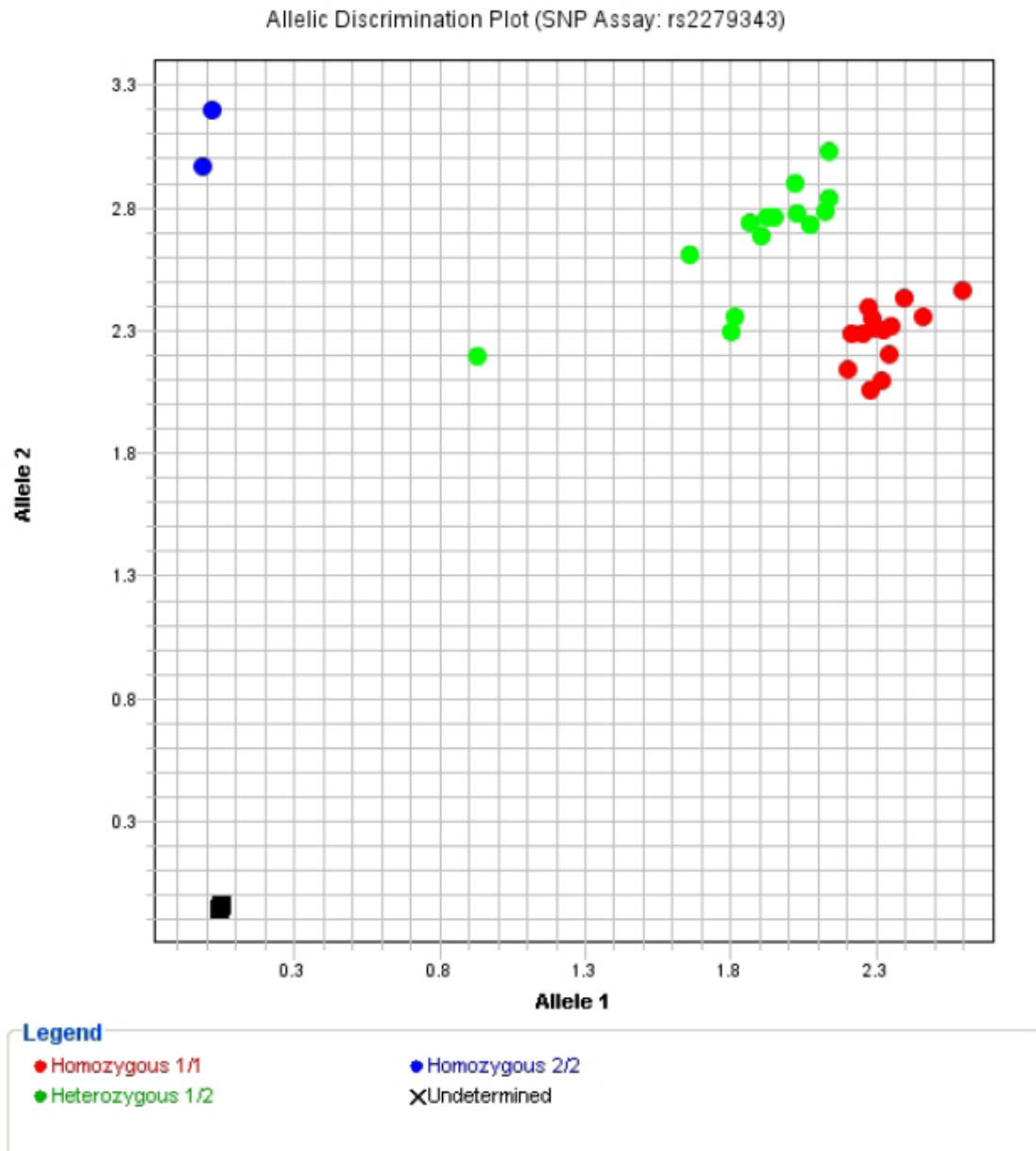


Figure 49: A typical allelic discrimination plot for the A785G SNP.

Where homozygous 1/1 stands for 785 AA subjects, 1/2 stands for 785 AG subjects and homozygous 2/2 represents 785 GG subjects. As shown in the legend undetermined samples are denoted by a X. No post-mortem subjects were undetermined during A785G SNP genotyping. The black square denotes the negative control. All samples were run in duplicate together with positive controls.

Table 31: A785G genotypes for the 84 post-mortem samples.

Sample	A785G genotype	Sample	A785G genotype	Sample	A785G genotype	Sample	A785G genotype
DC1	AG	DC22	AA	DC43	AG	DC64	AA
DC2	AA	DC23	AG	DC44	AG	DC65	AA
DC3	AA	DC24	AA	DC45	AA	DC66	AG
DC4	AG	DC25	AG	DC46	AG	DC67	AA
DC5	AA	DC26	AA	DC47	AG	DC68	AA
DC6	AA	DC27	AG	DC48	AG	DC69	AG
DC7	AG	DC28	AG	DC49	AA	DC70	AA
DC8	AG	DC29	AG	DC50	AA	DC71	AA
DC9	AA	DC30	AG	DC51	AA	DC72	AA
DC10	AG	DC31	AA	DC52	AG	DC73	AG
DC11	AG	DC32	AA	DC53	AA	DC74	AG
DC12	AG	DC33	AG	DC54	AG	DC75	AG
DC13	AA	DC34	AA	DC55	AG	DC76	AG
DC14	AA	DC34	AA	DC56	AA	DC77	AG
DC15	AG	DC36	AA	DC57	AA	DC78	AG
DC16	AA	DC37	AG	DC58	AA	DC79	AG
DC17	AA	DC38	GG	DC59	AA	DC80	AA
DC18	AG	DC39	AG	DC60	AA	DC81	AA
DC19	AG	DC40	AA	DC61	AG	DC82	AG
DC20	AA	DC41	AA	DC62	AA	DC83	AG
DC21	AA	DC42	AA	DC63	GG	DC84	AG

In total 40 of the post-mortem subjects were heterozygous for the G516T SNP, 2 subjects were homozygous for the T allele, and 42 subjects were homozygous for the G allele.

3.3 Control Sample Examination

3.3.1 Control Sample Study

All of the control samples collected were successfully quantified and genotyped for the *OPRM1* A118G, and *CYP2B6* T750C, G516T and A785G SNPs. The results for DNA quantification and SNP genotyping are reported below.

3.3.2 Buccal DNA quantification

All of the 100 extracted control samples were successfully quantified using the human quantifiler® kit (Table 32).

Samples	DNA yield ng/µl	Samples	DNA yield ng/µl	Samples	DNA yield ng/µl	Samples	DNA yield ng/µl
CC1	11.32	CC26	6.77	CC51	5.51	CC76	3.98
CC2	3.86	CC27	8.05	CC52	2.84	CC77	6.98
CC3	2.88	CC28	5.44	CC53	1.93	CC78	2.40
CC4	7.05	CC29	2.56	CC54	2.72	CC79	5.26
CC5	1.18	CC30	10.77	CC55	4.13	CC80	6.26
CC6	11.32	CC31	1.11	CC56	3.94	CC81	4.58
CC7	3.86	CC32	5.48	CC57	7.38	CC82	5.26
CC8	2.88	CC33	6.02	CC58	3.05	CC83	3.97
CC9	7.05	CC34	6.02	CC59	6.30	CC84	4.45
CC10	7.33	CC35	5.11	CC60	1.97	CC85	2.25
CC11	7.84	CC36	6.79	CC61	4.87	CC86	1.79
CC12	5.67	CC37	4.51	CC62	6.25	CC87	3.39
CC13	3.47	CC38	4.60	CC63	7.16	CC88	3.42
CC14	8.67	CC39	4.01	CC64	4.88	CC89	5.80
CC15	4.22	CC40	5.41	CC65	3.65	CC90	1.0
CC16	8.63	CC41	3.83	CC66	10.76	CC91	1.96
CC17	5.16	CC42	6.40	CC67	5.42	CC92	1.0
CC18	3.59	CC43	9.41	CC68	4.23	CC93	0.34
CC19	10.61	CC44	5.01	CC69	5.50	CC94	2.30
CC20	6.18	CC45	6.29	CC70	5.99	CC95	2.79
CC21	3.39	CC46	4.28	CC71	15.48	CC96	6.96
CC22	4.38	CC47	6.28	CC72	7.39	CC97	3.36
CC23	7.19	CC48	5.90	CC73	8.90	CC98	2.08
CC24	11.33	CC49	9.94	CC74	9.07	CC99	4.02
CC25	5.88	CC50	4.56	CC75	7.50	CC100	0.77

Table 32: DNA yield for control group buccal extractions.

3.3.3 A118G SNP genotyping

Table 33: A118G genotypes for the 100 control samples.

Samples	A118G genotype	Samples	A118G genotype	Samples	A118G genotype	Samples	A118G genotype
CC1	AA	CC26	AA	CC51	AA	CC76	AG
CC2	AA	CC27	AA	CC52	AA	CC77	AG
CC3	AG	CC28	AG	CC53	AA	CC78	AG
CC4	AA	CC29	AA	CC54	AG	CC79	AA
CC5	GG	CC30	AA	CC55	AG	CC80	AG
CC6	AG	CC31	AA	CC56	AA	CC81	AA
CC7	AA	CC32	AG	CC57	AA	CC82	AA
CC8	AA	CC33	AA	CC58	AA	CC83	AG
CC9	AA	CC34	AG	CC59	AA	CC84	AA
CC10	GG	CC35	AG	CC60	AA	CC85	AA
CC11	AA	CC36	AA	CC61	AA	CC86	AG
CC12	AA	CC37	AA	CC62	AA	CC87	AA
CC13	AG	CC38	AA	CC63	AA	CC88	AA
CC14	AA	CC39	AA	CC64	AA	CC89	AA
CC15	AG	CC40	AA	CC65	AG	CC90	AG
CC16	AG	CC41	AA	CC66	AA	CC91	AA
CC17	AA	CC42	AA	CC67	AA	CC92	AA
CC18	AG	CC43	AA	CC68	AA	CC93	AA
CC19	AG	CC44	AG	CC69	AA	CC94	AA
CC20	AG	CC45	AA	CC70	AA	CC95	AA
CC21	AA	CC46	AA	CC71	AA	CC96	AG
CC22	AG	CC47	AA	CC72	AG	CC97	AA
CC23	AA	CC48	AA	CC73	AA	CC98	AA
CC24	AG	CC49	AA	CC74	AA	CC99	AG
CC25	AA	CC50	AG	CC75	AG	CC100	AA

In total 30 subjects were heterozygous for the A118G SNP, two were homozygous for the G allele (CC5 & CC10) and 68 were homozygous for the A allele. The frequency of the A118G variation is statistically higher in the control population than the post-mortem population sampled (difference of 15.7 %, $P = 0.0046$).

3.3.4 T750C SNP genotyping

Table 34: T750C genotypes for the 100 control samples.

Samples	T750C genotype	Samples	T750C genotype	Samples	T750C genotype	Samples	T750C genotype
CC1	TC	CC26	CC	CC51	CC	CC76	TT
CC2	TC	CC27	TT	CC52	CC	CC77	TT
CC3	TC	CC28	CC	CC53	TT	CC78	TC
CC4	TT	CC29	TC	CC54	CC	CC79	TC
CC5	TT	CC30	TT	CC55	TC	CC80	TT
CC6	CC	CC31	TT	CC56	TC	CC81	TC
CC7	TT	CC32	CC	CC57	TC	CC82	TC
CC8	TT	CC33	TC	CC58	TC	CC83	TT
CC9	TC	CC34	TC	CC59	TC	CC84	TC
CC10	TC	CC35	TC	CC60	TC	CC85	TT
CC11	TC	CC36	TC	CC61	TC	CC86	TT
CC12	TC	CC37	TT	CC62	TT	CC87	TT
CC13	TC	CC38	TT	CC63	TC	CC88	CC
CC14	CC	CC39	TT	CC64	TT	CC89	TC
CC15	CC	CC40	CC	CC65	TT	CC90	TC
CC16	CC	CC41	TT	CC66	CC	CC91	TC
CC17	TC	CC42	TT	CC67	TT	CC92	TC
CC18	TC	CC43	TC	CC68	CC	CC93	TC
CC19	TC	CC44	TT	CC69	TC	CC94	TC
CC20	TT	CC45	CC	CC70	TT	CC95	TC
CC21	CC	CC46	TT	CC71	TC	CC96	TC
CC22	TC	CC47	TC	CC72	TT	CC97	TC
CC23	TC	CC48	TT	CC73	TC	CC98	TC
CC24	TC	CC49	TT	CC74	CC	CC99	TC
CC25	TC	CC50	TT	CC75	TT	CC100	TT

In total 49 of the control subjects were heterozygous for the T750C variation, 17 were homozygous for the C allele and 34 were homozygous for the T allele. This is a similar frequency to the post-mortem population sampled (19 %, 2 % difference between populations).

3.3.5 G516T SNP genotyping

Table 35: G156T genotypes for the 100 control samples.

Samples	G516T genotype	Samples	G516T genotype	Samples	G516T genotype	Samples	G156T genotype
CC1	GG	CC26	GG	CC51	GG	CC76	GT
CC2	GG	CC27	GG	CC52	GG	CC77	GG
CC3	GG	CC28	GG	CC53	GG	CC78	GG
CC4	GT	CC29	GT	CC54	GG	CC79	GG
CC5	GT	CC30	GT	CC55	GG	CC80	GG
CC6	GG	CC31	GT	CC56	GG	CC81	GG
CC7	GG	CC32	GG	CC57	GG	CC82	GG
CC8	GT	CC33	GT	CC58	GG	CC83	GG
CC9	GT	CC34	GG	CC59	GG	CC84	GG
CC10	GG	CC35	GT	CC60	GT	CC85	GT
CC11	GT	CC36	GG	CC61	GT	CC86	GT
CC12	GT	CC37	GT	CC62	GT	CC87	GT
CC13	GG	CC38	GT	CC63	GG	CC88	GG
CC14	GG	CC39	GG	CC64	GT	CC89	GG
CC15	GG	CC40	GG	CC65	GG	CC90	GT
CC16	GG	CC41	GT	CC66	GG	CC91	GG
CC17	GG	CC42	GG	CC67	GT	CC92	GG
CC18	GG	CC43	GG	CC68	GG	CC93	GT
CC19	GG	CC44	GG	CC69	GG	CC94	GG
CC20	TT	CC45	GG	CC70	GG	CC95	GG
CC21	GG	CC46	GG	CC71	GT	CC96	GT
CC22	GT	CC47	GG	CC72	GT	CC97	GT
CC23	GG	CC48	GG	CC73	GG	CC98	TT
CC24	GT	CC49	GG	CC74	GG	CC99	GT
CC25	GT	CC50	GG	CC75	TT	CC100	GT

In total 34 subjects were genotyped as being heterozygous for the G516T variant, three were homozygous for the TT genotype and 63 were homozygous for the GG genotype. The frequency of G516T variants was higher in the post-mortem population however this result was not statistically significant ($P = 0.92$).

3.3.6 A785G SNP genotyping

Table 36: A785G genotypes for the 100 control samples.

Samples	A785G genotype	Samples	A785G genotype	Samples	A785G genotype	Samples	A785G genotype
CC1	AA	CC26	AA	CC51	AG	CC76	AG
CC2	AA	CC27	AA	CC52	AA	CC77	AA
CC3	AG	CC28	AA	CC53	AA	CC78	AA
CC4	AG	CC29	AG	CC54	AA	CC79	AA
CC5	AG	CC30	AG	CC55	AA	CC80	AA
CC6	AA	CC31	AG	CC56	AA	CC81	AA
CC7	AA	CC32	AG	CC57	AA	CC82	AA
CC8	AG	CC33	AG	CC58	AA	CC83	AA
CC9	AG	CC34	AA	CC59	AA	CC84	AA
CC10	AA	CC35	AG	CC60	AG	CC85	AG
CC11	AG	CC36	AA	CC61	AG	CC86	AG
CC12	AG	CC37	AG	CC62	AG	CC87	AG
CC13	AA	CC38	AG	CC63	AA	CC88	AA
CC14	AA	CC39	AA	CC64	AG	CC89	AA
CC15	AA	CC40	AA	CC65	AA	CC90	AA
CC16	AA	CC41	AG	CC66	AA	CC91	AA
CC17	AA	CC42	AA	CC67	AG	CC92	AA
CC18	AA	CC43	AA	CC68	AG	CC93	AG
CC19	AG	CC44	AA	CC69	AA	CC94	AA
CC20	GG	CC45	AA	CC70	AA	CC95	AA
CC21	AA	CC46	AA	CC71	AG	CC96	AG
CC22	AG	CC47	AA	CC72	AG	CC97	AG
CC23	AA	CC48	AA	CC73	AA	CC98	GG
CC24	AG	CC49	AA	CC74	AA	CC99	AG
CC25	AG	CC50	AA	CC75	GG	CC100	AG

In total 38 of the control subjects were genotyped as heterozygous carriers of the A785G variant, three were homozygous for the GG genotype and 59 were homozygous for the AA genotype. The frequency for A785G is lower in the control population than the post-mortem population however this result is not statistically significant ($P = 0.90$).

3.4 *CYP2B6* Cloning

3.4.1 Cloning of promoter region of human *CYP2B6* gene

3.4.1.1 Examination of the plasmid by *Hind*III & *Xba*I Digest

In preparation for the experimental cloning work a double digest using the restriction enzymes *Hind*III and *Xba*I was conducted. The results are displayed in Figure 50.

Banding is clear for both the uncut DNA and the DNA cut with *Hind*III and *Xba*I. If Figure 4 within section 2.4.1 *Primary Cloning Strategy* is examined it is possible to see that these enzymes were used to cut the relevant sections out of the two vectors (hSVCT2 and pYEGFP3) to create specific vectors to examine *CYP2B6* expression in response to promoter regions variations.

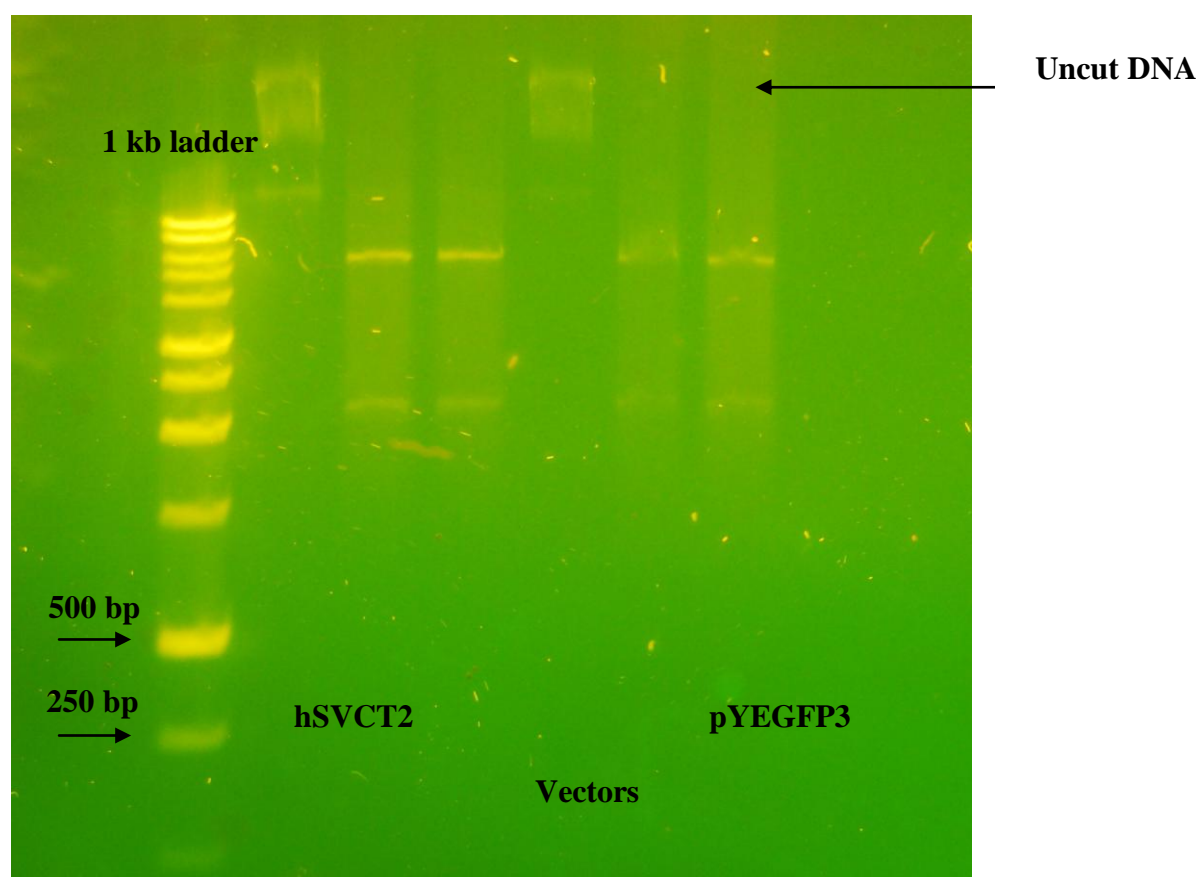


Figure 50: Double restriction digest using *Hind*III and *Xba*I for Cloning method development.

Agarose gel (2 %), run at 70 volts. Two DNA bands following the *Hind*III and *Xba*I double digest are shown for hSVCT2 and pyEGFP3.

3.4.1.2 Gel Extraction of pYEGFP3 Gene

Aliquots of double digested (*Hind*III, *Xba*I) pyEGFP DNA were run on a 2% gel in order to conduct the gel extraction (Figure 51). After the removal and collection of the DNA bands, gel extraction was conducted and confirmed through gel electrophoresis (Figure 52).

1 kb ladder

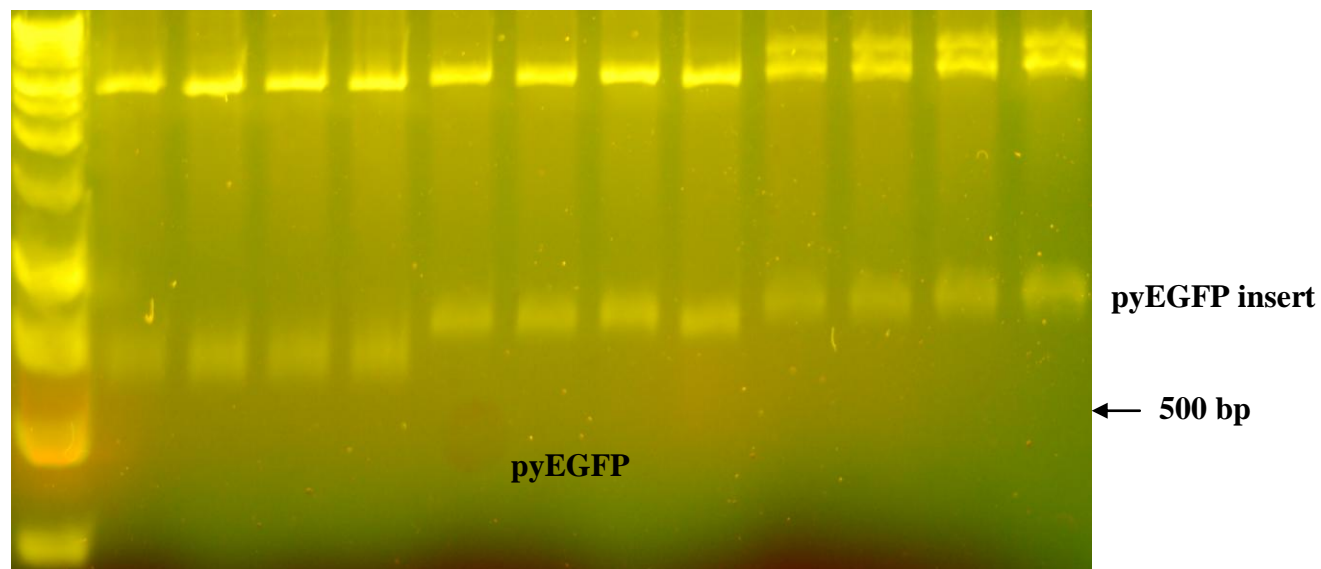


Figure 51: Double restriction digest of pyEGFP using *Hind*III and *Xba*I for Gel Extraction. Agarose gel (2 %), run at 70 volts. The pyEGFP3 DNA fragments (748 bp) are indicated.

1 kb ladder

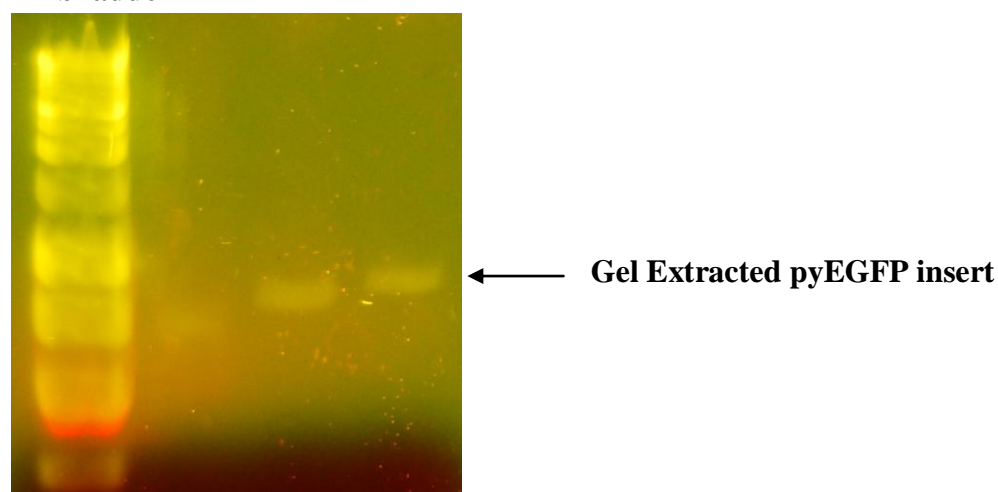


Figure 52: Gel Extracted pyEGFP inserts for cloning strategy.

Agarose gel (2 %), run at 70 volts. Purified pyEGFP3 fragments following Qiaquick gel extraction.

3.4.1.3 Gel Extraction of hSVCT2 Vector

Aliquots of triple digested (*HindIII*, *BamHI* *XbaI*) hSVCT2 DNA were run on a 2% gel in order to conduct the gel extraction (Figure 53). After the removal and collection of the DNA bands, gel extraction was conducted and confirmed through gel electrophoresis (Figure 54).

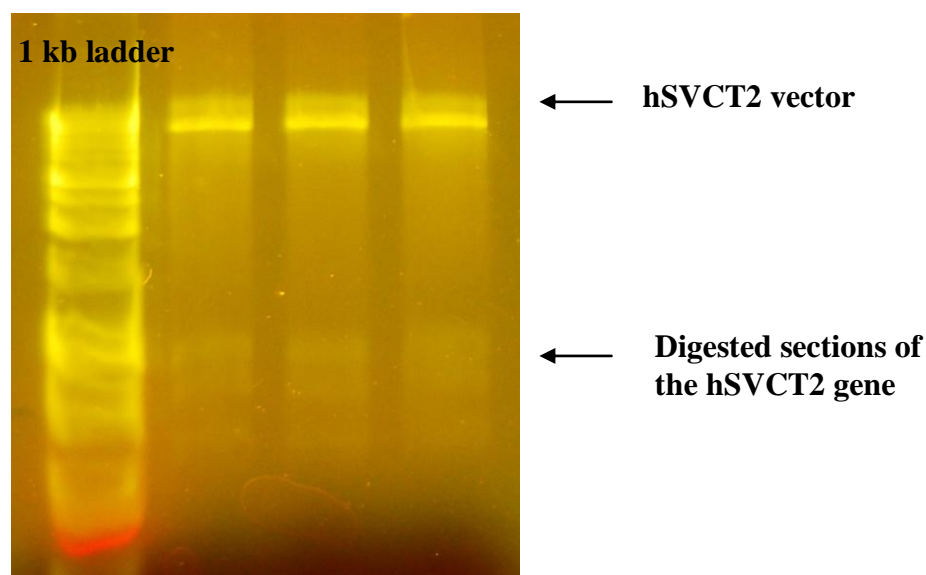


Figure 53: Triple restriction digest of hSVCT2 using *HindIII*, *BamHI* and *XbaI* for Gel Extraction.

Agarose gel (2 %), run at 70 volts. The arrows indicate the hSVCT2 vector and the digested hSVCT2 gene.

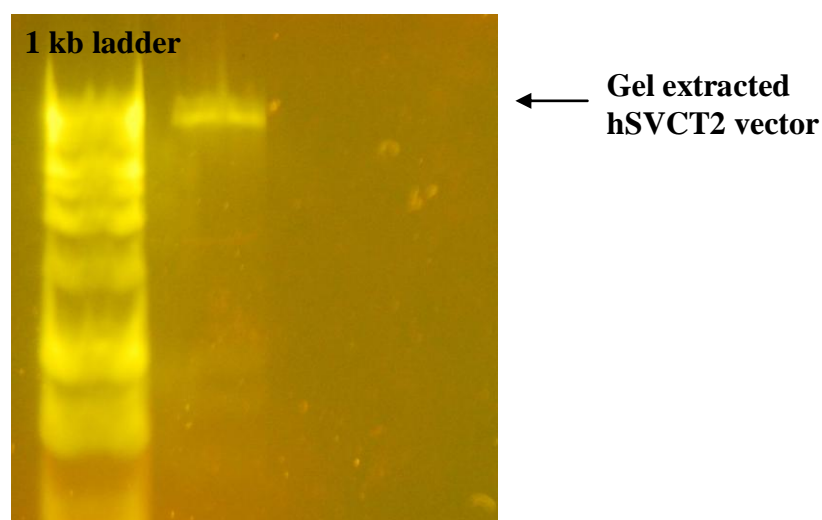


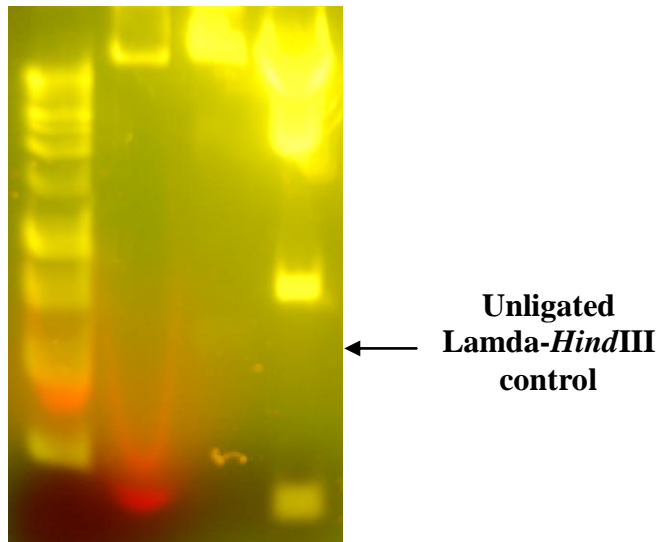
Figure 54: Gel Extracted hSVCT2 vector for cloning strategy.

Agarose gel (2 %), run at 70 volts. Purified hSVCT2 vector following QIAquick gel extraction.

3.4.1.4. Ligation of pyEGFP into hSVCT2 vector

The efficiency of the ligation of pyEGFP into the hSVCT2 vector was tested by a *Lamda-HindIII* ligation. As Figure 55 shows the two *Lamda-HindIII* ligated controls (LDH) had single bands indicating a successful ligation experiment.

1 kb ladder



LHD, LHD, Control

Figure 55: Ligated *Lamda-HindIII* positive controls.

Agarose gel (2 %), run at 70 volts. Arrow indicates the unligated *Lamda-HindIII* control sample.

3.4.1.5. *NdeI* confirmation of hSVCT2-EGFP vector transformation.

Following transformation, 43 clones were identified:

B (1:3 vector: insert ratio) – B21, B22, B23, B24, B25, B26, B31.

C (1:2 vector: insert ratio) – C21, C22, C31.

D (1:1 vector: insert ratio) – D31, D32, D33, D34, D35, D36.

E (2:1 vector: insert ratio) – E21, E22, E23, E24, E25, E26, E27, E31, E32, E33, E34,
E35, E36, E37.

F (3:1 vector: insert ratio) – F21, F22, F23, F24, F25, F26, F27, F28, F29, F210, F211,
F31, F32.

As expected no clones grew in the negative controls (A 0:1; G 1:0).

Clone identity was tested by conducting an *NdeI* digest on the samples. With the successful ligation of EGFP into the hSVCT2 vector, *NdeI* should cut the clones twice. If Figures 56, 57, 58, & 59 are examined there is only a single cut, suggesting that instead of ligating EGFP into hSVCT2, the vector had ligated to itself creating an empty vector.

1 kb ladder

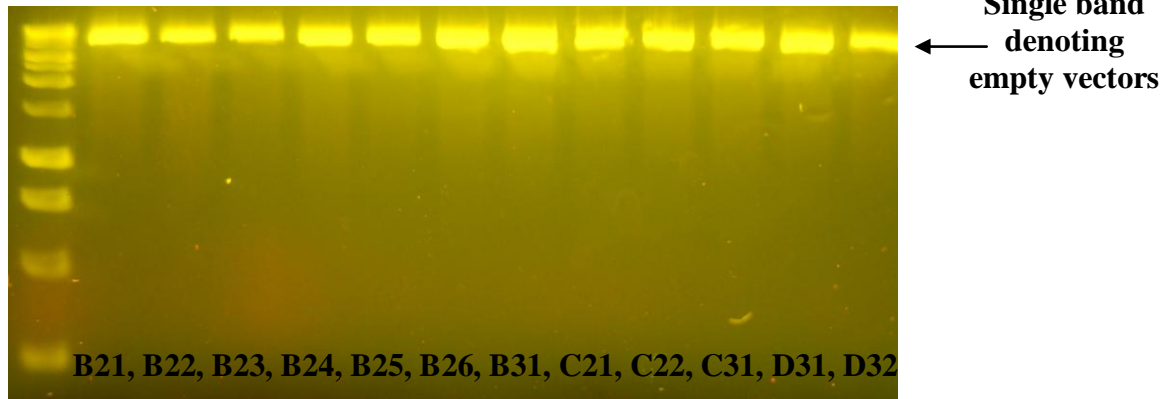


Figure 56: Single restriction digest of hSVCT2-EGFP clone using *NdeI*.

Agarose gel (2 %), run at 70 volts. Arrow indicates single cut following the *NdeI* digest.

1 kb ladder

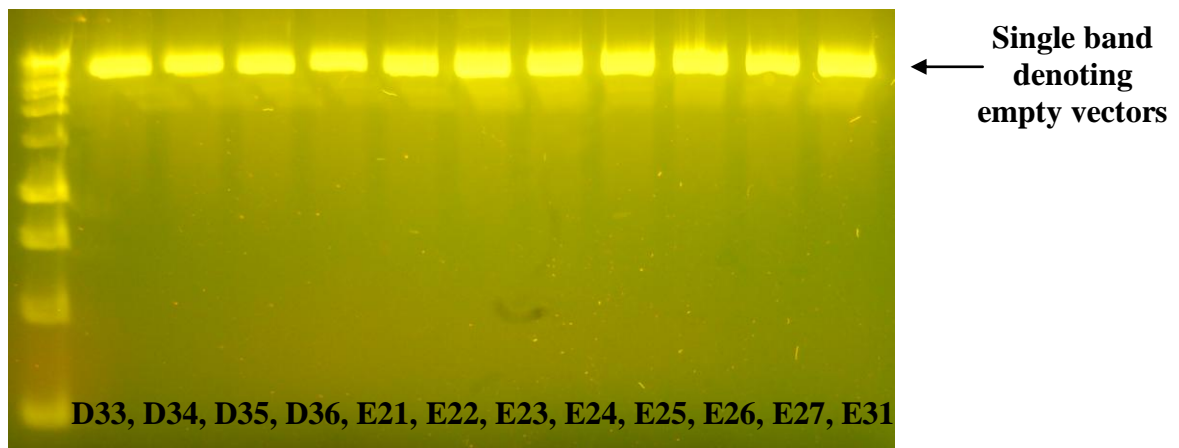


Figure 57: Single restriction digest of hSVCT2-EGFP clone using *NdeI*.

Agarose gel (2 %), run at 70 volts. Arrow indicates single cut following the *NdeI* digest.

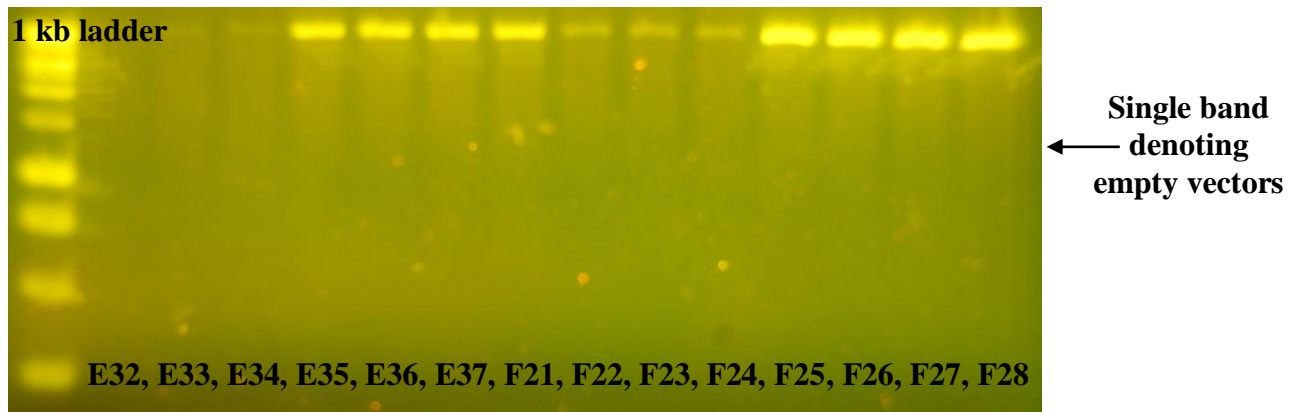


Figure 58: Single restriction digest of hSVCT2-EGFP clone using *NdeI*.

Agarose gel (2 %), run at 70 volts. Arrow indicates single cut following the *NdeI* digest.

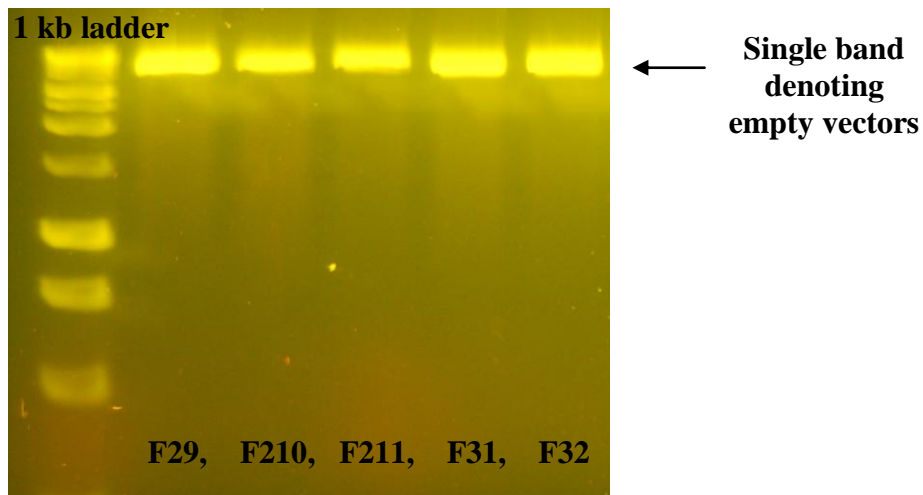


Figure 59: Single restriction digest of hSVCT2-EGFP clone using *NdeI*.

Agarose gel (2 %), run at 70 volts. Arrow indicates single cut following the *NdeI* digest.

In order to continue with cloning the *CYP2B6* promoter region the Invitrogen TOPO® kit was employed and a new cloning strategy constructed (Figure 5).

3.4.1.6. *CYP2B6* Promoter Region Primer Validation

As Figure 60 demonstrates the primary amplification of the *CYP2B6* promoter region had poor selectivity with lots of smearing visible. Banding for *CYP2B6* is visible however the bands are faint and require improvement for the TOPO® cloning strategy.

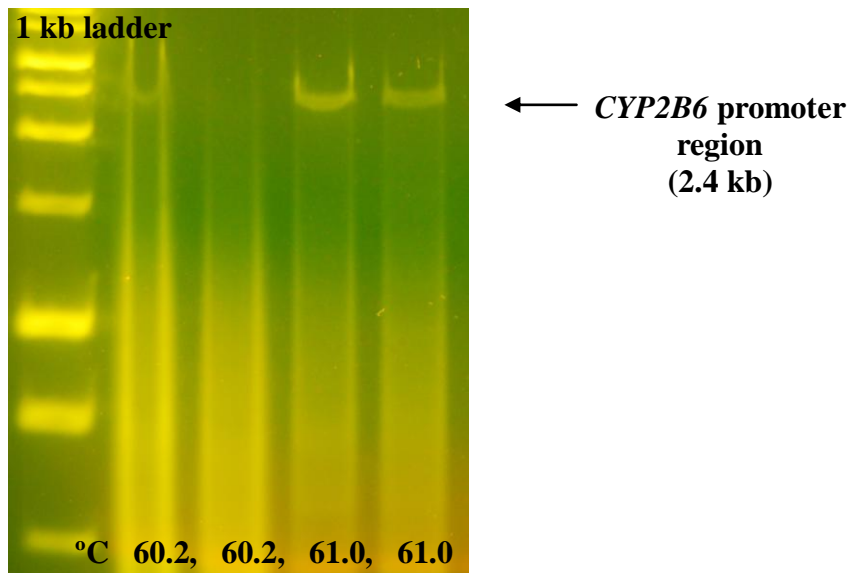


Figure 60: Amplification of *CYP2B6* promoter region for primer optimisation.

Agarose gel (2 %), run at 70 volts. Arrow indicates amplified *CYP2B6* promoter region (2.4 kb).

3.4.1.7 PCR Temperature Development

The gradient reaction demonstrated that the optimal temperature range for *CYP2B6* promoter region amplification was between 61.0 and 62.3 °C (Figure 61). However, there was still poor selectivity with faint banding for *CYP2B6*.

1 kb ladder

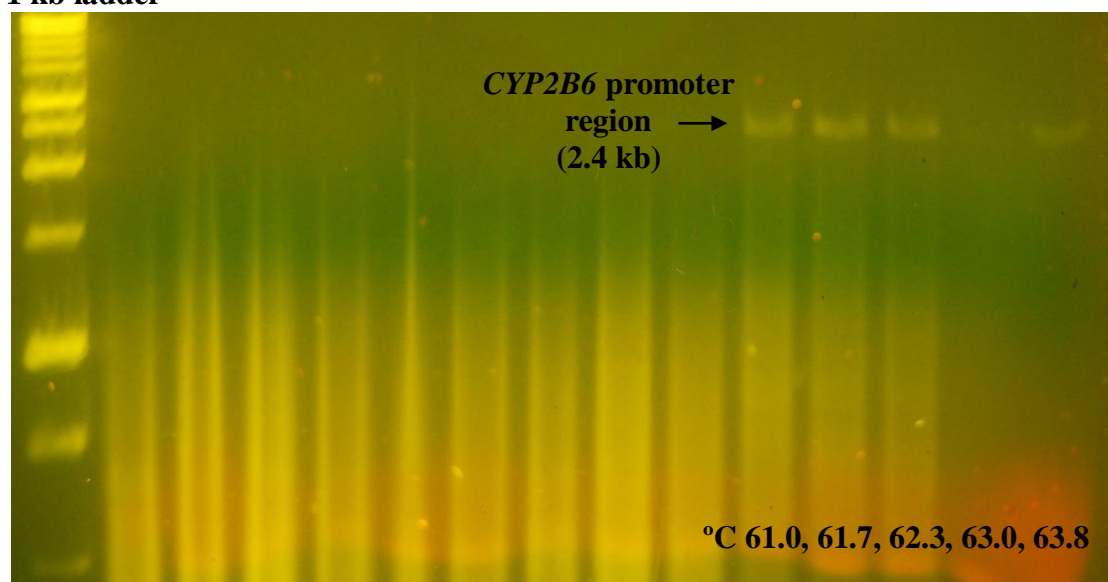


Figure 61: Gradient reaction to improve amplification selectivity for *CYP2B6* promoter.

Agarose gel (2 %), run at 70 volts. Arrow indicates amplified *CYP2B6* promoter region (2.4 kb).

3.4.1.8 Amplification of *CYP2B6* promoter region

1 kb ladder

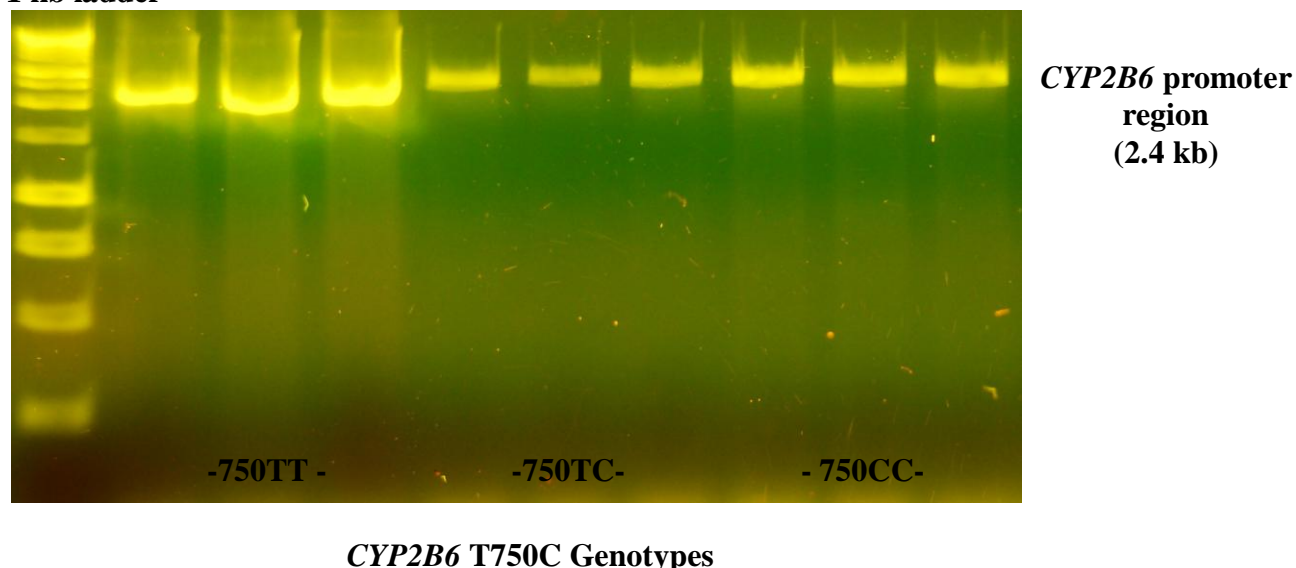


Figure 62: Amplification of *CYP2B6* promoter regions for 750TT, 750TC, & 750CC genotypes.

Agarose gel (2 %), run at 70 volts. Amplified *CYP2B6* promoter variants to analyse the influence of the T750C SNP.

As Figure 62 shows the optimal annealing temperature for *CYP2B6* promoter amplification had been identified at 60.2 °C. Adequate banding for all three T750C genotypes had been yielded to continue with the molecular cloning strategy (Figure 5) using the TOPO® Cloning Reaction (Invitrogen, UK).

3.4.1.9 Transformation of *CYP2B6* 750TT, 750TC, & 750CC into TOPO® vector

The ligation and transformation of the amplified *CYP2B6* regions for the three T750C genotypes was successful and clones for each were isolated. Each of the clones were confirmed by conducting a *Bgl*III & *Hind*III double restriction digest to confirm the presence of three bands (Figures 63, 64, 65). The orientation of the *CYP2B6* promoter region was then confirmed by conducting a single *Bgl*III digest to identify two bands (Figures 63, 64, 65).

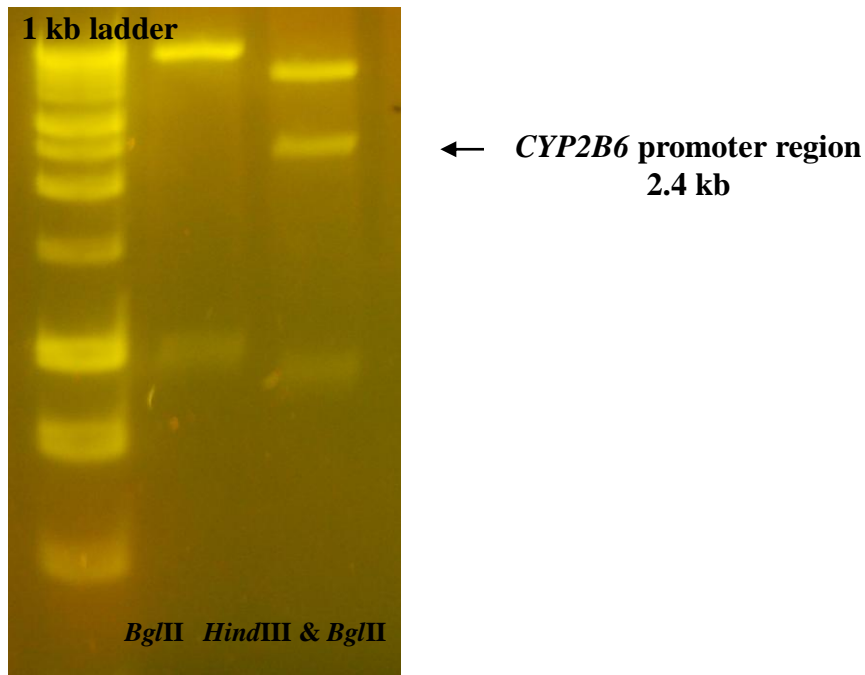


Figure 63: Validation of the *CYP2B6* promoter region transformation and orientation for the 750 TT genotype.

Agarose gel (2 %), run at 70 volts. The arrow indicates the *CYP2B6* promoter region visible after the *Hind*III/*Bg*III double digest. The orientation is correct as shown by the two bands for the *Bg*III single digest.

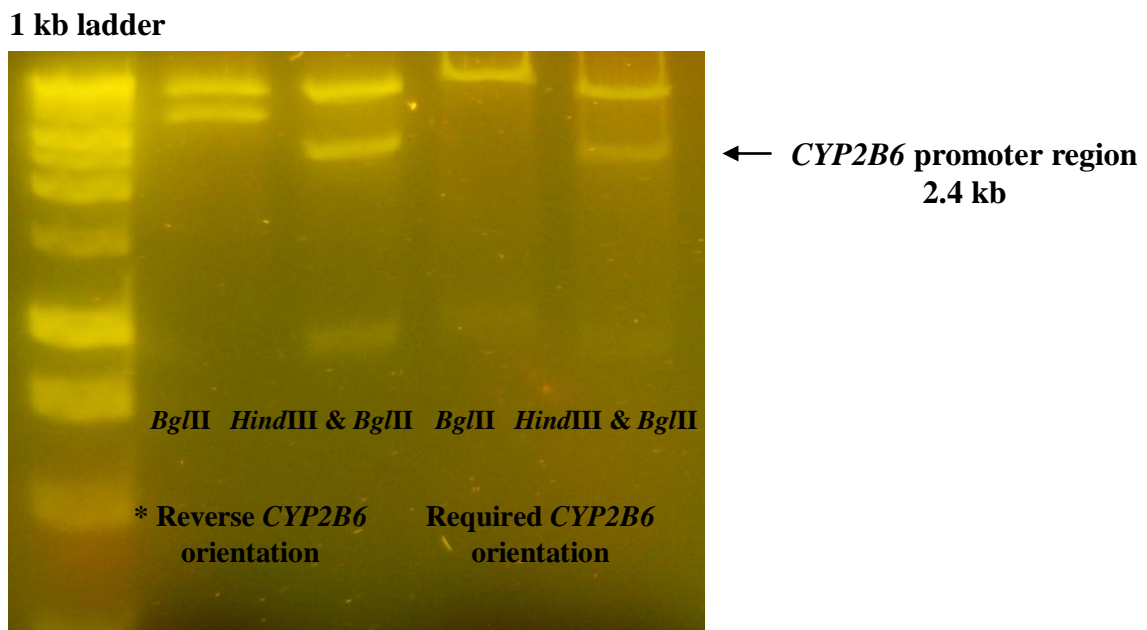


Figure 64: Validation of the *CYP2B6* promoter region transformation and orientation for the 750 TC genotype.

Agarose gel (2 %), run at 70 volts. The arrow indicates the *CYP2B6* promoter region visible after the *Hind*III/*Bg*III double digest. The orientation is correct as shown by the two bands for the *Bg*III single digest. The reverse *CYP2B6* orientation is indicated by *.

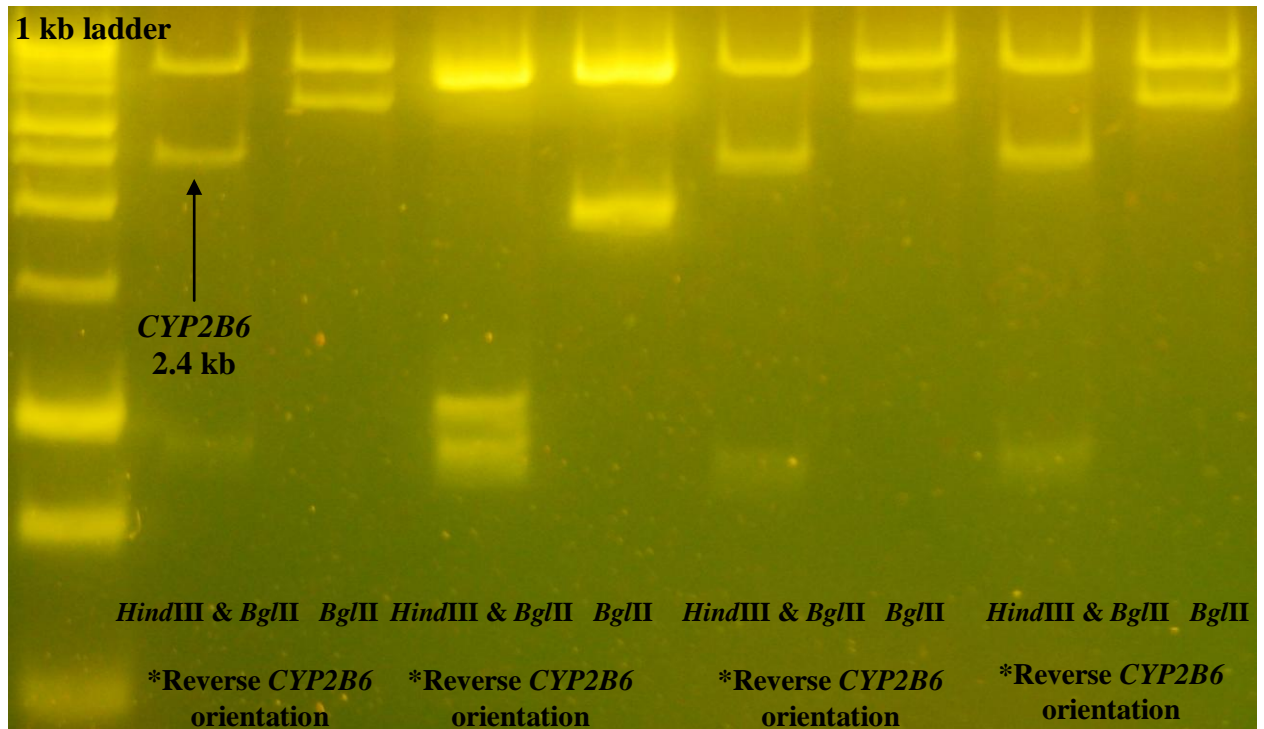


Figure 65: Validation of the *CYP2B6* promoter region transformation and orientation for the 750 CC genotype.

Agarose gel (2 %), run at 70 volts. The arrow indicates the *CYP2B6* promoter region visible after the *HindIII/BglIII* double digest. The orientation of *CYP2B6* is reversed as indicated by *.

As Figures 63 and 64 show the *CYP2B6* promoter regions for the 750 TT and TC genotypes were successfully ligated into the TOPO® TA vector creating the p2B6-GFP-HB-750 TT and p2B6-GFP-HB-750 TC clones. However, for the 750 CC genotype the *CYP2B6* promoter region was successfully ligated into the vector, however the orientation was reversed (Figure 65). Therefore, no p2B6-GFP-HB-750 CC clone was created.

3.5 A118G Methadone Binding Study

3.5 A118G Methadone Binding Study

The effects of the the A118G SNP on μ opioid receptor internalisation following methadone treatment was studied using Human primary CLL cell lines. DNA samples extracted from the CLL cells were quantified (Table 37) and genotyped for the A118G SNP (Table 38). Then, CLL cell lines for the 118 AA and 118 AG genotypes were exposed to varying concentrations of methadone to measure the effect of A118G on internalisation. The results from this study are discussed below.

3.5.1 B-cell line DNA Quantification

All of the 44 Human CLL cell lines were extracted and quantified successfully (Table 37).

Table 37: DNA yield for human CLL cell lines.

Cell Sample	Mean DNA Concentration (ng/ μ l)	Cell Sample	Mean DNA Concentration (ng/ μ l)
CL1	20.83	CL23	19.85
CL2	7.87	CL24	21.0
CL3	5.50	CL25	12.88
CL4	18.79	CL26	25.36
CL5	5.71	CL27	528
CL6	14.05	CL28	15.96
CL7	20.74	CL29	35.34
CL8	16.15	CL30	234
CL9	4.12	CL31	7.88
CL10	4.54	CL32	13.03
CL11	20.78	CL33	12.44
CL12	24.80	CL34	2.74
CL13	25.00	CL35	38.47
CL14	7.50	CL36	8.63
CL15	16.70	CL37	18.91
CL16	23.0	CL38	17.05
CL17	5.30	CL39	32.42
CL18	6.60	CL40	1.05
CL19	12.38	CL41	2.22
CL20	8.73	CL42	5.04
CL21	6.96	CL43	12.64
CL22	18.87	CL44	19.55

3.5.2 A118G SNP Genotyping

Of the 44 human CLL cell lines genotyped for the *OPRM1* A118G variation 28 were homozygous for the AA genotype, 15 were heterozygous (AG) and 1 was homozygous for the GG genotype (Table 38).

Table 38: A118G SNP Genotypes for CLL Subjects.

Cell Sample	A118G SNP Genotype	Cell Sample	A118G SNP Genotype
CL1	AG	CL23	AG
CL2	AG	CL24	AG
CL3	AG	CL25	AA
CL4	AA	CL26	AA
CL5	AA	CL27	AA
CL6	AA	CL28	AA
CL7	AG	CL29	AA
CL8	AA	CL30	AA
CL9	AA	CL31	AA
CL10	AA	CL32	AA
CL11	AA	CL33	AA
CL12	AA	CL34	AA
CL13	AG	CL35	AG
CL14	AG	CL36	GG
CL15	AA	CL37	AA
CL16	AA	CL38	AA
CL17	AA	CL39	AA
CL18	AG	CL40	AG
CL19	AG	CL41	AG
CL20	AG	CL42	AG
CL21	AA	CL43	AA
CL22	AA	CL44	AA

3.5.3 Receptor Internalisation

3.5.3.1 Primary anti- μ and secondary anti-rabbit IgGFITC validation

As shown in Table 39 the optimal antibody concentration for visualising cell surface μ opioid receptor presence was P 1:20, S 1:10, closely followed by P 1:20, S 1:20. It was observed that the negative control mean fluorescence intensity was higher than expected with a geometric mean of 4.7. It was postulated that the goat polyclonal to

rabbit IgG-FITC secondary antibody may be binding to other locations, for example Fc receptors.

Table 39: The mean fluorescence intensity for antibody bound μ opioid receptors.

Tube	Reaction		Geometric Mean	Receptor Visualisation (% change from S 1:10)
1	P 1:10	S 0	3.34	
2	P 0	S 1:10	4.70	
3	P1:10	S 1:10	4.72	0.4 %
4	P1:10	S 1:20	7.65	63 %
5	P1:10	S 1:50	2.85	- 39 %
6	P1:20	S 1:10	29.31	524 %
7	P1:20	S 1:20	19.28	310 %
8	P1:20	S 1:50	3.85	-18 %
9	P1:50	S 1:10	9.66	106 %
10	P1:50	S 1:20	3.44	- 27%
11	P1:50	S 1:50	3.92	- 17%
12	Kappa/Lamda control		11.02	134 %

3.5.3.2 Blockage of Fc Receptors to improve Antibody-Receptor Binding

In order to minimise secondary antibody binding to Fc receptors a blocking experiment using human AB (HAB) serum was tested (Table 40).

Table 40: The mean fluorescence intensity for antibody bound μ opioid receptors following HAB blocking of Fc receptors.

Tube	Reaction		Geometric Mean	Receptor Visualisation (% change from S 1:10)
1	P 1:20	S 0	1.5	
2	P 0	S 1:20	2.09	
3	P1:20	S 1:10	1.91	-9 %
4	P1:20	S 1:20	2.12	1.4 %
5	Kappa/Lamda control		2.45	17 %

As shown in Table 40 the addition of HAB serum may have reduced the geometric mean result for S 1:20, however, the percentage change from the negative control was

minimal. The difference between the sample geometric mean and the S1:20 controls were used to identify the effects of methadone concentration and the A118G polymorphism on μ opioid receptor internalisation.

3.5.3.3 Primary anti- μ and secondary anti-rabbit IgGPE Optimisation

Previous works from this study used a goat polyclonal to rabbit IgG-FITC secondary antibody and it was postulated that non-specific binding could be interfering with the results. No improvement was observed using the HAB blocking agent. An experiment was conducted using the mouse monoclonal to rabbit IgG-PE secondary antibody to determine whether this improved visualisation of μ receptors. However as shown in Table 41 little μ receptor visualisation was observed. It was proposed that the rabbit monoclonal [EP1470Y] to μ opioid receptor primary antibody was degraded, possibly as a result of freeze/thawing.

Table 41: The mean fluorescence intensity for PE antibody bound μ opioid receptors.

Tube	Reaction	Geometric Mean	Receptor Visualisation (% change from S 1:10)
1	P 1:10 S 0	1.11	
2	P 0 S 1:10	1.12	0 %
3	P1:10 S 1:10	1.13	0.9 %
4	P1:10 S 1:20	1.13	0.9 %
5	P1:10 S 1:50	1.12	0 %
6	P1:20 S 1:10	1.13	0.9 %
7	P1:20 S 1:20	1.13	0.9 %
8	P1:20 S 1:50	1.12	0 %
9	P1:50 S 1:10	1.14	1.8 %
10	P1:50 S 1:20	1.13	0.9 %
11	P1:50 S 1:50	1.12	0 %
12	Kappa/Lamda control	1.18	5.4 %

3.5.3.4 Primary anti- μ and secondary anti-rabbit IgGFITC Optimisation

As shown in Table 42 the optimal μ opioid receptor (ab10275) primary antibody concentration was 1:10, and the optimal secondary antibody (goat polyclonal to rabbit IgG-FITC) was also 1:10. This was then followed by P 1:100, S 1:10, and P 1:1000, S 1:10. It is also clear from these results that the mouse monoclonal to rabbit IgG-PE secondary antibody was not suitable for this experiment. Therefore the primary μ opioid primary antibody (ab10275) 1:10 and goat polyclonal to rabbit IgG-FITC secondary 1:10 antibody concentrations were used to determine the effects of methadone concentration and the A118G polymorphism on μ opioid receptor internalisation.

Table 42: The mean fluorescence intensity for FITC and PE antibody bound μ opioid receptors.

Tube	Reaction	Geometric Mean	Receptor Visualisation (% change from S 1:10)
1	P 1:10 S 0	1.39	
2	P 0 S 1:10 FITC	2.21	
3	P0 S 1:10 PE	1.09	
4	P1:10 S 1:10 FITC	9.92	349 %
5	P1:10 S 1:100 FITC	1.94	-12 %
6	P1:10 S 1:1000 FITC	1.09	-51 %
7	P1:100 S 1:10 FITC	2.71	23 %
8	P1:100 S 1:100 FITC	1.56	-29 %
9	P1:100 S 1:1000 FITC	1.09	-51 %
10	P1:1000 S 1:10 FITC	2.4	9 %
11	P1:1000 S 1:100 FITC	1.6	-28 %
12	P1:1000 S 1:1000 FITC	1.08	-51 %
13	P1:10 S 1:10 PE	1.10	-50 %
14	P1:10 S 1:100 PE	1.10	-50 %
15	P1:10 S 1:1000 PE	1.09	-51 %
16	P1:100 S 1:10 PE	1.10	-50 %
17	P1:100 S 1:100 PE	1.09	-51 %
18	P1:100 S 1:1000 PE	1.09	-51 %
19	P1:1000 S 1:10 PE	1.09	-51 %
20	P1:1000 S 1:100 PE	1.07	-52 %
21	P1:1000 S 1:1000 PE	1.09	-51 %
22	Kappa/Lamda control	2.45	11 %

3.5.4 Racemic Methadone Binding Study

3.5.4.1 The effects of cell culture incubation interval on cell apoptosis

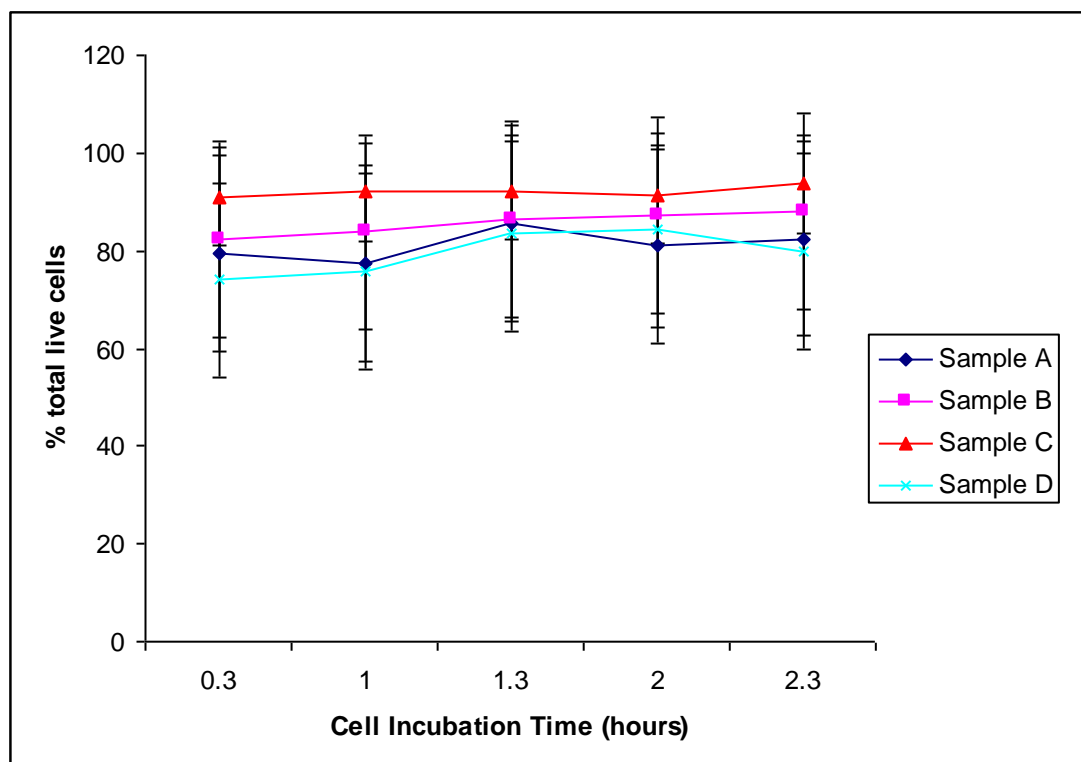


Figure 66: The influence of cell culture incubation time on cell apoptosis following freezing and thawing.

There is an increase in % live cells for Samples A and D over the 1.3 and 2 hour time intervals, however the increase is not significant.

As Figure 66 shows the difference in cell apoptosis between different incubation intervals was not significant. An incubation time of one hour was selected for the apoptosis and μ opioid receptor internalisation experiments. This incubation time was the same as other works (Keith *et al.* 1998; Trapaidze *et al.* 2000).

3.5.4.2 Cell culture of B-lymphocytes in methadone

3.5.4.2.1 Cell Apoptosis Trial

The effects of the A118G polymorphism and methadone exposure on cellular apoptosis were examined. As shown in Figures 67 and 68, typically there was an

increase in the percentage of total cells positive for Annexin V. This trend is clearer in Figure 68 and could be a result of the 118 AG genotype.

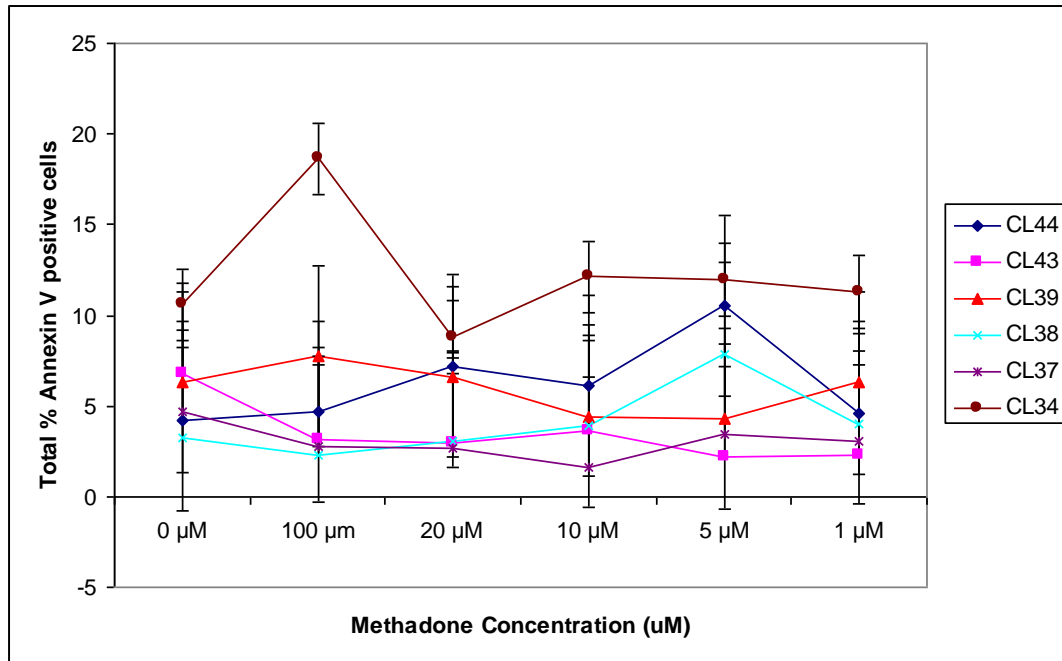


Figure 67: The influence of methadone concentration on early stage cell apoptosis for 118 AA subjects, determined by the % of Annexin V-FITC positive cells.

For 118 AA subjects there is an increase in apoptosis for the 100uM treatment.

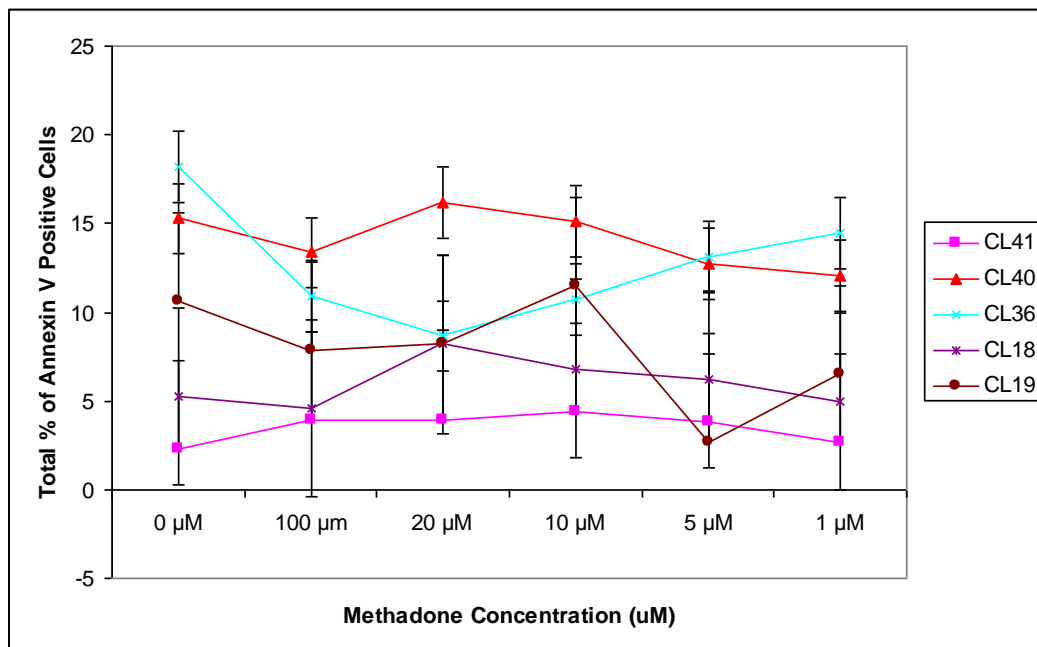


Figure 68: The influence of methadone concentration on early stage cell apoptosis for 118 AG subjects, determined by the % of Annexin V-FITC positive cells.

For 118 AG subjects there is an increase in apoptosis for the 20 and 10uM treatments.

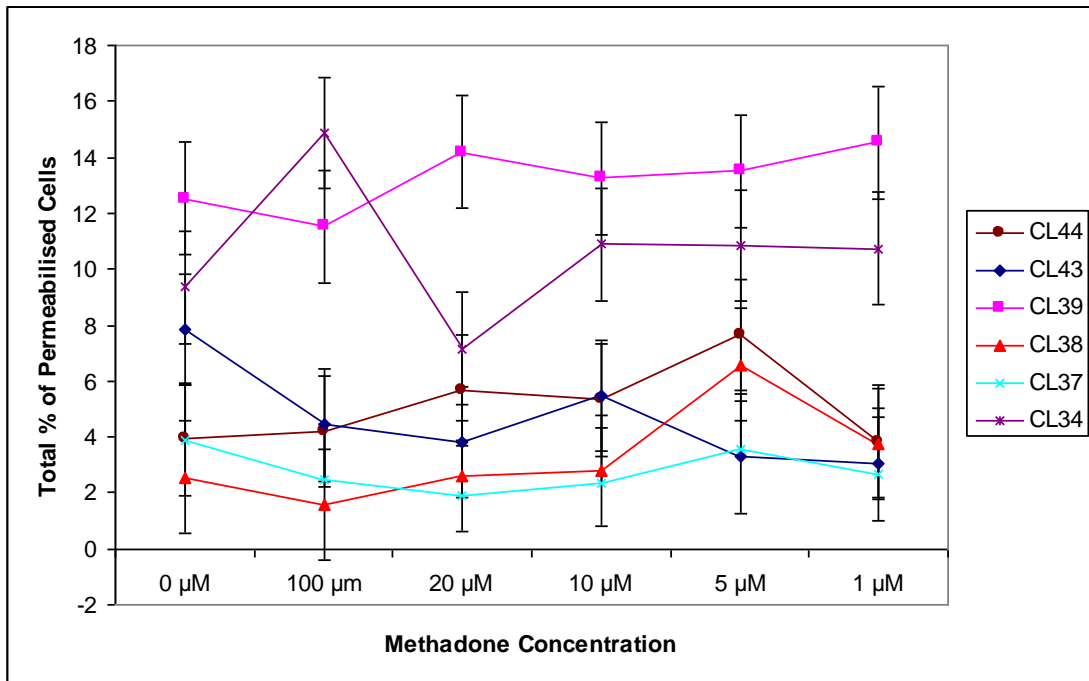


Figure 69: The influence of methadone concentration on late stage cell apoptosis for 118 AA subjects, determined by the % of propidium iodide permeabilised cells.

For 118 AA subjects there is a decrease in apoptosis for the 100μM treatment for all subjects except CL34 and CL44.

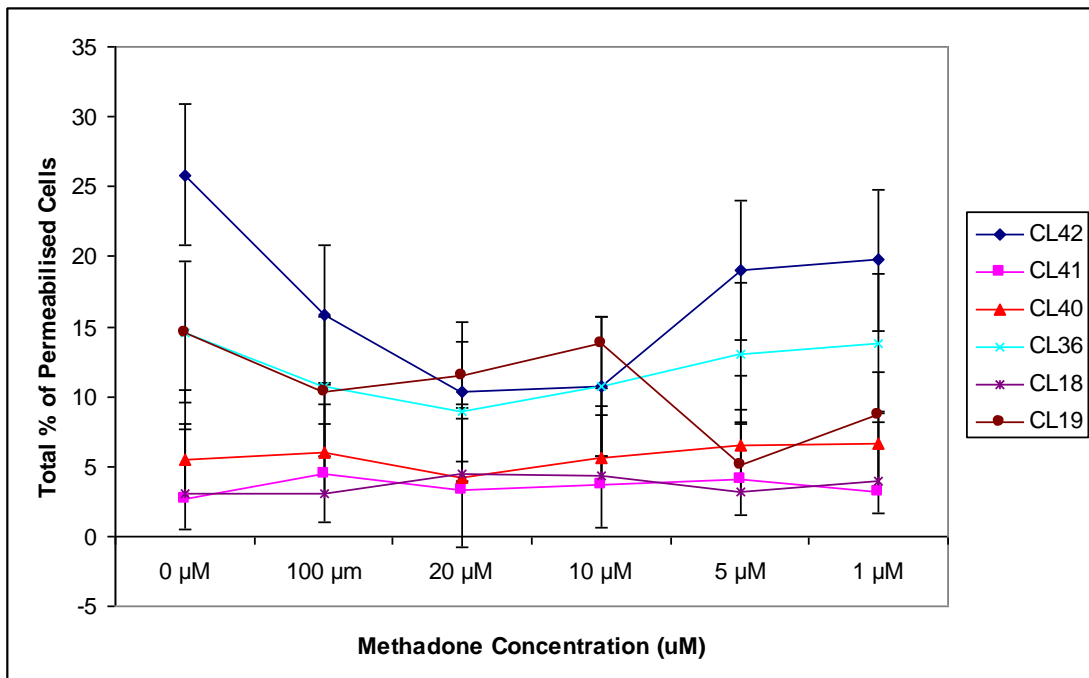


Figure 70: The influence of methadone concentration on late stage cell apoptosis for 118 AG subjects, determined by the % of propidium iodide permeabilised cells.

For 118 AG subjects there is a decrease increase in apoptosis until the 20 μM treatment.

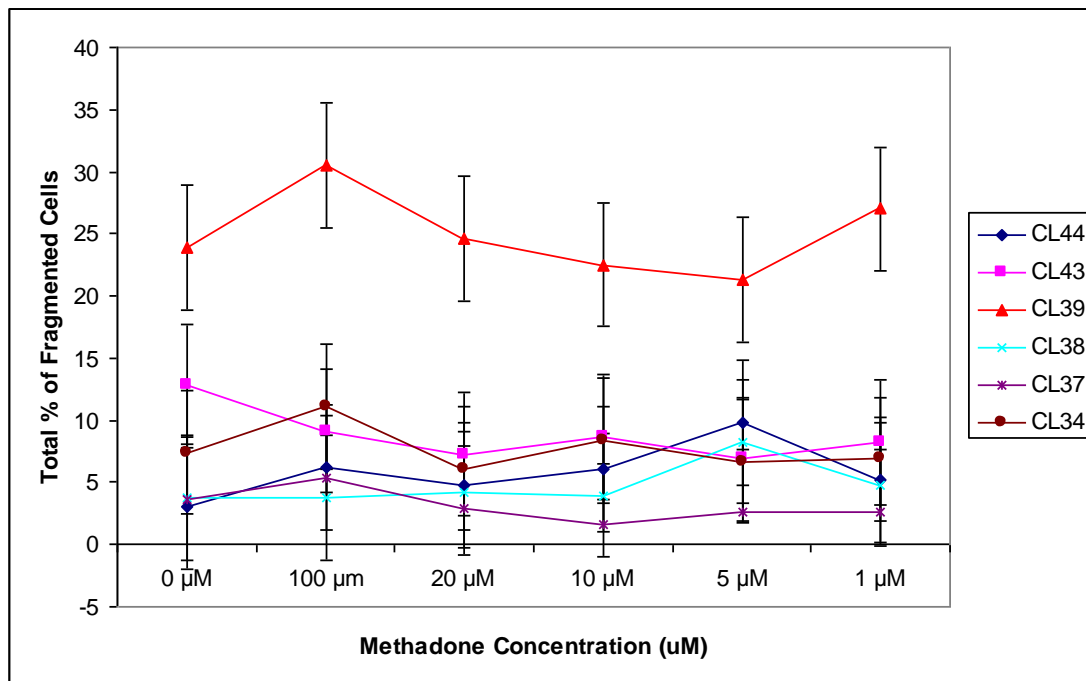


Figure 71: The influence of methadone concentration on late stage cell apoptosis for 118 AA subjects, determined by the % of propidium iodide fragmented cells.

For 118 AA subjects there is an increase in cell fragmentation after the 100μM treatment, which decreased for the following methadone treatments.

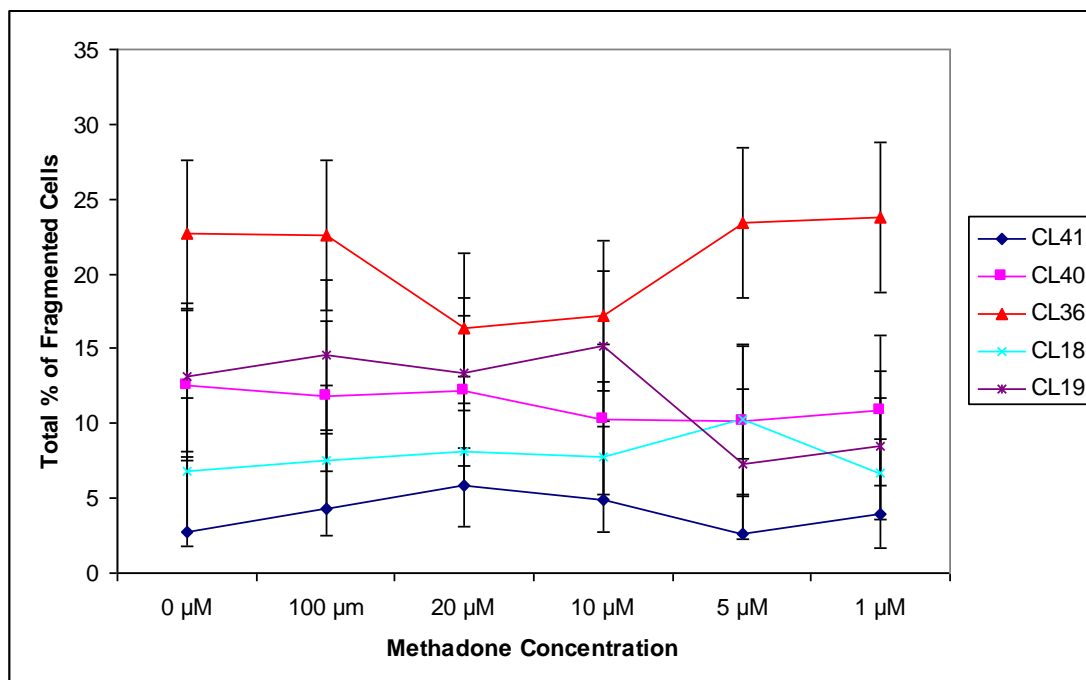


Figure 72: The influence of methadone concentration on late stage cell apoptosis for 118 AG subjects, determined by the % of propidium iodide fragmented cells.

For 118 AG subjects there is a noticeable increase in cell fragmentation between the 20 μM and 10 μM methadone treatments.

The propidium iodide results for cell permeabilisation show an increase for the 20 μM and 10 μM methadone concentrations (Figures 69 & 70). As shown in Figure 71 an increase in cell fragmentation for 118 AA subjects following the 100 μM methadone concentration and between 20 and 5 μM methadone was observed. For the 118 AG subjects the trend was clearer with the majority of subjects demonstrating an increase in cell fragmentation following the 100 μM and 20 μM methadone concentrations (Figure 72). These results are discussed in Chapter 8.

3.5.4.2.2 μ Receptor Internalisation

The effect of the A118G polymorphism and methadone exposure on μ -opioid receptor internalisation was examined to determine whether alterations to receptor internalisation are associated with individual susceptibility to methadone.

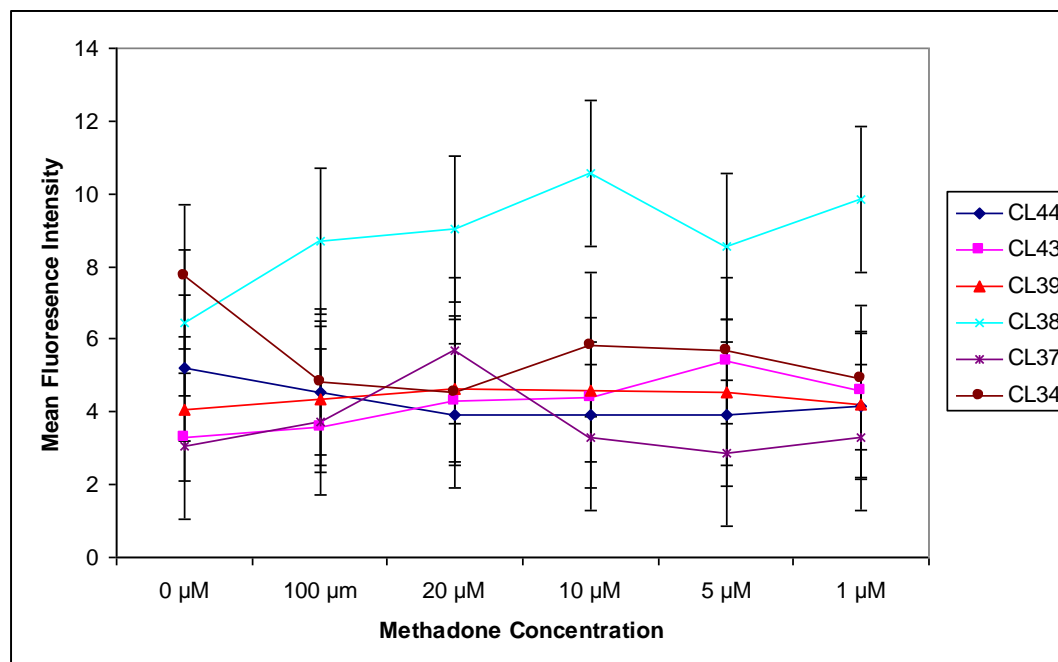


Figure 73: The influence of methadone concentration on μ opioid receptor internalisation for 118 AA subjects.

For 118 AA subjects there is an increase in cell fragmentation following methadone treatment for CL38.

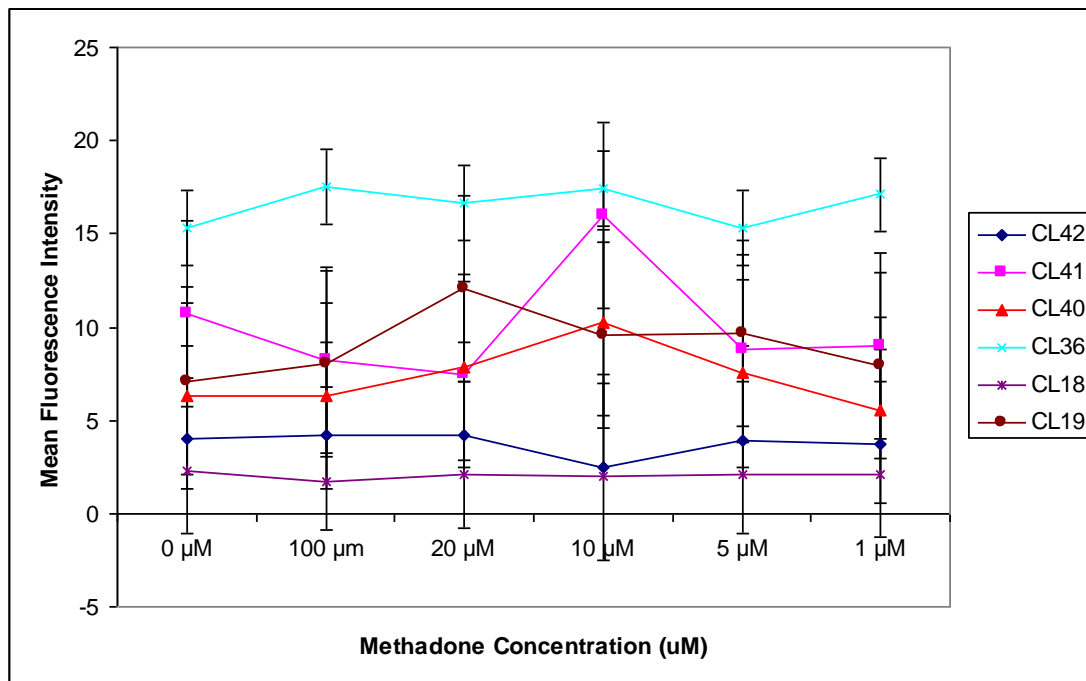


Figure 74: The influence of methadone concentration on μ opioid receptor internalisation for 118 AG subjects.

For 118 AG subjects the mean fluorescence intensity is significantly higher than 118 AA subjects indicating a higher reduction in μ receptor internalisation for 118 AG subjects compared with 118 AA subjects following methadone treatment.

Interestingly the mean fluorescence intensity for 118 AA subjects (Figure 73) was lower than that of 118 AG subjects (Figure 74). It was postulated that this might be associated with μ opioid receptor accumulation at the cell surface as a result of methadone exposure. However it could also be linked with alterations to *OPRM1* gene expression as a result of the A118G polymorphism. There was a significant increase in the mean fluorescence intensity for 118 AG subjects compared with 118 AA subjects (Figure 74). For both 118 AA and AG subjects the mean fluorescence intensity increased after the 20 μ M and 10 μ M methadone treatments (Figure 73 & 74). For a discussion of these results see Chapter 8.

3.6 Statistical Analysis

3.6.1 Data Normalisation

Data normality was checked for *CYP2B6* T750C, G516T, A785G and *OPRM1* A118G, with a normal distribution for all of the SNPs.

3.6.2 Post-mortem Drug Correlations

3.6.2.1 Post-mortem Drug Concentrations

The association between post-mortem methadone concentrations and post-mortem morphine, benzodiazepine, SSRIs, SNRIs, Ethanol, Tricyclic Antidepressants were examined (Figures 75 to 80). It was not possible to examine the association between methadone and dihydrocodeine as there were only two cases of methadone and dihydrocodeine. There was no significant correlation between methadone concentration and other drugs examined (Figures 75 to 80). However, although these results do not appear to be significant statistically, as an isolated number from the measurements given, the plots for methadone and morphine (Figure 75), methadone and ethanol (Figure 79) and methadone and tricyclic antidepressants (Figure 80) do show a trend.

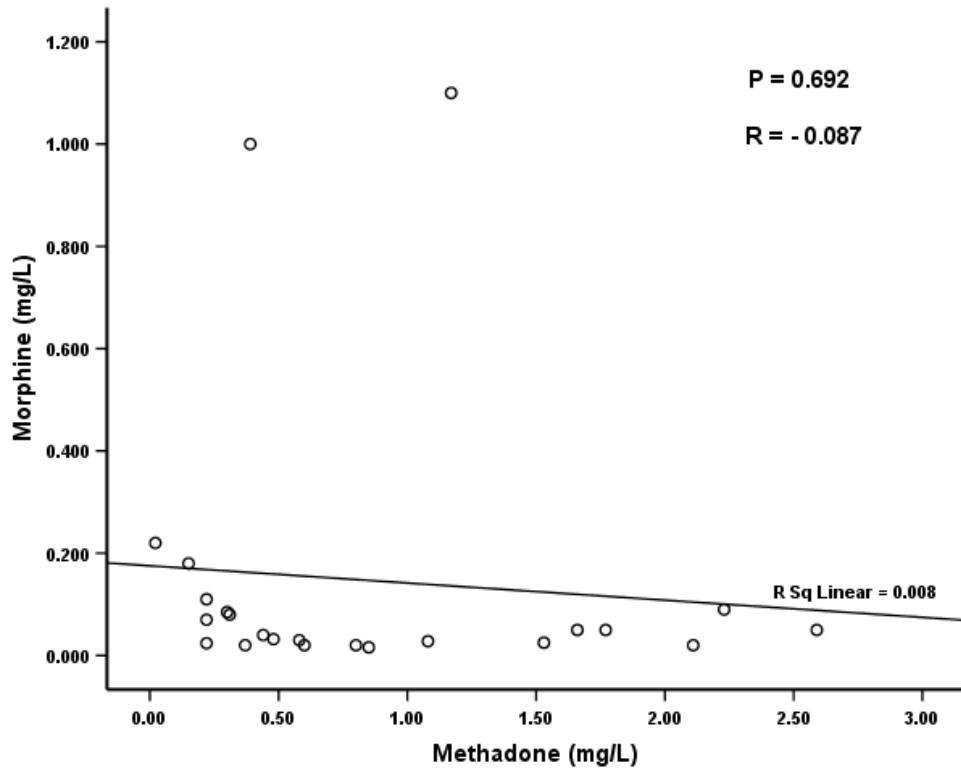


Figure 75: The correlation between post-mortem methadone concentrations and post-morphine concentrations.

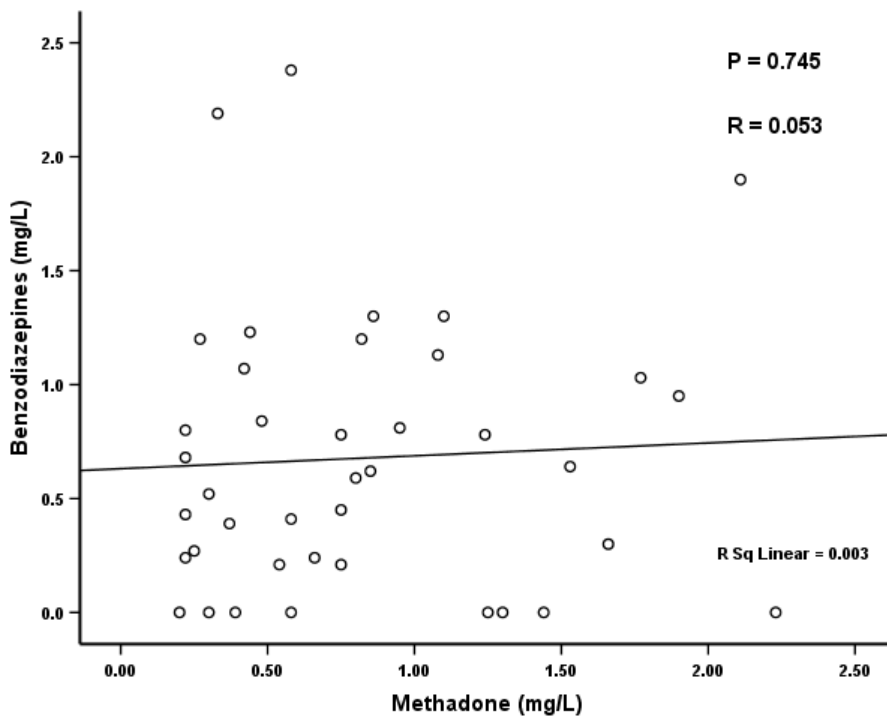


Figure 76: The correlation between post-mortem methadone concentrations and post-mortem benzodiazepine concentrations.

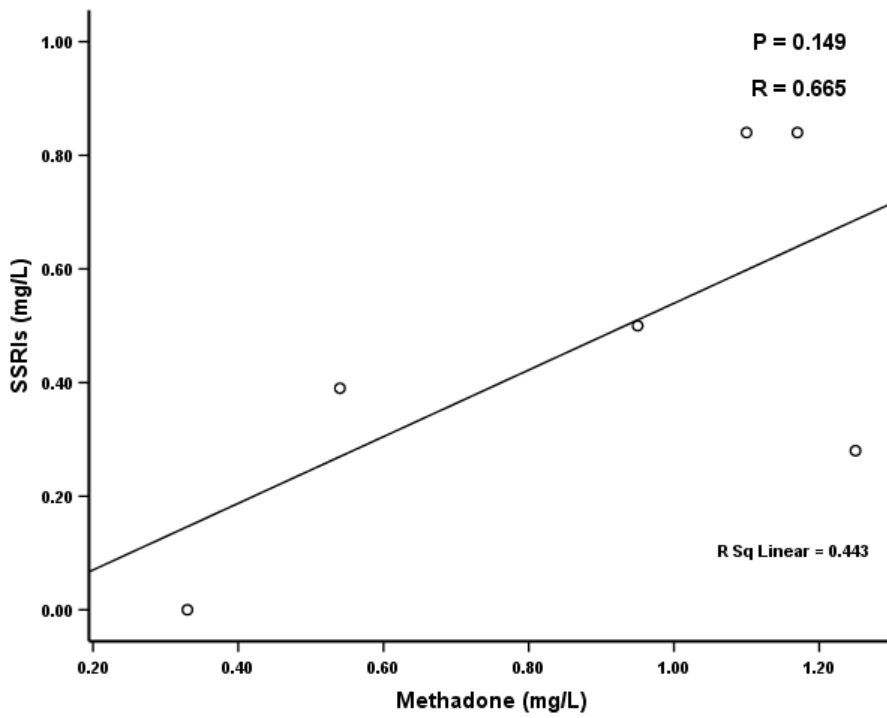


Figure 77: The correlation between post-mortem methadone concentrations and post-mortem SSRI concentrations.

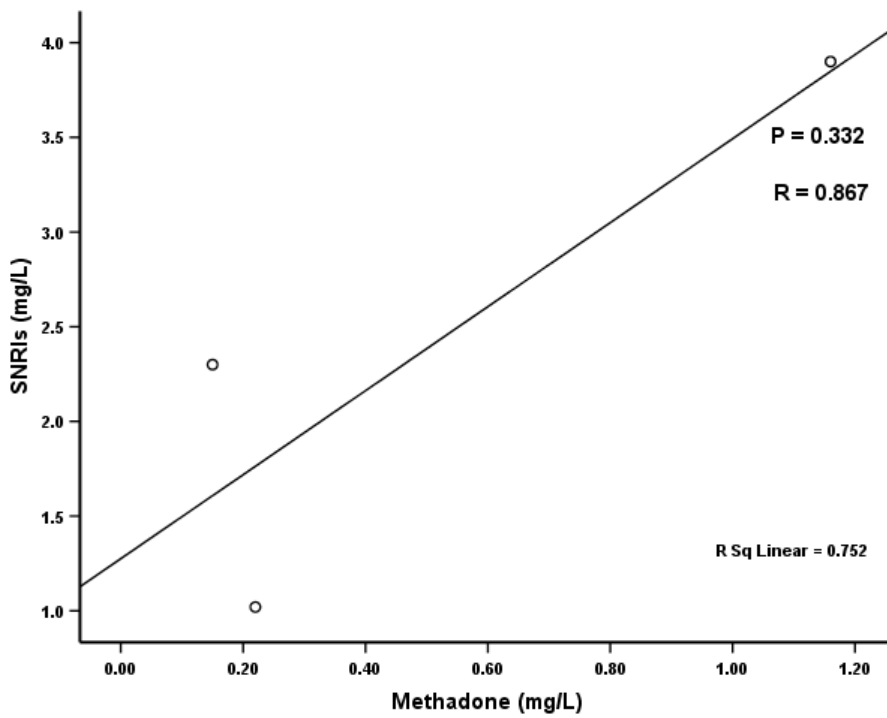


Figure 78: The correlation between post-mortem methadone concentrations and post-mortem SNRI concentrations.

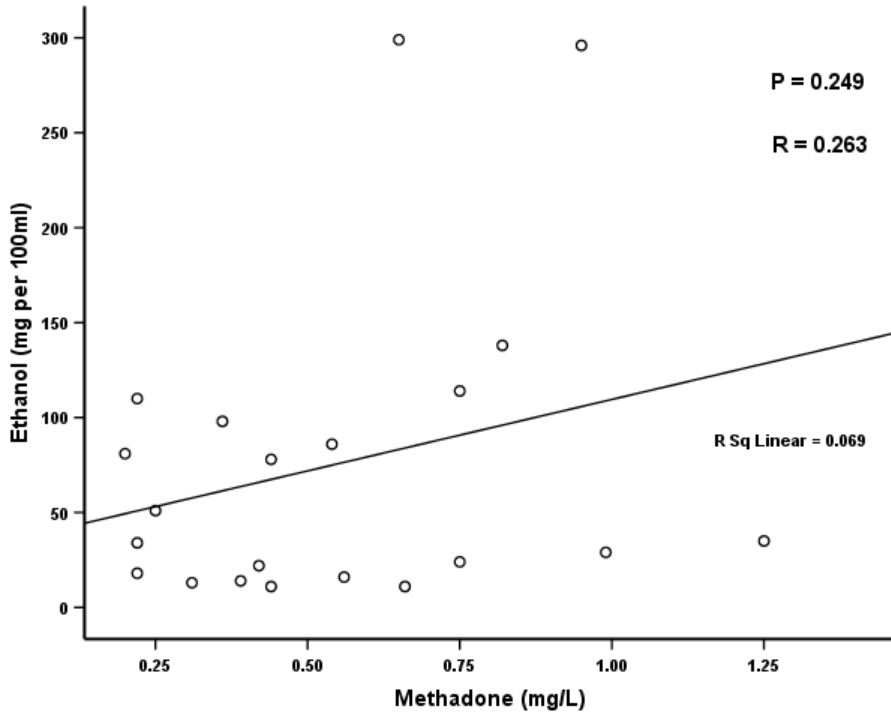


Figure 79: The correlation between post-mortem methadone concentrations and post-mortem ethanol concentrations.

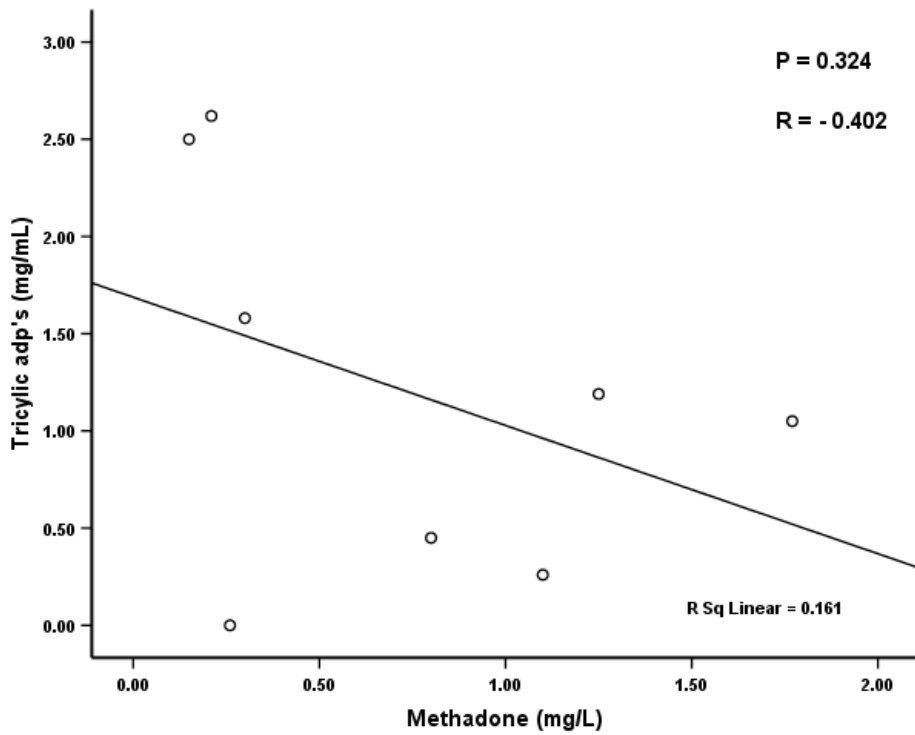


Figure 80: The correlation between post-mortem methadone concentrations and post-mortem tricyclic antidepressant concentrations.

3.6.3 Independent T test

Using the Independent T-Test significant associations between the *CYP2B6* G516T, and A785G gene variations and increased post-mortem methadone concentrations were identified (see Chapters 4, 5, 6). There was no association between T750C and methadone concentration observed in this study. For the first post-mortem population sampled (40 subjects) there was no significant difference in post-mortem methadone concentrations for the A118G SNP (Chapter 4). However when this population was increased to 69 subjects a statistically significant association was identified (Chapter 5; $P = 0.05$).

3.6.4 Hardy Weinberg equilibrium

3.6.4.1 *CYP2B6*

3.6.4.1.1 T750C SNP

Post-mortem population

Table 43: Post-mortem expected and observed frequencies for the T750C SNP.

Genotype	Expected	Observed
750 TT	24.11	37
750 TC	41.79	16
750 CC	18.11	31

P allele frequency is 0.54; Q allele frequency is 0.46

Table 44: Hardy Weinberg results for the T750C SNP in the post-mortem population.

	750 TT	750 TC	750 CC	p allele freq	q allele freq
750 TT	2.06	16	31	0.21	0.79
750 TC	37	67.73	31	0.52	0.48
750 CC	37	16	1.73	0.82	0.18

$X^2 = 31.99$, 1 degree of freedom, $P < 0.001$.

The null hypothesis that the population is in Hardy-Weinberg equilibrium is rejected.

Control population

Table 45: Control expected and observed frequencies for the T750C SNP.

Genotype	Expected	Observed
750 TT	33.06	49
750 TC	48.87	17
750 CC	18.06	34

P allele frequency is 0.57; Q allele frequency is 0.43

Table 46: Hardy Weinberg results for the T750C SNP in the control population.

	750 TT	750 TC	750 CC	p allele freq	q allele freq
750 TT	2.13	17	34	0.2	0.8
750 TC	49	81.63	34	0.55	0.45
750 CC	49	17	1.47	0.85	0.15

$X^2 = 42.53$, 1 degree of freedom, $P < 0.001$.

The null hypothesis that the population is in Hardy-Weinberg equilibrium is rejected.

3.6.4.1.2 G516T SNP

Post-mortem population

Table 47: Post-mortem expected and observed frequencies for the G516T SNP.

Genotype	Expected	Observed
516 GG	15.43	35
516 GT	41.14	2
516 TT	27.43	47

P allele frequency is 0.43; Q allele frequency is 0.57

Table 48: Hardy Weinberg results for the G516T SNP in the post-mortem population.

	516 GG	516 GT	516 TT	p allele freq	q allele freq
516 GG	0.02	2	47	0.02	0.98
516 GT	35	81.12	47	0.46	0.54
516 TT	35	2	0.03	0.97	0.03

$X^2 = 76.03$, 1 degree of freedom, $P < 0.001$.

The null hypothesis that the population is in Hardy-Weinberg equilibrium is rejected.

Control population

Table 49: Control expected and observed frequencies for the G516T SNP.

Genotype	Expected	Observed
516 GG	11.9	33
516 GT	45.19	3
516 TT	42.9	64

P allele frequency is 0.35; Q allele frequency is 0.66

Table 50: Hardy Weinberg results for the G516T SNP in the control population.

	516 GG	516 GT	516 TT	p allele freq	q allele freq
516 GG	0.04	3	64	0.02	0.98
516 GT	33	91.91	64	0.42	0.58
516 TT	33	3	0.07	0.96	0.04

$X^2 = 87.16$, 1 degree of freedom, $P < 0.001$.

The null hypothesis that the population is in Hardy-Weinberg equilibrium is rejected.

3.6.4.1.3 A785G SNP

Post-mortem population

Table 51: Post-mortem expected and observed frequencies for the A785G SNP.

Genotype	Expected	Observed
785 AA	16.3	36
785 AG	41.4	2
785 GG	26.3	46

P allele frequency is 0.44; Q allele frequency is 0.56

Table 52: Hardy Weinberg results for the A785G SNP in the post-mortem population.

	785 AA	785 AG	785 GG	p allele freq	q allele freq
785 AA	0.02	2	46	0.02	0.98
785 AG	36	81.39	46	0.47	0.53
785 GG	36	2	0.03	0.97	0.03

$X^2 = 76.08$, 1 degree of freedom, $P < 0.001$.

The null hypothesis that the population is in Hardy-Weinberg equilibrium is rejected.

Control population

Table 53: Control expected and observed frequencies for the A785G SNP.

Genotype	Expected	Observed
785 AA	15.6	38
785 AG	47.8	3
785 GG	36.6	59

P allele frequency is 0.4; Q allele frequency is 0.61

Table 54: Hardy Weinberg results for the A785G SNP in the control population.

	785 AA	785 AG	785 GG	p allele freq	q allele freq
785 AA	0.04	3	59	0.02	0.98
785 AG	38	94.7	59	0.45	0.55
785 GG	38	3	0.06	0.96	0.04

$X^2 = 87.84$, 1 degree of freedom, $P < 0.001$.

The null hypothesis that the population is in Hardy-Weinberg equilibrium is rejected.

3.6.4.2 OPRM1

3.6.4.2.1 A118G SNP

Post-mortem population

Table 55: Post-mortem expected and observed frequencies for the A118G SNP.

Genotype	Expected	Observed
118 AA	5.25	21
118 AG	31.5	0
118 GG	47.25	63

P allele frequency is 0.25; Q allele frequency is 0.75

Table 56: Hardy Weinberg results for the A118G SNP in the post-mortem population.

	118 AA	118 AG	118 GG	p allele freq	q allele freq
118 AA	0	0	63	0	1
118 AG	21	72.75	63	0.37	0.63
118 GG	21	0	0	1	0

$X^2 = 84$, 1 degree of freedom, $P < 0.001$.

The null hypothesis that the population is in Hardy-Weinberg equilibrium is rejected.

Control population

Table 57: Control expected and observed frequencies for the A118G SNP.

Genotype	Expected	Observed
118 AA	9.61	30
118 AG	42.78	2
118 GG	47.61	68

P allele frequency is 0.31; Q allele frequency is 0.69

Table 58: Hardy Weinberg results for the A118G SNP in the control population.

	118 AA	118 AG	118 GG	p allele freq	q allele freq
118 AA	0.01	2	68	0.01	0.99
118 AG	30	90.33	68	0.4	0.6
118 GG	30	2	0.03	0.97	0.03

$X^2 = 90.87$, 1 degree of freedom, $P < 0.001$.

The null hypothesis that the population is in Hardy-Weinberg equilibrium is rejected.

3.6.5 CYP2B6 and OPRM1 SNP-SNP Correlations

In all cases where the *CYP2B6* G516T was identified, A785G was also found. This is in agreement with previous reports where it was noted that G516T acts as a marker of A785G. Linkage between G516T and A785G presence was identified with a χ^2 (32.471), 1 df, $P < 0.001$. Linkage between the T750C, G516T and A785G gene variants was identified in both populations (see Chapter 6). In the post-mortem population the T750C, G516T and A785G variants were identified together in 17 cases (20 %) and in the control population the SNPs were found in 17 % of cases. No linkage was found between A118G and T750C, G516T and A785G in the control population ($P = 0.479$, $P = 0.572$, $P = 0.479$ respectively). Interestingly linkage was identified between A118G and G516T ($P < 0.01$) and A785G ($P < 0.01$) in the post-mortem population.

3.6.6 The Influence of Age, Gender and Involvement in Methadone Maintenance

The binary logistic regression model revealed that gender and age were significantly associated with population and this is discussed in Chapter 7.

Table 59: Variables entered into the Binary Logistic Regression Equation to determine the effects of Age and Gender on *CYP2B6* and *OPRM1* SNP prevalence.

		B	S.E.	Wald	df	Sig.
Step 1(a)	A118G			.228	2	.892
	A118G(1)	19.601	27237.521	.000	1	.999
	A118G(2)	19.399	27237.521	.000	1	.999
	G516T			.364	2	.834
	G516T(1)	21.726	21843.516	.000	1	.999
	G516T(2)	22.238	21843.516	.000	1	.999
	A785G			.000	1	.985
	A785G(1)	.015	.817	.000	1	.985
	T750C			2.306	2	.316
	T750C(1)	-.132	.577	.053	1	.819
	T750C(2)	-.651	.536	1.474	1	.225
	Gender(1)	1.748	.411	18.104	1	.000
	Age	.145	.026	31.464	1	.000
	Constant	-46.341	34914.348	.000	1	.999

Variable(s) entered on step 1: A118G, G516T, A785G, T750C, Gender, and Age.

Chapter 4

Identification of a rapid screening method to differentiate methadone susceptible individuals using *OPRM1* and *CYP2B6* gene variants.

This chapter has been published and has been presented here in paper format.

4.1 ABSTRACT

Methadone is a medication valued for its effectiveness in the treatment of heroin addiction, but with many fatal poisonings reported over the years. We have examined the association between *CYP2B6* and μ -opioid receptor (*OPRM1*) gene variations and apparent susceptibility to methadone poisoning. Genomic DNA was extracted from post-mortem whole blood of 40 individuals whose deaths were attributed to methadone poisoning. Presence of *CYP2B6**4,*9, and *6 alleles and the *OPRM1* A118G variant were determined by SNP genotyping. *CYP2B6* *4, *9, and *6 alleles were associated with higher post-mortem methadone concentrations ($P \leq 0.05$). *OPRM1* A118G was also associated with higher post-mortem methadone concentrations but not at a level of statistical significance ($P = 0.39$). In these methadone deaths *OPRM1* 118GA was associated with higher post-mortem benzodiazepine concentrations ($P = 0.04$), a finding not seen for morphine. The risk of a methadone fatality during treatment may be evaluated in part by screening for *CYP2B6**6 and A118G.

Keywords:

Methadone; Benzodiazepines; μ -opioid receptor; *CYP2B6*; Fatal; Post-mortem blood

4.2 Introduction

Methadone is a μ -receptor agonist valued for its effectiveness in the treatment of opioid dependency and pain management. Administered in a racemic mixture, methadone has a long plasma elimination half-life (between 13 to 55 hours) and high oral bioavailability (70-90%) (Wolff *et al.* 1997; Foster *et al.* 1999; Corkery *et al.* 2004; Moffat *et al.* 2004; Nettleton *et al.* 2007). Extensively metabolised in the liver methadone is converted into its primary metabolite 2-ethylidene-1, 5-dimethyl-3, 3-diphenylpyrrolidine (EDDP) by the cytochrome P450 enzymes *CYP3A4*, *CYP2B6* and to a lesser extent *CYP2D6* (Crettol *et al.* 2007).

Inter-individual variation in blood methadone concentration and toxic drug accumulation have been increasingly reported (Osselton *et al.* 1984; Buster *et al.* 2002; Corkery *et al.* 2004; Maxwell *et al.* 2005; Eap *et al.* 2007; Shields *et al.* 2007) and might be explained by pharmacogenomics (Foster *et al.* 1999; Corkery *et al.* 2004; Eap *et al.* 2007). In drug tolerant individuals blood methadone concentrations can reach > 0.84 mg/L, whilst in fatal cases blood methadone concentrations typically range between 0.4 mg/L to > 1.8 mg/L. However many fatalities occur with concentrations as low as 0.05 mg/L, significantly lower than the average blood concentration (Caplehorn & Drummer, 2002). Genetic variations in the cytochrome enzymes responsible for methadone metabolism may affect drug pharmacokinetics explaining this inter-individual variation. Although a number of *CYP3A4* variants have been identified and *CYP3A4* gene expression levels demonstrate up to 40-fold inter-individual differences (Dai *et al.* 2001; Plant *et al.* 2007) thus far no significant association between *CYP3A4* variants and methadone metabolism has been documented (Westlind *et al.* 2001).

CYP2B6 is of interest because it is involved in the metabolism of a number of drugs including midazolam (Lang *et al.* 2001), ketamine (Yanagihara *et al.* 2001), bupropion (Faucette *et al.* 2000), and methadone (Crettol *et al.* 2007; Eap *et al.* 2007). Although expressed predominantly in the liver *CYP2B6* can also be found at lower levels in the brain, stomach, lung, kidney and heart (Park *et al.* 2000). *CYP2B6* is highly polymorphic and a number of different genotypes have been identified (Lang *et al.* 2001). *CYP2B6**4/*4 is associated with allele * 4 (A785G single nucleotide polymorphism, SNP) and this genotype produces a fast metaboliser phenotype. When allele * 9 (G516T SNP) is found in combination with allele * 4 they form a haplotype corresponding to allele * 6. The *CYP2B6**6/*6 genotype produces a slow or poor metaboliser phenotype and is present at a frequency of about 6% in Caucasian populations (Lang *et al.* 2001; Crettol *et al.* 2007; Eap *et al.* 2007). Slow metabolisers have reduced enzymatic activity, which can result in drug accumulation and increased toxicity.

Genetic variations within the opioid receptors may also affect drug pharmacodynamics impacting the response to methadone. The μ opioid receptor (*OPRM1*) is of particular interest since it is the preferential binding target of methadone. A number of *OPRM1* variants have been identified and the A118G missense SNP in exon 1 has been linked with significant reductions in β -endorphin binding (Bond *et al.* 1998), increased morphine requirements (Klepstad *et al.* 2005), protection from morphine-6-glucuronide (M6G) induced toxicity (Lötsch *et al.* 2002), and susceptibility to drug addiction (Bart *et al.* 2004). Therefore gene variations such as the *OPRM1* A118G variation could affect drug binding and drug response. The association between A118G and methadone is unclear and requires further investigation.

Benzodiazepines are often administered to methadone maintenance patients to treat anxiety associated with drug addiction and heroin withdrawal (Darke *et al.* 1995), however concomitant use of benzodiazepines and methadone can increase lethal respiratory depression (McCormick *et al.* 1984).

We explored the possibility that genetic variations in the μ opioid receptor *OPRM1* and *CYP2B6* may be linked with susceptibility to methadone toxicity by analysing the prevalence of the *OPRM1* A118G variation and *CYP2B6**4, *9 and *6 alleles in 40 fatalities attributed to methadone toxicity.

4.3 Materials and Methods

Case Selection

A retrospective review (2007-2008) of methadone-associated deaths from a geographically defined area of Scotland (Tayside, Fife and Central regions) was conducted.

Toxicological Analyses

The toxicological analysis for each subject was conducted at the Centre for Forensic and Legal Medicine, Dundee University. Following cross-clamping of the femoral vein, blood samples were collected by needle and syringe distally. Methadone was extracted from post-mortem blood specimens using liquid/liquid extraction followed by high pressure liquid chromatography with a diode array detector (HPLC – DAD). Post-mortem blood specimens were made alkaline using 0.2M carbonate buffer and extracted with 1-chlorobutane. A Waters Spherisorb 5 μ m OD/CN HPLC column (4.6 x 150mm) and a guard column were used with acetonitrile (25% acetonitrile in aqueous TEAP buffer) as the mobile phase.

DNA Extraction and Quantitation

Genomic DNA was isolated from leukocytes (sodium fluoride anticoagulated blood) by the DNeasy Blood and Tissue Kit (Qiagen, Crawley, UK) and quantified using the Human Quantifiler® Kit (Applied Biosystems, Warrington, UK) in accordance with the manufacturer's instructions.

OPRM1 & CYP2B6 Genotyping by Conventional PCR

Samples were amplified by PCR to identify homozygous wild type, homozygous variant and heterozygous controls. For the A118G SNP in exon 1 of *OPRM1* primer EX1F_HB (forward: 5' ATGCCTTGGCGTACTCAAGTTG) and primer EX1R_HB (reverse: 5' CTA ACTCCCAAGGCTCAATGTTG) were used. G516T in exon 4 was amplified using primer C2B6E4F (forward: 5' GTACATAATTAGCTGTTACGG) and primer C2B6E4R (reverse: 5' AAGTCTGGTAGAACAAGTTCA). A785G in exon 5 of *CYP2B6* was amplified using primer C2B6E5F (forward: 5' AGGAGATATAGAGTCAGTGAG) and primer C2B6E5R (reverse: 5' AGTTCCTCCTCCCTATTTTCT). PCRs were performed with a reaction volume of 50 µl, including 27.5 µl PCR grade water, 10 µl of 5x GoTaq™ buffer, 3.0 mM MgCl₂, 1 µl of 10 mM deoxynucleoside triphosphates (dNTPs) (final concentration of 0.25 mM), 1 µl Forward and Reverse primers, 10 ng/ µl DNA and 0.5 µl GoTaq™ DNA polymerase. PCR reactions were performed with a Primus 96 advanced machine (Alpha Laboratories, Eastleigh, UK). The cycling conditions were as follows: initial denaturation at 95°C for 5 minutes; subsequent denaturation at 95°C for 1 minute; annealing at 65.3°C (118 A>G), 59.5°C (516 G>T), and 62.1°C (785 A>G) for 30 seconds; primer extension at 72°C for 2 minutes, repeated for 30 cycles, followed by final extension at 72°C for 5 minutes. PCR products were visualised by

electrophoresis with a 2 % Cyber Green-agarose gel on blue light. Samples were purified using the QIAquick PCR Purification Kit (Qiagen, Crawley, UK) in accordance with the manufacturer's instructions. DNA sequencing was conducted by COGENICS (COGENICS, Essex, UK).

OPRM1 Genotyping by Real-time PCR

Samples were genotyped for the A118G variation using the commercialised TaqMan® SNP Genotyping assay (Applied Biosystems, Warrington, UK, product no. 4351379) following the manufacturers instructions.

CYP2B6 Genotyping by Real-time PCR

Samples were genotyped for the G516T variation using the commercialised TaqMan® Drug Metabolism Genotyping assay (Applied Biosystems, Warrington, UK, product no. 4362691). A custom designed TaqMan® assay (Applied Biosystems, Warrington, UK, product no. 4331349) was used to genotype for A785G. Genotyping was performed according to the manufacturer's instructions.

Statistical Analysis

Data are presented as median, means \pm SE of the mean. The statistical significance of the differences between methadone mean concentrations and the G516T and A785G variants and methadone/benzodiazepine mean concentrations and A118G was determined using the two-tailed Independent T test. Linkage between gene variants was determined using Pearson's Chi-square test and Spearman's rank correlation. A P value of ≤ 0.05 was considered to indicate statistical significance. All analyses were performed with SPSS Software (version 14.0).

4.4 Results

The 40 post-mortem cases where methadone had been implicated in the cause of death included 34 men and 6 women, the majority of whom were Caucasian (97.5%). The mean age of the case subjects was 31 ± 1.6 (17 – 60 range). Methadone together with benzodiazepines was present in 20 of the 40 subjects. Other drugs detected in the post-mortem blood samples are listed in Table 60.

Table 60: Drugs detected at post-mortem in 40 fatalities attributed to methadone as a cause of death.

Psychoactive substance	Total
Blood	40 (100%)
Ethanol	
Negative	25 (62.5 %)
≤ 100 mg/100ml	11 (27.5 %)
100-200 mg/100ml	2 (5 %)
200-300 mg/100ml	2 (5 %)
Antidepressants	11 (27.5 %)
Benzodiazepines	20 (50 %)
Morphine	15 (37.5 %)
Dihydrocodeine	2 (5 %)
Quetiapine	2 (5 %)
Amfetamine	1 (2.5 %)
Propanolol	1 (2.5 %)
Urine	
Codeine	3 (7.5 %)
6-MAM	2 (5 %)
Cannabinoids	11 (27.5 %)
Cocaine and or metabolites	1 (2.5 %)

CYP2B6 alleles and post-mortem methadone blood concentrations

Of the 40 methadone related fatalities, 14 were genotyped as heterozygous carriers of allele * 9, a frequency of 35% and 1 was genotyped as a homozygous carrier, an allelic frequency of 2.5%. This result is higher than previous reports (Kircheiner *et al.* 2003; Crettol *et al.* 2005; Crettol *et al.* 2007) but within the expected range detailed on the National Center for Biotechnology Information (NCBI) website for Caucasian populations (www.ncbi.nlm.nih.gov/SNP). Heterozygous carriers of allele * 4 were identified in 16 cases, a frequency of 40% which is noticeably higher than other reports from Caucasian populations (Kircheiner *et al.* 2003; Jacob *et al.* 2004; Crettol *et al.* 2005; Crettol *et al.* 2007). Allele * 6 was identified in 15 cases, an allelic frequency of 37.5%, once again an elevated frequency compared with other studies (Kircheiner *et al.* 2003; Jacob *et al.* 2004; Crettol *et al.* 2005). As expected the post-mortem methadone blood concentrations (mean 0.56 mg/L, $P < 0.05$) for the CYP2B6*1/*1 (wild type) genotype were statistically lower than the other genotypes identified (Table 61). The frequency of CYP2B6*1/*1 (57.5%) was higher than other reports (43%, 22%) conducted on living subjects (Lang *et al.* 2001; Crettol *et al.* 2005), although only 3 alleles were observed from the post-mortem subjects in this study.

All of the CYP2B6 alleles tested (*4, *9 and * 6) were associated with higher mean post-mortem methadone blood concentrations ($P < 0.05$, Independent T-test), reflecting poor methadone metabolism (Figures 81 & 82, Table 61).

In all cases where allele * 9 was identified, allele *4 was also found. This is in agreement with previous reports where it was noted that allele * 9 acts as a marker of allele *4 (Crettol *et al.* 2007; Eap *et al.* 2007). Linkage between allele * 9 and allele * 4 presence was identified with a χ^2 (32.471), 1 df, $P < 0.001$. Only one subject was

identified with the CYP2B6*6/*6 genotype, this subject had a post-mortem blood methadone concentration of 1.38 mg/L, a concentration 3.45 fold higher than the normally recognised fatal threshold, but this result was not statistically significant (Table 61). CYP2B6*1/*4 was identified in two cases, a frequency of 5%. By itself allele * 4 has been linked with fast metabolism (Lang *et al.* 2001) however our results did not show this trend, with a mean post-mortem concentration of 0.86 mg/L (Table 61). No CYP2B6*4/*4 genotypes were identified.

Table 61: CYP2B6*4,*9, and *6 alleles and post-mortem methadone blood concentrations.

	Frequency	Mean	Std. Deviation	Std. Error Mean	Median	P value
<i>CYP2B6</i>						
A785G						
(allele * 4)						
AA	23	0.56 mg/L	0.296	0.062	0.56	
GA & GG	17	0.95 mg/L	0.608	0.148	0.97	0.024*
G516T						
(allele * 9)						
GG	25	0.58 mg/L	0.353	0.071	0.56	
TG & TT	15	0.96 mg/L	0.598	0.154	0.97	0.039*
Allele * 6	15	0.96 mg/L	0.598	0.154	0.97	0.039*
*1/*1	23	0.56 mg/L	0.296	0.618	0.56	0.024*
*1/*4	2	0.86 mg/L	0.948	0.670	0.86	0.690
*1/*6	14	0.93mg/L	0.609	0.163	0.91	0.041*
*6/*6	1	1.38 mg/L				0.153

Significance at < 0.05 is denoted by *.

Table 62: *OPRM1* and *CYP2B6* Genotyping Data for the Post-mortem Methadone-attributed fatalities.

Case	<i>CYP2B6</i> G516T Genotype GG, GT, TT	<i>CYP2B6</i> A785G Genotype AA AG GG	<i>OPRM1</i> A118G Genotype AA, AG, GG	Methadone (mg/L)	Sample
1	GG	AA	AA	0.27	Fm
2	GG	AA	AA	0.86	Fm
3	GT	AG	AA	1.16	Fm
4	GG	AA	AA	0.30	Fm
5	GG	AA	AA	1.1	Fm
6	GT	AG	AA	0.82	Fm
7	GT	AG	AA	0.97	Fm
8	GG	AA	AA	0.22	Fm
9	GT	AG	AA	0.20	Fm
10	GT	AG	AG	1.44	Fm
11	GG	AA	AA	0.48	Fm
12	GG	AA	AA	1.25	Fm
13	GT	AG	AG	1.08	Fm
14	GG	AA	AA	0.44	Fm
15	GG	AA	AA	0.58	Fm
16	GT	AG	AG	0.33	Fm
17	GG	AA	AA	0.95	Fm
18	GG	AA	AA	0.58	Fm
19	GG	AA	AA	0.65	Fm
20	GT	AG	AA	1.66	Fm
21	GG	AA	AA	0.60	Fm
22	GT	AG	AA	0.54	Fm
23	GT	AG	AA	0.26	Fm
24	GT	AG	AA	2.23	Fm
25	GG	AA	AA	0.39	Fm
26	GG	AA	AA	0.25	Fm
27	GT	AG	AA	0.15	Cd
28	GG	AA	AA	0.37	Fm
29	GG	AA	AA	0.22	Fm
30	GG	AA	AA	0.22	Fm
31	GT	AG	AA	1.3	Fm
32	TT	GG	AA	1.38	Fm
33	GT	AG	AA	0.19	Fm
34	GG	AA	AA	0.75	Fm
35	GG	AA	AA	0.24	Fm
36	GG	AA	AA	1.53	Fm
37	GG	AA	AA	0.56	Fm
38	GG	AA	AA	0.80	Fm
39	GG	AA	AA	0.75	Fm
40	GT	AG	AG	0.85	Fm

Where Fm = femoral.

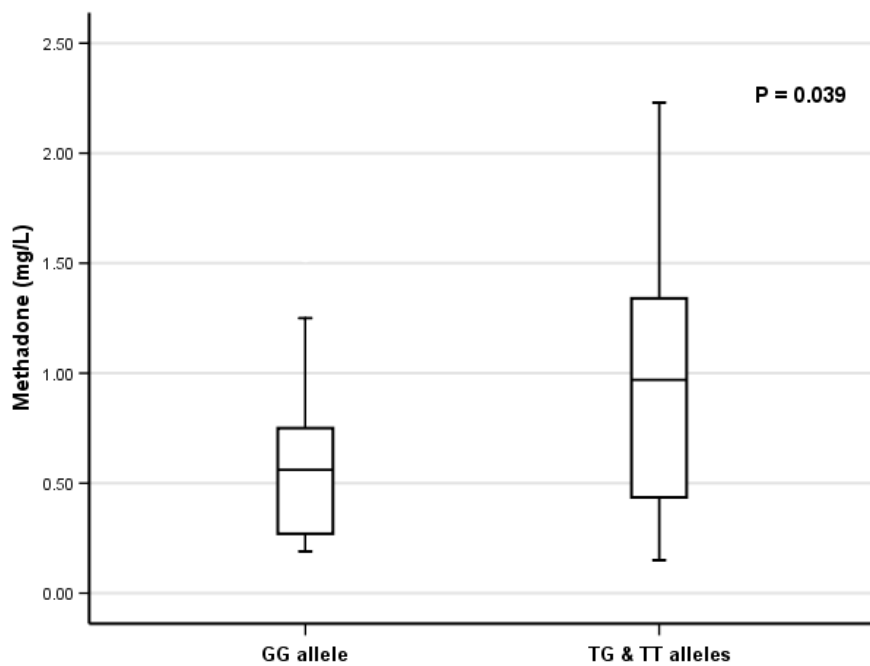


Figure 81: Distribution (median and interquartile range) of post-mortem methadone concentrations for the 516GG, 516GT, and 516TT genotypes.

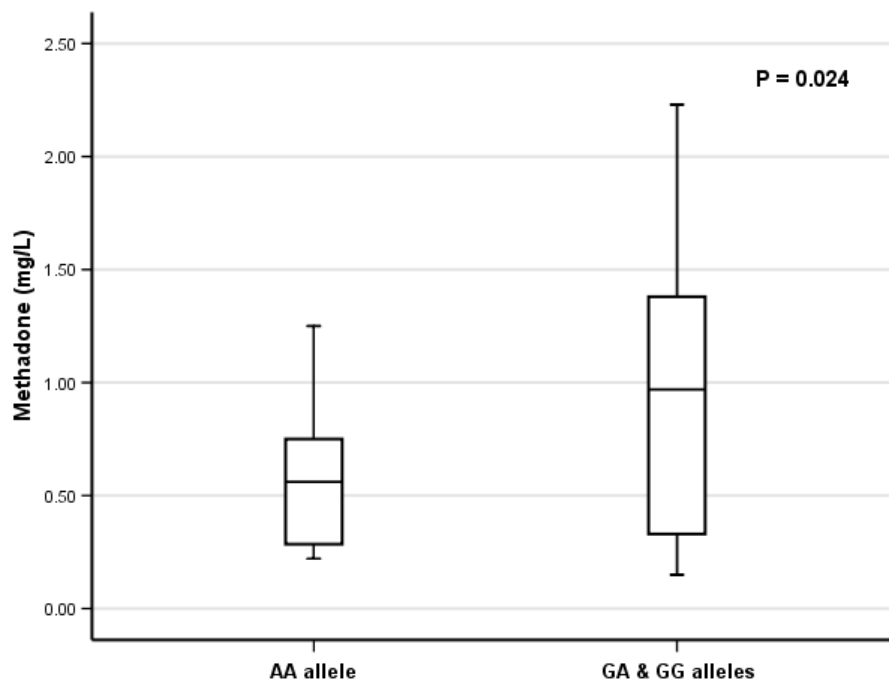


Figure 82: Distribution (median and interquartile range) of post-mortem methadone concentrations for the 785AA, 785AG and 785 GG genotypes.

OPRM1 A118G and post-mortem methadone blood concentrations

The A118G SNP demonstrated an allelic frequency of 10%, a similar result to that reported in other studies conducted on living subjects (Bergen *et al.* 1997; Lotsch *et al.* 2002). No significant association was seen between A118G and post-mortem methadone blood concentrations ($P > 0.05$, Table 63). However the median methadone concentration for 118 GA carriers is higher than 118 AA carriers at 0.97 mg/L and 0.58 mg/L respectively (Figure 83). No homozygote for the G allele was identified in this study. A significant association was identified in this study between 118G allele and CYP2B6 * 9 allele, and 118G allele and CYP2B6 * 4 allele by using Spearman's rank correlation ($P < 0.01$, $P < 0.05$ respectively).

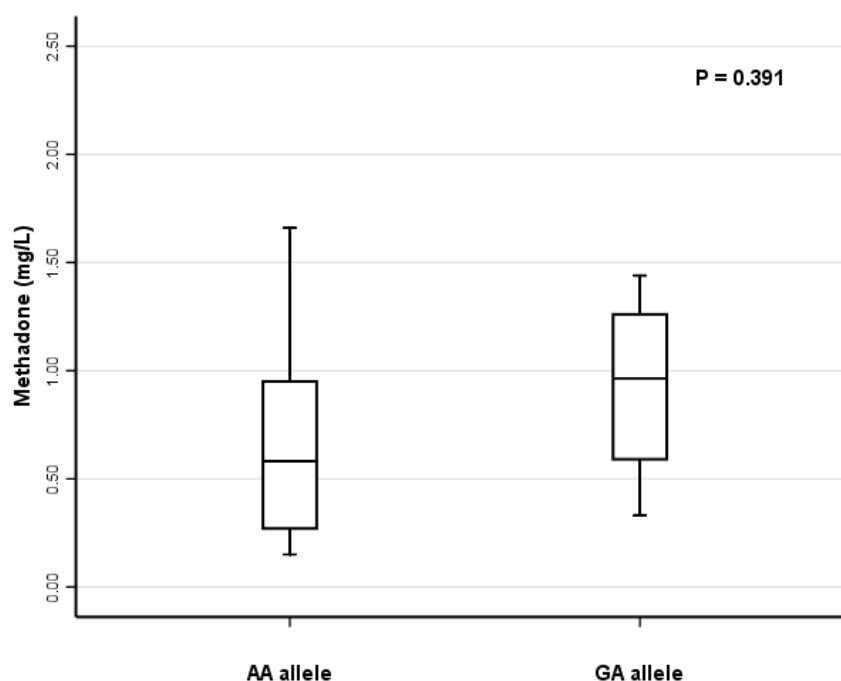


Figure 83: Distribution (median and interquartile range) of post-mortem methadone concentrations for the 118AA, 118GA and 118GG genotypes.

OPRM1 A118G and post-mortem benzodiazepine blood concentrations

Benzodiazepines are concurrently administered with methadone to addicts for the treatment of substitute related anxiety. The additive effect of benzodiazepines and methadone in causing respiratory depression has been well documented (McCormick *et al.* 1984; Lintzeris *et al.* 2007). Concomitant use of methadone and benzodiazepines was demonstrated in 50% of the subjects (Table 60). There was a significant association between the A118G SNP and mean post-mortem benzodiazepine concentrations, $P < 0.01$ (Table 63). Heterozygous individuals demonstrated a 2.4 fold higher mean benzodiazepine concentration compared to homozygous wild type (Figure 84).

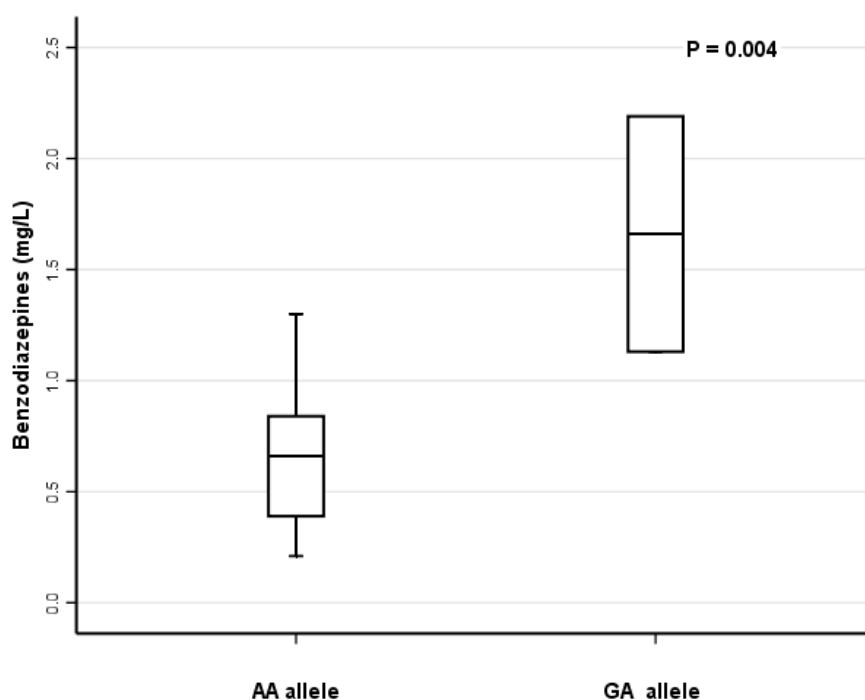


Figure 84: Distribution (median and interquartile range) of post-mortem benzodiazepine concentrations for the 118AA, 118GA and 118GG genotypes.

Table 63: A118G genotypes and post-mortem methadone and benzodiazepine concentrations for a population of methadone-attributed fatalities (population 1) and A118G genotypes and post-mortem morphine and benzodiazepine concentrations for a population of morphine-attributed fatalities (population 2).

Population 1					
A118G genotype	Frequency	Mean	Std. Deviation	Std. Error Mean	Median
Methadone					
AA	36	0.70 mg/L	0.493	0.082	0.58
GA	4	0.93 mg/L	0.465	0.233	0.97
2-tailed Sig.	0.391				
Benzodiazepines					
AA	18	0.69 mg/L	0.363	0.086	0.66
GA	2	1.66 mg/L	0.749	0.530	1.66
2-tailed Sig.	0.004*				
Population 2					
A118G genotype	Frequency	Mean	Std. Deviation	Std. Error Mean	Median
Morphine					
AA	25	0.45 mg/L	0.86	0.172	0.22
GA	2	0.12 mg/L	0.05	0.035	0.16
2-tailed Sig.	0.593				
Benzodiazepines					
AA	25	1.62 mg/L	1.57	0.315	0.58
GA	2	1.05 mg/L	0.10	0.705	0.97
2-tailed Sig.	0.626				

4.5 Discussion

Use of methadone in maintenance programmes worldwide (Buster *et al.* 2002; Maxwell *et al.* 2005) has been associated with methadone-associated fatalities. Patients prescribed methadone for heroin withdrawal are reported to be 6.7 times more likely to experience an adverse drug reaction during the drugs induction phase (Caplehorn & Drummer, 2002), at a time when either drug tolerance may be overestimated or other drugs are in use (Corkery *et al.* 2004). In this study, a significant association was revealed between the CYP2B6*4, *9 and *6 alleles and high methadone concentrations in post-mortem blood, characteristic of the slow metaboliser phenotype. This is the first time such a genetic association has been demonstrated in methadone related fatalities (Table 61) i.e. deaths in which methadone toxicity was assessed as a probable significant factor by the autopsy pathologist. Furthermore, the allelic frequencies of these target alleles were considerably higher than those reported in live patients (Crettol *et al.* 2007; Eap *et al.* 2007) supporting the concept that there is linkage between these gene variants and methadone toxicity. This observation is in agreement with the results of a study examining *CYP2D6* SNPs in post-mortem cases and methadone metabolism, where the prevalence of poor metabolisers exceeded the reported frequencies in general population reports (Wong *et al.* 2003). Thus the risk of a methadone fatality may be predetermined in part by screening for *CYP2B6* variants, in particular CYP2B6*6. Therefore there is potential value in screening for *CYP2B6* variants before prescribing methadone for drug addiction, and possibly also in palliative care where methadone may be used as an alternative to morphine for analgesia (Ripamonti *et al.* 1997). It would be interesting to examine *CYP2B6* allele frequencies in an opioid abusing

population to identify whether there are higher frequencies among opioid abusers compared with the general population.

The CYP2B6*4 allele has been linked with increased enzymatic activity (Lang *et al.* 2001; Kircheiner *et al.* 2003) and fast metaboliser status but the anticipated lower drug levels were not observed in the present study. Only two subjects were CYP2B6*1/*4 carriers limiting further interpretation (Table 61). Future studies which take into account individual drug history, the time period between drug administration and death, and post-mortem interval might strengthen our findings, which this far only identify a trend. The inevitable post-mortem interval between death and sampling could potentially increase blood drug concentrations due to post-mortem redistribution (Pounder & Jones *et al.* 1990). The sampling site and manner of sample collection used in this study should ameliorate this. Nevertheless, even femoral venous blood samples are subject to post-mortem increase (Moriya & Hashimoto, 1997).

A number of studies have examined the association between *OPRM1* variants and inter-individual variability in morphine metabolism (Lotsch *et al.* 2002; Klepstad *et al.* 2005), but there is limited information on the relationship between this genotype and response to methadone. The *OPRM1* A118G SNP has been shown to affect opioid efficacy (Klepstad *et al.* 2005). This SNP, located in exon 1, results in an amino acid change from asparagine to aspartic acid causing the loss of a putative N-linked glycosylation site, which might be associated with changes in receptor trafficking to the membrane (George *et al.* 1999). *In vitro* expression studies at the transcription level examining this SNP also noted significant increases in wild-type expression over 118 GA carriers (Zhang *et al.* 2005). Since *OPRM1* 118AA receptors have ten times more binding sites than that of 118GA (Zhang *et al.* 2005) it was postulated that the residue of 118 may be attributed to a *cis*-acting factor. Reductions

in cell surface μ receptors may limit the availability of drug binding sites.

Significantly increased post-mortem methadone concentrations were not found in association with *OPRM1* 118 GA (Table 63), however there is a distinct separation between the median post-mortem methadone concentrations for 118 AA and 118 GA carriers at 0.70 mg/L, 0.93 mg/L respectively (Figure 83), without considering two data outliers (1.66 & 1.44 mg/L) which could be falsely elevating the 118 AA mean drug concentration. Since A118G reduces receptor binding sites (Zhang *et al.* 2005) this might offer an explanation for the increased drug concentrations observed in this study. Therefore the possibility of an association between A118G and methadone blood concentration cannot be excluded. An increased sample size would assist in exploring this potential relationship.

When benzodiazepines were found in conjunction with methadone (Table 63, Population 1), carriers of *OPRM1* 118 GA had a 2.4 fold higher post-mortem mean blood benzodiazepine concentration ($P < 0.01$). Although the study has a limited sample size it has to be noted that a clear difference was observed. Interestingly this was not seen in morphine-associated fatalities (Table 63, Population 2) suggesting a specific link between methadone and benzodiazepines. Given that both methadone and morphine bind to the mu opioid receptor similarly, this raises the question why the interaction varies for different opioids. It may be postulated that this is linked with receptor endocytosis which is induced by methadone but not morphine (Keith *et al.* 1998). However the reason for this interaction remains unknown and it would be interesting to study this further. A potential pharmacokinetic mechanism for interactions between methadone and benzodiazepines may take place via a shared CYP metabolic pathway. A number of benzodiazepines are metabolised by *CYP3A4* & *CYP2B6* including diazepam (Schminder *et al.* 1996), midazolam (Lang *et al.* 2001), and flunitrazepam, (Hesse *et al.* 2001). Furthermore, some benzodiazepines have

been theorised to act as weak inhibitors of *CYP3A4* (Spaulding *et al.* 1974). Increased methadone concentrations in liver and brain have been reported when diazepam was administered following methadone exposure (Shah *et al.* 1979). It has been reported that benzodiazepine inhibition of *CYP3A4* is weak and unlikely to be of clinical significance (Foster *et al.* 1999). Other drugs known to inhibit methadone metabolism include ketoconazole (Baldwin *et al.* 1995), nelfinavir (Hesse *et al.* 2001), paroxetine (Walsky *et al.* 2006), and sertraline (Walsky *et al.* 2006), therefore concomitant use of these drugs may lead to increased methadone concentrations post-mortem. Drug interactions cannot therefore be excluded as additional factors in the increased methadone concentrations reported in this study.

It is well documented that the co-administration of methadone and benzodiazepines can result in lethal respiratory depression (McCormick *et al.* 1984; Borron *et al.* 2002; Lintzeris *et al.* 2007). Since benzodiazepines bind to GABA_A receptors and not opioid receptors this does not involve a direct association (Borron *et al.* 2002). However, both receptor systems share common signal transduction pathways (Dan'ura *et al.* 1988). Animal models have indicated the occurrence of associations between the opioid and GABA_A receptor systems, where for example benzodiazepines have been shown to potentiate the respiratory effects of fentanyl (Bailey *et al.* 1990). In the rat concomitant use of benzodiazepines with the partial μ -opioid agonist buprenorphine resulted in the increased recruitment of μ -opioid receptors (Poisonel *et al.* 2009). Consequently it may be postulated that benzodiazepines affect μ -opioid receptor regulation through signal transduction and regulatory pathways. Our findings suggest that susceptibility to methadone and benzodiazepines is associated with the A118G genotype by a presently unknown mechanism.

A significant association between *OPRM1* A118G genotype and CYP2B6 *4, 9* and 6* alleles was revealed in this study. Both genes are vital to methadone action *in vivo* and this assemblage of gene variants may reflect the nature of coordinated action of the enzyme and receptor in contributing to susceptibility to methadone. Agonist-occupancy at μ -receptors leads to receptor phosphorylation and rapid receptor desensitization (Koch *et al.* 1998). This in turn facilitates receptor internalisation reducing agonist response (Koch *et al.* 2005), and is thought to be a mechanism involved in the acquisition and development of drug tolerance (Koch *et al.* 2005). Receptor internalisation should reduce the number of potential drug binding sites, protecting against methadone toxicity in the presence of poor drug metabolism. However, concomitant use of methadone and benzodiazepines may up-regulate μ receptors (Poisnel *et al.* 2009) neutralising the reduction in available binding sites, leading to methadone toxicity. The A118G genotype of *OPRM1* has been linked also with susceptibility to heroin addiction (Bart *et al.* 2004). As demonstrated in our study CYP2B6*9 & *6 alleles can be linked with poor drug metabolism as expressed by higher post-mortem blood drug concentrations. The combination of *OPRM1* A118G genotype and CYP2B6*9 & *6 variants could lead to predisposition to opioid addiction and greater susceptibility to methadone fatality. The sensitivity of the μ -opioid receptor to methadone will be reduced in 118 GA subjects, therefore these subjects may reach higher concentrations before toxic effects appear.

In this retrospective review of case fatalities, potential confounding factors such as the presence and concentrations of all other drugs, mode of drug intake, previous opiate use or recent abstinence, and rapid or delayed death cannot be excluded. In summary, *CYP2B6* variants, specifically the CYP2B6*6 allele are associated with higher methadone concentrations in the post-mortem blood of fatalities from methadone toxicity, likely as a consequence of “poor” or “slow” drug

metabolism. This genotype clearly correlates with higher methadone concentrations; we can therefore postulate that for a normal population subjects with this genotype will experience higher methadone accumulation and are therefore more at risk of methadone toxicity. This suggests that the CYP2B6*6 allele may be a suitable risk factor for screening for individual susceptibility to methadone toxicity. The 118 GA genotype may have a similar value, which needs to be explored in a larger study. The presence of the A118G SNP on the *OPRM1* gene may also be of forensic value when interpreting the potential toxic relationship between methadone and benzodiazepines. Given that methadone maintenance therapy has been effective in reducing heroin associated mortalities for many years (Esteban *et al.* 2003) it would be beneficial to reduce methadone-associated mortality by assessing and monitoring its adverse effects on individuals with slow-metaboliser genotypes. Genetic screening for “susceptibility” variations prior to maintenance therapy could therefore be used to identify patients who may be at increased risk, since it is not routine practice for patients undergoing methadone maintenance treatment to undergo therapeutic drug monitoring (TDM). Typically TDM is employed for substances with a low therapeutic index such as cardio-toxic, neuroleptic and immunosuppressive drugs where the difference between beneficial therapeutic and toxic blood/plasma concentrations is small. Although TDM offers a scientific approach to selecting a drug regime to optimise therapy it involves regular clinic visits, can involve costly analysis and in many instances clinical response does not correlate with plasma drug concentration. Genetic screening of subjects prior to methadone maintenance treatment would involve a single rapid diagnostic test. Specific screening to identify CYP2B6*6 and *OPRM1* A118G carriers prior to addiction treatment could therefore be valuable as part of a cost-effective risk management strategy.

Chapter 5

Validation of a screening method to differentiate methadone susceptible individuals using *OPRM1* and *CYP2B6* gene variants.

This chapter has been drafted for publication and has been presented here in paper format.

5.1 ABSTRACT

The last chapter examined the association between *CYP2B6* and μ -opioid receptor (*OPRM1*) gene variations and apparent susceptibility to methadone poisoning. In this chapter the effect of *CYP2B6* and *OPRM1* variations will be studied for a larger population of subjects whose deaths were attributed to methadone. Genomic DNA was extracted from post-mortem whole blood of 69 individuals whose deaths were attributed to methadone poisoning. Presence of *CYP2B6**4, *9, and *6 alleles and the *OPRM1* A118G variant were determined by SNP genotyping. *CYP2B6* *4, *9, and *6 alleles were associated with higher post-mortem methadone concentrations ($P \leq 0.05$). *OPRM1* A118G was also associated with higher post-mortem methadone concentrations at a level of statistical significance ($P = 0.05$). This confirms that the risk of a methadone fatality may be evaluated in part, by screening for *CYP2B6**6 and A118G.

Keywords:

Methadone deaths; μ -opioid receptor; *CYP2B6*; MMT; Gene promoters

5.2 Introduction

Methadone is used in the treatment of opioid dependence, resulting in the decrease and often suspension of illicit opioid abuse (Shields *et al.* 2007). However, methadone has a long and unpredictable half life which can result in drug accumulation and delayed overdose (Sawe, 1986; Kreek *et al.* 1996; Foster *et al.* 2000; Manfredi *et al.* 2001). This can be complicated further by gene variations resulting in considerable inter-and intra-individual pharmacokinetic and pharmacodynamic variability (Kharasch *et al.* 2009).

Methadone action *in vivo* is largely mediated through *CYP2B6* metabolism and drug-receptor interactions at the μ opioid receptor (Chapter 4; Bunten *et al.* 2010). The primary metabolic route for methadone metabolism is N-demethylation and spontaneous decyclisation converting the drug into EDDP (Kobek *et al.* 2009). Earlier work revealed a significant association between the cytochrome P450 *CYP2B6**4, *9 and *6 alleles and high methadone concentrations in post-mortem blood, characteristic of the slow metaboliser phenotype (Chapter 4; Bunten *et al.* 2010). However, despite, an established genotype-phenotype relationship, the molecular basis of the *6 allele remains unclear with effects at the transcription, splicing, protein stability and substrate specificity levels (Hofmann *et al.* 2008). Clarification of the molecular role of *CYP2B6* could assist in explaining inter-individual variability in blood methadone concentrations and drug toxicity (Chapter 4; Bunten *et al.* 2010).

This has particular significance for the interpretation of post-mortem methadone concentrations which can be complex due to a significant overlap between therapeutic and lethal concentrations, for example, therapeutic plasma methadone concentrations range between 0.075 and 1.1 mg/L, toxic concentrations between 0.2 and 2.0 mg/L and lethal concentrations between 0.4 and 2.8 mg/L (Moffat *et al.* 2004;

Schulz & Schmoltdt, 2003). The interpretation of post-mortem results is further complicated by the fact that in a significant number of opioid-related deaths, several hours may elapse between the time the drug enters the body and the time of death, during which extensive metabolism may take place. The identification of gene variations responsible for inter-individual variability in blood methadone concentrations, such as CYP2B6*6 could aid toxicological interpretation identifying poor metabolisers at autopsy.

cis-Acting functional polymorphisms that affect transcription, mRNA processing, mRNA stability, and protein translation may also represent a cause of human phenotypic variability (Zhang *et al.* 2005). The CYP2B6 T750C promoter region single nucleotide polymorphism (SNP) could also be of importance in individual methadone susceptibility. T750C is one of the most frequently identified SNPs in the CYP2B6 promoter region (Zukunft *et al.* 2005), and has been reported to decrease CYP2B6 expression which would result in alterations to methadone metabolism. (Lang *et al.* 2001; Lamba *et al.* 2003).

The μ opioid receptor is a critical factor in methadone response that could influence the post-mortem concentration. The work presented in Chapter 4 identified a trend between higher methadone concentrations and the μ opioid receptor (*OPRM1*) A118G variation (Chapter 4; Bunten *et al.* 2010). This result was not statistically significant ($P = 0.39$) however, and could be a consequence of a limiting sample size. *In vitro* expression studies on A118G report significant increases in wild-type expression over 118 GA carriers (Zhang *et al.* 2005). Since A118G reduces receptor binding sites (Zhang *et al.* 2005) this might offer an explanation for increased post-mortem blood methadone concentrations and should be further explored with a larger sample size.

μ opioid receptor *OPRM1* and *CYP2B6* gene variations were examined in a post-mortem population where the deaths had been attributed to methadone to confirm the role of *CYP2B6**6 in methadone susceptibility. Whilst trying to clarify the role of the *OPRM1* A118G variation to methadone toxicity.

5.3 Materials and Methods

Case Selection

A retrospective review (2007-2010) of methadone-associated deaths from a geographically defined area of Scotland (Tayside, Fife and Central regions) was conducted.

Toxicological Analyses

The toxicological analysis for each subject was conducted at the Centre for Forensic and Legal Medicine, Dundee University. Following cross-clamping of the femoral vein, blood samples were collected by needle and syringe distally. Methadone was extracted from post-mortem blood specimens using liquid/liquid extraction followed by high pressure liquid chromatography with a diode array detector (HPLC – DAD). Post-mortem blood specimens were made alkaline using 0.2M carbonate buffer and extracted with 1-chlorobutane. A Waters Spherisorb 5 μ m OD/CN HPLC column (4.6 x 150mm) and a guard column were used with acetonitrile (25% acetonitrile in aqueous TEAP buffer) as the mobile phase.

DNA Extraction and Quantitation

Genomic DNA was isolated from leukocytes (sodium fluoride anticoagulated blood) by the DNeasy Blood and Tissue Kit (Qiagen, Crawley, UK) and quantified using the

Human Quantifiler® Kit (Applied Biosystems, Warrington, UK) in accordance with the manufacturer's instructions.

OPRM1 & CYP2B6 Genotyping

The procedure for *OPRM1* A118G, *CYP2B6**4, *9, and *6 genotyping was described previously (Chapter 4; Bunten *et al.* 2010). For the *CYP2B6* T750C promoter SNP samples were amplified by PCR to identify homozygous wild type and heterozygous controls using primer C2B6PrF (forward: 5' CAGGTTCAAGTGATTCTCTTG) and primer C2B6PrR (reverse: 5' CATGTTCAAAACTGAGAGGCT). PCRs were performed with a reaction volume of 50 µl, including 27.5 µl PCR grade water, 10 µl of 5x GoTaq™ buffer, 3.0 mM MgCl₂, 1 µl of 10 mM deoxynucleoside triphosphates (dNTPs) (final concentration of 0.25 mM), 1 µl Forward and Reverse primers, 10 ng/µl DNA and 0.5 µl GoTaq™ DNA polymerase. PCR reactions were performed with a Primus 96 advanced machine (Alpha Laboratories, UK). The cycling conditions were as follows: initial denaturation at 95°C for 5 minutes; subsequent denaturation at 95°C for 1 minute; annealing at 65°C for 30 seconds; primer extension at 72°C for 2 minutes, repeated for 30 cycles, followed by final extension at 72°C for 5 minutes. PCR products were visualised by electrophoresis with a 2 % Cyber Green-agarose gel on blue light. Samples were purified using the QIAquick PCR Purification Kit (Qiagen, UK) in accordance with the manufacturer's instructions. DNA sequencing was conducted by COGENICS (The Sequencing Company, Essex, United Kingdom Corporation). Samples were then genotyped for the T750C SNP using the validated TaqMan® SNP Genotyping assay (4362691)

Statistical Analysis

Data are presented as median, means \pm SE of the mean. The statistical significance of the differences between methadone mean concentrations and the *CYP2B6* T750C, G516T, A785G variants and the *OPRM1* A118G was determined using the two-tailed Independent T test. Linkage between gene variants was determined using Pearson's Chi-square test and Spearman's rank correlation. The effect of subject participation in methadone maintenance on post-mortem methadone concentration was explored using the Independent T-test. The association between participation in methadone maintenance and SNP presence was examined using Pearson's Chi-square test. A P value of ≤ 0.05 was considered to indicate statistical significance. All analyses were performed with SPSS Software (version 14.0).

5.4 Results

The 69 post-mortem cases where methadone had been implicated in the cause of death included 50 men and 19 women, the majority of whom were Caucasian (99.94%). The mean age of the case subjects was 33 ± 1.38 (17 – 60 range).

CYP2B6 alleles and post-mortem methadone blood concentrations

Of the 69 methadone related fatalities, 27 were genotyped as heterozygous carriers of allele * 9, a frequency of 39 % and 2 were genotyped as homozygous carriers, an allelic frequency of 2.9 %. This result is in accordance with the work presented in Chapter 4 (Bunten *et al.* 2010). Heterozygous carriers of allele * 4 were identified in 29 cases, a frequency of 42 %. Allele * 6 was identified in 29 cases, an allelic frequency of 42 %, an elevated frequency compared with other studies (Kircheiner *et al.* 2003; Jacob *et al.* 2004; Crettol *et al.* 2005). For the T750C promoter region SNP

30 individuals were heterozygous, a frequency of 43.5 % and 14 were genotyped as homozygous for the CC genotype (20.1 %). This is in accordance with other reports from Caucasian populations (Zukunft *et al.* 2005).

All of the CYP2B6 alleles tested (*4, *9 and * 6) were associated with higher mean post-mortem methadone blood concentrations ($P < 0.05$, Independent T-test), indicative of poor methadone metabolism (Table 64).

Two subjects were identified with the CYP2B6*6/*6 genotype, with post-mortem blood methadone concentrations of 1.38 mg/L, and 2.10 mg/L (mean 1.74 mg/L). CYP2B6*1/*4 was identified in two cases, a frequency of 2.9 %. By itself allele * 4 has been linked with fast metabolism (Lang *et al.* 2001) however our results did not show this trend, with a mean post-mortem concentration of 0.86 mg/L (Table 65). No CYP2B6*4/*4 genotypes were identified.

There was no significant difference in mean blood concentration for the T750C variation ($P = 0.302$), with a mean methadone blood concentration of 0.79 mg/L for heterozygous carriers, 0.69 mg/L for subjects homozygous for the CC genotype and 1.02 mg/L for homozygous TT subjects. Interestingly the mean post-mortem methadone concentration is lower in subjects with the T750C allele than wild type subjects.

OPRM1 A118G and post-mortem methadone blood concentrations

The A118G SNP demonstrated an allelic frequency of 13 %, higher than a previous study (Bunten *et al.* 2010) but within the range reported in other studies (Bergen *et al.* 1997; Lötsch *et al.* 2002). With an increased post-mortem sample size of 69 subjects a significant association was observed between A118G and post-mortem methadone blood concentrations ($P = 0.05$, Table 64). The median methadone concentration for

118 GA carriers was 0.58 mg/L and for 118 AA carriers 1.08 mg/L respectively. No homozygote for the G allele was identified in this study.

Table 64: CYP2B6*4,*9, and *6 alleles and *OPRM1* A118G post-mortem methadone blood concentrations.

	Frequency	Mean	Std. Deviation	Std. Error Mean	Median	P value
<i>CYP2B6</i>						
A785G						
(allele * 4)						
AA	38	0.69	0.638	0.104	0.52	
GA & GG	31	1.06	0.729	0.131	0.97	0.028*
G516T						
(allele * 9)						
GG	40	0.70	0.640	0.101	0.52	
TG & TT	29	1.07	0.730	0.136	0.97	0.027*
<i>OPRM1</i>						
A118G						
AA	60	0.79	0.651	0.084	0.58	
AG	9	1.28	0.895	0.298	1.08	0.050*

Significance at < 0.05 is denoted by *.

CYP2B6 and OPRM1 Correlations

A significant association was identified in this study between 118G allele and CYP2B6 * 9 allele, and 118G allele and CYP2B6 * 4 allele using Pearson's Chi

Square Test ($P = 0.004$, $P = 0.002$ respectively). Furthermore, T750C presence correlated with CYP2B6*4, *9, & *6 alleles ($P < 0.01$), this result is in accordance with other reports (Zukunft *et al.* 2005).

Methadone Maintenance

The association between post-mortem methadone concentration and subject participation in methadone maintenance was explored for 32 of the 69 subjects sampled in this study. A significant association was identified between higher post-mortem methadone concentrations and subject enrolment in methadone treatment programmes ($P = 0.001$, 0.54 mg/L mean concentration for subjects not in methadone treatment, 1.44 mg/L mean concentration for subjects in methadone treatment) using the Independent T-test. Furthermore, post-mortem methadone concentration significantly correlated with methadone maintenance daily dosage (Figure 85) using Pearson's two-tailed correlation coefficient. There was no association between subject participation in methadone maintenance and the *CYP2B6* and *OPRM1* SNPs (Table 65). Furthermore, there was no significant association between methadone treatment daily dosage and the *CYP2B6* and *OPRM1* SNPs (Table 65).

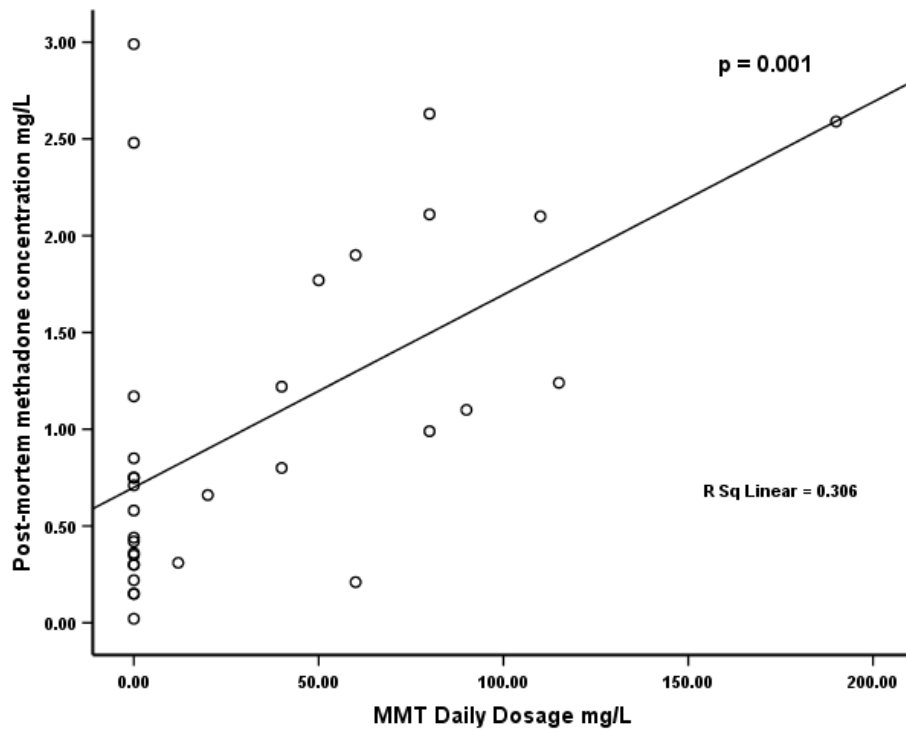


Figure 85: The association between post-mortem methadone concentration (mg/L) and methadone maintenance daily dosage (mg/L).

Table 65: The effect of *CYP2B6* T750C, G516T, A785G, *OPRM1* A118G, Gender and Age on subject participation in maintenance and daily methadone dosage.

Gene variants	R ² value	P value
Subject participation in methadone maintenance		
T750C	0.049	0.792
A785G	-0.122	0.507
G516T	-0.22	0.507
A118G	-0.030	0.870
Age	0.299	0.096
Gender	-0.181	0.320
Methadone Maintenance Daily Dosage		
T750C	-0.267	0.140
A785G	0.166	0.363
G516T	0.166	0.363
A118G	-0.108	0.557
Age	0.209	0.250
Gender	0.218	0.231

5.5 Discussion

Polymorphisms in metabolizing enzymes and transporters can be valuable biomarkers for variable pharmacokinetics, pharmacodynamics and adverse drug reactions. The human cytochrome P450 enzyme *CYP2B6* is highly polymorphic playing a key role in the biotransformation of drugs (Hofmann *et al.* 2007). Previous works have reported that heterozygous and homozygous carriers of the *CYP2B6**6 allele express up to 4-fold less protein with resulting changes in enzymatic activity (Desta *et al.* 2007). In this study the *CYP2B6**9 (G516T), *CYP2B6**4 (A785G), and *CYP2B6**6 (G516T & A785G) alleles all associated with statistically higher blood methadone concentrations (Table 64), this is in agreement with previous results indicating that *CYP2B6**6 (G516T, A785G) can be used to determine poor methadone metabolism (Chapter 4, Buntun *et al.* 2010). A study examining *CYP2B6**6 expression and function in human liver samples reported that the G516T SNP is the casual mutation leading to poor drug metabolism (Hofmann *et al.* 2008). Interestingly the study also reported that G516T is responsible for aberrant splicing leading to a major splice variant that lacks the region between exons 4 and 6 (Hofmann *et al.* 2008). This results in reduced levels of functional mRNA transcripts, protein and enzymatic activity (Hofmann *et al.* 2008). It was theorised that the *CYP2B6**6 allele might be a result of a pretranslational mechanism involving the T750C promoter variation, however, the study did not identify any such association (Hofmann *et al.* 2008).

In this study T750C was not associated with higher drug concentrations, with wild type carriers having higher blood methadone concentrations than heterozygous or wild type subjects. As T750C has been linked with decreased receptor expression (Lang *et al.* 2001; Lamba *et al.* 2003), higher methadone concentrations were expected due to a reduced ability to metabolise the drug. Additionally, T750C

associated with CYP2B6*6, which is in accordance with earlier studies where T750C is part of the CYP2B6*6B haplotype with the G516T and A785G variations (Lamba *et al.* 2003; Hesse *et al.* 2004; Zukunft *et al.* 2005). This assemblage of gene variants would result in reduced expression of a poorly functioning gene and could be expected to result in higher post-mortem methadone concentrations. However, there have also been contrasting reports documenting that the T750C SNP is not involved with reduced *CYP2B6* expression (Zukunft *et al.* 2005; Hofmann *et al.* 2008). T750C is also part of the CYP2B6*22 allele together with C1848A, G801T, and T82C which has been linked with high *CYP2B6* expression as a result of the T82C SNP (Faucette *et al.* 2000; Zukunft *et al.* 2005). A study examining human liver expression reported that the T82C variation significantly impacted *CYP2B6* mRNA expression ($P < 0.01$), with heterozygous carriers of T82C demonstrating 2.1 fold higher expression than subjects homozygous for the 82 TT genotype (Zukunft *et al.* 2005). Despite the significance of T82C for *CYP2B6* expression, there is considerable variability within the TT and TC groups indicating the involvement of additional unknown factors (Zukunft *et al.* 2005). The significance of CYP2B6*22 has not been explored in this study however examination of this allele would be interesting to determine the relevance of CYP2B6*22 for methadone susceptibility as it may result in an ultrarapid metaboliser phenotype (Zukunft *et al.* 2005). It is logical to suggest that the increased methadone concentrations identified for 750 TT subjects in this study may be linked with increased *CYP2B6* expression due to the CYP2B6*22 allele.

Opioid receptors belong to the family of seven trans-membrane protein coupled receptors and are involved in the modulation of numerous endogenous physiological and neurobiological systems (Binyaminy *et al.* 2008). μ receptors are located in brain and spinal regions, in addition to various circulating immune cells (Bidlack, 2000; Ross *et al.* 2005; Toskulkao *et al.* 2009). Methadone deaths are

primarily due to respiratory depression following the activation of the opioid system at the respiratory control centre within the brain resulting in reduced sensitivity to carbon dioxide (CO₂). A study on the post-mortem brain of heroin abusers reported exaggerated impairments to the opioid neuropeptide system in the presence of A118G carriers (Drakenberg *et al.* 2006). Such changes are likely to be associated with A118G effects on *OPRM1* expression and could impact respiratory function. A major effect of μ receptor activity in the brain is the decrease of neuronal membrane excitability, due to an increase in K⁺ conductance and hyperpolarization of the cell membrane (Chavkin, 1988; Mestek *et al.* 1995). Agonist binding at μ alters receptor conformation, facilitating coupling to heterotrimeric guanine nucleotide binding proteins (G proteins) inducing a variety of downstream effectors including the inhibition of adenylyl cyclase and intracellular cyclic AMP (cAMP) (Beyer *et al.* 2004; Krosiak *et al.* 2007). Chronic receptor activation results in a reduction of receptor responsiveness limiting the physiological response of the cell to external signals (Binyaminy *et al.* 2008). The exon 1 A118G variation has the highest overall frequency of any missense *OPRM1* variant reported and has been linked with a higher potency for activation of G protein-coupled potassium channels increasing receptor functionality (Bond *et al.* 1998). A previous study reported higher post-mortem methadone concentrations in the presence of the A118G variation (Bunten *et al.* 2010) however this result was not statistically significant (P = 0.391). In this study we examined an increased post-mortem sample size and revealed that the A118G variation significantly associated with higher blood methadone concentrations (Table 64, P = 0.05). As a clear functional role for A118G regulation of receptor expression has been documented (Zhang *et al.* 2005; Krosiak *et al.* 2007), it is theorised that the higher methadone concentrations observed are a result of A118G affecting receptor expression, resulting in a reduction of surface receptors (Chapter 4; Bunten *et al.*

2010). The attenuation of activated cell surface receptors could lead to increased methadone *in vivo*, with subsequent drug accumulation and a lack of sensitivity to the toxic effects of methadone (Chapter 4; Bunten *et al.* 2010). The A118G variation has also been linked with lower levels of forskolin-induced cAMP accumulation and differences in agonist-mediated cAMP signalling for methadone (Kroslak *et al.* 2007). A study using animal models reported that the adenylyl cyclase and cAMP pathways are involved in opioid analgesia, tolerance, and withdrawal (Kim *et al.* 2006). A118G induced disruptions to these signal transduction pathways could have subsequent effects on methadone response and susceptibility.

Methadone maintenance programmes have been shown to reduce the illicit use of opiates, and the risks of acquiring the human immunodeficiency virus (HIV) (Milroy & Forrest, 2000). Nevertheless, there continues to be concerns regarding the use of methadone (Lintzeris *et al.* 2007). The work in this study and the work described in Chapter 4 revealed that *CYP2B6* and *OPRM1* gene variations may contribute to individual susceptibility to methadone fatality (Chapter 4; Bunten *et al.* 2010). Information regarding subject participation in methadone maintenance was available for 32 subjects for this work. A total of 17 (53 %) of these post-mortem subjects were involved in methadone maintenance programmes with an average daily methadone prescription of 76.3 mg/L. Therefore, 47 % of the methadone toxicity deaths examined here were in people not in methadone treatment. This result is in accordance with other studies examining methadone toxicity and death (Sunjic & Zador, 1999; Heinemann *et al.* 2000; Bell *et al.* 2009). Fatal blood methadone concentrations have been reported to be almost two-fold higher in subjects involved in a methadone maintenance programme (Worm *et al.* 1993). A study on methadone maintenance treatment in Hamburg, Germany, reported higher post-mortem blood methadone concentrations (0.62 mg/L mean concentration) for subjects in treatment

compared with those not enrolled (0.43 mg/L mean concentration) in maintenance programmes (Heinemann *et al.* 2000). Furthermore, blood concentrations below the generally accepted fatal 0.4 mg/L concentration were identified in 48 % of subjects within methadone treatment and 68 % of subjects not in treatment, indicating that susceptibility to methadone overdose is higher in subjects not enrolled in methadone maintenance (Heinemann *et al.* 2000). In agreement with the work presented in Chapter 4, this study revealed statistically higher post-mortem methadone concentrations in subjects engaged in methadone maintenance at the time of death ($P < 0.01$). As expected, the post-mortem methadone concentrations were higher in subjects on high daily doses of methadone treatment (Figure 85). However, there was no significant association between methadone maintenance participation and the CYP2B6*6 allele and A118G. It is logical to assume that the association between high post-mortem methadone concentrations and enrolment in methadone maintenance is due to chronic methadone accumulation and the development of tolerance. A fatal dose for a methadone naïve/novice subject will be lower than an individual undergoing maintenance due to the acquisition of drug tolerance (Corkery *et al.* 2004). As there was no association between maintenance enrolment and SNP presence it can be postulated that tolerance as a result of chronic methadone treatment may result in higher post-mortem methadone concentrations. However, this does not alter the association identified between the CYP2B6*6 allele and A118G and post-mortem methadone concentration in this study.

Given the potential for such serious adverse events from methadone use, it is necessary to understand the molecular mechanisms responsible for methadone action *in vivo*. Earlier works documented the importance of pharmacogenomic research for certifying methadone mortality (Wong *et al.* 2003). The results described here will have important consequences for pharmacogenomic research. In addition to

identifying drug susceptible individuals (Chapter 4; Bunten *et al.* 2010), the CYP2B6*6 allele could also be used as a tool for the interpretation of forensic toxicological results. Forensic toxicology often contributes to the determination of cause and manner of death (Druid *et al.* 1999). Many fatal intoxications concern suicidal overdoses, however chronic administration of drugs such as methadone can complicate interpretation as it is difficult to differentiate between an acute overdose and chronic toxicity due to drug tolerance (Druid *et al.* 1999). *CYP2B6* genotyping could be used in cases where the toxicological results are unclear, confirming whether the cause of death was through overdose or as a result of poor methadone metabolism. Additionally the *OPRM1* A118G variation has also been demonstrated to correlate with higher post-mortem methadone concentrations indicating that this variation could also be of use for methadone pharmacogenomics.

Chapter 6

**Inter-individual variability in the prevalence of *OPRM1* and
CYP2B6 gene variations identify drug susceptible
populations.**

**This chapter has been drafted for publication and has been presented here in
paper format.**

6.1 ABSTRACT

Methadone is used worldwide for the treatment of heroin addiction; however fatal poisonings are increasingly reported. The prevalence of *CYP2B6* and μ -opioid receptor (*OPRM1*) gene variations were examined between a post-mortem population where the deaths were associated with methadone and a live non-drug using control population using Taqman™ SNP Genotyping assays. The *CYP2B6**6 allele was higher in the post-mortem population however the difference was not significant ($P = 0.92$). The *CYP2B6* T750C promoter variation was similar in frequency for both populations. Linkage between T750C, and *CYP2B6**6 was identified for both populations ($P < 0.01$). The prevalence of the *OPRM1* A118G variation was significantly higher in the control population ($P = 0.0046$) which might indicate a protective mechanism against opioid toxicity. Individual susceptibility to methadone may be determined by screening for *CYP2B6**6.

Keywords: Forensic Science, Pharmacogenomics, *OPRM1*, A118G, Methadone

6.2 Introduction

The application of pharmacogenomics for the interpretation of drug toxicity and individual drug susceptibility is steadily increasing and several studies indicate that the genotyping of single nucleotide polymorphisms (SNPs) may be a useful forensic tool (Wong *et al.* 2001; Janneto *et al.* 2002; Bunten *et al.* 2010). Most functionally important SNPs are located within genetic coding regions (exonic domains) and are ideal candidates to examine inter-individual drug responses (Giacomini *et al.* 2007). Gene variations in the Cytochrome P450 (CYP) enzymes can alter individual drug metaboliser status (Wong *et al.* 2003; Gerber *et al.* 2004, Eap *et al.* 2007; Bunten *et al.* 2010). Similarly linkage between receptor variations and drug response has been reported, with the μ opioid receptor gene (*OPRM1*) recognised as a key variable in individual sensitivity to opioids (Lötsch *et al.* 2002). A number of significant SNPs have also been identified within critical non-coding regions i.e. gene promoter regions (Mills *et al.* 2006).

Screening for SNPs involved in methadone action *in vivo* could identify individuals susceptible to methadone toxicity in addition to improving toxicological interpretation. *CYP2B6* is one of the cytochrome P450 enzymes responsible for methadone metabolism. The T750C variant is located in the proximal promoter region and has been linked with decreased gene expression. The influence of T750C on methadone susceptibility is currently unknown. The *CYP2B6**6/*6 genotype results from the combination of the G516T and A785G SNPs and has been associated with poor metabolism. *CYP2B6**6/*6 is present at a frequency of about 6% in Caucasian populations (Lang *et al.* 2001; Crettol *et al.* 2007; Eap *et al.* 2007). In living subjects the frequency of *CYP2B6**1/*6 has previously been reported at 24-26% (Kircheiner *et al.* 2003; Crettol *et al.* 2005) with *CYP2B6**1/*4 at 26% (Kircheiner *et al.* 2003).

However, the work conducted in Chapter 4 reported higher frequencies in post-mortem subjects whose deaths were attributed to methadone at 40 % and 37.5% respectively (Chapter 4, Bunten *et al.* 2010). This may be indicative of *CYP2B6* involvement in methadone toxicity. The work in Chapter 4 also documented a significant association between *CYP2B6* variants and increased post-mortem methadone concentrations (Chapter 4, Bunten *et al.* 2010).

OPRM1 is of special interest as it is the preferential binding target of methadone. The association between SNP frequencies in the *OPRM1* gene and drug response have been examined in Hispanic (Bond *et al.* 1998), African-American (Gerlernter *et al.* 1999), Caucasian (Klepstad *et al.* 2005), and Japanese populations (Ide *et al.* 2006). The A118G SNP has been reported at frequencies ranging between 2 and 48.5% across different populations (Bond *et al.* 1998; Gerlernter *et al.* 1999; Li *et al.* 2000; Ross *et al.* 2005).

The purpose of this study was to explore the joint effects of *OPRM1* and *CYP2B6* genes in predicting individual susceptibility to methadone. Using SNP genotyping the prevalence of the *OPRM1* A118G variation, the *CYP2B6* T750C promoter variation and *CYP2B6**4, *9 and *6 alleles were studied in 84 methadone associated fatalities comparing the gene frequencies against a non methadone using control population.

6.3 Materials and Methods

Case Subjects and Controls

A population of 84 subjects whose deaths were associated with methadone in the East of Scotland was selected. The control population consisted of 100 healthy non-

methadone using volunteers from Bournemouth University. This study was approved by the Bournemouth University Ethics Committee.

DNA Extraction and Quantitation

Genomic DNA for the post-mortem subjects was isolated from leukocytes (sodium fluoride anticoagulated blood) using the DNeasy Blood and Tissue Kit (Qiagen, Crawley, UK). For the control group buccal cells were collected using the Epicentre Catch-All Swab and extracted in 150µl of MasterAmp™ buccal extraction fluid (Epicentre Biotechnologies, Madison, USA). All DNA samples were quantified using the Human Quantifiler® Kit (Applied Biosystems, Warrington, USA) in accordance with the manufacturer's instructions.

Genotyping

The procedure for *OPRM1* A118G, *CYP2B6**4, *9, and *6 genotyping was described previously (Bunten *et al.* 2010). For the *CYP2B6* T750 promoter SNP samples were amplified by PCR to identify homozygous wild type and heterozygous controls using primer C2B6PrF (forward: 5' CAGGTTCAAGTGATTCTCTTG) and primer C2B6PrR (reverse: 5' CATGTTCAAACTGAGAGGCT). PCRs were performed with a reaction volume of 50 µl, including 27.5 µl PCR grade water, 10 µl of 5x GoTaq™ buffer, 3.0 mM MgCl₂, 1 µl of 10 mM deoxynucleoside triphosphates (dNTPs) (final concentration of 0.25 mM), 1 µl Forward and Reverse primers, 10 ng/ µl DNA and 0.5 µl GoTaq™ DNA polymerase. PCR reactions were performed with a Primus 96 advanced machine (Alpha Laboratories, Eastleigh, UK). The cycling conditions were as follows: initial denaturation at 95°C for 5 minutes; subsequent denaturation at 95°C for 1 minute; annealing at 65°C for 30 seconds; primer extension at 72°C for 2 minutes, repeated for 30 cycles, followed by final extension at 72°C for 5 minutes.

PCR products were visualised by electrophoresis with a 2 % Cyber Green-agarose gel on blue light. Samples were purified using the QIAquick PCR Purification Kit (Qiagen, Crawley, UK) in accordance with the manufacturer's instructions. DNA sequencing was conducted by COGENICS (COGENICS, Essex, UK). Samples were then genotyped for the T750C SNP using the validated TaqMan® SNP Genotyping assay (Applied Biosystems, Warrington, UK, product no. 4362691)

Statistical Analysis

Data are presented as means \pm SE of the mean. A Binary Logistic Regression model was used to examine the effects of *OPRM1* A118G, *CYP2B6**4, *9, *6, age, gender and race variables between the control and post-mortem population (95% confidence intervals). T-Test and Fisher's exact test were used to examine the difference between genotype frequencies for the control and post-mortem populations. Binary correlations were used to examine the association between the *CYP2B6* and *OPRM1* SNPs. A *P* value of ≤ 0.05 was considered to indicate statistical significance. All analyses were performed with SPSS Software (version 14.0).

6.4 Results

The 84 post-mortem cases where methadone had been implicated in the cause of death included 62 men and 22 women, the majority of whom were Caucasian (98 %). The mean age of the case subjects was 33.2 ± 1.12 (17 – 60 range). The 100 control subjects included 45 men and 55 women, the majority of whom were Caucasian (97%). The mean age of the control subjects was 24 ± 0.72 (18-55 range).

CYP2B6 G516T, A785G and T750C frequency data

Of the 84 post-mortem samples screened, 37 were genotyped as heterozygous carriers

of G516T (allele * 9), a frequency of 44 % and 2 were genotyped as homozygous carriers, an allelic frequency of 2.4 %. For the control group 34 % were genotyped as being heterozygous for allele * 9 (a difference of 10 %) and 3 % were homozygous for the variant allele (Figures 86 and 87). This difference was not statistically significant with a P value of 0.92 (Fishers exact test). Heterozygous carriers of A785G (allele * 4) for the post-mortem group were identified in 40 cases, a frequency of 47.6 % and 2.4 % were homozygous for the variant allele, which is noticeably higher than other reports from Caucasian populations (Kircheiner *et al.* 2003; Jacob *et al.* 2004; Crettol *et al.* 2005; Crettol *et al.* 2007). For the control group 38% of subjects were heterozygous for A785G. The difference between the post-mortem and control frequencies was 9.6 %, this result was not statistically significant (P = 0.90). For the methadone-attributed deaths allele * 6 was identified in 39 subjects, an allelic frequency of 46.4 %, which was higher than the control group where allele *6 was identified in 36% of subjects (P = 0.92).

The T750C promoter region SNP has been linked with alterations in gene expression (Lang *et al.* 2001). In the post-mortem population 37 subjects were heterozygous for T750C, a frequency of 44 %, a similar frequency to that identified in the control population (49%). 16 post-mortem subjects were homozygous for the CC genotype (19 %) again a similar frequency to the control population (17%) (Figure 87).

Linkage between the T750C, G516T and A785G gene variants was identified in both populations (Table 66). In the post-mortem population the T750C, G516T and A785G variants were identified together in 17 cases (20 %) and in the control population the SNPs were found in 17 % of cases. Interestingly wherever the variant homozygote for T750C was identified the G516T variant was not present. For the post-mortem

population the variant T750C homozygote was found in 16 subjects and for the control population in 17 subjects. Only one of the 9 post-mortem subjects also had the A785G variant and for the control group only 3 subjects also had the A785G variant.

Table 66: Genotype prevalence between the healthy control population and the post-mortem population whose deaths have been associated with methadone.

Gene variants	R ² value	P value
Post-mortem population		
T750C & G516T	-0.442**	0.001
T750C & A785G	-0.389**	0.001
T750C & A118G	-0.123	0.265
A118G & G516T	0.485**	0.001
A118G & A785G	0.495**	0.001
A785G & G516T	0.931**	0.001
Control population		
T750C & G516T	-0.365**	0.001
T750C & A785G	-0.274**	0.006
T750C & A118G	0.072	0.479
A118G & G516T	0.058	0.572
A118G & A785G	0.072	0.479
A785G & G516T	0.903**	0.001

** Correlation is significant at the < 0.01 level (two-tailed).

Allele frequencies for *OPRM1* and *CYP2B6* heterozygous subjects

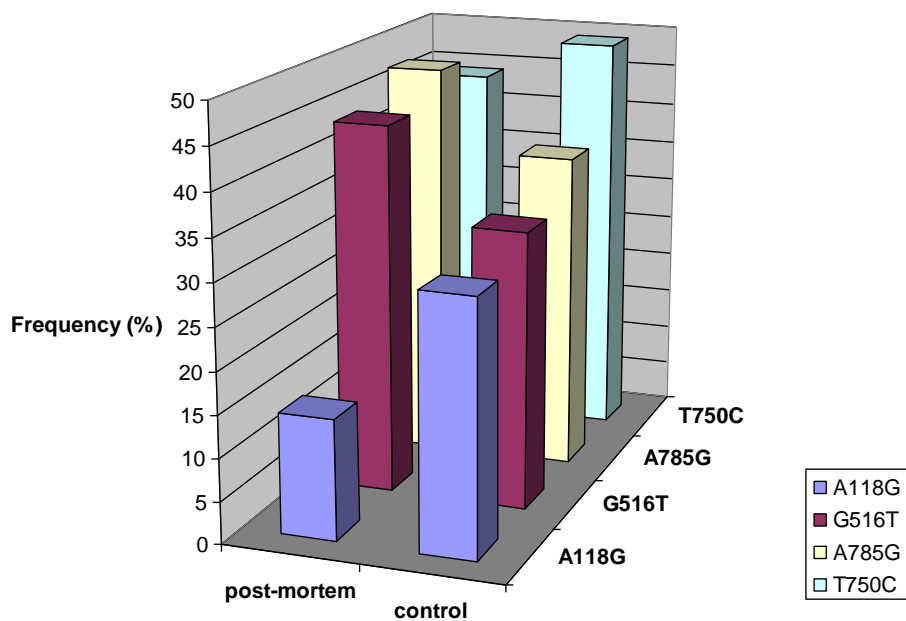


Figure 86: Heterozygous frequencies for *OPRM1* A118G & *CYP2B6* G516T, A785G & T750C genotypes.

Allele frequencies for *OPRM1* and *CYP2B6* homozygous wild type subjects

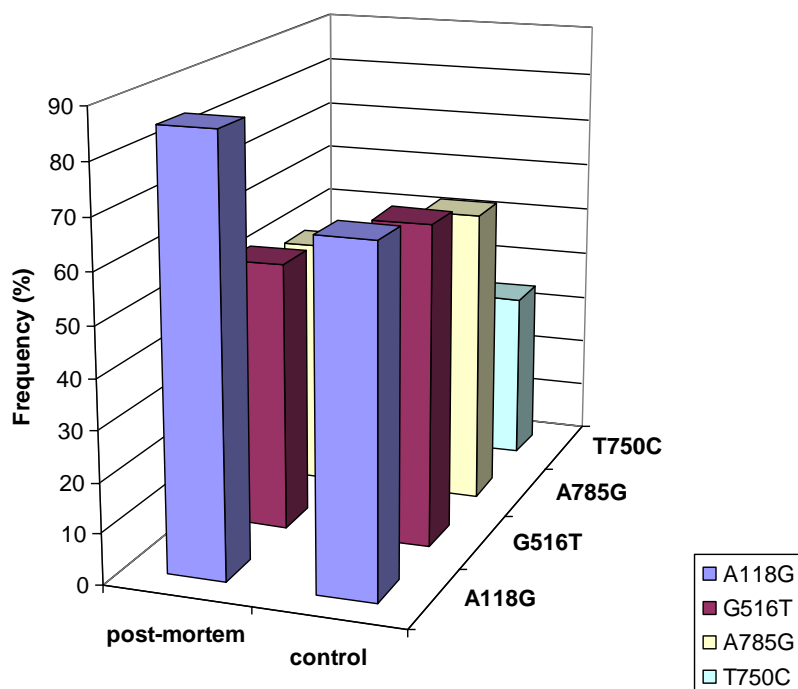


Figure 87: Homozygous variant frequencies for *OPRM1* A118G & *CYP2B6* G516T, A785G & T750C genotypes.

OPRM1 A118G frequency data

In the post-mortem group the A118G SNP was found in 12 subjects a frequency of 14.3 % (Figure 86) which is a similar result to previous studies (Bergen *et al.* 1997; Lotsch *et al.* 2002; Bunten *et al.* 2010). No homozygote for the G allele was identified. In the control group 30 subjects had the AG genotype and 2 subjects were homozygous for the G allele. The difference in frequency between the groups (15.7 %) was statistically significant with a P value of 0.0046.

No linkage was found between A118G and T750C, G516T and A785G in the control population. Interestingly linkage was identified between A118G and G516T and A785G in the post-mortem population (Table 66).

Age, gender and race effects

The logistic regression model demonstrated the importance of gender and age for the SNP associations reported in this study.

Gender correlated significantly with T750C in the post-mortem population ($-0.301 R^2$, P value = 0.005). This was not repeated in the control population ($0.039 R^2$, P value = 0.699). No SNP correlation with age were observed in the post-mortem population, however both G516T and A785G were associated with age in the control population ($0.256 R^2$, P value = 0.010; $0.293 R^2$, P value = 0.003 respectively).

Age and gender were also significantly correlated with population ($0.395 R^2$, P value = 0.001; $-0.375 R^2$, P value = 0.001 respectively).

6.5 Discussion

The importance of *CYP2B6* and *OPRM1* variations for individual susceptibility to methadone was reported in Chapters 4 and 5. Identification of methadone risk factors will improve the toxicological interpretation of methadone-related deaths at autopsy whilst assisting in the prevention of methadone toxicity particularly during the drug induction phase.

The present study examined the prevalence of *CYP2B6* and *OPRM1* SNPs in a post-mortem population where the deaths had been associated with methadone compared with a healthy control population of non-methadone using living subjects. The work presented in Chapters 4 and 5 noted higher incidences of the *CYP2B6* G516T and A785G variations in post-mortem subjects (Bunten *et al.* 2010) when compared with previous studies sampling live subjects (Crettol *et al.* 2007; Crettol *et al.* 2005; Kircheiner *et al.* 2003). Similarly the results from this study report higher frequencies of G516T and A785G in the post-mortem population than the control group (Figure 86). However, this difference was not statistically significant ($P = 0.92$, $P = 0.90$, respectively) and may be indicative of a trend that has been limited by sample size. A larger number of post-mortem subjects would elucidate the association between G516T and A785G prevalence and methadone susceptibility.

The T750C variant had a similar distribution across both populations sampled suggesting that the presence of this variant is not a suitable risk factor for methadone susceptibility. However, when examining linkage between T750C and G516T and T750C and A785G a significant association was discovered (Table 66). T750C has been reported to decrease *CYP2B6* expression (Lang *et al.* 2001). The work discussed in Chapter 4 revealed the importance of the G516T and A785G variants for methadone susceptibility with the *CYP2B6**6 allele correlating with poor methadone

metabolism (Crettol *et al.* 2007; Eap *et al.* 2007; Bunten *et al.* 2010). Subjects with all three *CYP2B6* variants would therefore experience reduced expression of an already poorly functioning gene. The resulting effect on metabolism would likely involve methadone accumulation and toxicity. The association between T750C, G516T and A785G was significant for both the post-mortem population and the control population suggesting the possibility of a haplotype between these three *CYP2B6* SNPs.

Identification of genetic mutations that alter the functional activity of *OPRM1* may also explain inter-individual responses to methadone (Befort *et al.* 2001). A118G is located in the N-terminal region of the receptor resulting in the loss of a putative N-glycosylation site which could result in alterations to *OPRM1* expression (Zhang *et al.* 2005). The frequency of the A118G SNP was significantly higher in the control group, with a 15.7 % difference between populations for heterozygous subjects (P = 0.0046). Several studies have reported that A118G may confer protection from opioid toxicity (Bond *et al.* 1998; Town *et al.* 1999; Lötsch *et al.* 2002). A118G has been associated with reductions in cell surface receptors limiting the availability of drug binding sites and as a result drug response (Zhang *et al.* 2005). However, it was reported in Chapter 4 that the A118G SNP may be associated with the lethal interaction between methadone and benzodiazepines, although this may be a consequence of benzodiazepine induced μ -receptor up-regulation (Bunten *et al.* 2010). A118G effects on gene expression have been well documented (Zhang *et al.* 2005; Mague *et al.* 2009). A Study on mRNA expression in post-mortem brain tissue reported a ten-fold reduction in protein levels for subjects with the G allele (Zhang *et al.* 2005). Furthermore, lower surface receptor expression and decreased forskolin-induced receptor activation has been identified in cell systems expressing the G allele (Kroslak *et al.* 2007). It seems logical therefore that receptor function will be reduced in

subjects with the G allele. This may confer protection from opioid toxicity at therapeutic levels. However these subjects will have a reduced sensitivity of the μ -receptor which could lead to higher methadone concentrations *in vivo* before toxic effects appear. As methadone has a long mean elimination half life of approximately 55 hours (Moffat *et al.* 2004) this could be especially pronounced in drug abusing subjects, limiting any possible protective function rendered by the G allele.

No linkage between the *OPRM1* A118G genotype and *CYP2B6* T750C, G516T and A785G genotypes was observed for the control population in this study (Table 66). However linkage was identified between A118G and G516T and A118G and A785G in the post-mortem population, this result is in agreement with Chapters 4 and 5 which documented a significant association between A118G and G516T and A118G and A785G in post-mortem subjects. In this study G516T, A785G, and A118G were found together in 8 of the post-mortem cases (66%) and 11% of the control population. An association between A118G, G516T and A785G would have significant impacts on methadone response. As discussed in Chapter 4 the *CYP2B6**6 allele associates with increased susceptibility to methadone fatality and A118G has been linked with increased heroin addiction (Bart *et al.* 2004). Therefore this combination of gene variants could lead to subjects with increased tendency to drug addiction and a reduced ability to metabolise methadone.

The logistic regression model detected statistically significant age and gender interactions. Furthermore, gender significantly correlated with *CYP2B6* T750C in the post-mortem population ($P < 0.01$). As the frequency of this SNP remained constant across both the post-mortem and control population it is proposed that T750C has an unknown influence on methadone susceptibility that requires further investigation. In the control population *CYP2B6* G516T and A785G significantly correlated with age.

However, as the control group was made up of a student population this may have influenced this result.

Both age and sex influences on the opioid system have previously been described (Gabilondo *et al.* 1995; Zubieta *et al.* 1999). Increased μ -opioid receptor densities have previously been found to correlate with age, with older subjects having significantly more receptors (Gabilondo *et al.* 1995). Gender influences could be linked with hormonal factors which can influence drug absorption, disposition, metabolism and pharmacodynamics (Lukas & Wetherington, 2005). This could contribute to differences in both drug action and response between males and females. It has been well documented that estrogen is involved in the enhancement of psycho-stimulants in females (Becker, 1990; Peris *et al.* 1991; Justice & de Wit, 1999, 2000). Conversely, it has also been reported that estrogen may confer protection against opioid toxicity as inter-individual variation in morphine potency is higher in males (Zubieta *et al.* 1999). A118G sex-specific associations (Munafò *et al.* 2006) have been reported previously however the functional significance of this is unclear (Mague *et al.* 2009).

Alternatively gender trends in drug abuse could be an influential factor in the significance reported in this study. It has been well documented that drug abuse and mortalities from drug overdose occur more frequently in males than females (Roth *et al.* 2004; Becker & Hu, 2008). With reports of men being between two and three times more likely to have a drug abuse/dependence disorder (Becker & Hu, 2008). Furthermore, studies using animal models indicate that sex differences in drug dependence may be a result of sexually dimorphic development of the brain (Peris *et al.* 1991). Socio-cultural and economic parameters can also not be excluded as years of education, employment status, medical health status and incidence of physical and sexual abuse are all underlying factors contributing to the development of drug abuse

and dependence (Lex, 1991; Brady & Randall, 1999; Lukas & Wetherington, 2005). The post-mortem population examined in this study only reported 9 females (16%), which could explain the significance identified in this study for gender.

In summary the CYP2B6*6 allele may be linked with increased susceptibility to methadone particularly when in combination with the *CYP2B6* T750C promoter variation. The association between the prevalence of T750C, G516T and A785G remained constant across both the post-mortem and control population. The role of the *OPRM1* A118G variation for methadone susceptibility remains unclear. The higher prevalence of A118G in the control population is in support of the theory that A118G is protective against opioid toxicity (Bond *et al.* 1998; Town *et al.* 1999; Lötsch *et al.* 2002). However, whilst, this protective function may work effectively with opioids such as morphine with a relatively short elimination half life (Moffat *et al.* 2004), for methadone, which has a significantly longer elimination half life, this could result in high concentrations accumulating *in vivo*, leading to methadone toxicity and in extreme cases death. Furthermore, no linkage was identified in this study between A118G and the *CYP2B6* G516T and A785G variations. It is suggested that a larger post-mortem sample size is required to effectively determine the role of A118G for methadone response. Genotyping CYP2B6*6 homozygotes and heterozygotes may therefore, assist in reducing adverse reactions to methadone during the drug induction phase whilst serving as a useful tool for certifying methadone toxicity at autopsy.

Chapter 7

The T750C single nucleotide polymorphism may be associated with *CYP2B6* gene expression.

This chapter has been drafted for publication and has been presented here in paper format.

7.1 ABSTRACT

There is significant inter-individual variability in hepatic *CYP2B6* expression and this has been associated with gene variations within the promoter region. The results from Chapters 5 and 6 revealed a significant association between the *CYP2B6**6 allele and the *CYP2B6* T750C promoter region polymorphism. However, the role of T750C for methadone action *in vivo* is unclear. In order to explore the effects of T750C on inter-individual susceptibility to methadone, subcloning of the proximal *CYP2B6* promoter region into an EGFP reporter system was employed. Using the TOPO® TA Expression kit and OneShot® chemically competent *E. coli* cells three clones for the 750 TT, 750 TC and 750 CC genotypes were created, to assess the promoter activity of *CYP2B6*, as a result of the T750C polymorphism.

Keywords: *CYP2B6*, T750C, Cloning, Expression, Methadone.

7.2 Introduction

CYP2B6 has long been thought to play a minor role in drug metabolism (Pascussi *et al.* 2003; Lemaire *et al.* 2004), however its role in methadone metabolism is still under investigation. Significant inter-individual differences in gene expression patterns are common and result from either environmental factors or *cis*- or *trans*-mediated genetic effects (Johnson *et al.* 2005). *CYP2B6* activity has been documented to vary more than 100-fold among different individuals (Ekins *et al.* 1998). *In vitro* studies have documented inter-individual variability in hepatic *CYP2B6* expression at the mRNA, protein and catalytic level, with male subjects demonstrating noticeably lower levels than females (Code *et al.* 1997; Ekins *et al.* 1998; Lang *et al.* 2001; Lamba *et al.* 2003). Understanding the molecular pathways leading to *CYP2B6* induction and regulation will lead to better models for the screening and prediction of drug interactions (Pascussi *et al.* 2003).

Many *CYP2B6* alleles have been reported, however there is an inherent bias towards sequencing and genotyping of coding regions (Johnson *et al.* 2005). A number of significant SNPs can also be found within critical non-coding regions i.e. gene promoter regions (Mills *et al.* 2006) and these include C1848A, G801T, T750C, and T82C (Zukunft *et al.* 2005). The T750C SNP (*CYP2B6**1G) located within the proximal promoter region correlated with lower levels of gene expression (Lang *et al.* 2004) and could therefore have cascade effects on both drug pharmacokinetics and pharmacodynamics. T750C forms part of the *CYP2B6**6B allele together with G516T and A785G. The work reported in Chapters 4 and 5 demonstrated the importance of G516T and A785G for methadone metabolism and individual susceptibility to methadone mortality (Bunten *et al.* 2010). Since, T750C has been linked with lower *CYP2B6* expression (Lang *et al.* 2004), it is logical to assume that the combination of

T750C together with the CYP2B6*6 allele could result in reduced expression of a gene associated with methadone accumulation. Interestingly, the work described in Chapter 5 showed that T750C was not associated with significantly higher post-mortem methadone concentrations despite correlating with the CYP2B6*6 allele. Furthermore, 750 TT subjects had higher post-mortem methadone concentrations (0.79 mg/L) than 750 TC and 750 CC subjects (0.69 mg/L, Chapter 5). It was postulated that this may also be due to T750C involvement in the CYP2B6*22 allele, which has been linked with higher *CYP2B6* expression as a result of the T82C polymorphism (Zukunft *et al.* 2005; Li *et al.* 2010).

Currently, the influence of T750C on *CYP2B6* expression and its subsequent association with methadone toxicity remains unclear. Linkage between SNPs located within the *CYP2B6* promoter region and exons such as the G516T SNP (Hoffman *et al.* 2008), requires further investigation, specifically with respect to their potential impact on gene transcription. A stable reporter construct was developed to study the effect of the *CYP2B6* T750C promoter variation on gene expression. To achieve this OneShot®TOP10 Chemically Competent *E. coli* cells were transfected with the entire *CYP2B6* proximal promoter region plus the *EGFP* reporter gene.

7.3 Materials and Method

CYP2B6 Cloning Strategy

A strategy was designed to clone the *CYP2B6* promoter region containing the 750 TT, 750 TC, and 750 CC genotypes into an Enhanced Green Fluorescence Protein (EGFP) reporter construct (Figure 4). A second strategy was then created to clone the *CYP2B6* promoter region into the pcDNA3.1/CT-GFP-TOPO® vector (Figure 5).

EGFP transformation into hSVCT2 plasmid

The *EGFP* gene was excised from pyEGFP (invitrogen) as a 0.7kb *XbaI/HindIII* fragment and recloned into *HindIII/XbaI* cut hSVCT2 vector (Liang *et al.* 2001).

Transformation was carried out using plasmid cDNA prepared by purification on Qiaquick™ spin columns (Qiagen, Crawley, UK). PyEGFP expressing plasmid was introduced into *E. coli* JM109 according to the manufacturer's instructions.

Transformants were verified by *NdeI* enzyme digestions of extracted plasmid DNA in gel electrophoresis.

CYP2B6 promoter region amplification

The *CYP2B6* promoter region for the 750 TT, 750 TC and 750 CC genotypes was amplified using primer C2B6F1 *BglII* (forward: 5' ata**AGATC**TTTCTGGTTTTACGGCTCAG) and primer C2B6R1 *HindIII* (reverse: 5' att**AAGCTT**CATCATCCAGGAGCATTAGCTT), which introduced *BglII* and *HindIII* restriction sites respectively. Promoter region amplifications were verified by agarose gel electrophoresis and the Sybergreen stained DNA fragments were visualised under blue light.

Cloning the CYP2B6 promoter variants into pcDNA3.1/CT-GFP-TOPO®

The *CYP2B6* promoter variants were extracted and purified using the Qiagen Gel Extraction Kit™ (Qiagen, UK) from the Agarose gel (1.6 %) after electrophoresis, and cloned into the pcDNA3.1/CT-GFP-TOPO® vector. The recombinant p2B6-GFP-HB DNA samples were introduced into OneShot® TOP10 Chemically Competent *E. coli* according to the manufacturer's protocol. Transformants bearing *CYP2B6* promoter variants in the correct orientation were verified by *BglII/HindIII* and *BglII* enzyme digestions followed by DNA electrophoresis in agarose gel. The genotypes of the 750 TT, 750TC, and 750 CC clones were confirmed by DNA sequencing (sense strand).

7.4 Results

Restriction Site Cloning Strategy

Subcloning of EGFP into hSVCT2 plasmid

In total 43 transformants were obtained after the ligation of the EGFP gene into the hSVCT2 plasmid. But there have been no correct clones obtained. The *NdeI* enzyme digestions revealed that the 43 clones were all empty vectors. It was anticipated that the cheaper/conventional strategy would be less efficient. Under the pressure in obtaining the clones for further studies on the promoter activity a more efficient but expensive strategy (Figure 5) was formulated using the TOPO® TA Expression Kit.

CYP2B6 promoter region amplification

The promoter regions for the *CYP2B6* 750 TT, 750 TC and 750 CC genotypes were successfully amplified using the C2B6F1 *BglI* and C2B6R1 *HindIII* primers (*Section 3.4 CYP2B6 Cloning, Figure 62*).

Subcloning CYP2B6 promoter variants into pcDNA3.1/CT-GFP-TOPO®

p2B6-GFP-HB transformation into the OneShot® *E. coli* cells was successfully verified through the *BglIII/HindIII* restriction digest. In total 40 transformants for p2B6-GFP-HB-750 TT were obtained, of these ten were analysed further with one correct *CYP2B6* transformant verified (Figure 88). For p2B6-GFP-HB-750 TC 50 transformations were obtained of the ten transformants analysed two were *CYP2B6* clones (Figure 88), however only one had the correct orientation (Figure 88). For p2B6-GFP-HB-750 CC five transformations were obtained, of these three were *CYP2B6* clones, however, all three clones were in the wrong orientation (Figure 88).

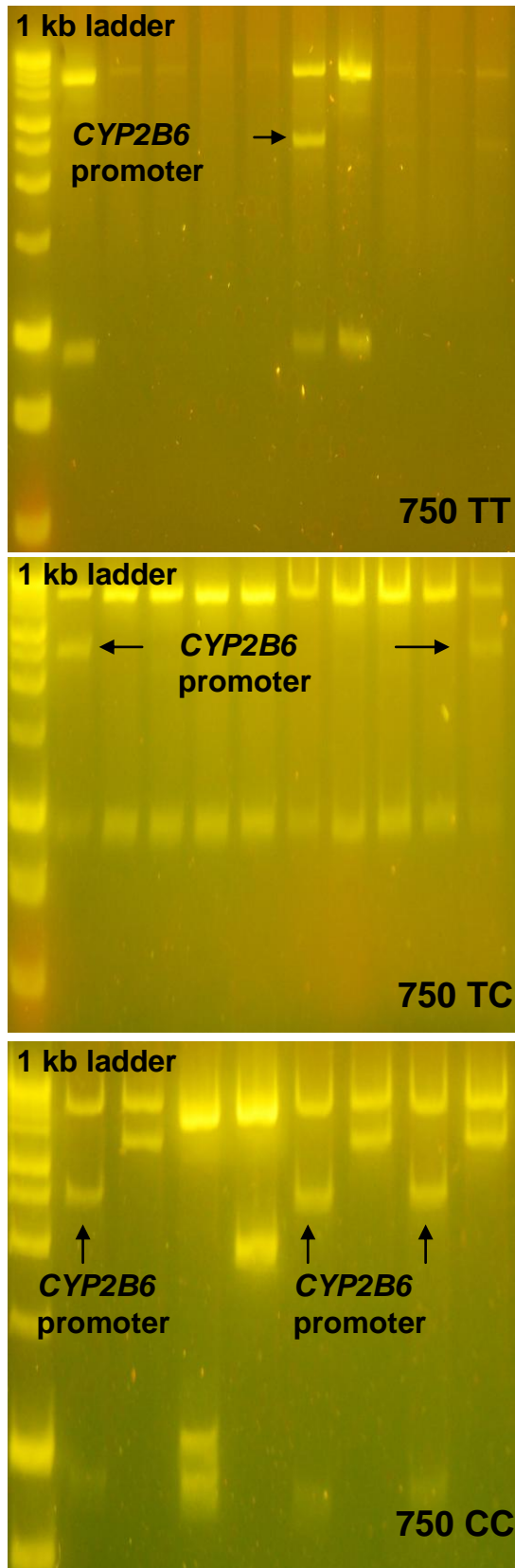


Figure 88: Total number of *CYP2B6* transformants obtained for T750C variants.

Agarose gel (2 %) and run at 70 volts. Arrows indicate *CYP2B6* promoter transformants.

7.5 Discussion

The molecular mechanisms responsible for methadone action *in vivo* are unclear. The hepatic expression of *CYP2B6* is highly variable and could be affected by a variety of factors including drug exposure, age, gender, diet, hormone production and genetics (Lamba *et al.* 2003; Lang *et al.* 2004; Lukas & Wetherington, 2005; Eap *et al.* 2008; Li *et al.* 2010). There is growing evidence that polymorphisms within gene promoter regions significantly influence gene expression by changing the level of RNA transcription (Day & Tuite, 1998; Rockman & Wray, 2002, Johnson *et al.* 2005). T750C is located in the putative HNF1-binding site and has been reported to be associated with alterations to *CYP2B6* protein levels (Lamba *et al.* 2003; Lang *et al.* 2004). However, the statistical significance of this association is unclear. A study examining variants within the *CYP2B6* promoter region and hepatic *CYP2B6* expression reported modest T750C effects, with 750 TC and 750 CC subjects having 1.42 and 1.81 fold less protein than 750 TT subjects (Lamba *et al.* 2003). Another study reported significant reductions in *CYP2B6* expression as a result of the T750C polymorphism (Lang *et al.* 2004).

The work described in Chapter 5 revealed a significant correlation between T750C and the *CYP2B6**6 allele (G516T & A785G) which could affect individual susceptibility to methadone. However there was no association between high post-mortem methadone concentrations and T750C, which was an unexpected result. Currently, the role of T750C for hepatic *CYP2B6* expression requires clarification to determine whether the polymorphism could be involved in individual susceptibility to methadone. It is postulated that p2B6-GFP-HB-750 TT and p2B6-GFP-HB-750 TC introduction into mammalian Chinese Hamster Ovary (CHO) cells may identify T750C effects on gene expression following methadone exposure in a controlled

system. The GFP protein is stable, species independent and can be observed non-invasively in living cells, therefore, monitoring GFP fluorescence is a suitable method for the reliable estimation of GFP expression levels (Nocarova & Fisher, 2009) and *CYP2B6* promoter activity for the T750C polymorphism.

The primary cloning strategy designed for the study (Chapter 2, Figure 4) involved the insertion of the EGFP gene into the hSVCT2 vector, to act as a marker of *CYP2B6* promoter activity, and to explore the effects of the T750C polymorphism on gene expression. However, the subcloning of EGFP into hSVCT2 was unsuccessful and no positive clone was identified as the EGFP-hSVCT2 clone. Ligation reaction was successful as tested by conducting a *Lamda/HindIII* control and was therefore not the factor responsible for cloning difficulties. However, the method used to prepare the hSVCT2 vector for ligation involved a *HindIII/XbaI* restriction digest to remove the hSVCT2 gene fragment followed by a further digest with *BamHI* to prevent recircularization of the original expression vector. It was then postulated that either the hSVCT2 gene was re-ligated back into the vector or the restriction double digest with *HindIII/XbaI* was not efficient enough such that only one site was digested leading to original vector self ligation back. An alternative *CYP2B6* cloning strategy was then designed using the CT-GFP TOPO® TA expression kit. This was chosen since TOPO® cloning involves a rapid and simple strategy allowing the direct fusion of the polymerase amplified *CYP2B6* promoter variants to a GFP reporter system. The amplification of the entire proximal *CYP2B6* promoter regions by C2B6F1 *BglI* and C2B6R1 *HindIII* was successful (Figure 62). The *CYP2B6* promoter variants were ligated into the pcDNA3.1/CT-GFP-TOPO vector taking advantage of the intensive Topoisomerases within the kit. The transformations of p2B6-GFP-HB-750 TT, and p2B6-GFP-HB-750 TC into the competent *E. coli* cells were successful, and two *CYP2B6* promoter variant constructs have been selected to explore T750C effects on

gene expression of GFP in the further studies on their association with methadone metabolism susceptibility.

The 84 post-mortem samples genotyped for the T750C polymorphism in Chapter 6 revealed a significant association between T750C and gender ($P < 0.01$). As discussed in Chapter 6, gender influences have been linked with hormonal factors influencing drug absorption, disposition, metabolism and pharmacodynamics (Lukas & Wetherington, 2005) and this requires further investigation. Lamba *et al.* (2003) reported significant differences in *CYP2B6* expression in liver between male and female subjects, with *CYP2B6* activity below quantifiable limits in 7.1 % of females and in 20 % of males. In the present study the male gender significantly correlated with T750C presence, with only 6 females subjects heterozygous for the T750C polymorphism and 2 homozygous for the C allele. As higher reductions in *CYP2B6* activity had been reported in males (Lamba *et al.* 2003) and T750C has been linked with reduced *CYP2B6* expression, it is postulated that the association between gender and T750C reported here is due to T750C alterations to *CYP2B6* activity. Further investigation is required to establish whether there are gender differences in *CYP2B6* expression as a result of T750C. Therefore, functionality trials using p2B6-GFP-HB-750 TT, p2B6-GFP-HB-750 TC, and p2B6-GFP-HB-750 CC clones following methadone exposure may determine the influence of T750C on *CYP2B6* expression and therefore the role of T750C for methadone susceptibility.

However, identifying the genetic alleles that are accounted for inter-individual differences in drug response is complex. The genetic components of complex inter-individual variations may require resolution of multiple gene variations which collectively yield recognizable phenotypes such as drug susceptibility (Li *et al.* 2010). For *CYP2B6* the studies described in Chapter 4 and 5 revealed that the presence of functional variations in exons 4 and 5 known to alter drug metabolism may interact

with T750C. Therefore, the association between methadone metabolism susceptibility and *CYP2B6* promoter variants will be explored further using p2B6-GFP-HB-750 TT and p2B6-GFP-HB-750 TC. However, it must be noted that inter-individual variability in *CYP2B6* expression may also be attributed to chemical-mediated induction through the activation of constitutive androstane receptor and/or the pregnane X receptor (Li *et al.* 2010). As *CYP2B6* transcription is correlated with constitutive androstane receptor (CAR) expression (Li *et al.* 2010), it is possible that polymorphisms in the *CAR* gene may also be responsible for altering the *CYP2B6* expression. Studies conducted in recent years have provided evidence that part of the human *CYP2B6* variability is caused by its drug-inducible regulation via proximal and distal response elements termed Phenobarbital-responsive enhancer module at -1.7kb (Sueyoshi *et al.* 1999; Goodwin *et al.* 2001; Wang *et al.* 2003) and xenobiotic-responsive enhancer module at -8.5 kb (Lamba *et al.* 2003; Wang *et al.* 2003B). Furthermore, it has been revealed that the relative levels of *CAR* mRNA are higher in female subjects than that in male subjects (Wei *et al.* 2000; Wang *et al.* 2003; Fery *et al.* 2010). Since, *CAR* influences *CYP2B6* expression, it seems likely that the association between T750C and gender reported in this study may also be due to an interaction between *CYP2B6* and *CAR*. The human pregnane X receptor induces *CYP2B6* transcription (Goodwin *et al.* 2001) forming a heterodimer with the retinoid X (RXR) receptor Lemaire *et al.* 2004). As the hPXR-RXR complex is thought to act as a drug-responsive transcription factor to regulate *CYP2B6* activity (Geick *et al.* 2001) it is also possible that this interaction is influential in the association between T750C and gender reported in this study.

In conclusion the role of the *CYP2B6* T750C polymorphism for methadone susceptibility is unclear and requiring further investigation. Reductions in hepatic *CYP2B6* activity as a consequence of T750C have been revealed (Lamba *et al.* 2003;

Lang *et al.* 2004), therefore, it seems likely that the gene expression level is associated with individual susceptibility to methadone toxicity and death. The present study has designed and created two *CYP2B6* promoter variant clones for the 750 TT, and 750 TC genotypes. These clones could now be used to determine the effect of *CYP2B6* promoter variants on GFP gene expression, to measure the effects of the T750C polymorphism on *CYP2B6* activity.

Chapter 8

The effects of the *OPRM1* A118G variation on cellular apoptosis and μ -receptor internalisation following methadone treatment.

This chapter has been drafted for publication and has been presented here in paper format.

8.1 ABSTRACT

Earlier work of this research project identified an association between the *OPRM1* A118G polymorphism and increased susceptibility to methadone and methadone and benzodiazepine fatality. It is known that methadone binding to μ -opioid receptors induces receptor internalisation and it was postulated that this might be linked with individual susceptibility to methadone. This study explored the association between the A118G polymorphism and methadone concentration on μ opioid receptor internalisation and cellular apoptosis in chronic lymphocytic leukaemia (CLL) cells using flow cytometry. It was observed in this study that the A118G polymorphism is associated with higher levels of cellular apoptosis as demonstrated by Annexin V and propidium iodide binding. Furthermore, the G allele is associated with significant reductions in receptor internalisation. The A118G polymorphism might be involved in receptor accumulation at the cell membrane as a result of poor receptor internalisation, which could induce methadone toxicity.

Keywords: A118G, Apoptosis, Internalisation, Methadone, *OPRM1*.

8.2 Introduction

The work presented in Chapters 5 and 6 of this research project demonstrated that the μ -opioid receptor is involved in individual susceptibility to methadone toxicity and death. However, the molecular mechanisms responsible for this remain unclear. The receptor-mediated activation of μ -opioid receptors is a complex process involving a number of downstream actions, including the regulation of adenylyl cyclase, mitogen-activated protein kinase (MAPK), G-protein-gated, inwardly rectifying K^+ channels and voltage-dependent calcium channels (Toskulkaeo *et al.* 2010). Agonist exposure at the μ -opioid receptor rapidly results in receptor internalisation modulating the number of active receptors at the plasma membrane (Trapaidze *et al.* 2000). The process of receptor internalisation occurs within minutes after opioid receptor activation and has been observed in opioid receptor transfected cells, neuroblastoma cells and native neurons (Koch & Hollt, 2008). Since, receptor internalisation is differentially regulated by distinct peptide agonists and alkaloid drugs it has been proposed that receptor internalisation plays an important role in individual response to opioids (Trapaidze *et al.* 2000).

A disruption to receptor internalisation as a result of gene variations could have significant effects on signal transduction and individual response to methadone (Trapaidze *et al.* 2000). The *OPRM1* A118G single nucleotide polymorphism codes for the N40D protein which is located within the second extracellular loop of the receptor, which is an important domain for the initial binding of opioids (Ferrer-Alcón *et al.* 2004). The A118G variation is responsible for the loss of an N-glycosylation site significantly affecting β -endorphin binding (Bond *et al.* 1998). The effect of A118G on receptor internalisation following methadone exposure is unclear, and recent work postulated that the A118G SNP reduces receptor internalisation resulting

in an accumulation of desensitised receptors at the membrane surface (Chapters 4 & 5). To study this further the present study used an *in vitro* methodology to investigate methadone induced receptor internalisation in primary chronic lymphocytic leukaemia (CLL) cells. CLL cell samples were selected because μ -opioid receptor presence on lymphocytes had been well reported (Mehrishi & Mills, 1983; Wu & Li, 1999; Toskulkaio *et al.* 2009 and CLL subjects possess high numbers of B-lymphocytes.

In addition to determining the effects of methadone on receptor internalisation, the effect of methadone concentration on cellular apoptosis was also investigated in this work, to determine whether methadone exposure induces cellular stress initiating intracellular apoptotic signalling and cell suicide. Studies have reported that morphine induces apoptosis in immunocytes and that this is directly associated with opioid tolerance and receptor desensitisation (Fecho *et al.* 1994; Wu *et al.* 1999; Mao *et al.* 2002; Tegeder & Geisslinger, 2004). Furthermore, due to the association between apoptosis and receptor desensitisation it has been postulated that receptor internalisation is a key event involved in the initiation of opioid-induced cell death (Tegeder & Geisslinger, 2004). Therefore the association between apoptosis and receptor internalisation requires further study, as this association may be involved in individual susceptibility to methadone.

8.3 Materials and Methods

DNA Extraction

Genomic DNA was isolated from 13 human cell lines using the DNeasy Blood and Tissue Kit (Qiagen). All DNA samples were quantified using the Human Quantifiler® Kit (Applied Biosystems) in accordance with the manufacturer's instructions.

OPRM1 A118G SNP Genotyping

A total of 44 chronic lymphocytic leukaemia (CLL) samples were genotyped for the A118G variation using the commercialised TaqMan® SNP Genotyping assay (Applied Biosystems, Warrington, UK, product no. 4351379) to identify A118G subjects.

Cell Culture and Ligand Binding Assay

Twelve human B-CLL cell lines (6 homozygous for the AA genotype, 5 heterozygous for the G allele and 1 homozygous for the GG genotype) were cultured in GIBCO® RPMI Media 1640 (supplemented with Penicillin, Streptomycin, L-Glutamine, and 10 % Fetal Calf Serum) and incubated with concentrations of 1 µM, 5 µM, 10 µM, 20 µM, and 100 µM methadone hydrochloride solutions for 1 hour at 37°C.

Annexin V FITC and propidium Iodide Staining of Apoptosing Cells

Cell surface staining was performed by washing 500µl of cultured cells with phosphate-buffered saline (PBS). Following this 1×10^6 cells for each treatment were incubated with 1µl of Annexin V FITC conjugate and 2µl of propidium iodide solution for 10 minutes at room temperature protected from the light. After cell staining flow cytometric analysis was performed.

µ-Opioid Receptor Internalisation

Receptor internalisation was performed by washing 500µl of cultured cells with FACSFlow. After this 1×10^6 cells for each treatment were incubated with 2µl of the rabbit polyclonal to µ opioid receptor (ab10272) for 30 minutes at 4°C. The cells were washed twice before being incubated with 2µl of Goat polyclonal to Rabbit IgG-FITC for 30 minutes at 4°C. The cells were then washed. After antibody binding flow cytometric analysis was performed.

Flow cytometric analysis

Flow cytometric analysis was performed using a Becton Dickinson FACS Analyser flow cytometer with argon ion laser excitation at (488) nm, with 10,000 events of each sample measured. Data were acquired using forward scatter, side scatter, μ antibody to Rabbit IgG FITC, Annexin V FITC and propidium iodide. Medians of fluorescent intensities (MFI) of antibody-stained μ -opioid receptors as a measure of receptor internalisation were determined.

Statistical Analysis

Data are presented as median, means \pm SE of the mean. The association between Annexin V and propidium iodide staining for the subjects was determined using the two tailed Spearman's rank test. The data was split using treatment grouping and genotype grouping to determine the effects of A118G and methadone treatment on cellular apoptosis. Spearman's rank testing was conducted to explore A118G effects on the apoptosis pathway using the following parameters: % live cells, % permeabilised cells, and % fragmented cells following methadone treatment. The independent T-test was used to determine the association between receptor internalisation for 118AA, and 118AG subjects, and the effect of A118G on cell apoptosis. The association between apoptosis and receptor internalisation was determined using Spearman's rank correlation. A P value of ≤ 0.05 was considered to indicate statistical significance. All analyses were performed with SPSS Software (version 14.0).

8.4 Results

OPRM1 A118G SNP Genotyping

In total 15 subjects were identified as heterozygous for the 118 G allele, a frequency of 34 %, one subject as homozygous for the 118 GG genotype (2 %) and 28 subjects as homozygous for the 118 AA genotype (64 %). This result is in agreement with early work (Chapter 6).

Annexin V FITC staining as a marker of cellular apoptosis

Annexin V binds to phosphatidylserine on the surface of the cell membrane of cells in the early stages of apoptosis. Following flow cytometry the Annexin V cells were divided into two separate groups (dead cells and live cells) using cell gating. The cells were then further sub-divided into % Annexin V positive, and % Annexin V negative. When examining the total cells (dead cells and live cells) there was a significant correlation between the % of Annexin V negative cells and the 118 AG genotype regardless of methadone treatment (Table 67). For the Annexin V dead cell group, the % of Annexin V negative cells was significantly associated with the control (0 μ M), 100 μ M, and 5 μ M methadone treatments in the presence of the 118 AG genotype ($P \leq 0.05$). This trend continued with the live cell group with the 100 μ M, 20 μ M, and 5 μ M methadone treatments associating with % of Annexin V negative cells for the 118 AG subjects. Interestingly there was no association between the % of cells positive for Annexin V and methadone treatment or subject genotype.

Table 67: The effect of the A118G variation on the total % of Annexin V negative cells.

Methadone Treatment	118 AA Genotype		118 AG & GG Genotypes	
	R ²	P value	R ²	P value
0 µM	0.086	0.872	0.886	0.019*
100 µM	0.143	0.787	0.943	0.005**
20 µM	0.314	0.544	0.943	0.005**
10 µM	0.314	0.544	0.829	0.042*
5 µM	0.314	0.544	0.943	0.05*
1 µM	0.314	0.544	-0.257	0.623

* Denotes ≤ 0.05 , ** denotes ≤ 0.01 .

The association between genotype and apoptosis was further examined using the Independent T-test. For the total cell group the 118 AG genotype was associated with significantly higher levels of Annexin V positive cells (19.92) compared with 118 AA subjects (5.83; $P = 0.001$). This trend continued for the % of Annexin positive cells within the live cell group ($P = 0.037$; 118 AA, 0.346; 118 AG, 0.603). As expected the A118G variation significantly associated with lower total % of Annexin V negative cells ($P = 0.002$; 118 AA 90.57; 118 AG 76.87).

Propidium Iodide staining as a marker of cellular apoptosis

Propidium iodide targets and binds to cells in the later stages of cellular apoptosis. After flow cytometry the cells were divided into % dead cells and the % live cells. Within these groupings three stages of cell apoptosis were designated: % live cells, % permeabilised cells, % fragmented cells. There was no association observed when examining the total number of cells (dead and live cells). In the dead cell group the % of live cells significantly correlated with the 118 AG genotype for the 20 µM and the 10 µM methadone treatments ($P = 0.019$, $P = 0.019$). Within the live cell group the % of permeabilised cells were significantly correlated with methadone treatment.

Furthermore, the 10 μM and 1 μM methadone treatments were associated with apoptosis for 118 AG subjects.

The association between genotype and propidium iodide for the total cells was further explored with the Independent T-test. The A118G variation associated with significantly lower live cells ($P = 0.007$; 84.09, 69.84 respectively), and significantly higher fragmented cells ($P = 0.006$; 9.22, 21.26 respectively). For the permeabilised cell group the 118 AG genotype associated with higher levels of cells permeabilisation however this result was not statistically significant ($P = 0.076$; 6.62, 8.75). This trend continued for the live cell group with significantly lower live cells for 118 AG subjects ($P = 0.022$), higher levels of fragmentation however this result was not statistically significant ($P = 0.096$) and significantly higher levels of permeabilisation ($P = 0.019$).

Annexin V and propidium Iodide joint effects

Interestingly there was a positive correlation between the total % of Annexin V positive cells and the total % of propidium iodide fragmented cells. Furthermore, this was associated with both treatment and genotype (Table 68).

Table 68: The association between the Total % of Annexin V positive cells and the Total % of propidium Iodide Live, Fragmented and Permeabilised Cells.

118 AA Genotype						
Treatment	PI % Live Cells		PI % Fragmented Cells		PI % Permeabilised Cells	
	R ²	P value	R ²	P value	R ²	P value
0 µM	-0.771	0.072	0.600	0.208	0.771	0.072
100 µM	-0.886	0.019*	0.886	0.019*	0.943	0.005**
20 µM	-0.600	0.208	0.371	0.468	0.771	0.072
10 µM	-0.600	0.208	0.371	0.468	0.600	0.208
5 µM	-0.600	0.208	0.143	0.787	0.657	0.156
1 µM	-0.600	0.208	0.314	0.544	0.886	0.019
118 AG/GG Genotype						
Treatment	PI % Live Cells		PI % Fragmented Cells		PI % Permeabilised Cells	
	R ²	P value	R ²	P value	R ²	P value
0 µM	-0.943	0.005**	0.943	0.005**	0.943	0.005**
100 µM	-0.829	0.042*	0.829	0.042*	0.771	0.072
20 µM	-0.829	0.042*	0.829	0.042*	0.429	0.397
10 µM	-0.829	0.042*	0.771	0.072	0.714	0.111
5 µM	-0.943	0.005**	0.886	0.019*	0.771	0.072
1 µM	-0.657	0.156	0.657	0.156	0.829	0.042*

* Denotes ≤ 0.05 , ** denotes ≤ 0.01 .

µ-Opioid Receptor Internalisation

Internalisation of the µ-opioid receptor was measured through µ-opioid receptor – anti rabbit IgG - FITC fluorescence. The effect of methadone treatment and A118G was tested by examining changes in the geometric mean. The average geometric mean for 118 AA subjects (5.17 mean fluorescence intensity, MFI) was significantly lower than 118 AG/GG subjects (8.13 MFI, $P = 0.002$). Furthermore, the mean fluorescence for both 118 AA and 118 AG/GG subjects increased from control levels when treated with the 20 µM to 5 µM methadone treatments (Figure 89).

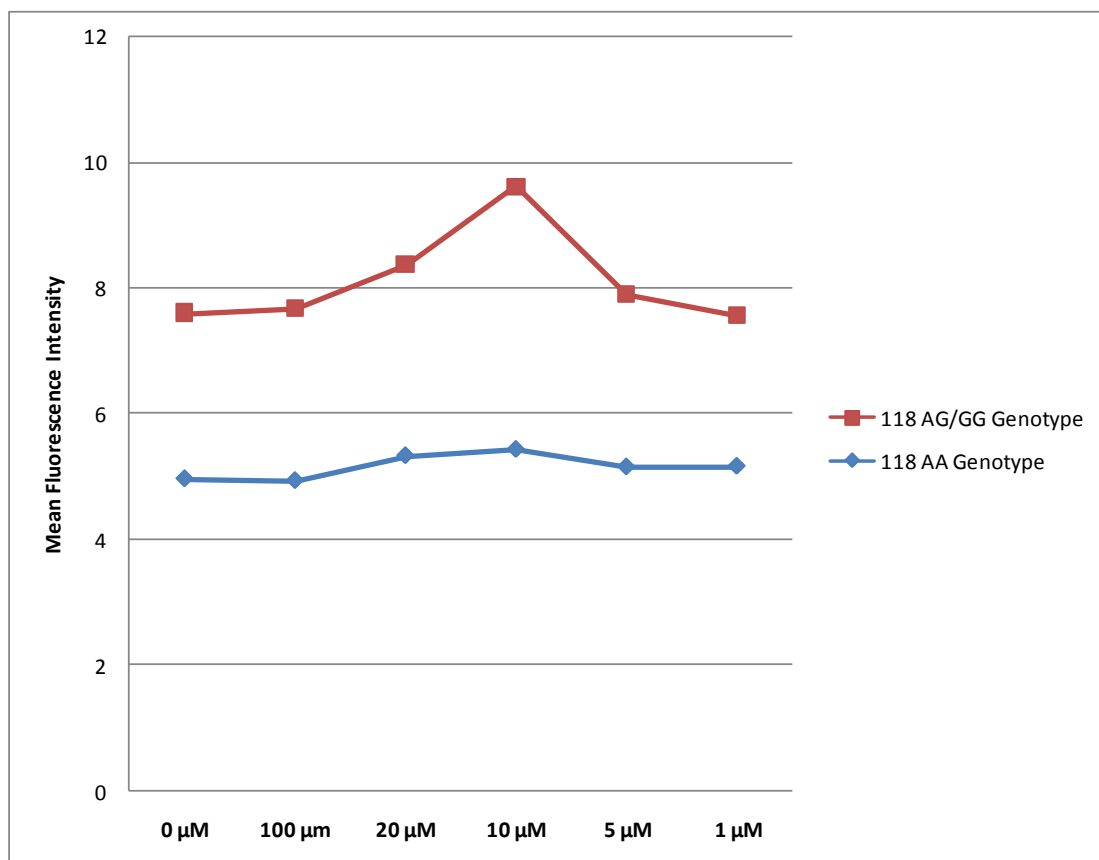


Figure 89: Mean receptor fluorescence for 118 AA and 118 AG/GG subjects following methadone treatment.

The Association between μ-Opioid Receptor Internalisation and Cellular Apoptosis

There was a significant correlation for 118 AG subjects between the geometric mean for μ-opioid receptor internalisation and the % of live Annexin V positive cells, for the 20 μM methadone treatment (R^2 0.829, $P = 0.042$).

8.5 Discussion

The interaction between the μ-opioid receptor and methadone is complex. *In vitro* analysis of μ may assist in elucidating the molecular mechanisms responsible for inter-individual susceptibility to methadone toxicity and death. In the present study two indicators of cellular apoptosis were used, Annexin V which detects the early

stages of apoptosis and propidium iodide which identifies the later stages of cellular apoptosis. Annexin V is a calcium dependent phospholipid binding protein that has a high affinity for negatively charged phospholipids (phosphatidylserine) on the cell surface. One of the earliest features of cellular apoptosis is the translocation of phosphatidylserine from the inner to the outer leaflet of the plasma membrane, thereby exposing phosphatidylserine to the external environment and Annexin V. Propidium iodide is a membrane impermeant dye and is therefore excluded from viable cells. In the later stages of apoptosis the cellular membrane becomes compromised allowing propidium iodide to enter the cells and stain the nucleus (Riccardi & Nicoletti, 2006). It was identified here that apoptosis correlated with the A118G polymorphism (Table 67), furthermore, this was associated with the 20 and 10 μ M methadone treatments ($P < 0.05$). When the association between the A118G genotype and apoptosis was examined further it was revealed that subjects with the 118 G allele had significantly higher levels of Annexin V positive cells ($P < 0.01$) and higher levels of cellular fragmentation ($P < 0.01$). Therefore it is postulated here that the A118G variation is linked with increased cellular apoptosis. Previous works have documented that methadone is a potent inducer of apoptosis (Maneckjee & Minna, 1994; Heusch & Maneckjee, 1998; Maneckjee & Heusch, 1999; Friesen *et al.* 2008). However, it was reported that this may be mediated through a non-opioid mechanism involving the autocrine growth-stimulatory factor bombesin (Maneckjee & Heusch, 1999). Friesen *et al.* (2008) reported that methadone is a potent inducer of cell death in leukaemia cells, and that this was due to the activation of apoptosis pathways by caspase -9 and caspase-3. Interestingly, the study also reported that there was no association between methadone induced apoptosis and nonleukemic cells (Friesen *et al.* 2008). However, the results from the present study indicate an association between cellular apoptosis and the μ -opioid receptor. Since, an association was reported

between the *OPRM1* A118G variation and methadone accumulation in Chapter 5 it is logical to postulate that this is linked with methadone-induced apoptosis in leukemic cells. It is clear that further investigation is required into the association between methadone-induced apoptosis and the μ -opioid receptor. However, the results from the work reported in this study indicate the *OPRM1* gene as a target for future work.

There was a statistically significant correlation between Annexin V positive cells and propidium iodide permeabilisation and fragmentation (Table 68). This is an expected result as both Annexin V and propidium iodide are markers of cellular apoptosis. It was observed during FACS analysis that no cells were positive for Annexin V and negative for propidium iodide (i.e. in early stages of cell apoptosis). Earlier works examining different methadone incubation times (Chapter 2, Figure 66) did not reveal a change in the % of Annexin V positive cells and propidium iodide negative cells. Therefore methadone may induce rapid cell apoptosis.

Opioid exposure has been postulated to induce changes in the number of opioid receptors present on lymphocytes in a similar manner to which opiates induce drug tolerance (Toskulkao *et al.* 2009). Following agonist-receptor activation, opioid receptors promote guanine nucleotide exchange of heterotrimeric G-protein (Toskulkao *et al.* 2009). This triggers a downstream signal transduction pathway involving adenylyl cyclase, mitogen-activated protein kinase (MAPK), K^+ channels and Ca channels (Zhang *et al.* 1998; Whistler *et al.* 1999; Trapideze *et al.*, 2000; Toskulkao *et al.* 2009), leading to receptor phosphorylation and internalisation. This results in a depletion of cell surface μ -opioid receptors. Previous work has reported significant reductions in μ receptors located on T-lymphocytes in chronic heroin abusers, which could be indicative of *OPRM1* down regulation (Ferrer-Alcon *et al.* 2004). Furthermore, chronic methadone exposure has been documented to affect

OPRM1 transcription resulting in the attenuation of μ receptor mRNAs leading to a reduction of receptors at the cell surface (Toskulkao *et al.* 2009). However, in the present study an association was revealed between the *OPRM1* A118G variation and increased receptor levels following methadone treatment. Furthermore, the work presented in Chapters 4 and 5 identified an association between A118G and increased blood methadone concentrations in post-mortem subjects. This was postulated to be representative of a reduction in receptor internalisation resulting in an accumulation of desensitised receptors at the membrane surface. Since, a significant association was identified here between the 118 AG genotype and increased MFI values it is logical to assume that the A118G polymorphism is responsible for reductions in receptor internalisation, and may be influential in inter-individual methadone susceptibility. However the A118G polymorphism had previously been associated with reductions in receptor binding sites, with 118 AA carriers possessing ten times more binding sites (Zhang *et al.* 2005). It would be interesting to explore this further with an increased sample size to determine the role of A118G for receptor internalisation and methadone susceptibility.

An agonist-receptor association was observed between the 20 and 10 μ M methadone concentration range (Figure 89). Since, the MFI for both 118 AG and to a lesser extent 118 AA subjects is increased between these methadone treatments, it is postulated that this is where methadone is detrimental to μ -receptor internalisation. Furthermore, for 118 AG subjects we identified an association between increased μ receptor fluorescence and increased Annexin V and propidium iodide apoptosis for this concentration range ($P < 0.01$, $P < 0.05$ respectively). Several studies indicate that opioids are involved in a variety of biological effects independent to analgesia that could effect cell survival (Pak *et al.* 1999; Yin *et al.* 1997; Yin *et al.* 1999; Tegeder *et*

al. 2003). It has been observed that opioid receptors can promote apoptosis through Fas regulation (Yin *et al.* 1999). Additionally, it has been documented that opioid involvement in apoptosis could be kinase dependent, with pertussis toxin (PTX) antagonising the pro-apoptotic effects of morphine in some cells (Yin *et al.* 1997), but not in others (Tegeder *et al.* 2003) in response to the kinase involved in receptor internalisation. Furthermore, as, heterodimerisation between opioid receptors and somatostatin (SSTRs) has been observed (Pfeiffer *et al.* 2002) it had also been postulated that cross-talk between these systems can activate apoptosis signalling pathways following opioid treatment. However, this was not identified in human U266 multiple myeloma cells (Kerros *et al.* 2009). Therefore it is likely that multiple systems are involved in the association between μ opioid receptor internalisation and cellular apoptosis following methadone treatment. However, it is clear from the results reported here that the *OPRM1* A118G variation is involved in both reductions in μ receptor internalisation and cellular apoptosis and that this is concentration dependent.

In summary, the *OPRM1* A118G variation is involved with higher levels of apoptosis in CLL cells, which could have beneficial implications for cancer therapy and research, in addition to elucidating the role of A118G for methadone susceptibility. An association between A118G and receptor accumulation at the cell membrane indicative of reduced receptor internalisation has also been reported in Chapter 5. This is in agreement with the earlier theory that A118G is associated with increased post-mortem methadone concentrations due to a reduced ability to internalise μ receptors (Chapters 4 & 5), resulting in an accumulation of de-sensitised receptors at the membrane. Finally an association between μ receptor internalisation and cellular apoptosis was established for the 118 AG genotype, however the

molecular mechanisms responsible for this remain unclear and require future investigation. Further research into the role of A118G for receptor internalisation and apoptosis following methadone treatment is required, nevertheless, it is clear from these results that A118G is involved in individual susceptibility to methadone at a cellular level.

Chapter 9

Thesis Conclusions, Limitations & Future Work

9.1 Thesis Conclusions

This thesis has presented a wide review on the application of forensic pharmacogenomics for methadone toxicity, focusing on the influence of gene variations on individual susceptibility to methadone toxicity and death. The early chapters have given a thorough description of methadone and its involvement in drug-related deaths and have included a review of the gene systems pertinent to the project. The current problems faced by forensic toxicologists for methadone-attributed deaths have been described. The safety profile of methadone has been reviewed and the genes vital to methadone action *in vivo* have been described with particular emphasis on *CYP2B6* and *OPRM1*.

This chapter summarises the work carried out for this project at each stage of its development. Section 9.2 discusses the main findings and the limitations of the work conducted. In section 9.3 the possibilities for further work are detailed, with attention to ultimate forensic application.

9.2 Results Summary

The application of clinical and forensic pharmacogenomics has been subject to considerable research over the last decade. However, the association between gene variations and methadone action *in vivo* has remained a difficult and rather neglected problem. The work described in this thesis has focused on the association between single nucleotide polymorphisms (SNPs) and individual susceptibility to methadone. Specifically, SNPs located within the *CYP2B6* gene and that of the μ -opioid receptor (*OPRM1*). Several contributions to this field have been made as part of this work and these include:

- 1: The *CYP2B6**6 allele and *OPRM1* A118G variation can be used to identify methadone susceptible individuals post-mortem.
- 2: The *OPRM1* A118G variation may be linked with the lethal association between methadone and benzodiazepines.
- 3: The development of two recombinant DNA clones for the 750 TT and 750 TC variants to study the association between the *CYP2B6* T750C promoter variant and methadone susceptibility.
- 4: The *OPRM1* A118G variation is involved in receptor accumulation at the cell membrane following methadone treatment as a result of poor receptor internalisation.

9.2.1 Conclusions

The use of methadone in maintenance programmes worldwide has been associated with methadone-attributed deaths. SNPs on the genes encoding the cytochrome P450 enzyme *CYP2B6* and that for the μ opioid receptor (*OPRM1*) have been explored in this study, to determine the association between the *CYP2B6* T750C, G516T, A785G, and *OPRM1* A118G polymorphisms and individual susceptibility to methadone. In Chapters 4 and 5 the applications of *CYP2B6* and *OPRM1* gene variants for the toxicological interpretation of deaths attributed to methadone are described. The gene encoding the human cytochrome P450 enzyme *CYP2B6* is highly polymorphic playing a key role in the biotransformation of many drugs (Hofmann *et al.* 2008). As described in Chapter 4, a significant association was identified between the *CYP2B6**4, *9, & *6 alleles and higher methadone concentrations ($P < 0.05$), characteristic of poor methadone metabolism. The *CYP2B6**6 allele had previously been associated with slow or poor drug metabolism, with heterozygous and homozygous carriers of the *CYP2B6**6 allele expressing up to 4-fold less protein than wild type individuals (Eap *et al.* 2005; Desta *et al.* 2007). However, this current work is the first study to report an association between *CYP2B6**6 and increased post-mortem methadone concentrations (Chapter 4; Bunten *et al.* 2010). Furthermore, the association between the *CYP2B6**6 allele and mean post-mortem methadone concentrations continued with an increased sample size of 69 subjects (Chapter 5; $P < 0.05$). A study examining *CYP2B6**6 expression in human liver samples reported that it is the G516T (allele *9) polymorphism that is primarily responsible for poor metabolism (Hoffman *et al.* 2008). In agreement with this, in all cases where G516T was identified, the A785G (allele *4) polymorphism was also found in this work. G516T has been linked with aberrant splicing resulting in a major splice variant

(SV1) between exons four and five (Hofmann *et al.* 2008). It has been postulated that SV1 may be associated with reductions in functional mRNA transcription, and enzymatic activity. Therefore, it would be interesting to determine whether SV1 is associated with individual methadone susceptibility.

It was observed in Chapter 6, that the allele frequencies for G516T and A785G were higher in the post-mortem population than the control population (G516T, 44 %, 34 %; A785G 47.6 %, 38 % respectively). However, this result was not statistically significant ($P = 0.23$, $P = 0.5$ respectively). It was postulated that this may be indicative of a trend that had been limited by sample size, and a larger number of post-mortem subjects may elucidate the association between G516T and A785G prevalence and methadone susceptibility. It would also be interesting to examine CYP2B6*6 allele frequencies in an opioid abusing population, to assist in the interpretation of the results, which is discussed further in *Section 9.3*.

There is growing evidence that polymorphisms within gene promoter regions significantly effect gene expression (Day & Tuite, 1998; Rockman & Wray, 2002; Johnson *et al.* 2005). The role of the *CYP2B6* promoter region variation T750C for methadone susceptibility is currently unclear and requires further investigation. In this study a significant association was identified between T750C and the CYP2B6*6 allele (Chapters 5 and 6). As described in Chapter 5, T750C correlated with both G516T ($P < 0.01$) and A785G ($P < 0.01$) in 69 post-mortem subjects. This association was also evidenced in 84 post-mortem subjects as described in Chapter 6 ($P < 0.01$, $P < 0.01$), respectively). This result is in agreement with other earlier studies, with T750C forming part of the CYP2B6*6B allele with G516T, and A785G (Lamba *et al.* 2003; Hesse *et al.* 2004; Zukunft *et al.* 2005). Unexpectedly, in the work presented in Chapter 6, T750C was not associated with higher post-mortem methadone concentrations, with 750 TT subjects having a higher post-mortem mean methadone

concentration (0.79 mg/L) than 750 TC and CC subjects (0.69 mg/L). Since, T750C associated with the CYP2B6*6 poor metabolism allele, higher post-mortem methadone concentrations were expected. Furthermore, T750C had been reported to be associated with reductions in hepatic *CYP2B6* expression (Lamba *et al.* 2003; Lang *et al.* 2004). Therefore the assemblage of T750C, G516T and A785G reported in Chapter 5 and 6 could result in a potentially lethal combination where a subject would experience poor methadone metabolism as a result of both reduced *CYP2B6* expression and the CYP2B6*6 allele. However, since, T750C was not associated with statistically higher post-mortem methadone concentrations in this study, the significance of the association between T750C, G516T and A785G is unclear (Chapter 5). Furthermore, T750C is also part of the CYP2B6*22 allele together with T82C, which has been linked with increased *CYP2B6* expression (Faucette *et al.* 2000; Zukunft *et al.* 2005; Li *et al.* 2010). As the significance of the CYP2B6*22 allele has not been studied in this study it cannot be excluded that the increased post-mortem methadone concentrations identified for the 750 TT genotype are a result of the CYP2B6*22 allele and the T82C polymorphism. It would therefore be interesting to investigate the CYP2B6*22 allele further to identify whether the T82C polymorphism results in an ultra-rapid metaboliser phenotype impacting methadone metabolism.

There was no significant difference in allele frequency observed in Chapter 6 for the T750C polymorphism between the post-mortem (44 %) and control populations (49 %), indicating that this polymorphism may not be a suitable risk factor for determining methadone susceptibility. However, it was also reported that the T750C variation was significantly correlated with gender in the post-mortem population. Earlier works have consistently reported that gender differences are associated with *in vivo* hormone levels affecting drug absorption, disposition,

metabolism and pharmacodynamics (Becker *et al.* 1990; Peris *et al.* 1991; Justice & de Wit, 2000; Lamba *et al.* 2003; Roth *et al.* 2004; Lukas & Wetherington, 2005; Becker & Hu, 2008). Significant differences in *CYP2B6* expression have been reported between male and female subjects, with higher reductions in *CYP2B6* activity in male subjects (Lamba *et al.* 2003). The results from this study were in agreement with this, with male subjects significantly correlating with the T750C polymorphism. Therefore, it is postulated that the association observed between T750C and gender here, is due to T750C alterations to *CYP2B6* activity. In order to study this further, two recombinant DNA clones (p2B6-GFP-HB-750 TT, and p2B6-GFP-HB-750 TC) were designed and created to determine the role of T750C for *CYP2B6* activity, and as a result susceptibility to methadone toxicity (Chapter 7). Functionality trials modelling the effects of T750C as a measure of green fluorescence protein (GFP) activity following methadone exposure would be a logical progression and this is discussed further in *Section 9.3 Further Work*.

The association between the human μ -opioid receptor and inter-individual variability in drug response had been well studied; however there is limited information on the association between the A118G polymorphism and response to methadone. The *OPRM1* A118G polymorphism has been shown to affect drug efficiency and response (Bond *et al.* 1998). As described in Chapter 4 no significant difference was observed between the A118G genotype and post-mortem methadone concentration. However, it was observed that subjects heterozygous for the 118G allele had higher post-mortem methadone concentrations (0.93 mg/L) than homozygous wild-type subjects (0.70 mg/L) which was thought to be indicative of a trend. It was postulated that the trend for higher post-mortem methadone concentrations in 118 AG subjects could be explained by μ receptor internalisation

following agonist binding, resulting in a reduction in the number of available receptors for methadone binding at the cell membrane. Interestingly it was observed that the *OPRM1* A118G polymorphism significantly associated with decreased receptor internalisation, with 118 AG subjects demonstrating less receptor internalisation (8.13 MFI) than 118 AA subjects (5.17 MFI, in Chapter 8). Earlier works reported that the *OPRM1* receptor in 118 AG subjects have ten times less binding sites than that with the 118 AA genotype (Zhang *et al.* 2005). In this study, higher MFI values were observed for 118 AG subjects indicative of an increase in μ -receptors at the cell surface. It is logical to propose however, that this is due to receptor accumulation due to an inability to internalise and not an effect of A118G on increased gene expression. It was also revealed that subjects heterozygous for the A118G polymorphism had significantly higher levels of early and late stage apoptosis, and this correlated with receptor internalisation and methadone concentration (Chapter 8, $P = 0.042$). A number of studies have examined the association between *OPRM1* and cell apoptosis (Pak *et al.* 1999; Yin *et al.* 1997; Yin *et al.* 1999; Pfeiffer *et al.* 2002; Tegeder *et al.* 2003; Kerros *et al.* 2009), with associations reported between *OPRM1* and Fas regulation (Yin *et al.* 1999), protein kinases (Tegeder *et al.* 2003) and somatostatin (Pfeiffer *et al.* 2002). Therefore, it is likely that multiple systems are involved in the association between μ opioid receptor internalisation and cellular apoptosis following methadone treatment. However, it is clear from these results that the *OPRM1* A118G variation is involved in both reductions in μ receptor internalisation and cellular apoptosis and that this is concentration dependent (Chapter 8).

The results from the *in vitro* methadone internalisation study could therefore explain the association between the A118G polymorphism and increased post-mortem methadone concentrations. Interestingly, when the sample size was increased from 40

subjects to 69 subjects the mean post-mortem methadone concentration for A118G heterozygous subjects was significantly higher than wild-type subjects (Chapter 5; 1.28 mg/L, 0.79 mg/L respectively, $P = 0.05$). Therefore it is postulated that the A118G variation is an important factor in methadone toxicity and fatality.

It was also observed that there was a significant association between the A118G polymorphism and accumulation of benzodiazepines (Chapter 4). It is well documented that the co-administration of methadone and benzodiazepines can result in lethal respiratory depression (McCormick *et al.* 1984; Borron *et al.* 2002; Lintzeris *et al.* 2007). When benzodiazepines were found in conjunction with methadone, 118 AG subjects had a 2.4 fold higher post-mortem mean blood benzodiazepine concentration (Chapter 4, $P < 0.01$). Interestingly, this association was not observed in morphine-related fatalities ($P = 0.626$) and is postulated to be linked with μ -receptor internalisation (Keith *et al.* 1998). Since animal studies have reported that the co-administration of opioids together with benzodiazepines induces increased μ -opioid receptor recruitment (Poisnel *et al.* 2009), the interaction between methadone and benzodiazepines observed in the work is postulated to involve signal transduction with benzodiazepines up-regulating μ -opioid receptors. The findings from the work described here indicate that the A118G polymorphism is involved in individual susceptibility to fatality from methadone and benzodiazepines, and requires further investigation with a larger sample size.

A significant association was observed for the A118G allele frequencies between the control and post-mortem populations, with a 15.7 % difference between populations for heterozygous subjects (Chapter 6, $P = 0.0046$). The works presented in Chapters 4 and 5 indicated that 118 AG subjects will have reduced receptor function, which could confer protection from opioid toxicity at therapeutic levels (Lötsch *et al.* 2002). However, these subjects would have reduced sensitivity to

methadone at μ -receptors resulting in higher methadone concentrations *in vivo* before toxic effects appear (Chapters 4 & 5). Since methadone has a long mean elimination half life (Moffat *et al.* 2004) drug accumulation in 118 AG subjects could be especially pronounced, limiting any possible protective effect of the G allele.

Finally, a significant association was revealed between the *OPRM1* A118G genotype and the *CYP2B6**4, *9, and *6 alleles in subjects whose deaths had been attributed to methadone (Chapter 4, 5, & 6). As, both genes are essential to methadone action *in vivo*, this assemblage could indicate the coordinated action of the enzyme and receptor in contributing to individual susceptibility to methadone. Interestingly, no linkage between the A118G genotype and *CYP2B6**4, *9, & *6 alleles was observed for the control population studied (Chapter 6). Therefore the combination of the *OPRM1* A118G genotype and *CYP2B6**6 could lead to greater susceptibility to methadone fatality.

In summary it is suggested that the *CYP2B6**6 allele and the *OPRM1* A118G variation can be utilised in part to determine individual susceptibility to methadone. Both the *CYP2B6**6 allele and the *OPRM1* A118G variation were associated with higher post-mortem methadone concentrations in subjects whose deaths were attributed to methadone. Furthermore, the A118G variation associated with higher post-mortem benzodiazepine concentrations indicating the possibility of cross-talk between the opioid and GABA_A systems. When *in vitro* models were used to explore the effects of *CYP2B6* and *OPRM1* variations, it was observed that the A118G polymorphism is associated with reductions in receptor internalisation and higher levels of cellular apoptosis following methadone treatment. This result suggests that A118G effects on μ internalisation could be responsible for the higher concentrations of post-mortem methadone revealed in 118 AG subjects. Therefore, genetic screening for the G516T, A785G, and A118G variations has potential value for risk

management before prescribing methadone for addiction treatment, in addition to assisting in the toxicological interpretation of deaths involving methadone. Further study is required for the *CYP2B6* T750C promoter region polymorphism to determine the role of this SNP for methadone susceptibility.

9.2.2 Limitations of this Study

This study had a number of limitations which restricted the manner in which the work was conducted and this will now be discussed. The first study limitation was sample size and this was discussed in Chapters 4, 5, 6, and 7. Access to methadone-attributed deaths was a limiting factor. The study examined post-mortem subjects to investigate the association between individual genotype (*CYP2B6* & *OPRM1*) and post-mortem methadone concentration. The *CYP2B6**4 allele had previously been linked with increased enzymatic activity (Lang *et al.* 2001; Kircheiner *et al.* 2007) and rapid metaboliser status however the anticipated lower methadone levels were not observed in this study (Chapters 4 & 5). Since, only two subjects were *CYP2B6**1/*4 carriers, further interpretation of this result was limited. Additionally, no 118 GG genotype was identified amongst the post-mortem population (Chapters 4 & 5) therefore it was not possible to distinguish any difference in post-mortem methadone concentration between 118 AG and 118 GG subjects. When exploring the association between A118G and post-mortem benzodiazepine concentration in methadone-attributed fatalities only two 118 AG subjects were identified. This limited the validity of the association identified between A118G and higher post-mortem benzodiazepine concentrations. During the study design period, power calculations were conducted to determine the optimal number of post-mortem subjects required to meet the study aim and objectives. It was determined that 100 post-mortem samples would be the optimal

requirement for statistical significance. Unfortunately, however, sampling 100 post-mortem subjects whose deaths had been attributed to methadone was not possible. Therefore this study analysed all post-mortem subjects available and acknowledge here that sample size may have been a limiting factor on the accuracy of the statistic results reported here, particularly for those reported in Chapters 4, 5 and 6. However, this limited sample size did not restrict the observation of the significant associations for both *CYP2B6* and *OPRM1* polymorphisms and post-mortem methadone concentrations, and this was the first study to report such an association (Chapters 4 & 5; Bunten *et al.* 2010).

It would also have been interesting to examine the prevalence of *CYP2B6* and *OPRM1* polymorphisms in a current opioid using population (i.e. subjects enrolled in methadone maintenance therapy). However, access to such subjects required significant ethical approval, a clinic willing to participate in the study, and an incentive to subjects for study participation (typically monetary). Furthermore, before this could be pursued a significant association between *CYP2B6* and *OPRM1* polymorphisms and individual susceptibility to methadone had to firstly be identified. It should however be mentioned, that since higher post-mortem methadone concentrations in subjects with the *CYP2B6**6 allele and the A118G polymorphism were revealed, future collaboration with a methadone maintenance clinic has been agreed.

A select number of polymorphisms were examined in this study *CYP2B6* T750C, G516T, A785G, and *OPRM1* A118G. These SNPs were selected after an extensive literature search indicated that there was likely to be an association between methadone susceptibility and *CYP2B6* and *OPRM1* polymorphisms. It would have been interesting to explore a larger number of SNPs such as the *CYP2B6* T82C promoter region polymorphism. As observed in Chapter 5, 750 TC subjects were

associated with lower post-mortem methadone concentrations compared with 750 TT subjects. This was an unexpected result, and postulated to be a result of the T82C polymorphism resulting in the increased *CYP2B6* expression. However due to a restricted financial bursary the association of T82C for individual methadone susceptibility could not be explored further.

In vitro functionality trials to explore the effects of the T750C polymorphism on *CYP2B6* expression and individual susceptibility to methadone would have been interesting. However due to both time and financial constraints this aspect of the *in vitro* study could not be conducted. Nevertheless, two recombinant DNA clones (p2B6-GFP-HB-750 TT, and p2B6-GFP-HB-750 TC) harbouring the promoter region of *CYP2B6* with SNPs was achieved. This was due to complications with the initial cloning strategy which involved the insertion of the EGFP gene into the hSVCT2 vector to act as a marker of *CYP2B6* promoter activity. However, despite extended efforts the transformation of EGFP into hSVCT2 was unsuccessful, which reflected the challenging nature of molecular cloning within a short period of time. It was determined that the method used to prepare the hSVCT2 vector for ligation was responsible. In response to these difficulties a second cloning strategy was designed using the CT-GFP TOPO® TA expression kit. This system was selected as TOPO® cloning is a one-step cloning strategy involving the direct fusion of polymerase amplified products to a GFP reporter. Using the TOPO® cloning system clones for the 750 TT, and 750 TC genotypes were created.

Finally, the μ -opioid receptor internalisation study was limited by both time and financial constraints. As a result, we used methadone concentrations and incubation time intervals comparable to other studies. An experiment was conducted to examine five different methadone incubation treatments (Chapter 2, Figure 66). It would be better to conduct an extensive series of pilot experiments examining the effects of

methadone concentration, and different incubation times. It was discussed in Chapter 8 that none of the cell samples treated with methadone were found to be in the early stages of cellular apoptosis, which might be due to insufficient cell recovery from thawing stress. Therefore, further investigations are needed to confirm the findings from this work.

9.3 Further Work

This thesis has presented a number of studies that contribute towards the development of *CYP2B6* and *OPRM1* as markers of individual susceptibility to methadone. During each investigation, particular areas were identified which required further work, and these are now presented. As discussed in *Section 9.2.2 Study Limitations*, post-mortem sample size was a limiting factor in this study. An increased post-mortem sample size is therefore required to fully investigate the role of *CYP2B6* and *OPRM1* polymorphisms for individual susceptibility to methadone. Currently the *CYP2B6**6 allele and the *OPRM1* A118G variation have been identified as susceptibility variations in 69 subjects whose deaths had been attributed to methadone. It would be interesting to establish whether this association continued in a much larger post-mortem sample population. Furthermore, it would be useful to explore the prevalence of the *CYP2B6**6 allele and the *OPRM1* A118G polymorphism in an opioid abusing population, and future collaboration with a methadone maintenance clinic has been agreed. The current study examined these variations in a post-mortem population where the deaths had been attributed to methadone and a control population of non-methadone using subjects. To further determine the role of *CYP2B6* and *OPRM1* SNPs for methadone susceptibility it is also necessary to identify the association between drug concentration and SNP prevalence in opioid users *in vivo* as it is logical to think

that these subjects are less susceptible to methadone toxicity. Alternatively the examination of an opioid using population could reveal a SNP interaction associated with adverse methadone responses in tolerant individuals repeatedly exposed to methadone. It might be that this could involve SNPs affecting *OPRM1* expression. Therefore it would also be beneficial to examine different *OPRM1* SNPs likely to influence gene expression. The G172T polymorphism is located in the *OPRM1* promoter region and could be involved in gene regulation (Ross *et al.* 2005). Ide *et al.* (2006) examined the association between *OPRM1* polymorphisms and methamphetamine (MAP) dependence in a Japanese population. Significant linkage disequilibrium in the 3' region of the *OPRM1* gene was identified indicating that polymorphisms within this region could be linked with gene expression. Furthermore, a significant association was identified between the intron 2 IVS2+G691C polymorphism and MAP dependence (Ide *et al.* 2006). Therefore, it would be interesting to explore the G172T and IVS2+G691C polymorphisms for methadone susceptibility in a Caucasian population.

In Chapter 7 two clones were created to explore the effect of the 750 TT and 750 TC genotypes on *CYP2B6* expression. Earlier works indicate that this SNP is associated with reductions in *CYP2B6* expression (Lamba *et al.* 2003; Lang *et al.* 2004). However, the role of the T750C polymorphism for methadone susceptibility is unclear and functionality trials exploring the effect of T750C on *CYP2B6* expression could elucidate this. The transformation of the *CYP2B6* 750CC promoter region into the TOPO® TA vector was confirmed with a *HindIII* / *BglIII* digest (Figure 88). However, when a single *BglIII* digest was conducted it was observed that the *CYP2B6* promoter region orientation was reversed (Figure 88). Therefore further work is required to create a p2B6-GFP-HB-750 CC clone. The p2B6-GFP-HB-750 TT, p2B6-GFP-HB-750 TC clones contain the GFP reporter gene, which is an important

reporter molecule for monitoring gene expression and protein localization *in vivo*, *in situ* and in real-time observation (Chalfie *et al.* 1994; Inouye & Tsuji, 1994; Cheng *et al.* 1996; Chishima *et al.* 1997; Nocarova & Fisher, 2009). It is proposed that p2B6-GFP-HB-750 TT and p2B6-GFP-HB-750 TC transformation into mammalian Chinese Hamster Ovary (CHO) cells may identify T750C effects on gene expression following methadone exposure. As GFP protein is stable, species independent and can be observed non-invasively in living cells, monitoring GFP fluorescence can be regarded as a suitable method for the reliable estimation of GFP expression levels (Nocarova & Fisher, 2009). Earlier works have utilised flow cytometry (Bi *et al.* 2001; Paparella *et al.* 2002), fluorometry (Pérez-Arellano & Pérez-Martínez, 2003; Denis-Quanquin *et al.* 2007) and confocal microscopy (Nocarova & Fisher, 2009) to assess GFP fluorescence. Further p2B6-GFP-HB-750 TT and p2B6-GFP-HB-750 TC for the purposes of this study would be conducted using flow cytometry.

As discussed in Chapter 4 an association between the A118G polymorphism and post-mortem benzodiazepine concentration for methadone attributed fatalities was identified. Interestingly this was not seen in morphine-associated fatalities suggesting a specific link between methadone and benzodiazepines. Since, methadone and morphine both preferentially bind to the μ opioid receptor, this raised the question why the interaction varies for different opioids (Bunten *et al.* 2010). It is postulated that this is linked with receptor internalisation which is induced by methadone but not morphine (Keith *et al.* 1998). The association between the A118G polymorphism and receptor internalisation following methadone exposure was investigated, and it was observed that 118 AG subjects had reduced internalisation compared with 118 AA subjects (Chapter 8). It would be interesting to explore the interaction between methadone and benzodiazepines using an *in vitro* model similar to that described in Chapter 8. CLL cells cultured in different concentrations of methadone and diazepam

will reveal whether differences in receptor internalisation are responsible for the lethal association between methadone and benzodiazepines. Early works reported that benzodiazepine binding to GABA_A receptors results in the increased recruitment of μ opioid receptors (Poisnel *et al.* 2007). Furthermore, animal models demonstrated that benzodiazepines can potentiate the respiratory effects of fentanyl (Bailey *et al.* 1990). Therefore, it would also be beneficial to design an A118G cloning strategy using the CT-GFP TOPO® TA expression kit to explore *OPRM1* expression following methadone and diazepam exposure. This would assist in determining the roles of the A118G polymorphism for individual methadone susceptibility.

Methadone has an asymmetric carbon atom, forming two enantiomers, (- *R*)-methadone and (+ *S*)-methadone (Chapter 1, Figure 2) and is primarily administered as an equal racemic mixture (Pham-Huy *et al.* 1997; Rudaz & Veuthey, 1999; Rodriguez Rosas *et al.* 2003; Gerber *et al.* 2004; Lehotay *et al.* 2005).

Pharmacological activity at the μ opioid receptor is mostly due to (*R*)-methadone, which has a 10-fold higher affinity at μ and is up to 50 times more potent than the (*S*)-enantiomer (Rudaz & Veuthey, 1996; Foster *et al.* 1999; Liang *et al.* 2004).

Activation of the μ receptor by methadone is associated with lethal respiratory depression (Chevillard *et al.* 2010), therefore it is logical to assume that (*R*)-methadone is responsible for any adverse effects on the respiratory system. Animal models support this conclusion, with (*R*)-methadone inducing significantly more respiratory depression in the neonatal guinea pig than racemic methadone (Silverman *et al.* 2009).

While (*S*)-methadone has limited pharmacological activity there have been reports of cardio-toxicity as a result of (*S*)-methadone exposure. In recent years, increases in cardiac episodes have been reported in individuals prescribed methadone for maintenance treatment (Eap *et al.* 2007). Methadone blocks the hERG (human

ether-à-gogo related gene) voltage-gated potassium channel prolonging the QT interval affecting cardiac repolarisation, which can lead to torsades de pointes and sudden death. Furthermore, blockage of hERG by methadone is stereoselective with the (*S*)-enantiomer being significantly more potent than (*R*)-methadone (Eap *et al.* 2007).

This work has identified a significant association between the CYP2B6*6 allele and increased post-mortem methadone concentrations in subjects where the cause of deaths was attributed to methadone (Bunten *et al.* 2010). Both *in vitro* and *in vivo* studies have documented CYP2B6 stereoselectivity for the (*S*)-methadone enantiomer (Gerber *et al.* 2004; Eap *et al.* 2007), with the CYP2B6*6/*6 genotype correlating with higher (*S*)-but not (*R*)-methadone concentrations (Crettol *et al.* 2005; Eap *et al.* 2007). Furthermore, it has been reported that CYP2B6 metaboliser status also influenced individual QTc intervals, with poor metabolisers having a mean QTc interval 18 ms longer than extensive metabolisers (Eap *et al.* 2007).

Methadone deaths are primarily linked with respiratory depression ((*R*)-methadone) or torsades de pointes (tdp) and sudden death ((*S*)-methadone). However, most post-mortem investigations do not allow differentiation between these two causes of death. As the CYP2B6*6/*6 genotype is associated with a potentially higher risk of cardiac arrhythmias and sudden death by (*S*)-methadone and respiratory depression is linked with (*R*)-methadone, it seems logical that in cases where death has been caused by methadone it would be possible to determine whether this was respiratory or cardiotoxic in nature through the presence of specific gene variants. It would be interesting to explore the association between the CYP2B6*6 allele and the OPRM1 A118G polymorphism for (*R*)-methadone and (*S*)-methadone to determine whether these SNPs demonstrate stereoselectivity.

Finally there are a number of genes that could be influential in methadone action and response and these include GABA_A (Bailey *et al.* 1990; Cox & Collins, 2001), *DRD1* (Lalley *et al.* 2004; Lalley *et al.* 2005; Crettol *et al.* 2008), *DRD2* (Barratt *et al.* 2006), hERG (Eap *et al.* 2007), *ABCB1* (Hoffmeyer, *et al.* 2000; Crettol *et al.* 2007), and the human pregnane X-receptor hPXR (Bauer *et al.* 2006). Therefore, building a causal relationship between *CYP2B6* and *OPRM1* variants and phenotypic responses is not a simple task and this in part relates to the interconnectivity between different genes (Figure 90). Methadone is a substrate for the efflux transporter P-glycoprotein (P-gp) where it influences methadone absorption, distribution, brain penetration, pharmacodynamics and analgesia (Thompson *et al.* 2000; Bauer *et al.* 2006; Kharasch *et al.* 2009). The gene that codes for P-gp is the *ABCB1* gene, *ABCB1* has a number of SNPs that influence P-gp, including C3435T which has been reported to lower gene expression (Hoffmeyer *et al.* 2000). This SNP alone, or a haplotype that includes this SNP and the G2677T SNP have been reported to decrease transporter function, which could lead to increased plasma concentrations or, if the outward transporter at the blood-brain barrier is decreased, to increased brain concentrations of methadone (Lötsch *et al.* 2006). In addition, the xenobiotic activation of the hPXR is involved in P-gp up-regulation reducing the efficacy of methadone (Dussault & Forman, 2002; Bauer *et al.* 2006). Therefore, functional hPXR polymorphisms are also likely to influence methadone action *in vivo* (Zhang *et al.* 2001).

The dopamine receptors *DRD1* and *DRD2* play significant roles in the rewarding effects of drugs of abuse (Kreek *et al.* 2005). An earlier work reported an association between the *DRD2* TaqI A SNP and opioid dependence (Lawford *et al.* 2000). *In vitro* analysis of the *DRD2* C957T polymorphism suggested that this variation may be associated with altered mRNA folding and stability affecting *DRD2* expression (Duan *et al.* 2003). Blockade of the *DRD1* receptor revealed the enhancement of the μ -

opioid receptor respiratory network, increasing the depressant effects of fentanyl on respiration in addition to increasing the duration of action (Lally *et al.* 2005). In a study on 238 methadone maintenance patients a significant association was revealed between the DRD2 C957T polymorphism and patient non-response (Crettol *et al.* 2008). Furthermore, animal models have reported significant down-regulation of the μ opioid receptor in DRD2 knockout mice (Léna *et al.* 2008). Therefore, analysis of the interaction between the dopamine DRD1 and DRD2 receptors and *OPRM1* may further elucidate the molecular pathways involved in individual methadone susceptibility.

In summary this thesis has presented a number of studies that contribute towards the development of *CYP2B6* and *OPRM1* as markers for identifying individual susceptibility to methadone. Furthermore, this work has demonstrated some of the important constraints and limitations of the method used in this study, and suggested a number of corrections and new techniques for overcoming such obstacles. Particular aspects that need further studies have been addressed, and these include the acquisition of a larger post-mortem sample size and analysis of a current opioid using population. The progression of *in vitro* analysis on the activities of the *CYP2B6* promoter variants can be conducted by using the p2B6-GFP-HB-750 TT and p2B6-GFP-HB-750 TC clones. Such study will advance current knowledge of the molecular pathways involved in methadone susceptibility. As methadone is a chiral drug further research focusing on the association between *CYP2B6* and *OPRM1* SNPs for both enantiomers, ((*R*)-methadone and (*S*)-methadone) is required. Finally the network of genes in response to methadone action *in vivo* is complex and identifying the molecular pathway for methadone susceptibility will involve not only extensive examination of each individual gene but also the cross-talk between genes.

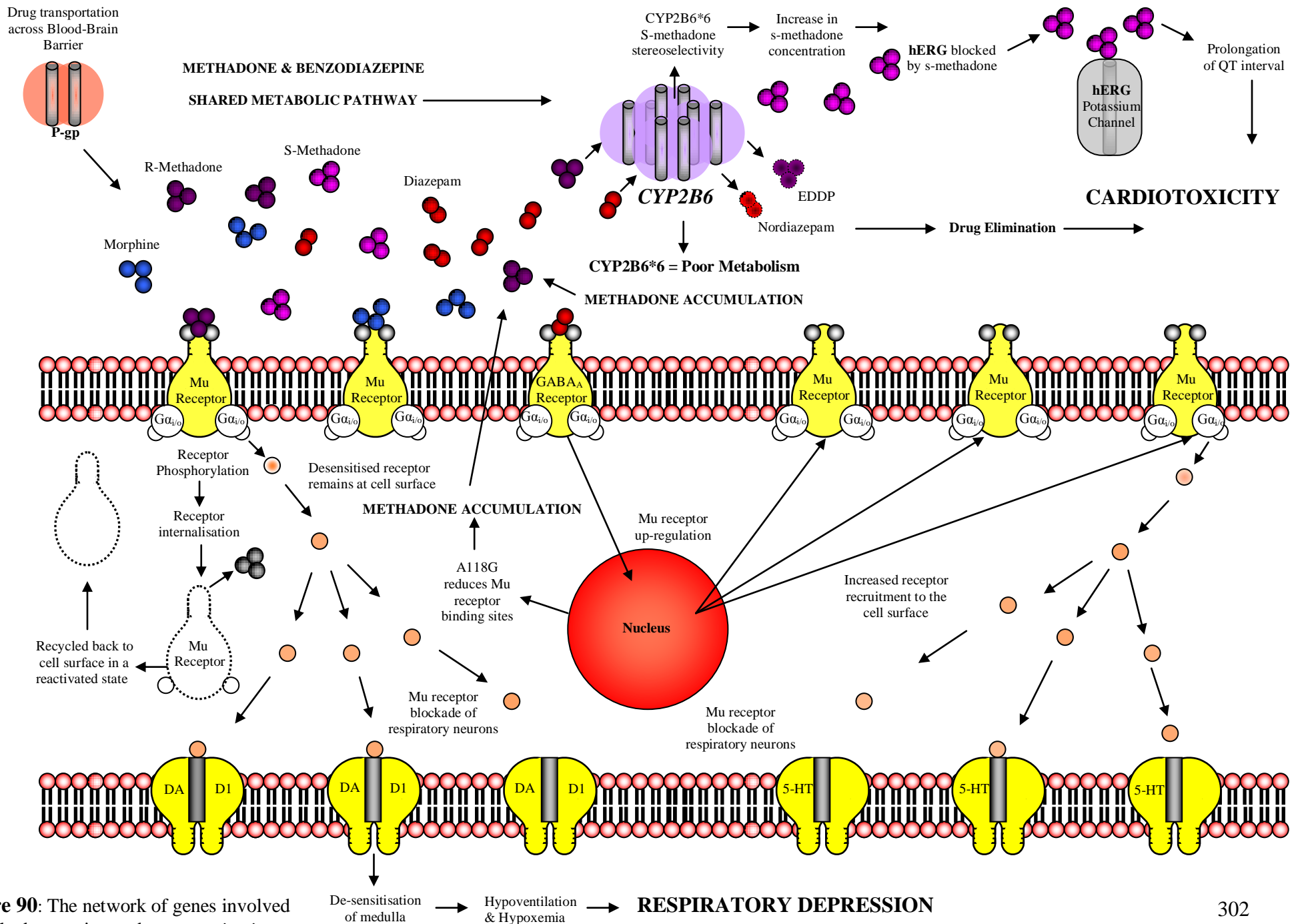


Figure 90: The network of genes involved in methadone action and response *in vivo*.

References

- Ahonen, J., Olkkola, K.T., & Neuvonen, P.J. (1997). Effect of route of administration of fluconazole on the interaction between fluconazole and midazolam. *European Journal of Clinical Pharmacology*, 51, 415-419.
- Ashby M, Fleming B, Wood M, Somogyi A. (1997). Plasma morphine and glucuronide (M3G and M6G) concentrations in hospice inpatients. *Journal of Pain and Symptom Management*, 14, 157–67.
- Ayonrinde, O.T.& Bridge, D.T. (2000). The rediscovery of methadone for cancer pain management. *The Medical Journal of Australia*, 172, 11-14.
- Bailey, C.P., Smith, F.L., Kelly, E., Dewey, W.L., & Henderson, G. (2006). How important is protein kinase C in μ -opioid receptor desensitization and morphine tolerance. *Trends in Pharmacological Sciences*, 27, (11), 558-565.
- Baldwin, S.J., Bloomer, J.C., Smith, G.J., Ayrton, A.D., Clarke, S.E., & Chenery, R.J. Ketoconazole and sulphaphenazole as the respective selective inhibitors of P4503A and 2C9. *Xenobiotica*. 25, 261-270 (1995).
- Barratt, D.T., Coller, J.K., & Somogyi, A.A. (2006). Association between the DRD2 A₁ allele and response to methadone and buprenorphine maintenance treatments. *American Journal of Medical Genetics, Part B (Neuropsychiatric Genetics)*, 141, (B), 323-331.
- Bart, G., Heilig, M., LaForge, K.S., Pollak, L., Leal, S.M., Ott, J., & Kreek, M.J. (2004). Substantial attributable risk related to a functional mu-opioid receptor gene polymorphism in association with heroin addiction in Central Sweden. *Molecular Psychiatry*, 9, 547-549.
- Bart, G., Kreek, M.J., Ott, J., LaForge, K.S., Proudnikov, D., Pollak, L., & Heilig, M. (2005). Increased attributable risk related to a functional μ -Opioid receptor gene polymorphisms in association with alcohol dependence in central Sweden. *Neuropsychopharmacology*, 30, 417-422.
- Baselt, R. C., 2004. *Disposition of toxic drugs and chemicals in man* 7th ed. Foster City, California: Biomedical Publications.
- Bauer, B., Yang, X., Hartz, A.M.S., Olson, E.R., Zhou, R., Kalvass, J.C., Pollack, G.M., & Miller, D.S. (2006). *In vivo* activation of human Pregnane X receptor tightens the blood-brain barrier to methadone through p-glycoprotein up-regulation. *Molecular Pharmacology*, 70, (4), 1212-1219.
- Bayerer, B., Stamer, U., Hoeft, A., & Stüber, F. (2007). Genomic variations and transcriptional regulation of the human μ -opioid receptor gene. *European Journal of Pain*, 11, 421-427.
- Becker, J.B. (1990). Estrogen rapidly potentiates amphetamine induced striatal dopamine release and rotational behaviour during microdialysis. *Neuroscience Letters*, 118, 169-171.

- Becker, J.B., & Hu, M. (2008). Sex differences in drug abuse. *Frontiers in Neuroendocrinology*, 29, (1), 36-47.
- Befort, K., Fillioi, D., Decaillot, F.M., Gaveriaux-Ruff, C., Hoehe, M.R. & Kieffer, B.L. (2001). A single nucleotide polymorphic mutation in the human mu-opioid receptor severely impairs receptor signalling. *Journal of Biological Chemistry*, 276, 3130-3137.
- Bell, J.R., Butler, B., Lawrance, A., Batey, R., & Salmelainen, P. (2009). Comparing overdose mortality associated with methadone and buprenorphine treatment. *Drug and Alcohol Dependence*, 104, 73-77.
- Bergen, A.W., Kokoszka, J., Peterson, R., Long, J.C., Virkkunen, M., Linnoila, M., & Goldman, D. (1997). Mu opioid receptor gene variants: lack of association with alcohol dependence. *Molecular Psychiatry*, 2, 490-494.
- Bergmann, T.K., Brasch-Andersen, C., Gréen, H., Mirza, M., Pedersen, R.S., Nielsen, F., Skougarrd, K., Wihl, J., Keldsen, N., Damkier, P., Friberg, L.E., Peterson, C., Vach, W., Karlsson, M.O., & Brosen, K. (2010). Impact of CYP2C8*3 on paclitaxel clearance: a population pharmacokinetic and pharmacogenomic study in 93 patients with ovarian cancer. *Pharmacogenomics Journal*, doi:10.1038/tpj.2010.19.
- Berrettini, W.H., Hoehe, M.R., Ferraro, T.N., DeMaria, P.A. & Gottheil, E. (1997). Human mu opioid receptor gene polymorphisms and vulnerability to substance abuse. *Addiction Biology*, 2, 303-308.
- Bertschy, G., Baumann, P., Eap, C.B., & Baettig, D. (1994). Probable metabolic interaction between methadone and fluvoxamine in addict patients. *Therapeutics Drug Monitoring*, 16, 42-45.
- Bhathena, A., & Spear, B.B. (2008). Pharmacogenetics: improving drug and dose selection. *Current Opinion in Pharmacology*, 8, 639-646.
- Bi, J.X., Wirth, M., Beer, C., Kin, E.J., Gu, M.B., & Zeng, A.P. (2001). Dynamic characterization of recombinant Chinese Hamster Ovary cells containing an inducible c-fos promoter GFP expression system as a biomarker. *Journal of Biotechnology*, 93, 231-241.
- Bidlack, J.M. (2000). Detection and function of opioid receptors on cells from the immune system. *Clinical Diagnosis and Laboratory Immunology*, 909, 1– 11.
- Binswanger, I.A., Stern, M.F., Deyo, R.A., Heagerty, P.J., Cheadle, A., Elmore, J.G., & Koepsell, T.D. (2007). Release from prison- a high risk of death for former inmates. *The New England Journal of Medicine*, 356, 157-165.
- Binyaminy, B., Gafni, M., Shapira, M., & Sarne, Y. (2008). Agonist-specific down regulation of mu-opioid receptors: different cellular pathways are activated by different opioid agonists. *Life Sciences*, 82, pp 831-839.

- Bohn, L.M., Lefkowitz, R.J., & Caron, M.G. (2002). Differential mechanisms of morphine antinociceptive tolerance revealed in (beta) arrestin-2 knock-out mice. *Journal of Neuroscience*, 22, 10494–10500.
- Bond, C., LaForge, K.S., Tian, M., Melia, D., Zhang, S., Borg, L., Gong, J., Schluger, J., Strong, J.A., Leal, S.M., Tischfield, J.A., Kreek, M.J., & Yu, L. (1998). Single-nucleotide polymorphism in the human mu opioid receptor gene alters β -endorphin binding and activity: possible implications for opiate addiction. *Proceedings of the National Academy of Sciences*, 95, pp 9608-9613.
- Borron, S.W., Monier, C., Risède, P., & Baud, F.J. (2002). Flunitrazepam variably alters morphine, buprenorphine, and methadone lethality in the rat. *Human Experimental Toxicology*, 21, 599-605.
- Brady, K.T., & Randall, C.L. (1999). Gender difference in substance use disorders. *Psychiatric Clinics of North America*, 22, 241-252.
- Broers, B., Junet, C., Bourquin, M., Déglon, J.J., Perrin, L., & Hirschel, B. (1998). Prevalence and incidence of HIV, hepatitis B and C among drug users on methadone maintenance treatment in Geneva between 1988 and 1995. *AIDS, Epidemiology and Social: Original papers*, 12, (15), 2059-2066.
- Bunten, H., Liang, W., Pounder, D.J., Seneviratne, C., Osselton, D. (2010). *OPRM1* and *CYP2B6* gene variants as risk factors in methadone-related deaths. *Clinical Pharmacology and Therapeutics*, 88, (3), 383-389.
- Buster, M.C., van Brussel, G.H., & van den Brink, W. (2002). An increase in overdose mortality during the first two weeks after entering or re-entering methadone treatment in Amsterdam. *Addiction*, 97, 993-1001.
- Butzbach, D.M. (2010). The influence of putrefaction and sample storage on post-mortem toxicology results. *Forensic Science and Medical Pathology*, 6, (1), 35-45.
- Camilleri, M. (2007). Pharmacogenomics and serotonergic agents: research observations and potential clinical practice implications. *Neurogastroenterology and motility*, 19, (s2), 40-45.
- Caplehorn, J.R.M. (2000). Knowledge of methadone toxicity among US maintenance clinic staff. *The Journal of Maintenance in the Addictions*, 1, 62-72.
- Caplehorn, J.R., & Drummer, O.H. (2002). Fatal methadone toxicity: signs and circumstances, and the role of benzodiazepines. *Australian and New Zealand Journal of Public Health*, 26, (4), 358-362.
- Caplehorn, J.R.M., & Ross, M.W. (1995). Methadone maintenance and the likelihood of risky needle sharing. *International Journal of the Addictions*, 30, 685-698.
- Catania, M.G. (2006). *An a-z guide to pharmacogenomics*, AACC Press, USA.
- Center for Substance Abuse Treatment, Methadone-Associated Mortality: Report of a National Assessment, May 8-9. 2003. SAMHSA Publication No. 04-3904. Rockville,

MD: Center for Substance Abuse Treatment, Substance Abuse and Mental Health Services Administration (2004).

Center for Substance Abuse Treatment. (2009). Emerging Issues in the Use of Methadone. HHS Publication No. (SMA) 09-4368. Substance Abuse Treatment Advisory, 8, (1), 1-8.

Chalfie, M., Tu, Y., Eukirchen, G., Ward, W.W., & Prasher, D.C. (1994). Green fluorescent protein as a marker for gene expression. *Science*, 263, 802-805.

Chartuvedi, K., Shahrestanifar, M., & Howells, R.D. (2000). μ Opioid receptor: role for the amino terminus as a determinant of ligand binding affinity. *Molecular Brain Research*, 76, 64-72.

Chavkin, C. (1988). Electrophysiology of opiates and opioid peptides. In: *The opiate receptors* (Pasternak, G.W., ed), pp 273-303. Clifton, NJ: Humana.

Cheng, L., Fu, F., Tsukamoto, A., & Hawley, R.G. (1996). Use of green fluorescent protein variants to monitor gene transfer and expression in mammalian cells. *Nature Biotechnology*, 14, 606-609.

Chevillard, L, Mègarbane, B, Baud, FJ, Risède, P, Dècleves, X, Mager, D, Milan, N, & Ricordel, I (2010) Mechanisms of respiratory insufficiency induced by methadone overdose in rats. *Addiction Biology* 15: 62-80.

Chishima, T., Miyagi, Y., Wang, X., Yamaoka, H., Shimada, H., Moossa, A.R., & Hoffman, R.M. (1997). Cancer invasion and micrometastasis visualised in live tissue by green fluorescent protein expression. *Cancer Research*, 57, 2042-2047.

Chugh, S.S., Socoteani, C., Reinier, K., Waltz, J., Jui, J., & Gunson, K. (2008). A community-based evaluation of sudden death associated with therapeutic levels of methadone. *The American Journal of Medicine*, 121, (1), 66-71.

Clarke, S.M., Mulcahy, F.M., Tijia, J., Reynolds, H.E., Gibbons, S.E., Barry, M.G., & Back, D.J. (2001). The pharmacokinetics of methadone in HIV-positive patients receiving the non-nucleoside reverse transcriptase inhibitor efavirenz. *British Journal of Clinical Pharmacology*, 51, 213-217.

Cobb, B.D., & Clarkson, J.M. (1994). A simple procedure for optimising the polymerase chain reaction (PCR) using modified Taguchi methods. *Nucleic Acids Research*, 22, (18), 3801-3805.

Code, E.L., Crespi, C.L., Penman, B.W., Gonzalez, F.J., Chang, T.K., & Waxman, D.J. (1997). Human cytochrome P4502B6: interindividual hepatic expression, substrate specificity and role in procarcinogen activation. *Drug Metabolism and Disposition*, 25, 985-993.

Corkery, J.M., Schifano, F., Ghodse, A.H., & Oyefeso, A. (2004). The effects of methadone and its role in fatalities. *Human Psychopharmacology*, 19, 565-576.

- Cook, D.S., Braithwaite, R.A., & Hale, K.A. (2000). Estimating antemortem drug concentrations from post-mortem blood samples: the influence of post-mortem redistribution. *Clinical Pathology*, 53, 282-285.
- Cox, R.F., & Collins, M.A. (2001). The effects of benzodiazepines on human opioid receptor binding and function. *Anesthesia and Analgesia*, 93, 354-358.
- Crettol, S., Dèglon, J.J., Besson, J., Croquette-Krokar, M., Gothuey, I., Hämmig, R., Monnat, M., Hüttemann, H., Baumann, P., & Eap, C.B. Methadone enantiomer plasma levels, *CYP2B6*, *CYP2C19*, and *CYP2C9* genotypes, and response to treatment. *Clinical Pharmacology and Therapeutics*, 78, 593-604 (2005).
- Crettol, S., Monnat, M., & Eap, C.B. (2007). Could pharmacogenetic data explain part of the interindividual sensitivity to methadone-induced respiratory depression? *Critical Care*, 11, (1), 119-120.
- Crettol, S., Besson, J., Croquette-Krokar, M., Hammig, R., Gothuey, I., Monnat, M., Deglon, J.J., Preisig, M., & Eap, C.B. (2008). Association of dopamine and opioid receptor polymorphisms with response to methadone maintenance treatment. *Progress in Neuro-Psychopharmacology & Biological Psychiatry*, 32, 1722-1727.
- Dai, D., Tang, J., Rose, R., Hodgson, E., Bienstock, R.J., Mohrenweiser, H.W., & Goldstein, J.A. (2001). Identification of variants of *CYP3A4* and characterization of their abilities to metabolize testosterone and chlorpyrifos. *The Journal of Pharmacology and Experimental Therapeutics*, 299, (3), 825-831.
- Dan'ura, T., Kurokawa, T., Yamashita, A., Yanagiuchi, H., & Ishibashi, S. (1988). Inhibition of rat brain adenylate cyclase activity by benzodiazepine through the effects on Gi and catalytic proteins. *Life Sciences*, 42, 469-475.
- Darke, S., Dufrou, J., & Torak, M. (2010). The comparative toxicology and major organ pathology of fatal methadone and heroin toxicity cases. *Drug and Alcohol Dependence*, 106, (1), 1-6.
- Darke, S.G., Ross, J.E., & Hall, W.D. (1995). Benzodiazepine use among injecting heroin users. *Medical Journal of Australia*, 162, 645-647.
- Davis, M.P., & Walsh, D. (2001). Methadone for relief of cancer pain: a review of pharmacokinetics, pharmacodynamics, drug interactions and protocols of administration. *Support Care Cancer*, 9, 73-83.
- Day, D.A., & Tuite, M.F. (1998). Post-transcriptional gene regulatory mechanisms in eukaryotes: an overview. *Journal of Endocrinology*, 157, (3), 361-371.
- Denis-Quanquin, S., Lamouroux, L., Lougarre, A., Mahéo, S., Saves, I., Paquereau, L., Demange, P., & Fournier, D. (2007). Protein expression from synthetic genes: Selection of clones using GFP. *Journal of Biotechnology*, 131, 223-230.
- Department of Health, Scottish Office Department of Health, Welsh Office, Department of Health, Department of Health and Social Services Northern Ireland,

- (1999). Drug misuse and dependence- guidelines on clinical management. The Stationary Office, London, 45-46.
- Desta, Z., Saussele, T., Ward, B., Bliedernicht, J., Li, L., Klein, K., Flockhart, D.A., & Zanger, U.M. (2007). Impact of *CYP2B6* polymorphism on hepatic efavirenz metabolism in vitro. *Pharmacogenomics*, 8, 547-558.
- De Vos, A., van der Weir, J., & Loovers, H.M. (2010). Association between *CYP2C19*17* and metabolism of amitriptyline, citalopram and clomipramine in Dutch hospitalized patients. *Pharmacogenomics*, doi: 10.1038/tpj.2010.39.
- de Vries, J.E., Wijnen, P.A.H.M., Hamulyák, K., van Dieijen-Visser, M.P., & Bekers, O. (2001). PCR on cell lysates obtained from whole blood circumvents DNA isolation. *Clinical Chemistry*, 47, 1701-1702.
- Dobler-Mikola, A., Hättenschwiler, J., Meili, D., Beck, T., Boni, E., & Modestin, J. (2005). Patterns of heroin, cocaine, and alcohol abuse during long-term methadone maintenance treatment. *Journal of Substance Abuse Treatment*, 29, 259-265.
- Donnelly, B., Balkon, J., Lasher, C., dePaul Lynch, V., Bidanset, J.H., & Bianco, J. (1983). Evaluation of methadone-alcohol interaction. I. Alterations of plasma concentration kinetics. *Journal of Analytical Toxicology*, 7, 246-248.
- Drakenberg, K., Nikoshkov, A., Horvath, M.C., Fagergren, P., Gharibyan, A., Saarelainen, K., Rahman, S., Nylander, I., Bakalkin, G., Rajs, J., Keller, E., Hurd, Y.L. (2006). Mu opioid receptor A118G polymorphism in association with striatal opioid neuropeptide gene expression in heroin abusers. *Proceedings of the National Academy of Sciences U.S.A.* 103, 7883–7888.
- Druid, H., Homgren, P., Carlsson, B., & Ahlner, J. (1999). Cytochrome P450 2D6 (*CYP2D6*) genotyping on post-mortem blood as a supplementary tool for interpretation of forensic toxicological results. *Forensic Science International*, 99, 25-34.
- Duan, J., Wainwright, M.S., Comeron, J.M., Saitou, N., Sanders, A.R., Gerlenter, T., & Gejman, P.V. (2003). Synonymous mutations in the human dopamine receptor D2 (*DRD2*) affect mRNA stability and synthesis of the receptor. *Human Molecular Genetics*, 12, 205-216.
- Dussault, I., & Forman, B.M. (2002). The nuclear receptor PXR: a master regulator of “homeland” defense. *Critical Reviews in Eukaryotic Gene Expression*, 12, 53-64.
- Dyer, K.R., Foster, D.J., White, J.M., Somogyi, A.A., Menalaou, A., & Bochner, F. (1999). Steady-state pharmacokinetics and pharmacodynamics in methadone maintenance patients: comparison of those who do and do not experience withdrawal and concentration-effect relationships. *Clinical Pharmacology and Therapeutics*, 65, 685-694.
- Eagling, V.A., Back, D.J., & Barry, M.G. (1997). Differential inhibition of cytochrome P450 isoenzymes by the protease inhibitors, ritonavir, saquinavir, and indinavir. *British Journal of Clinical Pharmacology*, 44, 190-194.

- Ekins, S., Vandenbranden, M., Ring, B.J., Gillespie, J.S., Yang, T.J., Gelboin, H.V., & Wrighton, S.A. (1998). Further characterization of the expression in liver and catalytic activity of *CYP2B6*. *Journal of Pharmacology and Experimental Therapeutics*, 286, 1253-1259.
- Eap, C.B., Bertschy, G., Powell, K., (1997). Fluvoxamine and fluoxetine do not interact in the same way with the metabolism of the enantiomers of methadone. *Journal of Clinical Psychopharmacology*, 17, 113-117.
- Eap, C.B., Broly, F., Mino, A. (2001). Cytochrome P450 2D6 genotype and methadone steady-state concentrations. *Journal of Clinical Psychopharmacology*, 21, 229-234.
- Eap, C.B., Buclin, T., & Baumann, P. (2002). Interindividual variability of the clinical pharmacokinetics of methadone. *Clinical Pharmacokinetics*, 41, (14), 1153-1193.
- Eap, C.B., Crettol, S., Rougier, J.S., Schlapfer, J., Sintra Grilo, L., Deglon, J.J., Besson, J., Croquette-Krokar, M., Carrupt, P.A., & Abriel, H. (2007). Stereoselective block of hERG channel by (s)-methadone and QT interval prolongation in *CYP2B6* slow metabolisers. *Clinical Pharmacology and Therapeutics*, 81, (5), 719-728.
- Ehret, G.B., Voide, C., Gex-Fabry, M., Chabert, J., Shah, D., Broers, B., Piguet, V., Musset, T., Gaspoz, J.M., Perrier, A., Dayer, P., & Desmeules, J.A. (2006). Drug-induced long QT syndrome in injection drug users receiving methadone high frequency in hospitalized patients and risk factors. *Archives of Internal Medicine*, 166, (12), 1280-1287.
- Eilers, H., & Schumacher, M.A. (2004). Opioid-induced respiratory depression: are 5-HT₄ receptor agonists the cure? *Molecular interventions*, 4, (4), 197-199.
- Ekhart, C., Rodenhuis, S., Smits, P.H.M., Beijnen, J.H., & Huitema, A.D.R. (2009). An overview of the relations between polymorphisms in drug metabolising enzymes and drug transporters and survival after cancer treatment. *Cancer Treatment Reviews*, 35, 18-31.
- Esteban, J., Gimeno, C., Barril, J., Aragones, A., Climent, J.M., & de la Cruz Pellin, M. (2003). Survival study of opioid addicts in relation to its adherence to methadone maintenance treatment. *Drug and Alcohol Dependence*, 70, 193-200.
- Fanoë, S., Hvidt, C., Ege, P., & Jensen, G.B. (2007). Syncope and QT prolongation among patients treated with methadone for heroin dependence in the city of Copenhagen. *Heart (British Cardiac Society)*, 93, 1051-1055.
- Faucette, S.R., Hawke, R.L., Lecluyse, E.L., Shord, S.S., Yan, B., Laethem, R.M., Lindley, C.M. (2000). Validation of bupropion hydroxylation as a selective marker of human cytochrome P450 2B6 catalytic activity. *Drug Metabolism and Disposition*, 10, 1222-1230.
- Fecho, K., Maslonek, K.A., Coussons-Read, M.E., Dykstra, L.A., & Lysle, D.T. (1994). Macrophage-derived nitric oxide is involved in the depressed concanavalin A

responsiveness of splenic lymphocytes from rats administered morphine in vivo. *The Journal of Immunology*, 152, (12), 5845-5852.

Ferguson, S.S., Zhang, J., arak, L.S., & Caron, M.G. (1996). Molecular mechanisms of G protein-coupled receptor kinases and arrestins. *Canadian Journal of Physiology and Pharmacology*, 74, 1095-1110.

Ferner, R.E. (2008). Post-mortem clinical pharmacology. *British Journal of Clinical Pharmacology*, 66, (4), 430-443.

Ferrer-Alcon, M., La Harpe, R., & García-Sevilla, J.A. (2004). Decreased immunodensities of μ -opioid receptors, receptor kinases GRK 2/6 and β -arresting-2 in post-mortem brains of opiate addicts. *Molecular Brain Research*, 121, 114–122.

Fery, Y., Mueller, S.O., & Schrenk, D. (2010). Development of stably transfected human and rat hepatoma cell lines for the species-species assessment of xenobiotic response enhancer module (XREM) –dependent induction of drug metabolism. *Toxicology*, doi:10.1016/j.tox.2010.08.008

Fonseca, F., Marti-Almor, J., Pastor, A., Cladellas, M., Farré, M., de la Torre, R., & Torrens, M. (2009). Prevalence of long QTc interval in methadone maintenance patients. *Drug and Alcohol Dependence*, 99, 327-332.

Foster, D.J.R., Somogyi, A.A., & Bochner, F. (1999). Methadone n-demethylation in human liver microsomes: lack of stereoselectivity and involvement of *CYP3A4*. *Journal of Clinical Pharmacology*, 47, 403-412.

Foster, D.J.R., Upton, R.N., Somogyi, A.A., Grant, C., & Martinez, A. (2005). The acute distribution of (r)- and (s)- methadone in brain and lung of sheep. *Journal of Pharmacokinetics and Pharmacodynamics*, 32, (3-4), 547-570.

Francisco, N.A. (2007). Control of breathing: how to better understand the respiratory effects of opioids. *European Journal of Pain Supplements*, 1, pp 61-65.

Friesen, C., Rischer, M., Alt, A., & Miltner, E. (2008). Methadone, commonly used as maintenance medication for outpatient treatment of opioid dependence, kills leukemia cells and overcomes chemoresistance. *Cancer Research*, 68, 6059-6064.

Funderburg, L.G., Vertrees, J.E., Truem J.E., & Miller, A.L. (1994). Seizures following addition of erythromycin to clozapine treatment. *American Journal of Psychiatry*, 151, 1840-1841.

Gabilondo, A.M., Meana, J.J., & Garcia-Sevilla, J.A. (1995). Increased density of μ -opioid receptors in the post-mortem brains of suicide victims. *Brain Research*, 682, 245-250.

Garrido, M.J., & Troconiz, I.F. (1999). Methadone: a review of its pharmacokinetic/pharmacodynamic properties. *Journal of Pharmacology and Toxicology Methods*, 42, 61–66.

- Geick, A., Eichelbaum, B., & Burk, O. (2001). Nuclear receptor response elements mediate induction of intestinal MDR1 by rifampicin. *Journal of Biological Chemistry*, 276, 14581-14587.
- George, S.T., Ruoho, A.E., & Malbon, C.C. N-glycosylation in expression and function of β -adrenergic receptors. (1999). *Journal of Biological Chemistry*, 261, 37-42.
- Gerber, J.G., Rhodes, R.J., & Gal, J. (2004). Stereoselective metabolism of methadone n-demethylation by cytochrome P4502B6 and 2C19. *Chirality*, 16, 36-44.
- Ghodse, H., Schifano, F., Oyefeso, A., Jambert-Gray, R., Cobain, K., & Corkery, J. (2003). Drug-related deaths as reported by participating procurators fiscal and coroners in England & Wales, Northern Ireland, Scotland, Isle of Man, Guernsey, Jersey: Annual Review 2002 and no-SAD surveillance report no. 11. Centre for Addiction Studies, St Georges Hospital Medical Hospital: London.
- Giacomini, K.M., Brett, C.M., Altman, R.B., Benowitz, N.L., Dolan, M.E., Flockhart, D.A., Johnson, J.A., Hayes, D.F., Klein, T., Krauss, R.M., Kroetz, D.L., Nguyen, A.T., Ratain, M.J., Relling, M.V., Reus, V., Roden, D.M., Schaefer, C.A., Shuldiner, A.R., Skaar, T., Tantisira, K., Tyndale, R.F., Wang, L., Weinshilboum, R.M., Weiss, S.T., & Zineh, I. (2007). The pharmacogenetics research network: from SNP discovery to clinical drug response. *Clinical Pharmacology and Therapeutics*, 81, (3), 328-345.
- Gill, M., Sala, M., Anguera, I., Chapinal, O., Cervantes, M., Guma, J.R., & Segura, F. (2003). QT prolongation and torsades de pointes in patients infected with human immunodeficiency virus and treated with methadone. *American Journal of Cardiology*, 92, 995-997.
- Goodwin, B., Moore, L.B., Stoltz, C.M., McKee, D.D., & Kliwer, S.A. (2001). Regulation of the human *CYP2B6* gene by the nuclear pregnane X receptor. *Molecular pharmacology*, 60, 427-431.
- Gossop, M., Marsden, J., Stewart, D., & Treacy, S. (2001). Outcomes after methadone maintenance treatment and methadone reduction treatments: two-year follow-up results from the National Treatment Outcome Research Study, *Drug and Alcohol Dependence*, 62, 255-264.
- Gowing LR, Farrell M, Bornemann R, Sullivan LE, Ali RL. (2006). Brief report: methadone treatment of injecting opioid users for prevention of HIV infection. *Journal of General Internal Medicine*, 21(2), 193-195.
- Grecksch, G., Bartzsch, K., Widera, A., Becker, A., Höllt, V., & Koch, T (2006). Development of tolerance and sensitization to different opioid agonists in rats. *Psychopharmacology*, 186, 177-184.
- Gupta, A., Lawrence, A.T., Krishnan, K., Kavinsky, C.J., & Trohman, R.G. (2007). Current concepts in the mechanisms and management of drug-induced QT prolongation and torsades de pointes. *American Heart Journal*, 153, 891-899.

Haga, H., Yamada, R., Ohnishi, Y., Nakamura, Y., Tanaka, T. (2002). Gene-based SNP discovery as part of the Japanese Millennium Genome Project: identification of 190 562 genetic variations in the human genome. *Journal of Human Genetics*, 47, 605-610.

Hancox, J.C., McPate, M.J., El Harchi, A., & Zhang, Y.H. (2008). The hERG potassium channel and hERG screening for drug-induced torsades de pointes. *Pharmacology and Therapeutics*, 119, 118-132.

Harding-Pink, D. (1993). Opioid toxicity, Methadone: one person's maintenance dose is another's poison. *Lancet*, 341, 665-666.

Harkcom, W.T., & Abbott, G.W. (2010). Emerging concepts in the pharmacogenomics of arrhythmias: ion channel trafficking. *Expert Review of Cardiovascular Therapy*, 8, (8), 1161-1173.

Heinemann, A., Iwersen-Bermann, S., Stein, S., Schmoldt, A., & Püschel, K. (2000). Methadone related fatalities in Hamburg 1990-1999: implications for quality standards in maintenance treatment? *Forensic Science International*, 113, 449-455.

Hesse, L.M., von Moltke, L., Shader, R.I., & Greenblatt, D.J. (2001). Ritonavir, Efavirenz, and Nelfinavir inhibit *CYP2B6* activity *in vitro*: potential drug interactions with bupropion. *Drug Metabolism and Disposition*, 29, (2), 100-102.

Hesse, L.M., He, P., Krishnaswamy, S., Hao, Q., Hogan, K., von Moltke, L.L., Greenblatt, D.J., & Court, M.H. (2004). Pharmacogenetic determinants of interindividual variability in bupropion hydroxylation by cytochrome P450 2B6 in human liver microsomes. *Pharmacogenetics*, 14, 225-238.

Heusch, W.L., & Maneckjee, R. (1998). Signalling pathways in nicotine regulation of apoptosis of human lung cancer cells. *Carcinogenesis*, 19, (4), 551-556.

Hoffmeyer S, Burk O, von Richter O, Arnold HP, Brockmoller J, John A, Cascorbi I, Gerloff T, Roots I, Eichelbaum M, Brinkmann U. (2000). Functional polymorphisms of the human multidrug-resistance gene: multiple sequence variations and correlation of one allele with P-glycoprotein expression and activity *in vivo*. *Proceedings of the National Academy of Sciences USA*, 97, 3473-3478.

Hofmann, M.H., Bliedernicht, J.K., Klein, K., Saussele, T., Schaeffeler, E., Schwab, M., & Zanger, U.M. (2008). Aberrant splicing caused by single nucleotide polymorphism c.516G>T [Q172H], a marker of *CYP2B6**6, is responsible for decreased expression and activity of *CYP2B6* in liver. *The Journal of Pharmacology and Experimental Therapeutics*, 325, (1), 284-292.

Ide, S., Han, W., Kasai, S., Hata, H., Sora, I., & Ikeda, K. (2005). Characterization of the 3' untranslated region of the human mu-opioid receptor (MOR-1) mRNA. *Gene*, 364, 139-145.

Ide, S., Kobayashi, H., Ujike, H., Ozaki, N., Sekine, Y., Inada, T., Harano, M., Komiyama, T., Yamada, M., Iyo, M., Iwata, N., Tanaka, K., Shen, H., Iwahashi, K., Itokawa, M., Minami, M., Satoh, M., Ikeda, K., & Sora, I. (2006). Linkage

- disequilibrium and association with methamphetamine dependence/psychosis of μ -opioid receptor gene polymorphisms. *The pharmacogenomics Journal*, 6, 179-188.
- Inouye, S., Tsuji, F.I. (1994). *Aequorea* green fluorescent protein: Expression of the gene and fluorescence characteristics of the recombinant protein. *FEBS Letters*, 341, 277-280.
- Ishani, D., Chakraborty, J., Gangopadhyay, P.K., Choudhury, S.R., & Das, S. (2010). Single-nucleotide polymorphism (A118G) in exon 1 of *OPRM1* gene causes alteration in downstream signalling by mu-opioid receptor and may contribute to the genetic risk for addiction. *Journal of Neurochemistry*, 112, (2), 486-496.
- Jacob, R.M., Johnstone, E.C., Neville, M.J., Walton, R.T. (2004). Identification of *CYP2B6* sequence variants by use of multiplex PCR with allele-specific genotyping. *Clinical Chemistry*, 50, 1372-1377.
- Janneto, P., Wong, S.H., Gock, S.B., Laleli-Sahin, E., Schur, B., Charles, C., & Jentzen, J.M. (2002). Pharmacogenomics as molecular autopsy for post-mortem forensic toxicology: genotyping cytochrome P450 2D6 for oxycodone cases. *Journal of Analytical Toxicology*, 26, (7), 438-447.
- Johnson, A. D., Wang, D., and Sadee, W. (2005). *Pharmacological Therapeutics*, 106, 19-38.
- Joseph, H., & Appel, P. (1985). Alcoholism and methadone treatment: Consequences for the patients and the program. *American Journal of Drug and Alcohol Abuse*, 11, 37-53.
- Justice, A.J., & de Wit, H. (1999). Acute effects of *d*-amphetamine during the follicular and luteal phases of the menstrual cycle in women. *Psychopharmacology*, 145, 67-75.
- Justice, A.J., & de Wit, H. (2000). Acute effects of *d*-amphetamine during the early and late follicular phases of the menstrual cycle in women. *Pharmacology Biochemistry and Behaviour*, 71, 259-268.
- Justo, D., Gal-Oz, A., Paran, Y., Goldin, Y., & Zeltser, D. (2006). Methadone-associated torsades de pointes (polymorphic ventricular tachycardia) in opioid-dependent patients. *Addiction*, 101, 1333-1338.
- Kantola, T., Kivisto, K.T., & Neuvonen, P.J. (1998). Erythromycin and verapamil considerably increase serum simvastatin and simvastatin acid concentrations. *Clinical Pharmacology and Therapeutics*, 64, 177-182.
- Katchman, A.N., McGroary, K.A., Kilborn, J. (2002). Influence of opioid agonists on cardiac human ether-a-go-go-related gene K (+) currents. *Journal of Pharmacology and Experimental Therapeutics*, 303, 688-694.
- Kaushik, R., Levine, B., & LaCourse, W.R. (2006). A brief review: HPLC methods to directly detect drug glucuronides in biological matrices (part I). *Analytica Chimica Acta*, 556, (2), 255-266.

Keith, D.E., Anton, B., Murray, S.R., Zaki, P.A., Chu, P.C., Lissin, D.V., Monteliliet-Agius, G., Stewart, P.L., Evans, C.J., & von Zastrow, M. (1998). Opiate drugs have differential effects on a conserved endocytic mechanism *in vitro* and in the mammalian brain. *Molecular Pharmacology*, 53, 377-384.

Kennedy, M.C. (2010). Post-mortem drug concentrations. *International Medical Journal*, 10, (3), 183-187.

Kerros, C., Cavey, T., Sola, B., Jauzac, P., & Allouche, S. (2009). Somatostatin and opioid receptors do not regulate proliferation or apoptosis of the human multiple myeloma U266 cells. *Journal of Experimental Clinical Cancer Research*, 28, (1), 77.

Kerwin, R. (1990). The answer lies within selective ligands and pharmacogenomics. *Addiction, commentaries*, 94, (7), 973-980.

Ketter, T.A., Jenkins, J.B., Schroeder, D.H., Pazzaglia, P.J., Marangell, L.B., Callahan, A.M., Hinton, M.L., Chao, J., & Post, R.M. (1995). Carbamazepine but not valproate induces bupropion metabolism. *Journal of Clinical Psychopharmacology*, 15, 327-333.

Kharasch, E.D., Walker, A., Whittington, D., & Bedynek, P.S. (2009). Methadone metabolism and clearance are induced by nelfinavir despite inhibition of P4503A (CYP3A) activity. *Drug and Alcohol Dependence*, 101, 158-168.

Kieffer, B.L. (1999). Opioids: first lessons from knockout mice. *Trends in Pharmacological Sciences*, 20, 19-26.

Kieffer, B.L. (2009). Live molecular recognition: visualizing opioid receptors trafficking *in vivo*. *Journal of Inclusion Phenomena and Macrocyclic Chemistry*, 65, 189-195.

Kienbaum, P., Heuter, T., Scherbaum, N., Gastpar, M., & Peters, J. (2002). Chronic μ -Opioid receptor stimulation alters cardiovascular regulation in humans: differential effects on muscle sympathetic and heart rate responses to arterial hypotension. *Journal of Cardiovascular Pharmacology*, 40, 363-369.

Kim, H., Yoon, Y.J., Kim, H., Kang, S., Cheon, H.G., Yoo, S.E., Shin, J.G., & Liu, K.H. (2006). Characterisation of the cytochrome P450 enzymes involved in the metabolism of a new cardioprotective agent KR-33028. *Toxicology Letters*, 166, 105-114.

Kircheiner, J., Klein, C., Meineke, I., Sasse, J., Zanger, U.M., Mürdter, T.E., Roots, I., & Brockmöller, J. (2003). Bupropion and 4-OH-bupropion pharmacokinetics in relation to genetic polymorphisms in *CYP2B6*. *Pharmacogenetics*, 13, (10), 619-626.

Klepstad, P., Dale, O., Skorpen, F., Borchgrevink, P.C., & Kaasa, S. (2005). Genetic variability and clinical efficacy of morphine. *Acta Anaesthesiologica Scandinavica*, 49, 902-908.

Kobek, M., Jabłoński, C.K., Kulikowska, J., Pieśniak, D., Chowaniec, C.Z. (2009). A rare case of lethal methadone intoxication of a 3-week infant. *Forensic Science International Supplement Series* 1, 88-90.

- Koch, T., & Höllt, V. (2008). Role of receptor internalisation in opioid tolerance and dependence. *Pharmacology and Therapeutics*, 117, pp 199-206.
- Koch, T., Krosiak, T., Mayer, P., Raulf, E., & Hollt, V. (1997). Site mutation in the rat μ -opioid receptor demonstrates the involvement of calcium/calmodulin-dependent protein kinase II in agonist-mediated desensitization. *Journal of Neurochemistry*, 69, 1767-1770.
- Koch, T., Schulz, S., Schröder, H., Wolf, R., Raulf, E., & Höllt, V. (1998). Carboxyl-terminal splicing of the rat μ -opioid receptor modulates agonist-mediated internalization and receptor resensitization. *Journal of Biological Chemistry*, 273, 13652-13657.
- Koch, T., Widera, A., Bartsch, K., Schulz, S., Brandenburg, L.O., Wundrack, N., Beyer, A., Grecksch, G., & Höllt, V. (2005). Receptor endocytosis counteracts the development of opioid tolerance. *Molecular Pharmacology*, 67, 280-287.
- Kornick, C.A., Kilborn, M.J., Santiago-Palma, J., Thaler, H.T., Keefe, D.L., Katchman, A.N., Pezzullo, J.C., Ebert, S.N., Woosley, R.L., Payne, R., & Manfredi, P.L. (2003). QTc interval prolongation associated with intravenous methadone. *Pain*, 105, 499-506.
- Kupiec, T.C., Raj, V., & Vu, N. (2006). Pharmacogenomics for the forensic toxicologist. *Journal of Analytical Toxicology*, 30, 65-72.
- Kraus, J., Borner, C., Giannini, E., Hickfang, K., Braun, H., Mayer, P., Hoehe, M.R., Ambrosch, A., König, W., & Hollt, V. (2001). Regulation of μ -Opioid receptor gene transcription by interleukin-4 and influence of an allelic variation within a STAT6 transcription factor binding site. *The Journal of Biological Chemistry*, 276, (47), 43901-43908.
- Kraus, J., Borner, C., Giannini, E., & Hollt, V. (2003). The role of nuclear factor kappaB in tumor necrosis factor-regulated transcription of the human mu-opioid receptor gene. *Molecular Pharmacology*, 64, (4), 876-884.
- Krantz, M.J., Lewkowiez, L., Hays, H., Woodroffe, M.A., Robertson, A.D., & Mehler, P.S. (2002). Torsades de pointes associated with very-high-dose methadone. *Annals of Internal medicine*, 137, 501-504.
- Kreek, M.J. (1978). Medical complications in methadone patients. *Annals of the New York Academy of Sciences*, 311, 110-134.
- Kreek, M.J. (1996). Opioid receptors: some perspectives from early studies of their role in normal physiology, stress responsivity, and in specific addictive diseases. *Neurochemical Research*, 21: 1469–1488.
- Kreek, M.J., Bart, G., Lilly, C., LaForge, K.S., & Nielsen, D.A. (2005). Pharmacogenetics and human molecular genetics of opiate and cocaine addictions and their treatments. *Pharmacological Reviews*, 57, 1-26.

- Kroslak, T., LaForge, K.S., Gianotti, R.J., Ho, A., Nielsen, D.A., & Kreek, M.J. (2007). The single nucleotide polymorphism A118G alters functional properties of the human mu opioid receptor. *Journal of Neurochemistry*, 103, 77-87.
- Joseph, R., & Moselhy, H.F. (2005). National survey of methadone prescribing for maintenance treatment: 'opiophobia' among substance misuse services? *Psychiatric Bulletin*, 29, 459-461.
- Laberke, P.J., & Bartsch, C. (2010). Trends in methadone-related deaths in Zurich. *International Journal of Legal Medicine*, DOI: 10.1007/s00414-010-0442-8.
- Lahiri, D.K., & Schnabel, B. (1993). DNA isolation by a rapid method from human blood samples: effects of MgCl₂, EDTA, storage, time, and temperature on DNA yield and quality. *Biochemical Genetics*, 31, (7-8), 321-328.
- Lalley, P.M., 2003. μ -opioid receptor effects on medullary respiratory neurons in the cat: evidence for involvement in certain types of ventilatory disturbances. *American Journal of Physiology, Regulatory, Integrative and Comparative Physiology*, 285, R1287–R1304.
- Lalley, P.M., 2004. D1-dopamine receptor agonists reverse respiratory network depression by opioids, increase CO₂ reactivity. *Respiratory Physiology and Neurobiology*, 139, 247–262.
- Lalley, P.M. (2005). D1-dopamine receptor blockade slows respiratory rhythm and enhances opioid-mediated depression. *Respiratory Physiology and Neurobiology*, 145, 13-22.
- Lamba, V., Lamba, J., Yasuda, K., Strom, S., Davila, J., Hancock, M.L., Fackenthal, J.D., Rogan, P.K., Ring, B., Wrighton, S.A., Schuetz, E.G. (2003). Hepatic *CYP2B6* expression: gender and ethnic differences and relationship to *CYP2B6* genotype and CAR (Constitutive Androstane Receptor) expression. *The Journal of Pharmacology and Experimental Therapeutics*, 307, (3), 906-922.
- Lang, T., Klein, K., Fischer, J., Nussler, A.K., Neuhaus, P., Hofmann, U., Eichelbaum, M., Schwab, M., & Zanger, U.M (2001). Extensive genetic polymorphism in the human *CYP2B6* gene with impact on expression and function in human liver. *Pharmacogenetics*, 11, (5), 399-415.
- Law, P.Y., Erickson, L.J., El-Kouhen, R., Dicker, L., Solberg, J., Wang, W., Miller, E., Burd, A.L., & Loh, H.H. (2000). Receptor density and recycling affect the rate of agonist-induced desensitization of μ -opioid receptor. *Molecular Pharmacology*, 58, 388-398.
- Lawford, B.R., Young, R.M., Noble, E.P., Sargent, J., Rowell, J., Shadforth, S., Zhang, X., & Ritchie, T. (2000). The D2 dopamine receptor A1 allele and opioid dependence: association with heroin use and response to methadone treatment. *American Journal of Medical Genetics*, 96B, 592-598.
- LeCluyse, E., Madan, A., Hamilton, G., Carroll, K., DeHaan, R., & Parkinson, A. (2000). Expression and regulation of cytochrome P450 enzymes in primary cultures

of human hepatocytes. *Journal of Biochemical and Molecular Toxicology*, 14, 177-188.

Lee, S.J., Jang, Y.J., Cha, E.Y., Kim, H.S., Lee, S.S., & Shin, J.G. (2010). A haplotype of *CYP2C9* associated with warfarin sensitivity in mechanical heart valve replacement patients. *British Journal of Clinical Pharmacology*, 70, (2), 213-221.

Lehmann, J.M., McKee, D.D., Watson, M.A., Willson, T.M., Moore, J.T., Kliewer, S. A. (1998). The human orphan nuclear receptor PXR is activated by compounds that regulate *CYP3A4* gene expression and cause drug interactions. *The Journal of Clinical Investigation*, 102, 1016-1023.

Lehotay, D.C., George, S., Etter, M.L., Graybiel, K., Eichhorst, J.C., Fern, B., Wildenboer, W., Selby, P., & Kapur, B. (2005). Free and bound enantiomers of methadone and its metabolite, EDDP in methadone maintenance treatment: relationship to dosage. *Clinical Biochemistry*, 38, 1088-1094.

Lemaire, G., de Sousa, G., & Rahmani, R. (2004). A PXR reporter gene assay in a stable cell culture system: *CYP3A4* and *CYP2B6* induction by pesticides. *Biochemical Pharmacology*, 68, 2347-2358.

Léna, I., Bradshaw, S., Pintar, J., & Ktchen, I. (2008). Adaptive changes in the expression of central opioid receptors in mice lacking the dopamine D2 receptor gene. *Neuroscience*, 153, (3), 773-788.

Lewanowitsch, T., White, J.M., & Irvine, R.J. (2004). Use of radiotelemetry to evaluate respiratory depression produced by chronic methadone administration. *European Journal of Pharmacology*, 484, 303-310.

Lex, B.W. (1991). Some gender differences in alcohol and polysubstance users. *Health Psychology*, 10, (2), 121-132.

Li, H., Ferguson, S., & Wang, H. (2010). Synergistically enhanced *CYP2B6* inducibility between a polymorphic mutation in *CYP2B6* promoter and PXR activation. *Molecular Pharmacology*, doi: 10.1124/mol.110.065185.

Li, J.L., Wang, X.D., Chen, S.Y., Liu, L.S., Fu, Q., Chen, X., Teng, L.C., Wang, C.X., & Huang, M. (2010). Effects of diltiazem on pharmacokinetics of tacrolimus in relation to *CYP3A5* genotype status in renal recipients: from retrospective to prospective. *Pharmacogenomics*, doi: 10.1038/tpj.2010.42.

Liang, H.R., Foltz, R.L., Meng, M., & Bennet, P. (2004). Method development and validation for quantitative determination of methadone enantiomers in human plasma by liquid chromatography/tandem mass spectrometry. *Journal of Chromatography B*, 806, 191-198.

Liang, W.J., Johnson, D., & Jarvis, S.M. (2001). Vitamin C transport systems of mammalian cells. *Molecular Membrane Biology*, 18, 87-95.

Lin, C, Somberg, T, Molnar, J, & Somberg, H. (2009). The effects of chiral isolates of methadone on the cardiac potassium channel IKr. *Cardiology* 113: 59-65.

- Lintzeris, N., Mitchell, T.B., Bond, A.J., Nestor, L., & Strang, J. (2007). Pharmacodynamics of diazepam co-administered with methadone or buprenorphine under high dose conditions in opioid dependent patients. *Drug and Alcohol Dependence*, 91, 187-194.
- Lintzeris, N., & Nielsen, S. (2010). Benzodiazepines, methadone and buprenorphine: interactions and clinical management. *American Journal of Addictions*, 19, (1), 59-72.
- Lukas, S.E., & Wetherington, C.L. (2005). Sex- and gender-related differences in neurobiology of drug abuse. *Clinical Neuroscience Research*, 5, (2-4), 75-87.
- Lötsch, J., Zimmermann, M., Darimont, J., Marx, C., Dudziak, R., Skarke, C., & Geisslinger, G. (2002). Does the A118G polymorphism at the μ -opioid receptor gene protect against morphine-6-glucuronide toxicity? *Anesthesiology*, 97, 814-819.
- Lötsch, J., & Geisslinger, G.A. (2005). Are μ -opioid receptor polymorphisms important for clinical opioid therapy? *Trends in Molecular Medicine*, 11, (2) 82-89.
- Lötsch, J., Skarke, C., Wieting, J., Oertel, B.G., Schmidt, H., Brockmoller, J., & Geisslinger, G. (2006). Modulation of the central nervous effects of levomethadone by genetic polymorphisms potentially affecting its metabolism, distribution, and drug action. *Clinical Pharmacology and Therapeutics*, 79, (1), 72-89.
- Luttrell, L.M., Daaka, Y., Della Rocca, G.J., & Lefkowitz, G. (1997). G protein-coupled receptors mediate two functionally distinct pathways of tyrosine phosphorylation in rat I a fibroblasts. *Journal of Biological Chemistry*, 272, 31648-31656.
- Lutrell, L.M., Ferguson, S.S.G., Daaka, Y., Miller, W.E., Maudsley, S., Della Rocca, G.J., Lin, F.T., Kawakatsu, H., Owada, K., Luttrell, D.K., Caron, M.G., & Lefkowitz, R.J. (1999). β -arrestin-dependent formation of β_2 adrenergic receptor-Src protein kinase complexes. *Science*, 283, 655-661.
- Magnusson, M.O., Dahl, M-L., Cederberg, J., Karlsson, M.O., & Sandström, R. (2008). Pharmacodynamics of carbamazepine-mediated induction of *CYP3A4*, *CYP1A2*, and Pgp as assessed by probe substrates midazolam, caffeine, and digoxin. *Clinical Pharmacology and Therapeutics*, 84, (1), 52-62.
- Mague, S.D., Isiegas, C., Huang, P., Liu-Chen, L.Y., Lerman, C., & Blendy, J.A. (2009). Mouse model of *OPRM1* (A118G) polymorphism has sex-specific effects on drug-mediated behaviour. *Proceedings of the National Academies of Sciences*, 106, (26), 10847-10852.
- Mäkinen, J., Frank, C., Jyrkkärinne, J., Gynther, J., Carlberg, C., & Honakoski, P. (2002). Modulation of mouse and human phenobarbital-responsive enhancer module by nuclear receptors. *Molecular Pharmacology*, 62, (2), 366-378.
- Maneckjee, R., & Minna J.D. (1994). Opioids induce while nicotine suppresses apoptosis in human lung cancer cells. *Cell Growth and Differentiation*, 5, (1), 1033-1040.

Maneckjee, R., & Heusch, W.L. (1999). Effects of bombesin on methadone –induced apoptosis of human lung cancer cells. *Cancer Letters*, 136, (2), 177-185.

Manfredi, P.L., Gonzales, G.R., Cheville, A.L., Kornick, C., & Payne, R. (2001). Methadone analgesia in cancer patients on chronic methadone maintenance therapy. *Journal of Pain Symptom Management*, 21, 169-174.

Mao, J., Sung, B., Ji, R.R., & Lim, G. (2002). Neuronal apoptosis associated with morphine tolerance: evidence for an opioid-induced neurotoxic mechanism. *The Journal of Neuroscience*, 22, (17), 7650-7661.

Martell, B.A., Arnsten, J.H., Krantz, M.J., & Gourevitch, M.N. (2005). Impact of methadone treatment on cardiac repolarization and conduction in opioid users. *The American Journal of Cardiology*, 95, 915-918.

Maxwell, J.C., Pullum, T.W., & Tannert, K. (2005). Deaths of clients in methadone treatment in Texas: 1994-2002. *Drug and Alcohol Dependence*, 78, 73-81.

McCormack, J.E., Baybut, H.N., Everington, D., Will, R.G., Ironside, J.W., & Manson, J.C. (2002). *PRNP* contains both intronic and upstream regulatory regions that may influence susceptibility to Creutzfeldt-Jakob Disease. *Gene*, 288, pp 139-146.

McCormick, G.Y., White, W.J., Zagon, I.S., Lang, C.M. (1984). Effects of diazepam on arterial blood gas concentrations and pH of adult rats acutely and chronically exposed to methadone. *Journal of Pharmacology and Experimental Therapeutics*, 230, 353-359.

McDonald, D.M. (1981). *Peripheral chemoreceptors in regulation of breathing*. New York, Dekker.

Megarbane, B., Decleves, X., Bloch, V., Bardin, C., Chast, F., & Baud, F.J. (2007). Case report: quantification of methadone-induced respiratory depression using toxicokinetic/toxicodynamic relationships. *Critical Care*, 11, (1), R5.

Mehrishi, J.N., & Mills, H. (1983). Opiate receptors on lymphocytes and platelets in man. *Clinical Immunology and Immunopathology*, 27, 240-249.

Meiler A, Mino A, Chatton A, Broers B (2005) Benzodiazepine use in a methadone maintenance programme: patient characteristics and the physician's dilemma. *Shweizer Archiv für Neurologie und Psychiatrie* 156: 310-317.

Mestek, A., Hurley, J.H., Bye, L.S., Campbell, A.D., Chen, Y., Tian, M. Liu, J., Schulman, H., & Yu, L. (1995). The human mu opioid receptor: modulation of functional desensitization by calcium/calmodulin-dependent protein kinase and protein kinase c. *Journal of Neuroscience*, 15, (2), 2396-2406.

Mills, R.E., Luttig, C.T., Larkin, C.E., Beauchamp, A., Tsui, C., Pittard, W.S., & Devine, S. (2006). An initial map of insertion and deletion (INDEL) variation in the human genome. *Genome Research*, 16, 1182-1190.

- Milroy, C.M., & Forrest, A.R.W. (2000). Methadone death: a toxicological analysis, *Journal of Clinical Pathology*, 53, 277-281.
- Modesto-Lowe, V., Brooks, D., & Petry, N. (2010). Methadone deaths: risk factors in pain and addicted populations. *Journal of General Internal Medicine*, 25, (4), 305-309.
- Moffat, A.C., M.D. Osselton, B. Widdop (Eds.), *Clarke's analysis of drugs, third edition*. 1233 (Pharmaceutical Press, London, 2004).
- Montagna, P. (2007). Recent advances in the pharmacogenomics of pain and headache. *Neurological Sciences*, 28, S208-S212.
- Moriya, F., & Hashimoto, Y. (1999). Redistribution of basic drugs into cardiac blood from surrounding tissues during early-stages post-mortem. *Journal of Forensic Sciences*, 44, (1), 10-16.
- Munafò, M.R., Elliot, K.M., Murphy, M.F., Walton, R.T., & Johnstone, E.C. (2007). Association of the mu-opioid receptor gene with smoking cessation. *Pharmacogenomics Journal*, 7, (5), 353-361.
- Mutolo, D., Bongianini, F., Einum, J., Dubuc, R., & Pantaleo, T. (2007). Opioid-induced depression in the lamprey network. *Neuroscience*, 150, 720-729.
- Nakamura, Y. (2008). Pharmacogenomics and Drug Toxicity. *New England Journal of Medicine*, 359, 856-858.
- Nallani, S.C., Glauser, T.A., Hariparsad, N., Setchell, K., Buckley, D.J., Buckley, A.R., & Desai, P.B. (2003). Dose-dependent induction of cytochrome P450 (CYP) 3A4 and activation of pregnane x receptor by topiramate. *Epilepsia*, 44, (12), 1521-1528.
- Neeleman, J., & Farrell, M. (1997). Fatal methadone and heroin overdoses: time trends in England and Wales. *Journal of Epidemiology and Community Health*, 51, 435-437.
- Nettleton, R.T., Ransom, T.A., Abraham, S.L., Nelson, C.S., & Olsen, G.D. (2007). Methadone-induced respiratory depression in the neonatal guinea pig. *Pediatric Pulmonology*, 42, pp 1134-1143.
- Nocarova, E., & Fisher, L. (2009). Cloning of transgenic tobacco BY-2 cells; an efficient method to analyse and reduce high natural heterogeneity of transgene expression. *BMC Plant Biology*, 9, 44-56.
- Oertel, B.G., Schmidt, R., Schneider, A., Geisslinger, G., & Lötsch, J. (2006). The μ -opioid receptor gene polymorphism 118A>G depletes alfentanil-induced analgesia and protects against respiratory depression in homozygous carriers. *Pharmacogenetics and Genomics*, 16, 625-636.
- Osselton, M.D., Blackmore, R.C., King, L.A., & Moffat, A.C. (1984). Poisoning-associated deaths for England and Wales between 1973 and 1980. *Human Toxicology*, 3, 201-221.

- Paice, J.A. (2007). Pharmacokinetics, pharmacodynamics, and pharmacogenomics of opioids. *Pain Management Nursing*, 8, (3), S2-S5.
- Pak, Y., O'Dowd, B.F., Wang, J.B., & George, S.R. (1999). Agonist-induced, G protein-dependent and -independent down-regulation of the mu opioid receptor. The receptor is a direct substrate for protein-tyrosine kinase. *Journal of Biological Chemistry*, 274, 27610-27616.
- Paparella, M., Kolossov, E., Fleischmann, B.K., Hescheler, J., & Bremer, S. (2002). The use of quantitative image analysis in the assessment of in vitro embryotoxicity endpoints based on a novel embryonic stem cell clone with endotherm-related GFP expression. *Toxicology in Vitro*, 16, 589-597.
- Park, B.K. (2000). Cytochrome P450 enzymes in the heart. *The Lancet*, 355, 945-946.
- Pascussi, J.M., Busson -Le Coniat, M., Maurel, P., & Vilarem, M.J. (2003). Transcriptional analysis of the orphan nuclear receptor constitutive androstane receptor (NR113) gene promoter: identification of a distal glucocorticoid response element. *Molecular Endocrinology*, 17, (1), 42-55.
- Pearson, E.C., & Woosley, R.L. (2005). QT prolongation and torsades de pointes among methadone users: reports to the FDA spontaneous reporting system. *Pharmacoepidemiological Drug Safety*, 14, 747-53.
- Peris, J., Decambre, C.H., Coleman-Hardee, M.L., & Simpkins, J.W. (1991). Estradiol enhances behavioural sensitization to cocaine and amphetamine-stimulated striatal [³H] dopamine release. *Brain Research*, 566, 255-264.
- Perez-Alvarez, S., Cuenca-Lopez, M.D., de Mera, R.M., Puerta, E., Karachitos, A., Bednarczyk, P., Kmita, H., Aguirre, N., Galindo, M.F., & Jordán, J. (2010). Methadone induces necrotic-like death in SH-SY5H cells by an impairment of mitochondrial ATP synthesis. *Biochimica et Biophysica Acta*, 1802, (11), 1036-1047.
- Pérez-Arellano, I., & Pérez-Martínez, G. (2003). Optimization of the green fluorescent protein (GFP) expression from a lactose-inducible promoter in *Lactobacillus casei*. *FEMS Microbiology Letters*, 222, 123-127.
- Pfeiffer, M., Koch, T., Schröder, H., Laugsch, M., Höllt, V., & Schulz, S. (2002). Heterodimerization of somatostatin and opioid receptors cross-modulates phosphorylation, internalization and desensitization. *Journal of Biological Chemistry*, 277, (22), 19762-19772.
- Pham-Huy, C., Chikhi-Chorfi, N., Galons, H., Sadeg, N., Laqueille, X., Aymnard, N., Massicot, F., Warnet, J.M., & Claude, J.R. (1997). Enantioselective high-performance liquid chromatography determination of methadone enantiomers and its major metabolite in human biological fluids using a new derivatized cyclodextrin-bonded phase. *Journal of Chromatography B*, 700, 155-163.
- Phillips, E.J., & Mallal, S.A. (2010). Pharmacogenetics of drug hypersensitivity. *Pharmacogenomics*, 11, (7), 973-987.

- Pimentel, L., & Mayo, D. (2008). Chronic methadone therapy complicated by torsades de pointes: a case report. *Clinical Communications: Adults*, 34, (3), 287-290.
- Pirmohamed, M. (2001). Pharmacogenetics and pharmacogenomics. *Journal of Clinical Pharmacology*, 52, 345-347.
- Plant, N. (2007). The human cytochrome P450 sub-family: transcriptional regulation, inter-individual variation and interaction networks. *Biochimica et Biophysica Acta*, 1770, 478-488.
- Poisnel, G., Dhilly, M., Le Boisselier, R., Barré, L., & Debruyne, D. (2009). Comparison of five benzodiazepine-receptor agonists on buprenorphine-induced μ -opioid receptor regulation. *Journal of Pharmacological Science*, 110, 36-46.
- Pounder, D.J., & Jones, G.R. (1990). Post-mortem drug redistribution – a toxicological nightmare. *Forensic Science International*, 45, (3), 253-263.
- Preston, K.L., Griffiths, R.R., Cone, E.J., Darwin, W.D., & Gorodetzky, C.W. (1986). Diazepam and methadone blood levels following concurrent administration of diazepam and methadone. *Drug and Alcohol Dependence*, 18, (2), 195-202.
- Prouty, R.W., & Anderson, W.H. (1990). The forensic implications and temporal influence on post-mortem blood-drug concentrations. *Journal of Forensic Science*, 35, 243-270.
- Quinney, S.K., Haehner, B.D., Rhoades, M.B., Lin, Z., Gorski, J.C., & Hall, S.D. (2008). Interaction between midazolam and clarithromycin in the elderly. *British Journal of Clinical Pharmacology*, 65, (1), 98-109.
- Raaska, K., & Neuvonen, P.J. (1998). Serum concentration of clozapine and N-desmethylclozapine are unaffected by the potent *CYP3A4* inhibitor itraconazole. *European Journal of Clinical Pharmacology*, 54, 167-170.
- Rebbeck, T.R., Jaffe, J.M., Walker, A.H., Wein, A.J., & Malkowicz, S.B. (1998). Modification of clinical presentation of prostate tumors by a novel genetic variant in *CYP3A4*. *Journal of the National Cancer Institute*, 90, 1225-1229.
- Rencurel, F., Stenhouse, A., Hawley, S.A., Friedberg, T., Hardies, D.G., Sutherland, C., & Wolf, C.R. (2005). AMP-activated protein kinase expression mediates Phenobarbital induction of *CYP2B6* gene expression in hepatocytes and a newly derived human hepatoma cell line. *The Journal of Biological Chemistry*, 280, (6), 4367-4373.
- Reyes-Gibby, C.C., Shete, S., Rakvåg, T., Bhat, S.V., Skorpen, F., Bruera, E., Kaasa, S., & Klepstad, P. (2007). Exploring joint effects of genes and the clinical efficacy of morphine for cancer pain: *OPRM1* and *COMT* genes. *Pain*, 130, 25-30.
- Reynaud, M., Petit, G., Potard, D., & Coutry, P. (1998). Six deaths linked to concomitant use of buprenorphine and benzodiazepines. *Addiction*, 93, 1385-1392.
- Ribera, E., Pou, L., Lopez, R.M., Crespo, M., Falco, V., Ocana, I., Ruiz, I., & Pahissa, A. (2001). Pharmacokinetic interaction between nevirapine and rifampicin in HIV-

- infected patients with tuberculosis. *Journal of Acquired Immune Deficiency Syndrome*, 28, 450-453.
- Riccardi, C., & Nicoletti, I. (2006). Analysis of apoptosis by propidium iodide staining and flow cytometry. *Analysis of apoptosis by propidium iodide staining and flow cytometry. Nature Protocols*, 1, 1458-1461.
- Richter, T., Murdter, T.E., Heinkle, G., Pleiss, J., Tatzel, S., Schwab, M., Eichelbaum, M., Zanger, U.M. (2004). Pharmacological mechanism-based inhibition of human *CYP2B6* by clopidogrel and ticlopidine. *Journal of Pharmacology and Experimental Therapeutics*, 308, 189-197.
- Ripamonti, C., Zecca, E., Bruera, E. (1997). An update on the clinical use of methadone for cancer pain. *Pain*, 70, 109-115.
- Roberts, J., Le Morvan, V., Smith, D., Pourquier, P., & Bonnet, J. (2005). Predicting drug response and toxicity based on gene polymorphisms. *Critical Reviews in Oncology/ Hematology*, 54, 171-196.
- Robertson, S., Maldarelli, F., Natarajan, V., Formentini, E., Alfaro, R.M., & Penzak., S.R. (2008). Efavirenz induces *CYP2B6*-mediated hydroxylation of bupropion in healthy subjects. *Journal of Acquired Immune Deficiency Syndromes*, 49, (5), 513-519.
- Rockman, M.V., & Wray, G.A. (2002). Abundant material for cis-regulatory evolution in humans. *Molecular Biology and Evolution*, 19, (11), 1991-2004.
- Rodriguez Rosas, M.E., Preston, K.L., Epstein, D.H., Moolchan, E.T., & Wainer, I.W. (2003). Quantitative determination of the enantiomers of methadone and its metabolite (EDDP) in human saliva by enantioselective liquid chromatography with mass spectrometric detection. *Journal of Chromatography B*, 796, 355-370.
- Romberg, R.R., Olofsen, E., Bijil, H., Taschner, P.E.M., Teppema, L.J., Sarton, E.Y., Van Kleef, J.W., & Dahan, A. (2005). Polymorphism of μ -opioid receptor gene (*OPRM1*: c.118A>G) does not protect against opioid-induced respiratory depression despite reduced analgesic response. *Anesthesiology*, 102, 522-530.
- Romelsjö, A., Engdahl, B., Stenbacka, M., Fugelstad, A., Davstad, I., Leifman, A., & Thiblin, I. (2010). Were the changes to Sweden's maintenance treatment policy 2000-06 related to changes in opiate-related mortality and morbidity? *Addiction*, 105, (9), 1625-1632.
- Ross, J.R., Rutter, D., Welsh, K., Joel, S.P., Goller, K., Wells, A.U., Du Bois, R., Riley, J. (2005). Clinical response to morphine in cancer patients and genetic variation in candidate genes. *The pharmacogenomics Journal*, 5, 324-336.
- Ross, K.S., Haites, N.E., & Kelly, K.F. (1990). Repeated freezing and thawing of peripheral blood and DNA in suspension: effects on DNA yield and integrity. *Journal of Molecular Genetics*, 27, 569-570.

- Roth, M.E., Cosgrove, K.P., & Carroll, M.E. (2004). Sex differences in the vulnerability to drug abuse: a review of preclinical studies. *Neuroscience and Biobehavioural Reviews*, 28, (6), 533-546.
- Routhier, D.D., Katz, K.D., & Brooks, D.E. (2006). QTc prolongation and torsades de pointes associated with methadone therapy. *Clinical Communications*, 32, (3), 275-278.
- Rudaz, S., & Veuthey, J.L. (1996). Stereoselective determination of methadone in serum by HPLC following solid-phase extraction on disk. *Journal of Pharmaceutical and Biomedical Analysis*, 14, 1271-1279.
- Runge, D., Köhler, C., Kostrubsky, V.E., Jäger, D., Lehmann, T., Runge, D.M., May, U., Beer Stolz, D., Strom, S.C., Fleig, W.E., & Michalopoulos, G.K. (2000). Induction of cytochrome P450 (CYP)1A1, *CYP1A2*, and *CYP3A4* but not of *CYP2C9*, *CYP2C19*, multidrug resistance (MDR-1) and multidrug resistance associated protein (MRP-1) by prototypical inducers in human hepatocytes. *Biochemical and Biophysical Research Communications*, 273, 333-341.
- Sagrieya, H., Berube, C., Wen, A., Ramakrishnan, R., Mir, A., Hamilton, A., & Altman, R.B. (2010). Extending and evaluating a warfarin dosing algorithm that includes *CYP4F2* and pooled rare variants of *CYP2C9*. *Pharmacogenetics and Genomics*, 20, (7), 407-413.
- SAMHSA, National Household Survey on Drug Abuse Series: H-12, 2000. Summary of findings from the 1999 National Household Survey on Drug Abuse, DHHS Publication Number (SMA) 00-3466, Rockville, MD.
- SAMHSA, National Household Survey on Drug Abuse Series: H-34, 2008. Results from the 2007 National Survey on Drug Use and Health: National Findings, DHHS Publication Number (SMA) 08-4343, Rockville, MD.
- Sánchez Hernández, A.M., AtinENZA Fernández, F., Arenal Maíz, A., González Torrecilla, E., Puchol Calderón, A., & Almendral Garrote, J. (2005). Torsades de pointes during methadone treatment. *Revista Española Cardiología*, 58, (10), 1230-1232.
- Santiago, T.V., Pugliese, A.C., & Edelman, N.H., (1977). Control of breathing during methadone addiction. *American Journal of Medicine*, 62, 347-354.
- Savas, S. (2010). Useful genetic variation databases for oncologist investigating the genetic basis of variable treatment response and survival in cancer. *Acta Oncologica*, doi: 10.3109/0284186X.2010.500297.
- Sawe, J. (1986). High-dose morphine and methadone in cancer patients. Clinical pharmacokinetic considerations of oral treatment. *Clinical Pharmacokinetics*, 11, 87-106.
- Sawyer, M.B., Innocenti, F., Das, S., Cheng, C., Ramirez, J., Pantle-Fisher, F.H., Wright, C., Badner, J., Pei, D., Boyett, J.M., Cook, .E., & Ratain, M.J. (2003). A

pharmacogenetic study of uridine diphosphate-glucuronosyltransferase 2B7 in patients receiving morphine. *Clinical Pharmacology and Therapeutics*, 73, 566-574.

Schminder, J., Greenblatt, D.J., von Moltke, L.L., & Shader, R.I. (1996). Relationship of *in vitro* data on drug metabolism to *in vivo* pharmacokinetics and drug interactions: Implications for diazepam disposition in humans. *Journal of Clinical Psychopharmacology*, 16, 267-272.

Schulz, M., & Schmoldt, A. (2003). Therapeutic and toxic blood concentrations of more than 800 drugs and other xenobiotics. *Pharmazie*, 58, 447-474.

Selley, D.E., Liu, Q., & Childers, S.R. (1998). Signal transduction correlates of mu opioid agonist intrinsic efficacy: receptor-stimulated [³⁵S] GTPγS binding in mMOR-CHO cells and rat thalamus. *The Journal of Pharmacology and Experimental Therapeutics*, 285, (2), 496-505.

Shah, N.S., Patel, V.O., & Donald, A.G. (1979). Effect of diazepam, desmethyylimipramine, and SKF 525-A on the disposition of levo-methadone in mice after single or double injection. *Drug Metabolism and Disposition*, 7, 241-242.

Shields, L.B.E., Hunsaker III, J.C., Corey, T.S., Ward, M.K., Stewart, D. (2007). Methadone toxicity fatalities: A review of medical examiner cases in a large metropolitan area. *Journal of Forensic Sciences*, 52, (6), 1389-1395.

Silverman, D.A.N., Nettleton, R.T., Spencer, K.B., Wallisch, M., & Olsen, G.D. (2009). S-Methadone augments R-methadone induced respiratory depression in the neonatal guinea pig. *Respiratory Physiology and Neurobiology*, 169, 252-261.

Skorpen, F., & Laugsand, E.A. (2008). Variable response to opioid treatment: any genetic predictors within sight? *Palliative medicine*, 22, 310-327.

Skjervold, B., Bathen, J., & Spigset, O. (2006). Methadone and the QT interval. Relations to the serum concentrations of methadone and its enantiomers (*R*)-methadone and (*S*)-methadone. *Journal of Clinical Psychopharmacology*, 6, 687-689.

Spaulding, T.C., Minium, L., Kotake, A.N., & Takemore, A.E. (1974). The effect of diazepam on the metabolism of methadone by the liver of methadone dependent rats. *Drug Metabolism and Disposition*, 2, 458-463.

Sueyoshi, T., Kawamoto, T., Zelko, I., Honkakoski, P., & Negishi, M. (1999). The repressed nuclear receptor CAR responds to Phenobarbital in activating the human *CYP2B6* gene. *The Journal of Biological Chemistry*, 274, (10), 6043-6045.

Sullivan, H.R., & Due, S.L. (1973). Urinary metabolites of DL-methadone maintenance subjects. *Journal of Medicinal Chemistry*.

Sunjic, S., & Zador, D. (1999). Methadone syrup-related deaths in New South Wales, Australia, 1990-95. *Drug and Alcohol Review* 18, 409-415.

Suzuki, Y., Sugai, T., Fukui, N., Watanabe, J., Ono, S., Inoue, Y., Ozdemir, V., & Someya, T. (2010). *CYP2D6* genotype and smoking influence fluvoxamine steady-

state concentration in Japanese psychiatric patients: lessons for genotype-phenotype association study design in translational pharmacogenetics. *Journal of Psychopharmacology*, doi: 10.1177/0269881110370504.

Tagliaro, F., & De Battisti, Z. (1999). Comments on White & Irvine's "Mechanisms of fatal opioid overdose". *Addiction*, 94, (7), 973-980.

Takeda, S., Eriksson, L., Yamamoto, Y., Joensen, H., Onimaru, H., & Lindahl, S.G. (2001). Opioid action on respiratory neuron activity of the isolated respiratory network in newborn rats. *Anesthesiology*, 95, (3), 740-749.

Tegeder, I., Grosch, S., Schmidtko, A., Haussler, A, Schmidt, H., Niederberger, E., Scholich, K., & Gesslinger, G. (2003). G protein-independent G(1) cell cycle block and apoptosis with morphine in adenocarcinoma cells: involvement of p53 phosphorylation. *Cancer Research*, 63, 1846-1852.

Tegeder, I., & Geisslinger, G. (2004). Opioids as modulators of cell death and survival – unravelling mechanisms and revealing new indications. *Pharmacological Reviews*, 56, (3), 351-369.

The International HapMap Consortium. (2003). The international HapMap project. *Nature*, 789-796.

Thompson, S.J., Koszdin, K., & Bernards, C.M. (2000). Opiate-induced analgesia is increased and prolonged in mice lacking P-glycoprotein. *Anesthesiology*, 92, 1392-1399.

Tomlinson, B., Young, R.P., Ng, M.C.Y., Anderson, P.J., Kay, R., & Critchley, J.A.J.H. (1996). Selective liver enzyme induction by carbamazepine and phenytoin in Chinese epileptics. *European Journal of Clinical Pharmacology*, 50, 411-415.

Toskulkao, T., Pornchai, R., Akkarapatumwong, V., Vatanatunyakum, S., & Govitrapong, P. (2010). Alteration of lymphocyte opioid receptors in methadone maintenance subjects. *Neurochemistry International*, 56, 285-290.

Town, T., Abdullah, L., Crawford, F., Schinka, J., Ordorica, P.I., Francism E., Hughes, P., Duara, R., Mullan, M. (1999) Association of a functional μ -opioid receptor allele (C118A) with alcohol dependency. *American Journal of Medical Genetics*, 88, 458–461.

Trapaidze, N., Gomes, I. Cvejic, S., Bansinath, M., & Devi, L.A. (2000). Opioid receptor endocytosis and activation of MAP kinase pathway. *Molecular Brain Research*, 76, 220-228.

Tross S, Campbell AN, Cohen LR, Calsyn, D., Pavlicova, M., Miele, G.M., Hu, M.C., Haynes, L., Nugent, N., Gan, W., Hatch-Maillette, M., Mandler, R., McLaughlin, P., El-Bassel, N., Crits-Christoph, P., & Nunes, E.V. (2008). Effectiveness of HIV/STD sexual risk reduction groups for women in substance abuse treatment programs: results of NIDA Clinical Trials Network Trial. *Journal of Acquired Immune Deficiency Syndromes*, 48(5), 581–589.

- Tsuang, M.T., Lyons, M.J., Meyer, J.M., Doyle, T., Eisen, S.A., Goldberg, J., True, W., Lin, N., Toomey, R., & Eaves, L. (1998). Co-occurrence of abuse of different drugs in men. *Archives of General Psychiatry*, 55, 967-972.
- Turpeinen, M., Nieminen, R., Juntunen, T., Taavitsainen, P., Raunio, H., & Pelkonen, O. (2004). Selective inhibition of *CYP2B6*-catalyzed bupropion hydroxylation in human-liver microsomes in vitro. *Drug Metabolism and Disposition*, 32, (6), 626-631.
- Unterwald, E.M., Horne-King, J., & Kreek, M.J. (1992). Chronic cocaine alters brain mu opioid receptors. *Brain Research*, 584, 314-318.
- Verster, A., & Buning, E. (2000). European methadone guidelines.
- Vesell, E.S. (2000). Advances in pharmacogenetics and pharmacogenomics. *Journal of Clinical Pharmacology*, 40, (9), 930-938.
- von Zastrow, M., Svingos, A., Haberstock-Debic, H., & Evans, C. (2003). Regulated endocytosis of opioid receptors: cellular mechanisms and proposed roles in physiological adaptation to opiate drugs. *Current Opinions in Neurobiology*, 13, 348-353.
- Walsky, R.L., Astuccio, A.V., & Obach, R.S. (2006). Evaluation of 227 drugs for *in vitro* inhibition of cytochrome P450 2B6. *Journal of Clinical Pharmacology*, 46, 1426-1438.
- Wang, D., & Sadee, W. (2006). Searching for polymorphisms that affect gene expression and mRNA processing: example ABCB1 (MDR1). *The AAPS Journal*, 8, (3), E515-E520.
- Wang, H., Faucette, S., Sueyoshi, T., Moore, R., Ferguson, S., Negishi, M., & LeCluyse, E.L. (2003A). A novel distal enhancer module regulated by Pregnane X receptor/constitutive androstane receptor is essential for the maximal induction of *CYP2B6* gene expression. *The Journal of Biological Chemistry*, 278, (16), 14146-14152.
- Wang, H., Faucette, S.R., Gilbert, D., Jolley, S.L., Sueyoshi, T., Neigishi, M., * LeCluyse, E.L. (2003B). Glucocorticoid receptor enhancement of pregnane X receptor-mediated *CYP2B6* regulation in primary human hepatocytes. *Drug Metabolism and Disposition*, 31, (5), 620-630.
- Wang, D., Guo, Y., Wrighton, S.A., Cooke, G.E., & Sadee, W. (2010). Intronic polymorphism in *CYP3A4* affects hepatic expression and response to statin. *Pharmacogenomics Journal*, doi:10.1038/tpj.2010.28.
- Wakeman, S.E., Bowman, S.E., McKenzie, M., Jeronimo, A., & Rich, J.D. (2009). Preventing death among the recently incarcerated: an argument for naloxone prescription before release. *Journal of Addiction Disorders*, 28, (2), 124-129.
- Walker, P.W., Klein, D., & Kasza, L. (2003). High dose methadone and ventricular arrhythmias: a report of three cases. *Pain*, 103, 321-324.

- Wei, P., Zhang, J., Egan-Hafley, M., Liang, S., & Moore, D.D. (2000). The nuclear receptor CAR mediates specific xenobiotic induction of drug metabolism. *Nature*, 407, 920-923.
- Wendel, B., & Hoehe, M.R. (1998). The human μ opioid receptor gene: 5' regulatory and intronic sequences. *Journal of Molecular Medicine*, 76, 525-532.
- Weschules, D.J., Bain, K.T., & Richeimer, S. (2008). Actual and potential drug interactions associated with methadone. *Pain Medicine*, 9, (3), 315-344.
- Westlind, A., Malmebo, S., Johansson, I., Otter, C., Andersson, T.B., Ingelman-Sundberg, M., & Oscarson, M. (2001). Cloning and tissue distribution of a novel human cytochrome p450 of the cyp3a subfamily, *CYP3A4*. *Biochemical and Biophysical Research Communications*, 281, 149-1355.
- Whistler, J.L., Chuang, H.H., Chu, P., Jan, L.Y., & von Zastrow, M. (1999). Functional dissociation of μ opioid receptor signalling and endocytosis. *Neuron*, 23, (4), 737-746.
- Whistler, J.L., & von Zastrow, M. (1999). Dissociation of functional roles of dynamin in receptor-mediated endocytosis and mitogenic signal transduction. *Journal of Biological Chemistry*, 274, 24575-24578.
- White, J.M., & Irvine, R.J. (1999). Mechanisms of fatal opioid overdose. *Addiction*, 94, 961-972.
- White, R.M., & Wong, S.H.Y. (2005). Pharmacogenomics and its applications. *Medical Laboratory Observer, Clinical Issues*, 37, pp 20-27.
- Wilson, M.E., Schwartz, R.P., O'Grady, K.E., Jaffe, J.H. (2010). Impact of interim methadone maintenance on HIV risk behaviours. *Journal of Urban Health: Bulletin of the New York Academy of Medicine*, 87, (4), doi:10.1007/s 11524-101-945-7.
- Wolff, K. (2002). Characterization of methadone overdose: clinical considerations and the scientific evidence. *Therapeutics and Drug Monitoring*, 24, 457-470.
- Wolff, K., Rostami-Hodjegan, A., Shires, S., Hay, A.W.M., Feely, M., Calvert, R., Raistrick, D., & Tucker, G.T. (1997). The pharmacokinetics of methadone in healthy volunteers and opiate users. *British Journal of Clinical Pharmacology*, 44, 325-334.
- Wong, S.H., Wagner, M.A., Jentzen, J.M., Schur, C., Bjerke, J., Gock, S.B., & Chang, C.C. (2003). Pharmacogenomics as an aspect of molecular autopsy for forensic pathology/toxicology: does genotyping CYP2D6 serve as an adjunct for certifying methadone toxicity? *Journal of Forensic Science*, 48, (6), pp 1-10.
- Wood, P.L., & Iyengar, S. (1988). Central actions of opiates and opioid peptides: in vivo evidence for opioid receptor multiplicity. In: *The opiate receptors* (Pasternak, G.W, ed), 307-356. Clifton, NJ: Humana.
- Worm, K., Steentoft, A., & Krinsholm, B. (1993). Methadone and drug addicts. *International Journal of Legal Medicine*, 106, 199-123.

- Wu, D.Y., Ugozzoli, L., Pal, B.K., Qian, J., & Wallace, R.B. (1991). The effect of temperature and oligonucleotide primer length on the specificity and efficiency of amplification by the polymerase chain reaction, *DNA and Cell Biology*, 10, (3), 233-238.
- Wu, T., Li, X.Y. (1999). Evidence for mu opioid receptor on mouse spleen lymphocyte. *Acta Pharmacologica & Sinica* 20, 835-843.
- Yamamoto, J., Kawamata, T., Niiyama, Y., Omote, K., & Namiki, A. (2008). Down-regulation of mu opioid receptor expression within distinct subpopulations of dorsal root ganglion neurons in a murine model of bone cancer pain. *Neuroscience*, 151, 843-853.
- Yanagihara, Y., Kariya, S., Ohtani, M., Uchino, K., Aoyama, T., Yamamura, Y., & Iga, T. (2001). Involvement of *CYP2B6* in N-demethylation of ketamine in human liver microsomes. *Drug Metabolism and Disposition*, 29, (6), 887-890.
- Yin, D.L., Ren, X.H., Zheng, Z.L., Pu, L., Jiang, L.Z., Ma, L., & Pei, G. (1997). Etorphine inhibits cell growth and induces apoptosis in SK-N-SH cells: involvement of pertussis toxin-sensitive G proteins. *Neuroscience Research*, 29, 121-127.
- Yin, D., Mufson, R.A., Wang, R., & Shi, Y. (1999). Fas-mediated cell death promoted by opioids. *Nature*, 397, (6716), 218.
- Zador, D., Mayet, S., & Strang, J. (2006). Commentary: Decline in methadone-related deaths probably relates to increased supervision of methadone in UK. *International Journal of Epidemiology*, 35, 1586-1587.
- Zhang, J., Ferguson, S.S.G., Barak, L.S., Bodduluri, S.R., Laporte, S.A., Law, P.Y., & Caron, M.G. (1998). Role for G protein-coupled receptor kinase in agonist-specific regulation of mu-opioid receptor responsiveness. *Proceedings of the National Academy of Science*, 95, 7157-7162.
- Zhang, J., Kuehl, P., Green, E.D., Touchman, J.W., Watkins, P., Daly, A., Hall, S.D., Maurel, P., Relling, M., Brimer, C., Yasuda, K., Wrighton, S.A., Hancock, M., Kim, R.B., Strom, S., Thummel, K., Russek, C.G., Hudson J.R.Jr., Schuetz, E.G., & Boguski, M.S. (2001). The human pregnane X receptor: genomic structure and identification and functional characterization of natural allelic variants. *Pharmacogenetics*, 11, 555-572.
- Zhang, Y., Wang, D., Johnson, A.D., Papp, A.C., & Sadee, W. (2005). Allelic expression imbalance of human mu opioid receptor (*OPRM1*) caused by variant A118G. *Journal of Biological Chemistry*, 280, 32618-32624.
- Zubieta, J.K., Dannals, R.F., & Frost, J.J. (1999). Gender and age influences on human-brain mu-opioid receptor binding measured by PET. *American Journal of Psychiatry*, 156, (6), 842-848.
- Zünkler, B.J., & Wos-Maganga, M. (2010). Comparison of the effects of methadone and heroin on Human ether-à-go-go Related gene channels. *Cardiovascular Toxicology*, 10, (3), 161-165.

Zunkuft, J., Lang, T., Richter, T., Hirsch-Ernst, K.I., Nussler, K., Klein, K., Schwab, M., Eichelbaum, M., & Zanger, U.M. (2005). A natural *CYP2B6* TATA box polymorphism (-82T-C) leading to enhanced transcription and relocation of the transcriptional start site. *Molecular Pharmacology*, 67, 1772-1782.

Appendix

OPRM1 Sequence information

The sequence information demonstrating SNP and primer location is shown below.

>PROTEIN SEQUENCE FOR OPRM1

```
MDSSAAPTNASNCTDALAYSSCSPAPSPGSWVNLSHLDGNLSDPCGPNRTDLGGRDS
LCPPTGSPSMITAITIMALYSIVCVVGLFGNFLVMYVIVRYTKMKTATNIYIFNLAL
ADALATSTLFPQSVNYLMGTWPFGTILCKIVISIDYINMFTSIFTLCTMSVDRYIAV
CHPVKALDFRTPRNAKIINVCNWILSSAIGLPVMFMATTKYRQGSIDCTLTFSHPTW
YWENLLKICVFIFAFIMPVLIITVCYGLMILRLKSVRMLSGSKEKDRNLRRITRMVL
VVVAVFIVCWTPIHIIYVIKALVTIPETTFQTVSWHFCIALGYTNSCLNPVLYAFLD
ENFKRCFREFCIPTSSNIEQQNSTRIRQNTRDHPSTANTVDRTNHQPPLAVSMAQIF
TRYPPPTHREKTCNDYMKR
```

AJ000341

> 5'UTR for OPRM1

and

>NC_000006 OPRM1 (480 amino acids)

```
aaaaaatcaccagattggtttatTTTTATTTATATTATTTATCACCAGATTGCA
tatatTTTAtgccattatctgggtataatggcataaaatatatgctaatacattttt
caactgaattcaaataattatgcacattaataattcatatatgtTTAATATAGAAAGAA
acacagagagtgagggagggaggtccactatgtattaagTACTGTGTTAGTGAGCAGA
cctcccttaggaaccttattacggagtacaaagctaggagagtaaataaagtatatt
aaaaatgcatacaaaagatgacagaatcaccattccaaaagatcctgggtggataag
aatcatgaattggatctaacaagatgtaacttaaaagtgaaaaaatctatagtgttg
tactgagctccctccaaagcaactataaatttataggagatgaaacatatgattcac
caggcataagaagaaagtttccgtaatacaaacactattgtatccatctTTTTAAACT
ccagctcctatcacagcacctgggtccaaagcagatctttagtatttTGTGGAAGTGGC
ttggattgtgttttaggaaatTTTGTcattggtaaacctaaggagagtcaagagaaca
acgtgacaaaaaataaaaactaaaaaaaaaaaaagggactttcattgtactggtag
aaagacaaagtttataatctggcttagtttctTTTTTGTGTTGTTGTTTTTGG
tcagggcaaatttaggtcattatTTTTTAACACTGGAAGTGTAGTTTCAGAGCAGATA
gacaaactatcaatgagaatagatgaacagcaaggccactgaaaggactcagaacta
catcttataagaacaactgaatgatgctaatagtTTAACTTGCAAAAGAGAAAACCTC
agttgatttcaaataatgaaataatagtggtaaggagttatcacttattaagcaatt
actattgcaatgtatactcatttaATCCTGCTAACAGACATATGAGgtgaatattat
tagcctaccctcgcctTTTTTAAGTAATGAGAAGACTGTCATCCTGTAGGGTAAAGT
aacatgtccaaactcacacagctacaaagttacaaagctgatttataaaatgattga
ctccaaggtcaggaattattatactgtgtcttTGTCTTCCACATGAACTAAGCACAAA
ggaactgaatgcaggcagacagatttcagctcaatataagagaattgttacattagt
```

tcatggaagaatatgttttaaggatTTTTTgTTAgTctctaggaatctctgtaaca
TTTTattgtgtaaaattatatgctTTaatgtaagaggataaaaaataatagtgaacatt
ggcaaaatagcctatgattaatagagTTTaccTatgagTTatctgTTTctaagataa
atgccaaaaataatattggaattaaatgTTCctTTTcaagatctTccctccctgctc
cctgaaattgcagTgaattTTTcaagaccaactgaggacatgtattTTTcaatgTTTa
TggtTaaaagatatgtacatgcacagatatatacatgtacagaaatgagaattactT
cagaattggTgTTaactTTtagaaaaaaaagaccaagaactTactctTggtattTac
aaatttattTctaaaa**tagaagcactcatggacttag**aagtaaggTataaaattcaa
aacgtatccatgTttTctcaaggatctTgTTgtaggcaactctaattccatataatta
TgtggctTTTcctagaattTTTtac**a**ctagaaaacagactgaatgcaaattTgTTT
gTTTtaacaacctTctT**ct**cagaagca**tatgtctatcgaggaagtcttc**agataaaa
aagataaacaattccaaacaggtctatgagattTaaagatgtgaaagatcaacattat
ctTtagTgactTtactggatgccacaacctTctgattTctgTaaaccactTcttatg
cct**cctaccocactgaaacaaaatc**agaggcaaacagagctTcacctagaaattggg
gaaaatgaggaacaggtTTT**ctgcacaaaagTTTattTgTTTctc**attTctTTTtca
gaaaataaaggatcgctgTtTgTTcccaacaggtTTgtagggaagaaaattggagaaa
cattattacctTTTcttagatgTtggcaacggaggcaacaaggactgcaaaagaaaa
TtTgTgTccccattcctaaataatcaaaattTggcagtagggatggaagagcattg
gggTTTtagggctgTtagggTTTcatcaagccaatgtattccctgccagattTTaag
gagaaaaaggcgctggaaaattgagTgatgTtagccccctTctattTTTg**cactg**
ctaccaagactaactctatctctctccccaccctTctctccatctccctcctTta
gatgTgTTTgcacagaagagTgcccagTgaagagacctactcctTggatcgctTTTgc
gcaaaatccaccctTTTccctcctccctccctccagcctccgaatcccgcatggc
ccacgctccccctcctgcagcggTgcggggcaggtgatgagcctctgtgaactactaa
ggTgggagggggctatacgcagaggagaatgtcagatgctcagctcggTccccctcg
cctgacgctcctctctgtctcagc**caggactggTTTctgTaaagaaa**cagcaggagct
gtggcagcggcgaaaggaagcggtgagggcgtTggaaccgaaaagtctcggTgct
cctggctacctcgcacagcggTgcccggccggcgtcagTacc**atggacagcagcgc**
Tgccccacgaacgccagcaattgcactg**atgcottggcgtactcaagTTg**ctccc
agcaccagccccggTtctTggTcaactTgtcccactTtagatggc**a**acctgtccga
ccatgCGgtccgaaccgcaccgacctgggCGggagagacagcctgtgcccTccgac
cggcagTccct**c**atgatcacggccatcacgatcatggccctctactccatcgtgtg
cgtggTggggctctTcgaaactTcctggTcatgTatgtgattgtcaggtaaagaaa
gcgccagggctccgagcggagggtTcagcggctTaaaggggtacaaagagacac**cta**
actcccaaggctcaatgTTgggcgggaggatgaaagaggggaggTaaactgggggga
ctctggaggagaccacggacagTgattgTtattTctatgagaaaacctactTTTctg
TTTTTctTcaactgataaagaaagaattcaaaattTcaggagcagagaagTtGctT
TggtaaaagctacaaatgtctaggggTggggggcggagggaagctatagcatagact
TggagcgtTcctTatactgagcaaaagggctcctTggcagagTcctacactcagTc
cctctgcaggagctatggaaagagTaaagTtGtaataatgg

ccTacaaaagTTTTTTaaaattaacagggTatggTggcatgcacctgggatccag
TtattcaggaggtgaggcaagaggatctcctTgagTccaggaggTtaaagctgtagTg
agctctgTtcataccattacactccagcctgggTaaacagggcaagatccTatccaaa
aaaaaaaaaaaaaggaagaaactcaacaaagcagcatcgtTgctattattTgcagctat
TtagccaataggtacatcattgacatcattgTaaatagccaagctgatactggaaaa
caattctatatctaatctcaaaaaagctTTTctactaattcatgcaaaTTTattattg
gaagctTaccTatattTTTtacactagTgtctTTTtactgattctcactctTctTcctTt
atctcctag**atacaccaagatgaagactgccaccaacatctacatTTTcaacctTgc**
TctggcagatgccttagccaccagTaccctgcct**ccagagTgtgaattacctaT**

gggaacatggccatttggaaaccatcctttgcaagatagtgatctc catagattacta
t aacatggtccaccagcatattcaccctctgcaccatgagtggtgatcgatacattgc
agtctgccaccctgtcaaggccttagatttccgtactccccgaaatgccaaaattat
caatgtctgcaactggatcctctcttcagccattggctctctgtaatgttcatggc
tacaacaaaatacagg caaggtgagtgatggttaccag cctgaggggaaggagggttca
cagcctgatatggttgatgtcataagcaaagcagtat tttatggagtgccccattg
tcttagtcacattgtaatttttaattattcttcttagcaaaaaaagcctttgaatact
taaaaataggaattttctcataaatttttaggcctattaaatcctttaagagaatgt
aatctatttatttctgatttctctgtatttacttcataaaaaatgggtgtgtaaattag
tacatagctctcccaagagtaattggagcttaaacc caaagagtattacactgaggc
ttgtttaaaattatcaagtggctgactacatggcaa atgtatctttctacaccta at
atcagaatattgaacaatccatcaaaaaatga agtgaaaacatccattacctggagc
cgctagagactttggacaattattacattttttat atcaatatagacctcatggag
gatctagctcatggttgagaggttcattttttgtt ccctgaacgaaagcttaatgtgat
cgaagtggactgcaaaaatgggaaatttagaaaaaa caaaaaacattagaagtaaaa
ctttctttgaaaagtaacaaacaactgagtttctt ccacaatttctttatagcctta
agttagctctggcaaggctaaaaatgaatgagcaaa atggcagtat taaacacctta
tgacataattaaatggttgctgctaatttttctt ttaaattcctttcttctaggttcc
atagattgtacactaac attctctcatccaacctgg tac tgggaaaacctgctgaag
atctgtgttttcatcttctgccttcattatgcc agtgctcatcattaccgtgtgctat
ggactgatgatcttgc cctcaagagtgtc gcatgctctctggctccaaagaaaag
gacaggaatcttcgaaggatcaccaggatgggtgct ggtgggtggctgtgttcatc
gtctgctggactcccattcacatttacgtcatc attaaagccttggttacaatcca
gaaactac ttccagactgtttcttggcacttctgc attgctctaggttacacaaac
agctgc tcaaccagtcctttatgcat tttctggatgaaaacttcaaacgatgcttc
agagagttctgtatcccaacctcttccaacattg agcaacaaaactccactcgaatt
cgtcagaacactagagaccaccctccacggcca atacagtggatagaactaatcat
caggtacgcagctctctagaattaggtatatct actggggatgacataaaaaattataa
ggctttgtgctaaactaggagtttaatccattat agaggatgagaatggaggggaaga
ggggaagcaaatgtggttctagtgttagagaag aggtttgttatataaactgtgtt
ctttatatttgactgtacatatcatttaggtataa agatacaccaatgagaaatcc
atgaaactattcaaaataactat ttttatggccttacttctatgcaaaatttatga

***CYP2B6* Sequence information**

The sequence information for *CYP2B6* demonstrating SNP and primer locations is shown below.

ttctggttttacggctcag ggggcatcatggaacctgccgacatgtgatgtctcccc
cggacccccagctttaaaatttctctcttttgtgctctgtccctttatttctcaggc
tgcccgacacttagggagaacagaaaagaacctacgtggaatattgggggtgaattt
tgcccgatatctggctgaatttcccctgataatgccactctctatgtccatgtgtac
acattgtttagcaccacttatgaatgagaacatgtgatattcactttctgtgcctg
gcttgtttacttaagataatcccctccagttgtatccatggttgctataaaagacat
tattttattcctttttatggctaa atagtattcaatgggtgatataaccacatttt
at ttaaccattcatctgttgatccctat tttttgctattgtaaatagcatttggacc
acatttcaagtacttaattagtgggccacatgcagcaagtgactatcacattggacaa
tgtagccccaaccactgtatgaccttgggtaagacttgcaaac tgcattgcttca
atatctccatctataaaatggggatggcaacaatacctcactaagagtgtaaagact

ga gttactgtgtgtaaaagcactt cacgcctccccatcggtgcttcaccctggggctg
caatgagcacccaatcttagtgtcagatgacacagcacagcaagaccgagggccttg
gttcaggaaagtccatgctgccacctcttcagggtcaggaaagtacagtttccacct
cttacaatataggactgtttgtctgctcctcctgggtcaaagtaacttcgggttcagg
tcttgatccagcaaagggtttgcttaacattgcaagaaagatggtgcctcatggtc
aaaagtcaggcgtaggatgagacagggcagacacgcacacattcacaccacgttttg
caaagatggactgaccctgtcagaggatgtgtgggtgaaggtgcacagtgaggatag
agacatatgggagtcagtagacatcaatcaaactggactcagtttgcacacacctg
gagctcaagagtctccaggggaaaacagagacacaaagtcagacagagagagagcc
agagaaatttctgcaccgtgaagatagtcagaggcaggggaagaaactccttagcac
tagttagagtgatcagaaaccaagaggacctgatcgctgtacctgccaggtctcagt
ttctgtctcctccaactgaccacctcttctctgagactcaccagttctgcatctc
ttgctcctccttctgtttctccgaccacttccacctgtggctgtcacagaaggggcg
atgaaggaggggacactggagatagactcagcatctgcaggcttcaaagagagggg
ctaggagatccaccaacacaccagcacaaatacaccagcacacacagatacacacaa
ttggttcatgtattgctagggttacagttt gctatgctacaaaggcagt aggccaaat
ttgattgaattgaataattccttattttcatcagcttctccttttttttttttttt
tttttttttgagatggagtattgctgtgtcaccaggctggagtgcagtggtgtaat
cttggtcactgcagcctccacctcccaggttcaagtgattctcttgccctcagcctc
ccgagtagctgggattaaaagtaccaccatcacgcccggtaatttttggttttt
agtacagatggggttttgccaatgtgggcccaggatggtctcgaactcttgacctaat
tgatctgccccctcagcttcccacgtgctgggattacaggtgtgagccaccgcac
ccagccagcctctcagttttgaacatgcaactaccaccacctccacaacacacaaatg
taaatgcactttcgtatataaaaactgtataaatacaaggaagctcatacacatgcaa
ggatacacacataagcacccccagattcaaccacagaaatatacgccagtaatttg
cataaattcaaacacccctttacatgtaaaaatcatataagcacatacagggatgca
agcaggcatggacaaatgcatgcaagcacagacaaacagacaaagctaagtaaaaa
gtgcaagctcacctatgcttacaaaaatagacatacatatacccacaaaccacaca
cccacacattcacttgctcacctggactttgatatctctaccactgtatccttgcca
atatctacagagtgggtaaagggataggcatcaggctcactgggttgcccaagcagga
agtctgggttccctaacaactttttctaag ctaatgctcctggatgat gatgaaaa
ggaggtggggaatggatgaaattttataacaggggtgcagaggcaggggtcaggataaa

gactctatagctgtgttgctgggtctaaatcctggcctcagtaatgagtagctgtg
caactttgggtcaaattactcagcctctcgggtctgccatctataaactggagctaat
aatcaaattgcatctgctcacattggtgtagtgagagttcaatggaattacgcgtg
acgtgctggtacataaattagctgttacggttattctcatgtttaccattactgagtg
atggcagacaatcacacagagatagggtgacagcctgatgttccccaggcacttcagt
ctgtgtccttgacctgctgcttcttcttag gggccctcatggaccccaccttctct
tcc agtccattaccgccaacatcatctgctccatcgtctttggaaaacgattccact
accaagatcaagagttcctgaagatgctgaacttggtctaccagactttttcactca
tcagctctgtattcggccag gtcagggagacggagaggggacaggggggtggtgggggtg
agggtgaacacccagaaacacacagagaaaaggatgacctgtcttgggggctcagaaatg
cagcttatccttgaagaaacgcagacatgtgaagaatcaggacatggagacctgg
agggaggagagacgggtgagacagggatagagacactgagagagagaatgaggcgtga
tggggaggcagaaatagagtcaagagagagactgagagaaggaagatgagcaaaaaa
agacaaagaagagcagaaatcaagagattctgagagacagagttgatgagaatgagt
gtgaaagagaggggagagagagagaacgaataaggcttgggcttcatgtctattctg
ctcctggatgtcatttctgtttttatttttttttagacggagtctcgtgtttcattcc

aagaggtaaatgtgagatagatcaaaggagatatagagtcagtgagtgaggggttca
gaggcagaggggagtggggaagtggggttcccatggagggattggggcccaggaggc
gctctctccctgtgacctgctagctcagccctaggcacaacctcaccacccttcttt
cttgagctggtttgagctcttctctggcttcttgaaatactttcctggggcacacag
gcaagtttacaaaaacctgcaggaaatcaatgcttacattggccacagtgaggagaa
gcaccgtgaaacctggacccagcgccccaaggacctcatcgacacctacctgct
ccacatggaaaaagtgggggtctgggagaggaaaaaggggaagggaggggagggg
aagatggagaggtgagaagaggaggaaaaagggtaggggaaggggaagatggggag
ggaagaagaagactaggaggaggagaaatagggaagggaggagagaacatgaggaa
ggaagaagaatgaggtgaaaggaggagaaataggaggaggagaaactgagacaggg
agagaggggaggtgggaagacagaatgaaagacagagggagagagagaagactgg
ctgaggaaggaattcggggcaagggacaaaaatacagcaacaagagaaaaaactcac

pcDNA3.1/CT-GFP-TOPO® Vector Sequence

gacggatcgggagatctcccgatcccctatggctgactctcagtacaatctgctctg
atgccgcatagttaagccagtatctgctccctgcttgtgtggtggaggtcgctgagt
agtgcgcgagcaaaaatttaagctacaacaaggcaaggcttgaccgacaattgcatga
agaatctgcttagggttaggcgttttgcgctgcttcgcgatgtacggggccagatata
cgctgtgacattgattattgactagttattaatagtaatacaattacgggggtcatttc
Atagcccatatatggagttccgcgttacataacttacggtaaatggcccgcctggca
ccgcccacgacccccgcccattgacgtcaataatgacgtatggtcccatagtaacg
ccaatagggactttccattgacgtcaatgggtggactatttacggtaaaactgcccac
ttggcagtacatcaagtgtatcatatgccaaagtacgccccctattgacgtcaatgac
ggtaaatggcccgcctggcattatgccagtacatgaccttatgggactttcctact
tggcagtacatctacgtattagtcacgctattaccatgggtgatgagggttttggcag
tacatcaatgggcgtggatagcgggttgactcacggggatttccaagtctccacccc
attgacgtcaatgggagtttgttttggcaccaaaatcaacgggactttccaaaatgt
cgtaacaactccgccccattgacgcaaatgggcggtagggcgtgtacgggtgggaggtc
tatataagcagagctctctggctaactagagaaccactgcttactggcttatcgaa
attaatacgactcactatagggagaccctaaagtggctagttaagcttggtaaccgagc
tcggatccactagtcacagtggtggaattctgcagatatccagcacagtgggcgcc
gctcgagtctagaatgctagcaaaaggagaagaacttttcaactggagttgtccc
tcttgtgaattagatgggtgatgtaaatgggcacaaattttctgtcagtgaggagg
tgaaggtgatgctacatacggaaagccttacccttaaatttatttgcactactggaa
actacctgttccatggccaacacttgtcactactttctcttatgggtgttcaatgctt
ttcccgttatccggatcatatgaaacggcatgacttttcaagagtgccatgcccga
aggttatgtacaggaacgcactatatctttcaaagatgacggggaactacaagacgcg
tgctgaagtcaagtttgaaggtgatacccttgttaatcgatcgagttaaaaggat
tgattttaaagaagatggaaacattctcggacacaaactcgagtacaactataactc
acacaatgtatacatcacggcagacaaacaaagaatggaatcaaagctaacttcaa
aattcgccacaacattgaagatggatccgttcaactagcagaccattatcaacaaaa
tactccaattggcgatggccctgtccttttaccagacaaccattacctgtcgacaca
atctgccctttcgaaagatcccaacgaaaagcgtgaccacatggctccttcttgagtt
tgaactgctgctgggattacacatggcatggatgagctctacaataatgaattaa
acccgctgatcagcctcgactgtgccttctaagtggccagccatctgttgtttgccc
tccccgtgccttcccttgaccctggaaggtgccactcccactgtcctttcttaataa
aatgaggaatgcatcgcatgtctgagtaggtgtcattctattctgggggggtggg
gtggggcaggacagcaagggggaggattgggaagacaatagcaggcatgctggggat

gcggtgggctctatggcttctgaggcggaaagaaccagctggggctctagggggtat
ccccacgcgccctgtagcggcgcattaagcgcggcggtgtgggtggttacgcgcagc
gtgaccgctacacttgccagcgccttagcggccgctcctttcgctttcttcccttc
tttctcgccacgttcgcccggctttccccgtcaagctctaaatcggggcatccctta
gggttccgatttagtgctttacggcacctcgacccccaaaaaacttgattaggggtgat
ggttcacgtagtgggcatcgccctgatagacggtttttcgccccttgacggttgag
tccacgttctttaatagtgactctgttccaaactggaacaacactcaaccctatc
tcggtctattcttttgatttataagggattttggggatttcggcctattggttaaaa
aatgagctgatttaacaaaaatttaacgcgaattaattctgtggaatgtgtgtcagt
taggggtgtggaagtccccaggctccccaggcaggcagaagtatgcaaagcatgcat
ctcaattagtcagcaaccagggtgtggaagtccccaggctccccagcaggcagaagt
atgcaaagcatgcatctcaattagtcagcaaccatagtcccgcccctaactccgccc
atcccccccctaactccgcccagttccgcccattctccgcccctaggctgactaatt
ttttttatttatgcagaggccgaggccgctctgcctctgagctattccagaagtag
tgaggaggcttttttgaggcctaggcttttgcaaaaagctcccgggagcttgata
tccattttcggatctgatcaagagacaggatgaggatcgtttcgcatgattgaacaa
gatggattgcacgcaggttctccggccgcttggttgagaggctattccggctatgac
tgggcacaacagacaatcggctgctctgatgccgccgtgttccggctgtcagcgcag
gggcgcccgggttctttttgtcaagaccgacctgtccgggtgccctgaatgaactgcag
gacgaggcagcgcggctatcggtggctggccacgcagggcggttccttgccgagctgtg
ctcgacgttgctactgaagcgggaagggactggctgctattggggaagtgcggggg
caggatctcctgtcatctcaccttgctcctgcccagaaaagtatccatcatggctgat
gcaatgcggcggtgcatacgttgatccggctacctgccattccgaccaccaagcg
aaacatcgcatcgagcgcagcacgtactcggatggaagccggctcttgctgatcaggat
gatctggacgaagagcatcaggggctcgcgccagccgaactgttcgccaggctcaag
gcgcgcagccccgacggcgaggatctcgtcgtgacctatggcgatgctgtcttgccg
aatatcatgggtggaatggccgcttttctggattcatcgactgtggccggctgggt
gtggcgaccgctatcaggacatagcgttggtaccgctgatattgctgaagagctt
ggcggcgaatgggctgaccgcttctcgtgctttacggtatcgcgctcccgattcg
cagcgcagctgccttctatcgccttcttgacgagttcttctgagcgggactctgggt
tcgcaaatgaccgaccaagcgcagcccaacctgccatcacgagatttcgattccac
cgccgcttctatgaaagggtgggcttcggaatcgtttccgggacgcggctggat
gatcctccagcgcgggatctcatgctggagttcttcgcccccacttgtttat
tgcagcttataatgggttacaataaagcaatagcatcacaatttcacaaataaagc
attttttctactgcattctagttgtggtttgtccaaactcatcaatgtatcttatca
tgtctgtataaccgtcgaccttagctagagcttggcgtaatcatggctcatagctgtt
tctgtgtgaaattgttatccgctcacaattccacacaacatacagagccggaagcat
aaagtgtaaagcctggggtgcctaatgagtgagctaaactcacattaattgcgttgcg
ctactgcccgcttccagtcgggaaacctgtcgtgcccagctgcattaatgaatcgg
ccaacgcgcggggagaggcggtttgctgattgggctcttccgcttctcgtcac
tgactcgtgctcggtcgttcggctgcccgcagcgggtatcagctcactcaaaggc
ggtaatacggttatccacagaatcaggggataacgcaggaaagaacatgtgagcaaa
aggccagcaaaaggccaggaaccgtaaaaaggccgcgttgctggcggttttccatag
gctccgccccctgacgagcatcacaataatcgacgctcaagtcaagtgaggtggcgaaa
cccagcaggactataaagataccaggcgtttccccctggaagctcctcgtgcgctc
tctgttccgaccctgccgcttaccggatacctgtccgcctttctccctcgggaag
cgtggcgcttctcaatgctcacgctgtaggtatctcagttcgggtgtaggtcgttcg
ctccaagctgggctgtgtgcacgaacccccgttcagcccagcgtgcgcttatc
cggtaactatcgtcttgagtccaacccggtaagacacgacttatcgccactggcagc
agccactggtaacaggattagcagagcaggtatgtaggcgggtgctacagagttctt
gaagtgggtggcctaactacggctacactagaaggacagtatgttggtatctgcgctc
gctgaagccagttaccttcggaaaaagagttggtagctcttgatccggcaacaac

caccgctggtagcgggtgggttttttggtttgcaagcagcagattacgcgcagaaaaaa
aggatctcaagaagatcctttgatcttttctacgggggtctgacgctcagtggaacga
aaactcacgtaagggttttgggtcatgagattatcaaaaaggatcttcacctagat
ccttttaaatataaaaatgaagttttaaatcaatctaaagtatatatgagtaaacttg
gtctgacagttaccaatgcttaatcagtgaggcacctatctcagcgatctgtctatt
tcgttcatccatagttgcctgactccccgtcgtgtagataactacgatacgggaggg
cttaccatctggccccagtgctgcaatgataccgcgagaccacgctcaccggctcc
agatttatcagcaataaaccagccagccggaagggccgagcgcagaagtggctcctgc
aactttatccgcctccatccagtcattaattggttgccgggaagctagagtaagtag
ttcgccagttaatagtttgcgcaacggtggtgccattgctacaggcatcgtgggtgc
acgctcgtcgtttgggtatggcttcattcagctccggttcccaacgatcaaggcgagt
tacetgatcccccatggttgcaaaaaagcgggttagctccttcggctcctccgatcgt
tgtcagaagtaagttggccgcagtggtatcactcatgggttatggcagcactgcataa
ttctcttactgtcatgccatccgtaagatgcttttctgtgactgggtgagtactcaac
caagtcattctgagaatagtgatgcgggcagccgagttgctcttgcccggcgtcaat
acgggataataccgcgccacatagcagaactttaaaagtgctcatcattggaaaacg
ttcttcggggcgaaaactctcaaggatcttaccgctgttgagatccagttcgatgta
accactcgtgcacccaactgatcttcagcatcttttactttcaccagcgtttctgg
gtgagcaaaaacagggaaggcaaaatgccgcaaaaaagggaataaggcgacacggaa
atggtgaataactcatactcttcctttttcaatattattgaagcatttatcagggtta
ttgtctcatgagcggatacatatttgatgtatttagaaaaataaacaataggggt
tccgcgcacatttccccgaaaagtgccacctgacgctc

DNA Extraction and Purification Protocols

MasterAmp™ Buccal Swab DNA Extraction Kit, Cambio

Protocol

1. Thaw the appropriate number of tubes containing the DNA Extraction Solution.
2. Divide the Extraction mixture into aliquots of 150 µl, using fresh labelled tubes.
3. Collect tissue (buccal cells) by rolling the buccal brush firmly on the inside of the cheek, approximately 20 times on each side making sure to move the brush over the entire cheek.
4. Air dry the brush for 10-15 minutes at room temperature at this point you can either continue straight to extraction or alternatively you can store the brush in its original packaging at 22-37°C for up to one month before extraction. For longer term storage, keep the dry brushes at -20°C for up to 6 months.
5. For extraction place the buccal brush into a tube containing the required amount of extraction fluid and rotate the brush a minimum of 5 times within

the fluid. Press the brush against the side of the tube, rotating slightly whilst removing it from the tube to ensure maximum DNA yield.

6. Cap the tube and vortex for 15 seconds.
7. Incubate the tube at 65°C for 2 minutes.
8. Repeat step 6.
9. Transfer the tube to 98°C and incubate for 3 minutes.
10. Repeat step 6.
11. Leave to cool at room temperature before storing at -20°C.

Promega Wizard® Genomic DNA purification Kit

Protocol

Use Table 5 to calculate the appropriate volume to perform the DNA extraction.

1. Combine the appropriate volumes of cell lysis solution and blood in a sterile eppendorf. Then mix by inversion.
2. Incubate at room temperature for ten minutes.
3. Centrifuge the sample as follows:

For samples $\leq 300\mu\text{l}$ spin at maximum speed (13,000 – 16,000 x g) for 20 seconds. For samples 1-10ml spin at 2,000 x g for 10 minutes.
4. Discard the supernatant and vortex the pellet.
5. Using the above table to calculate the required amount of Nuclei lysis solution, add to the tube and mix by inversion.
6. Add the protein precipitation solution, vortex for 20 seconds.
7. Centrifuge the sample as follows:

For samples $\leq 300\mu\text{l}$ spin at maximum speed (13,000 – 16,000 x g) for 3 minutes. For samples 1-10ml spin at 2,000 x g for 10 minutes.
8. Transfer the supernatant to a new tube containing isopropanol (use table for correct volume to add) and mix.
9. Centrifuge the sample as follows:

For samples $\leq 300\mu\text{l}$ spin at maximum speed (13,000 – 16,000 x g) for 1 minute. For samples 1-10ml spin at 2,000 x g for 1 minute.

10. Discard the supernatant. Add 70% ethanol (at the same volume as the isopropanol).
11. Repeat step 9.
12. Aspirate the ethanol and air-dry the pellet for 10-15 minutes.
13. Rehydrate the DNA in the appropriate volume of DNA rehydration solution for 1 hour at 65°C or overnight at 4°C.

Qiagen DNeasy Blood and Tissue Kit

Protocol

1. Pipet 20 μl proteinase K into a 1.5ml or 2ml microcentrifuge tube.
2. Add 50-100 μl anticoagulated blood. Adjust the volume to 220 μl with PBS.
3. Add 200 μl Buffer AL and mix thoroughly by vortexing (to ensure a homogenous solution) and incubate at 56°C for ten minutes.
4. Add 200 μl ethanol (96-100% to the sample and vortex.
5. Pipet the solution into a DNeasy mini spin column (placed in the 2ml collection tube) and centrifuge at ≥ 6000 x g (8000 rpm) for 1 minute. Discard flow-through and collection tube.
6. Place the spin column into a new 2ml collection tube and add 500 μl Buffer AW1, and centrifuge for 1 minute at ≥ 6000 x g (8000 rpm). Discard the flow-through and collection tube.
7. Place the spin column in a new 2ml collection tube and add 500 μl Buffer AW2, and centrifuge for 3 minutes at 20,000 x g (14,000 rpm) to dry the DNeasy membrane. Discard the flow-through and collection tube.
8. Place the DNeasy mini spin column in a clean 1.5ml or 2 ml collection tube and pipet 200 μl Buffer AE directly onto the DNeasy membrane. Incubate at room temperature for 1 minute and then centrifuge for 1 minute at ≥ 6000 x g (8000 rpm) to elute.

QIAquick PCR Purification Kit

Protocol

1. Add 200µl of PBI buffer to 40µl of the PCR product being purified. Mix thoroughly using a pipette.
2. Add the mixture carefully to a QIAGEN Quickspin Column.
3. Centrifuge at 13,000 rpm for 1 minute.
4. Discard the waste.
5. Add 750µl of PBE Buffer to wash the column.
6. Repeat step 3.
7. Discard the waste.
8. Repeat step 3 to ensure all the waste is removed.
9. Transfer the Quickspin column to a clean, labelled tube and leave to air dry for 5 minutes.
10. Add 40µl of EB Buffer to the centre of the Quickspin Column to elute the DNA.
11. Leave to air dry for 5 minutes.
12. Centrifuge at 13,000 rpm for 1 minute.
13. Eluted DNA can now be sent off for sequencing.

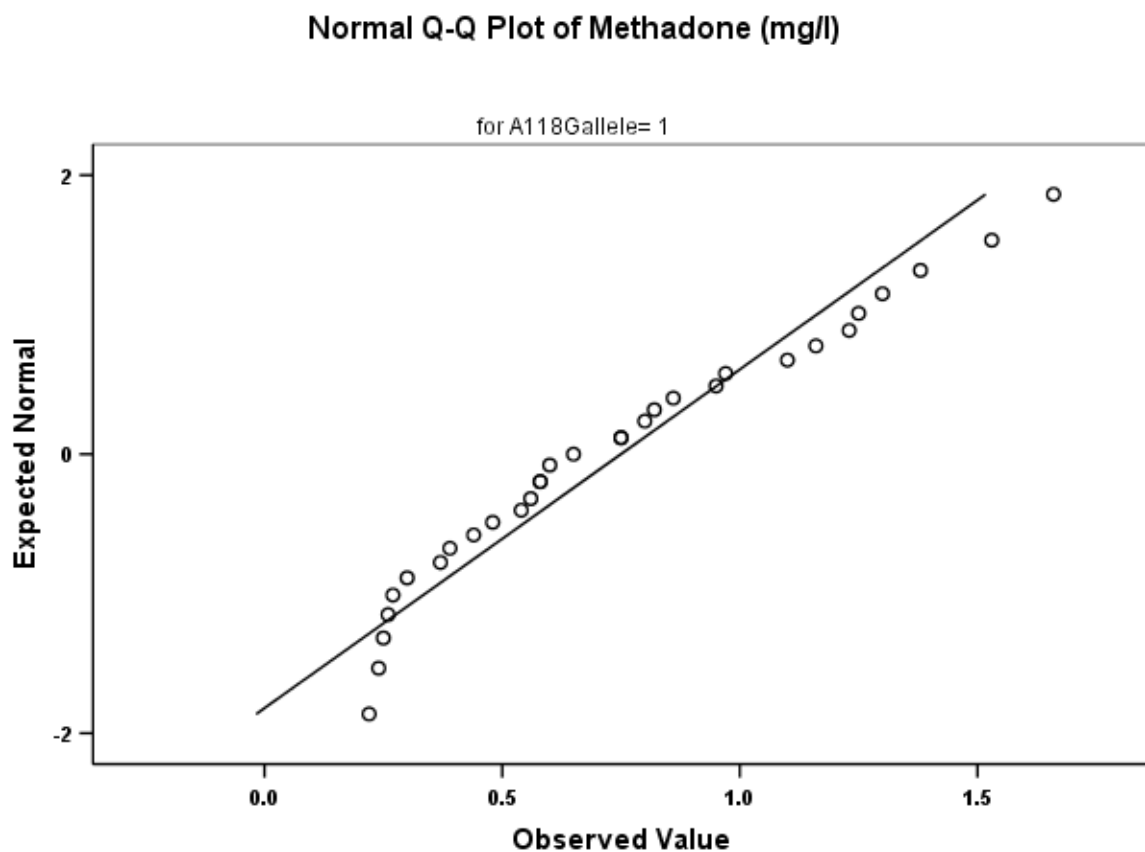
Data Normality

Data normality was examined with SPSS 14.0 software using the Shapiro-Wilks test, where a P value above 0.05 indicated a normal data distribution.

OPRM1 A118G SNP

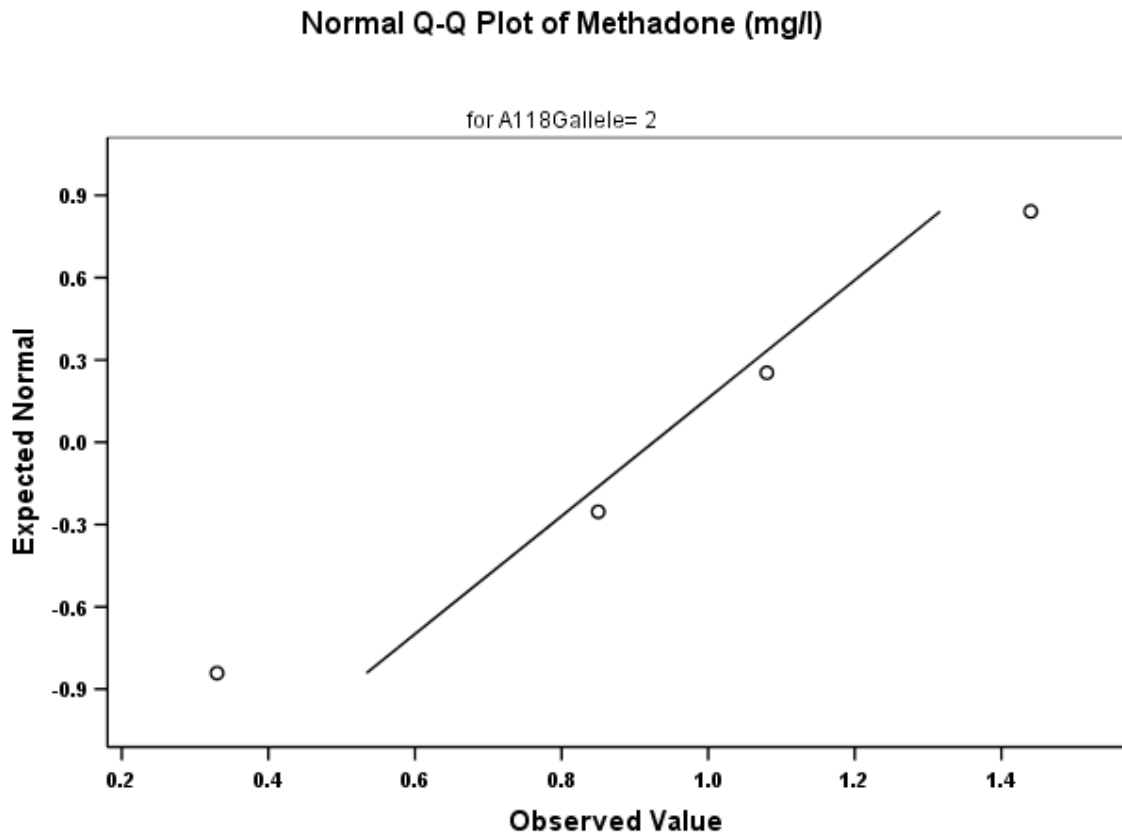
A118G Genotype	Statistic	df	Significance
118 AA	0.937	31	0.069
118 AG	0.989	4	0.953

118 AA Genotype



Normality plot for the 118 AA genotype, with post-mortem methadone concentration as the dependent variable and A118G as the factor, where $P > 0.05$.

118 AG Genotype

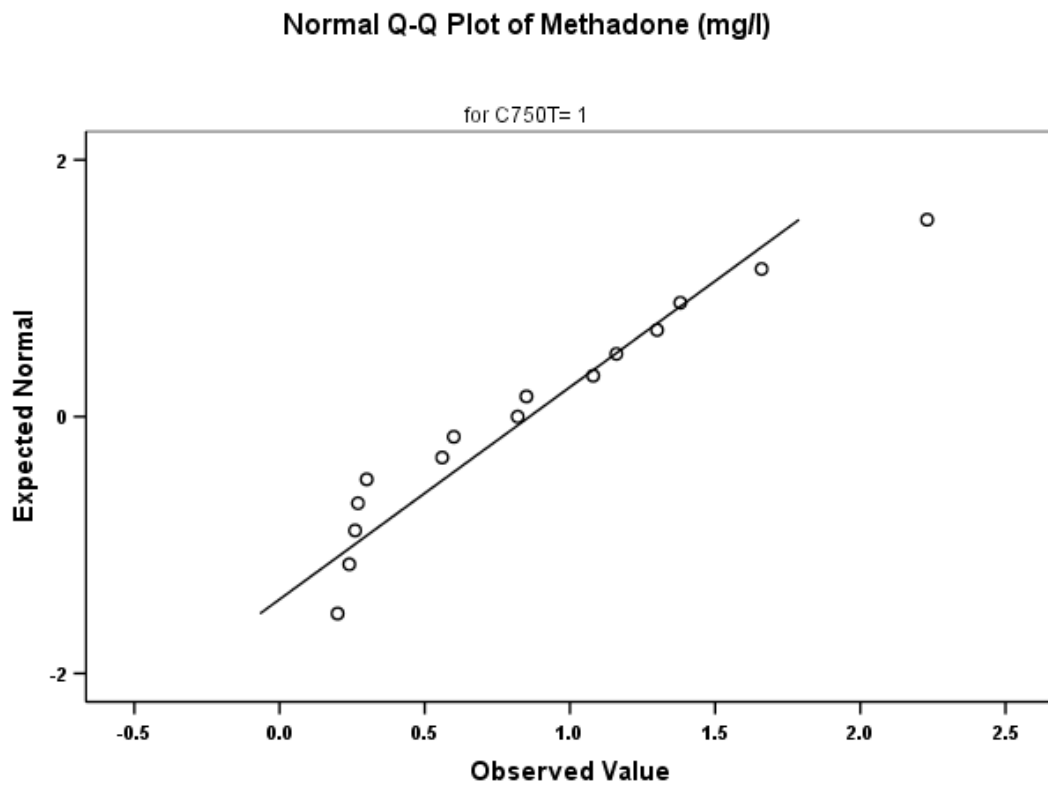


Normality plot for the 118 AG genotype, with post-mortem methadone concentration as the dependent variable and A118G as the factor, where $P > 0.05$.

CYP2B6 T750C SNP

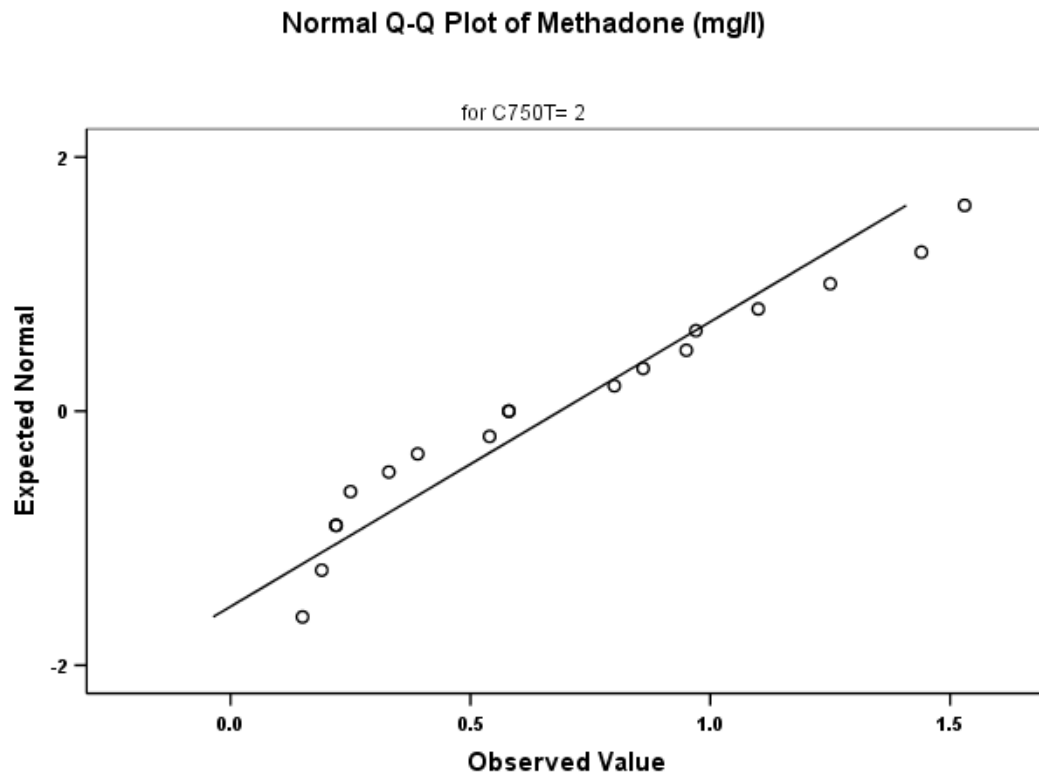
T750C Genotype	Statistic	df	Significance
750 TT	0.912	15	0.145
750 TC	0.919	18	0.127
750 CC	0.928	7	0.535

750 TT Genotype



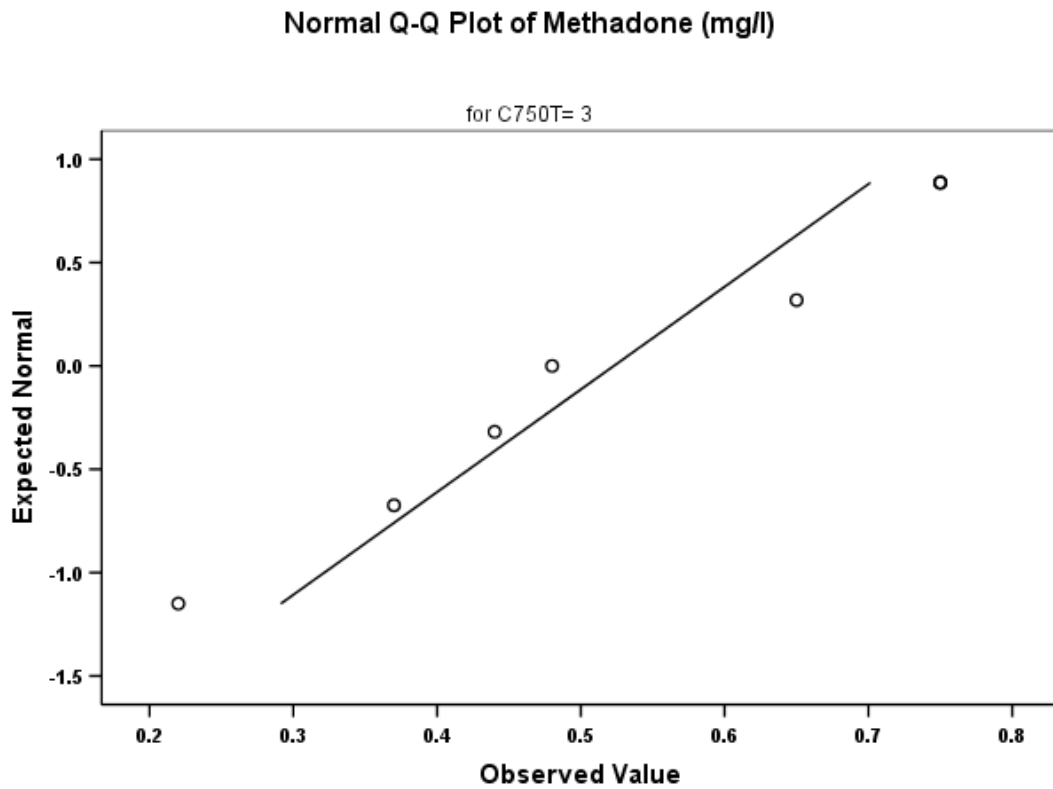
Normality plot for the 750 TT genotype, with post-mortem methadone concentration as the dependent variable and T750C as the factor, where $P > 0.05$.

750 TC Genotype



Normality plot for the 750 TC genotype, with post-mortem methadone concentration as the dependent variable and T750C as the factor, where $P > 0.05$.

750 CC Genotype

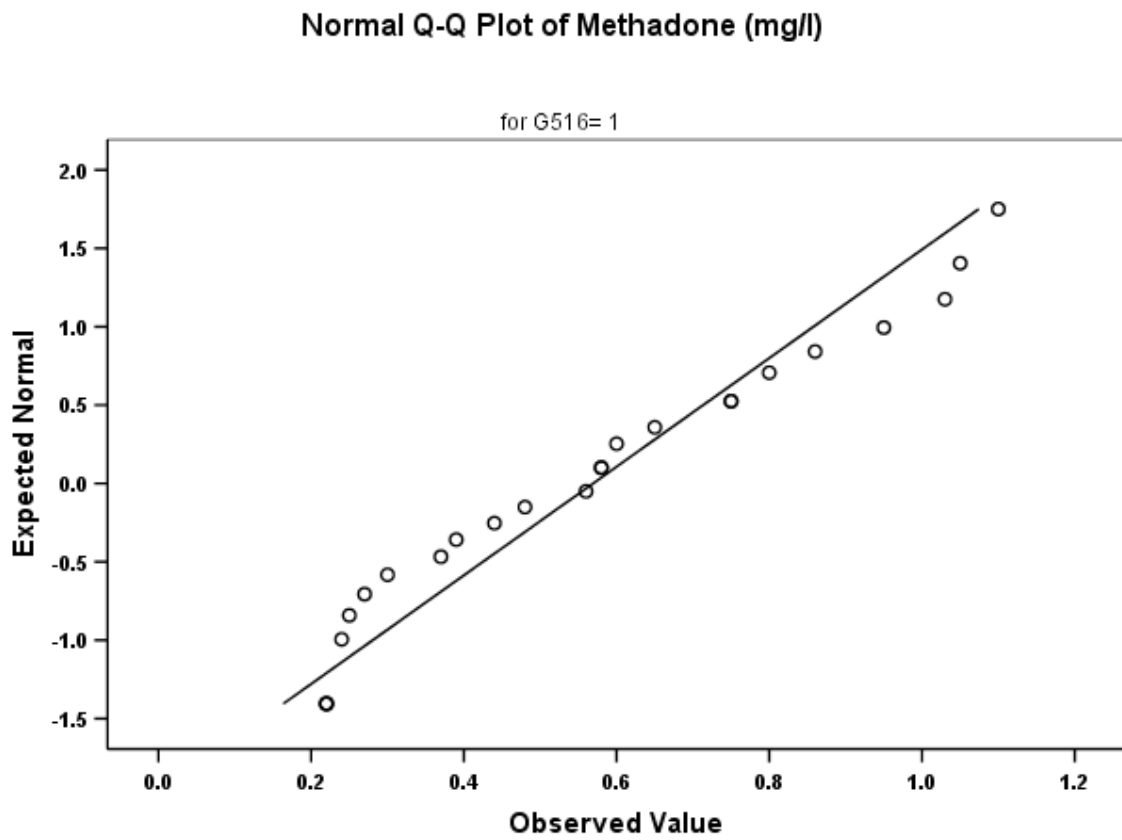


Normality plot for the 750 TC genotype, with post-mortem methadone concentration as the dependent variable and T750C as the factor, where $P > 0.05$.

CYP2B6 G516T SNP

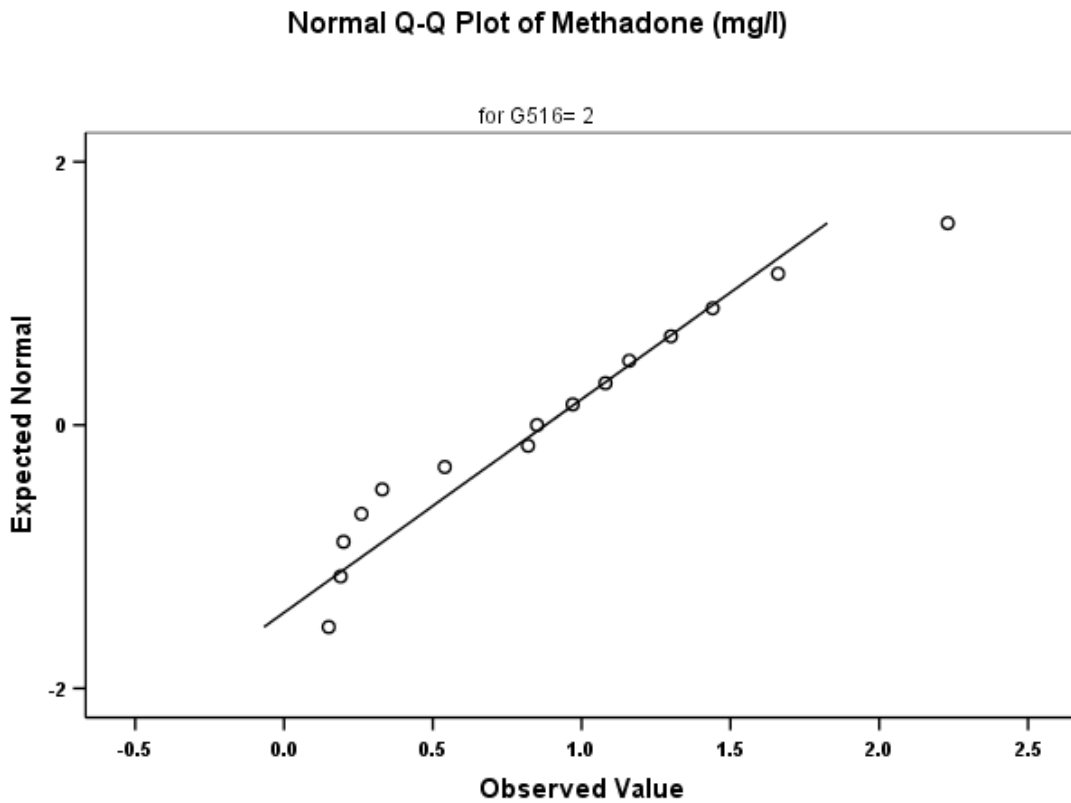
G516T Genotype	Statistic	df	Significance
516 GG	0.921	24	0.062
516 GT	0.932	15	0.295

516 GG Genotype



Normality plot for the 516 GG genotype, with post-mortem methadone concentration as the dependent variable and G516T as the factor, where $P > 0.05$.

516 GT Genotype

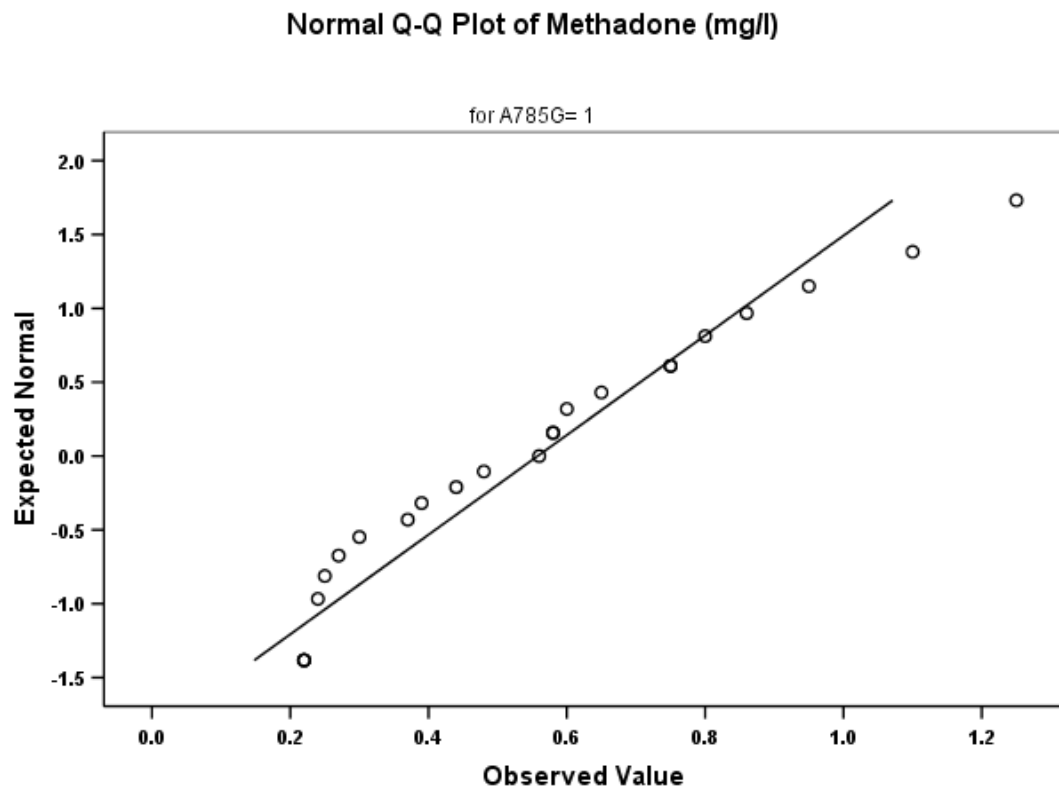


Normality plot for the 516 GT genotype, with post-mortem methadone concentration as the dependent variable and G516T as the factor, where $P > 0.05$.

CYP2B6 A785G SNP

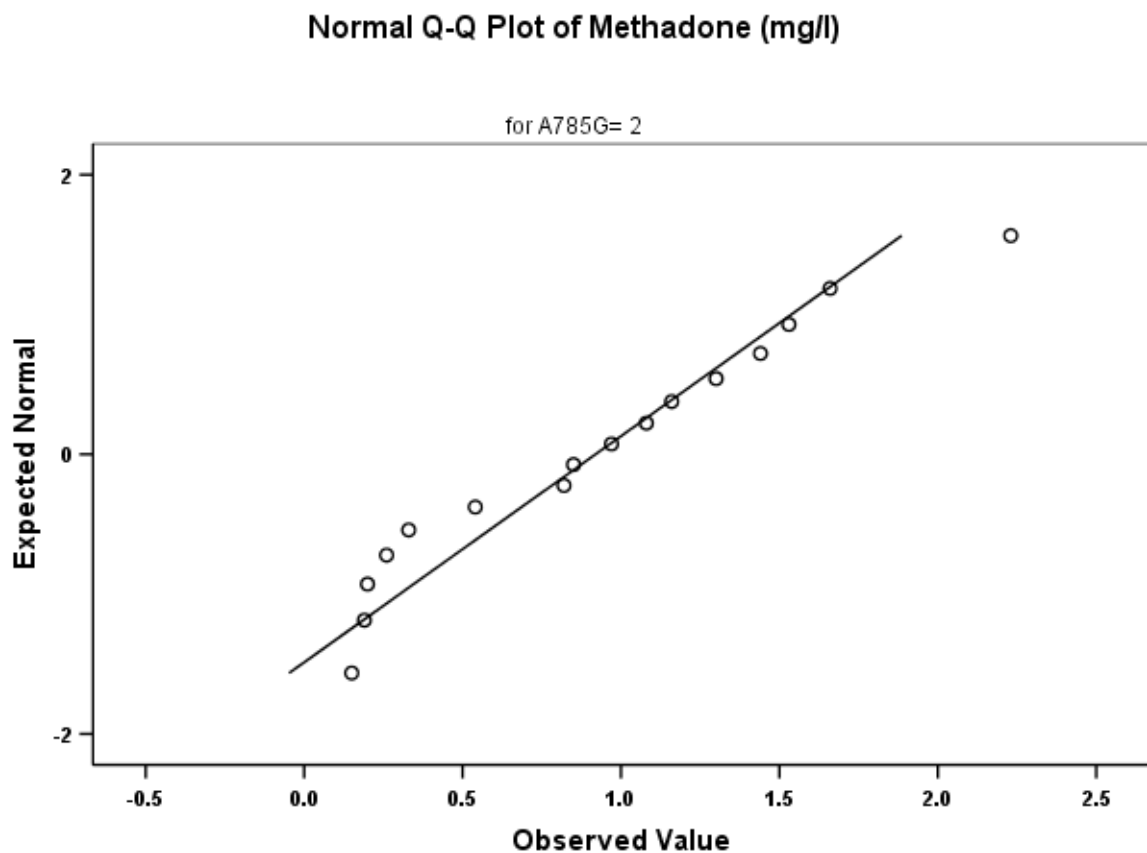
A785G Genotype	Statistic	df	Significance
785 AA	0.923	23	0.077
785 AG	0.940	16	0.352

785 AA Genotype



Normality plot for the 785 AA genotype, with post-mortem methadone concentration as the dependent variable and A785G as the factor, where $P > 0.05$.

785 AG Genotype



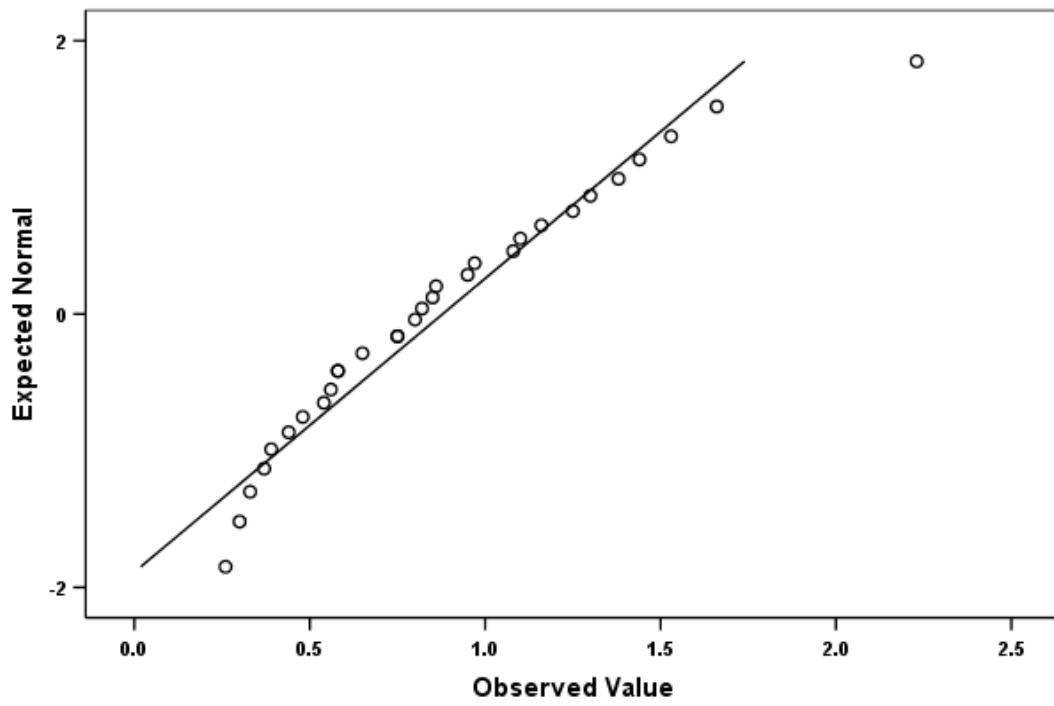
Normality plot for the 785 AG genotype, with post-mortem methadone concentration as the dependent variable and A785G as the factor, where $P > 0.05$.

Post-mortem Methadone Concentration

In order to examine the data distribution of the post-mortem methadone concentrations normality testing using the Shapiro Wilks test and SPSS 14.0 software was conducted. With methadone concentration as the dependent variable, no factor was selected.

	Statistic	df	Significance
Methadone (mg/L)	0.937	30	0.075

Normal Q-Q Plot of Methadone (mg/l)



Normality plot for post-mortem methadone concentration, where $P > 0.05$.

Glossary

5'	Five prime end of a DNA/RNA single strand
3'	Three primer end of a DNA/RNA single strand
<i>ABCB1</i>	Gene that encodes the p-glycoprotein transporter
Allele	Any of the forms of the same gene that differ in base sequence
Apoptosis	Is the process of programmed cell death.
Annexin V	Is a cellular protein that detects the early stages of apoptosis.
Arrhythmia	Irregular heartbeat, loss of rhythm
AV-12 cells	Mammalian cell line used for <i>in vitro</i> expression studies
β -endorphin	An endogenous opioid peptide that binds to the mu (μ) opioid receptor.
CAR	Constitutive androstane expression , a gene transcription factor
Cardiomyopathy	A disease of the heart muscle.
CCAAT	Sequence to signal the binding site for RNA transcription factor
Chiral	A molecule that is non-superimposable on its mirror image.
<i>Cis</i> -element	DNA sequences that regulate via transcription factors gene expression
CLL	Chronic Lymphocytic Leukemia
COMT	Catechol-O-methyl transferase, an enzyme involved in dopamine, epinephrine, and norepinephrine degradation.
COS-1 cells	Mammalian cell line used for <i>in vitro</i> expression studies
Cytochrome P450	A large and diverse family of enzymes involved in drug metabolism.
<i>CYP2A6</i>	Cytochrome P450 member involved in phase I metabolism
<i>CYP2B6</i>	Cytochrome P450 member involved in phase I metabolism
<i>CYP2C9</i>	Cytochrome P450 member involved in phase I metabolism
<i>CYP2C19</i>	Cytochrome P450 member involved in phase I metabolism
<i>CYP2D6</i>	Cytochrome P450 member involved in phase I metabolism
<i>CYP3A4</i>	Cytochrome P450 member involved in phase I metabolism
DIS-III-R	Diagnostic interview schedule 3 revised, measures symptoms of drug abuse
DNA	Deoxyribonucleic acid
Enantiomer	Either of a pair of stereoisomers
Endocytosis	The process by which cells absorb molecules.
Exon	Coding regions of a DNA sequence that will be expressed by mRNA
Fc Receptor	A protein found on the surface of specific cells including: natural killer cells, neutrophils, macrophages and mast cells.
FITC	Fluorescein isothiocyanate (FITC), a commonly used fluorescent dye for flow cytometry analysis.
Genotype	The total genetic constitution of an organism
GPCR	G-protein Coupled Receptor, involved in cellular signalling.
HAB serum	Human AB serum used to minimize non-selective antibody binding.
Haplotype	Set of SNPs on a single chromatid that are statistically associated
Hardy Weinberg Equilibrium	Relationship between gene and genotype frequencies in a population
HEK293 cells	Human embryonic kidney 293 cell line for use in <i>in vitro</i> studies
hERG	Human <i>Ether-à-go-go</i> gene coding for a potassium ion channel
Heterodimer	A protein composed of two polypeptide chains differing in composition in the order, number, or kind of their amino acid.
Heterozygous	A cell or organism with two different alleles for the same gene
Homozygous	A cell or organism with two identical alleles for the same gene
Huh-7 cells	Human hepatoma cell line for <i>in vitro</i> studies
I_{hERG}	Measurement of ionic current
Immunoglobulin (IgG)	Proteins produced by the immune system to fight infection.
Induction Phase	The beginning of methadone maintenance treatment, adverse responses to methadone are often reported in the induction phase (2 weeks).
Intron	Non coding regions of DNA that will not be expressed by mRNA
<i>In vitro</i>	Occurring outside of the body
<i>In vivo</i>	Occurring inside of the body
Isomer	Compounds with the same molecular formula but different structural formulas (Chiral).
<i>KCNH2</i>	The gene name for hERG
K_i value	Denotes the disassociation constant between a ligand and a protein

Ligand.....	A substance that is able to bind to and form a complex with a receptor to serve a biological purpose, e.g. methadone.
Linkage disequilibrium.....	Preferential association of linked genes/DNA markers in a population
Luciferase.....	Monooxygenase enzyme that catalyses bioluminescent reactions
Medulla.....	Lower portion of the brainstem, involved in respiration.
Mean Fluorescence Intensity (MFI).....	A measure of fluorescence intensity for flow cytometry to measure changes at the cellular level e.g. receptor internalisation.
mRNA.....	Messenger RNA, involved in DNA translation
Mu (μ) opioid receptor.....	The preferential binding target for many opioids including morphine
Myocardial Fibrosis.....	A type of heart disease where healthy heart muscle is replaced with fibrous tissues.
Myocarditis.....	Inflammation of the heart muscle.
Np-SAD.....	National Programme on substance abuse deaths report
<i>OPRM1</i>	The gene name for the μ opioid receptor
Pharmacodynamics.....	Biochemical and biophysical effects of a drug on the body
Pharmacokinetics.....	Biochemical and biophysical effects of the body on a drug
Phenotype.....	An observable characteristic or trait determined by the genotype
Phosphorylation.....	The addition of a phosphate group to a protein, involved in the activation or deactivation of many protein enzymes.
PE.....	Phycocerythrin, a commonly used fluorescent dye for flow cytometry analysis.
pKa.....	An acid dissociation constant, which measures the strength of an acid in a solution and can be used to determine the extent to which a drug will enter the blood stream.
Polymorphism.....	Multiple alleles of a gene within a population, usually expressing different phenotypes.
Pre-Botzinger Complex.....	An important region of the medulla for respiration.
Pregnane X Receptor.....	A nuclear factor involved in the upregulation of detoxification and clearance proteins in the presence of xenobiotics.
Promoter Region.....	A regulatory DNA region found upstream of a gene that controls gene expression.
Propidium Iodide.....	A dye used to measure apoptosis as it can only cross the membrane of non-viable cells.
Pulmonary Oedema.....	Fluid accumulation in the lungs.
QT interval.....	Measurement of the heart's electrical cycle between the Q and T waves
Racemic.....	A mixture that has equal amounts of left and right-handed enantiomers of a chiral molecule e.g. methadone.
Respiratory depression.....	Inadequate ventilation which can lead to death
RNA.....	Ribonucleic acid
RT-PCR.....	Real-time PCR used to amplify and simultaneously quantify a target
SNRIs.....	Serotonin–norepinephrine reuptake inhibitors – antidepressant drug.
SNP.....	Single nucleotide polymorphism
Splice variant.....	Variation from the original DNA sequence due to alternative splicing
SSRIs.....	Selective serotonin reuptake inhibitors- antidepressant drug.
Stereoselectivity.....	Preferential formation or targeting of one of a pair of enantiomers
TATA.....	The core promoter sequence involved in the initiation of transcription
TDM.....	Therapeutic Drug Monitoring, involves the measurement of medication in blood levels to avoid toxicity.
Torsades de pointes.....	A rare ventricular arrhythmia characterised by a long QT interval
<i>UGT2B7</i>	Gene for UDP-glucuronosyltransferase 2B7, phase II metabolism
Wild type.....	The typical or normal form of an organism, gene or characteristic